MINING-INDUCED SEISMICITY OF THE NORTH STAFFORDSHIRE COALFIELD

NABEEL HAMEED AL-SAIGH
B.Sc. (Mosul), M.Sc. (Keele)

A thesis presented for the Degree of Doctor of Philosophy in the Department of Geology, University of Keele

July 1981

ABSTRACT

Since the latter part of the last century several areas in North Staffordshire have experienced occasional series of earth tremors which are known locally as "goths" or "bumps". In early 1975 a series of earth tremors, culminating in a large tremor on the 15th July, shook the Trent Vale-Hanford area in the south of Stoke-on-Trent where coal was being extracted. The occurrence of earth tremors in areas where coal was being mined suggested that the incidence of these earth tremors was associated with mining operations in the coalfield.

To establish the causes and mechanisms of earth tremor generation, a seismic network consisting of five vertical and two horizontal seismometers was installed in the Stoke area in order to locate the hypocentres of the seismic events. The monitoring of seismic activity was carried out for two years (between September 1975 and September 1977).

Dr. N. J. Kusznir and Dr. G. K. Westbrook have studied the seismic activity in the Trent Vale-Hanford area, in the southern part of the North Staffordshire coalfield. In this thesis the seismic activity in the northern part of the coalfield is investigated.

During the seismic monitoring period, more than 300 seismic events were recorded and found to have occurred in the northern part of the coalfield. 98 of these were located. Only events recorded on four or five seismometers were located. They had local magnitude values, M_L, ranging between 0.1 and 2.5. The cluster of these seismic events coincides with regions of active mine workings. The tremor hypocentres were found to cluster in five areas. In three of these areas (areas A, C and D) seismic activity occurred as a result of the interaction between the stress field of the current workings and the stress field associated with the old mine workings. In the other two areas (areas B and E) the seismic activity appeared to be associated with sliding movements along pre-existing faults

due to the effects of mining operations. The depths of the tremor foci were concentrated between 1,000 m below O.D. and the surface, i.e. within the depth range of the active mine workings. The accuracy of the location was estimated to be of about 500 m in plan and less than that in depth.

First motion analysis of seismic events enabled the mechanisms of these events to be determined. Two types of seismic events with different first motions were observed in the coalfield. The first group of tremors showed both anaseismic and kataseismic first motions on seismometers. This type of tremor is interpreted as occurring either as a result of sliding movements along pre-existing faults, or due to failure in shear of the rocks in pillars and ahead of the active faces. The second group of tremors produced kataseismic first motions on all seismometers. This type of tremor is interpreted as having either an implosional source mechanism, and occurred as a result of rock failures in compression (pressure bursts), or as having a collapse source origin, and occurred mainly in goafs as a result of strata collapse and roof caving.

ACKNOWLEDGEMENTS

I should particularly like to thank Dr. Nick Kusznir for his patient, continuous guidance, supervision and constructive criticism of the work.

I extend my gratitude to Mr. Jim Preston, Mr. John Eyhre and Mr. B. Rollins of the National Coal Board (Western Area) for their helpfulness in collecting the geological and mining data and their stimulating discussions.

Special thanks are due to all members of the technical staff in the Geology Department, particularly to Mr. D. W. Kelsall and Miss P. Douglass for their excellent photographs.

Thanks are extended to Mrs. Carolyn Parnell who kindly typed the final manuscript with great skill.

This work was financed by a grant from the Ministry of Higher Education and Scientific Research of the Iraqi Government, to whom I am indebted.

Finally, I would like to express my gratitude to all members of my family for their encouragement and support during this study.

CONTENTS

CHAPTER 1

CASE HISTORIES OF MINING INDUCED SEISMICITY

1.1 Introduction

Mining induced seismicity may be defined as "the incidence of seismic events caused by rock movements or failures resulting from changes in the state of stress in the rock near mine excavation brought about by the presence of those excavations". (Cook, 1976).

When an underground excavation is made the virgin state of stress in the ground is disturbed, which results in stress concentrations in the rocks surrounding the excavation. As the rock is subjected to pressures approaching its strength limit, minor displacements or failures occur within the rock mass which results in the emission of seismic pulses. If the stress exceeds the rock strength, the rock will fail. Sometimes the failure occurs suddenly and explosively with rocks being ejected violently from the face, roof and walls. The seismic waves generated from such failures can propagate to the surface and appear as earth tremors which can be felt by local inhabitants. Many names have been used to describe the rock failures, such as rock bursts, bumps, bounces and quakes. However, the term rock burst is mostly used.

The phenomenon of rock bursts has been associated with mines throughout the world. Some examples are discussed in this chapter. In many of these case histories, fatilities, injuries and loss of production have been reported as a result of rock bursts. Sometimes the tremors associated with the rock bursts caused damage to property on the surface as well as in the mines.

1.2 Mining induced seismicity in the Witwatersrand gold mines, South Africa

Until 1908 it was generally considered that South Africa was seismically quiet. However, in 1908, about twenty years after the beginning of gold mining in the Witwatersrand near Johannesburg, a series of local earth tremors around Witwatersrand occurred. Since that time, the rock bursts in Witwatersrand have constituted a serious problem in deep mining, often becoming hazards to life and property and also interrupting mining operations.

The geological succession of the gold field consists generally of alternating bands of argillaceous and arenaceous sediments. The gold bearing reef dips southward at about 40°. The mine working takes place at depths of between 2 and 3 km.

The occurrence of tremors in the immediate vicinity of Witwatersrand suggested that they might be connected with the mining operations in the area. Therefore in July 1910 a 200 kg Wiechert horizontal seismograph was installed at the Union Observatory, about 6.4 km north of the mining area, in order to study these tremors.

From the seismograph records, Wood (1914) concluded that the origin of the Witwatersrand tremors was due to the slip of rock masses which had become unstable as a consequence of the extraction of large amounts of rock and water from comparatively shallow mines. He suggested that the slipping was probably more frequent near existing faults.

Cazalet (1920) analysed seismic records obtained from the Wiechert seismograph for the ten years from 1910 to 1919. He found a close correlation between the mining activities and the occurrence of tremors. Two distinctive features were noticed. The weekly distribution of tremors showed that their maximum incidence occurred during the working days, with a peak on Thursday, while the daily distribution showed a peak at blasting times.

Finsen (1950) made a statistical analysis for 29,669 tremors recorded over a period from mid-1938 to 1949. He confirmed the observations of Cazalet, Stokes and Gane concerning the occurrence of the maximum number of tremors during working days and with peaks during blasting times.

The relationship of the Witwatersrand tremors and mining was first clearly established by Gane et al. (1946) by means of five seismographs deployed on the surface around the mining area. They studied the tremors particularly to determine their hypocentres. The observations were made between March and August 1939. During this time 271 tremors were located. They found that most of the tremors were located in areas mined within the last decade at an average depth of 1.64 km. The authors concluded that the tremors originated within mining areas. The energy released by the largest tremor was estimated to be of the order of 10^{11} joules. Any suggestion that the tremors were caused by minor incidents such as the fall of the rocks in the mines can be consequently rejected. Gane suggested that fracture and mass displacement on a much larger scale might be needed to liberate such an amount of energy.

An electronic seismic recording system was built for the purpose of studying the Witwatersrand tremors more precisely. Gane et al. (1949) described in detail this equipment which consisted of six seismometers distributed in and around the mining areas. Gane et al. (1952) used six vertical electromagnetic seismographs placed over a single mine, and all within 0.5 km diameter, in order to accurately investigate the association between earth tremors and mining. In particular, they wished to determine whether or not the earth tremors could occur at considerable depths below the level of the mine. About 100 tremors were recorded and located between July and August 1950. They found that most of the tremor foci were concentrated adjacent to and slightly above the working level. The foci had an average depth of about 2.3 km. Again, this indicated a close relationship

between the tremors and the mine workings. Some tremors were located in the old workings, probably as a result of collapses taking place in the old workings as a consequence of mine stabilization.

Cook (1962) investigated the seismic activity, in particular to determine the energy released by the rock failures. The investigations were conducted in a longwall shaft which had a consistent history of rock bursts. Eight vertical and horizontal seismometers were installed at the end of holes drilled from the excavation into solid rock. Seismic velocities necessary for tremor locations were obtained by detonated explosions at known points along the face. Location of the foci was carried out graphically by using a string model. The accuracy of the location was checked by comparing the actual co-ordinates of the blasting shots and their computed co-ordinates. He claimed an accuracy of ± 5 m. During the monitoring period from January to June 1961, a total of 187 tremors, each radiating energy in excess of 1.4×10^5 J, were located. The largest tremors were recorded at Pretoria, about 61 km away. In the same region, and during the same period, only seven rock bursts were reported. All the reported rock bursts radiated energy in excess of 1.4×10^5 J. Cook, therefore, concluded that not all the events which radiated energy in excess of 1.4×10^5 J caused damage to the workings. Cook found that the majority of the foci were located close to the faces which were being worked, and that the pattern of seismicity followed the advancing face very closely. This was clear evidence for the association of tremors with mining operations, particularly to blasting. The daily distribution of the seismic events and energy release showed that an increase in the number of bursts and energy release occurred at blasting times. It was also noticed that there was a tendency for a series of small rock bursts to occur following a major one. Cook suggested that this may indicate that a large burst redistributes the stresses in the mine, consequently causing other tremors.

A statistical study of the rock bursts by Pretorius (1964) confirmed that most of the rock bursts occurred shortly after blasting.

1.3 Mining induced seismicity in the U.S.A.

Since 1899, when coal mines were first opened in the Sunnyside area of Utah, rock bursts have occurred and have been a serious threat to life and property. In 1958 the U.S. Geological Survey commenced investigations in the mines to determine the relationship between geological features and coal mine rock bursts (Dunrud and Osterwald, 1965). The Sunnyside area is located along the Book Cliffs of the Northern Colorado Plateau, about 40 km east of Price, Utah. The plateau is about 2 km above sea level. The depth of the mine workings extend up to about 0.76 km below the surface. The beds dip gently eastward and north-eastward at 5°-15° (Osterwald and Dunrud, 1966). Two sets of steeply dipping faults trending approximately north-northwest and east-northeast occur in the area.

In 1962, a seismic network was installed to detect the seismic activity in the Book Cliffs Coalfield near Sunnyside. A violent and spontaneous release of coal and rock from faces, ribs and roofs was a common hazard (Dunrud and Osterwald, 1965; Osterwald and Dunrud, 1966). The network consisted of six seismometers. 50,000 tremors were recorded in the district between 1963 and 1966. Seasonal as well as daily patterns for tremor occurrence were noticed. Seasonal maxima occurred in November, December, May and June. They seemed to be related more to unknown natural causes than to mining. Daily maxima occurred every 5-9 days, and these appeared to be related to the rate of mining. Most of the large tremors occurred during the seasonal maxima when the daily tremor rate suddenly decreased. Some of the large tremors reached a magnitude of 4 on the Richter scale, and their foci lay within a few hundred feet of the mining level. This indicated that large amounts of energy were being released near the mining level. Many sources of large tremors were located near faults or fault

intersections. Some of them were located near faults in unmined areas. This may indicate spontaneous stress releases during local slippage along these faults, where the stress may be caused by mining activity or by tectonics or both. Therefore, the authors concluded that the danger from large tremor and mine stability problems are greater in areas near to faults than in other areas where no faults exist.

Barnes et al. (1969) noted that during 1967 more than 50,000 tremors were recorded by the seismic network near Sunnyside. 540 tremors were of sufficient magnitude to be accurately located. Again he found that most of the tremors were located near faults or fault intersections. The majority of tremor epicentres were located within less than 5 km of the mine workings, while the depth of the tremor foci ranged between 0.3 - 3.0km below the level of the mine. It has also been noticed that in the southern part of the district (near Geneva mine), many of the large tremors occurred at greater depths than those at the northern part of the district. This may be due to one or two of the following reasons:

1. The Sunnyside fault zone intersects a graben at the north edge of the Geneva mine.
2. The presence of a subsurface fault in the southern part of the mining area.

The unexpected high seismic activity in the Sunnyside district posed two questions:

1. Does the seismic activity occur at Sunnyside alone or does similar activity occur in other adjacent areas?
2. Is the seismic activity at Sunnyside due to mining or due to the geological structure, particularly the faults present in the district?

To answer these questions, Osterwald et al. (1971) carried out two experiments to study the mining induced seismicity in two different areas,

particularly in order to correlate them with the seismic activity at Sunnyside mines. The two areas are in the Gentry Mountains 60 km west of Sunnyside, and in the Little Park Wash, 24 km south of Sunnyside. During the experiments a seismic network consisting of six portable vertical seismometers was installed in the area to be studied. The monitoring was conducted for about two weeks in each area. In the Gentry Mountain area, 37 tremors were located. Most of the tremors were located within or near the mining area. Some tremors were located along the major north trending faults west of the mining area. These tremors probably result from release of stress concentrated along the faults. At Little Park Wash, 70 tremors were recorded. Most of the tremors were located in or near the southern part of the Geneva mine at a depth of about 900 m below the mining level and within 2.13 km laterally of the active mining area. No tremor was observed within or near a major west-northwest faulted zone. This zone is 6.4 km wide, and located at about 8 km to the south of the mining area.

Finally, Osterwald concluded that the seismic activity in the Sunnyside district is not unique in the area. He also found that faults are sources of many earthquakes but are not the main causes of earth tremors. The main cause is the removal of large amounts of coal which caused stress concentrations in many parts of the mine. The stress concentrations may extend hundreds of metres below the mining level and laterally as far as 3 km away from the active mining areas.

Smith et al. (1974) carried out a detailed micro-seismic survey for 33 days in 1970 in the Geneva and Columbia mines. These mines are situated in the northern part of the Sunnyside area. The aim of the survey was to determine the relationship between the submine tremors and the induced mechanism produced by mining activity. The monitoring network consisted of three vertical fixed seismometers arranged in a tripartite array with a radius of about 0.5 km. Another three portable vertical seismographs were

distributed near the centre of the area in a triangular array with an average radius of about 5 km. Seismic activity averaged several hundred events per day with magnitudes between -0.5 to + 2.8. About 272 hypocentres were located, of which 85 were accurate. Most of the tremors were located beneath one area in which pillar and barrier removal was being conducted. Foci of the events were concentrated between 0.5 and 1.5 km below the active mining area. No definite evidence indicated the association of seismic activity with any surface or subsurface faults. The fault-plane solutions obtained from the first motion of P-waves suggested a possible relationship between the stress producing the submine tremors and those stresses which produced the thrust faulting and folding of the San Rafael Swell. This indicated that the maximum principal stress σ_1 was nearly horizontal. When the pillars and barriers were removed the minor and vertical principal stress σ_3 was reduced further, while σ_1 remained constant. It is believed that this would cause the generation of earth tremors near the zones of stress redistribution beneath the area of pillar removal and may account for the concentrated seismic activity beneath the Geneva mine.

In the Somerset Coalmine, Colorado, coal mine bursts were a hazard. Osterwald et al. (1972) conducted an experiment in September 1969 to study the seismic activity in the mine, in particular to determine the effect of a nuclear explosion, which was going to be detonated 65 km NW of Somerset, on the occurrence of tremors in the mine. Seven portable vertical seismographs were deployed around the mine. There was also one fixed seismograph directly above the mine. The observation was continued for two weeks. During this time the portable seismographs recorded 38 tremors, of which 13 could be located. In the same period the fixed seismograph recorded 517 tremors. Most of the tremors were located under the actively mined areas or beneath the intersection of steeply dipping coal seams with several clastic dykes in the southern part of the mine. This was probably due to

the unequal redistribution of stress in the intersection zones as a result of mining. This stress was released as tremors during the mining progress.

Osterwald found no changes in the total number of tremors occurring per day after the nuclear explosion. However, the maximum number of large tremors per day increased.

Hardy and Mowrey (1976) carried out micro-seismic studies associated with a longwall coal mining operation in Central Pennsylvania. In particular, they hoped to locate zones of instability around mine workings. Seven geophones were installed at the surface over the active panel. The observations were carried out for six months in 1974. During this period the longwall face advanced about 244 m at 183 m below the surface. In the same period several hundred seismic events were recorded. Only seismic events recorded on five or more geophones were located. The micro-seismic events were located firstly by using an isotropic seismic velocity model. It was found that the majority of events were located within 61 m ahead of the face. The same events were located again using an anisotropic seismic velocity model. In this case the events were clustered along the actual longwall face, most of them lying within ± 18 m of the face position. Most of the foci were within a ± 30 m depth of the coal seam. Many of the seismic events generated in the vicinity of the coal seam were due to fracturing of the immediate roof and crushing of the coal. Some events possibly occurred below the panel due to elastic rebound of the temporarily unloaded floor area. Micro-seismic activity also appeared in one of the tailgate pillars. These pillars normally become highly stressed as the face passes and in many mines are badly damaged.

A good correlation was noticed between the occurrence of micro-seismic events and actual underground mining activity. It was noticed that the frequency of events reduced dramatically during shift changes. The subsequent rapid increase in micro-seismic activity occurred about 20 minutes

after the beginning of the next shift. A general increase in micro-seismic activity associated with underground blasts was also observed.

1.4 Mining induced seismicity in the U.S.S.R.

In the U.S.S.R. the extraction of coal from great depths has been carried out particularly in the Donets Coal Basin. The coal is extracted from a depth exceeding 500 m from more than 100 mines. Some new mines are now under construction at depths of 1200-1500 m.

In the 1940's rock bursts were first encountered in the U.S.S.R. in the Kizelovsk coalfield. After that they occurred in the Kuznetsk, Donets, Shurab, and Suchan coalfields. 425 reported rock bursts occurred in these fields from 1943 to 1962 (Avershin and Petukhov, 1964). In the Donbass coalfield 454 rock bursts were recorded between 1946 to 1960 (Mirer, 1966). In 1952 work was started in the U.S.S.R. to develop seismo-acoustic equipment and methods to study the coal seams during mining at great depths (Antsyferov, 1966). The object was to find reliable warning signs of imminent rock bursts and to find ways of combating them.

In the steep seams of the Donbass coalmine, it was noticed that a "sagging roof" occurred after 15-20 days at normal production rates. The sagging is preceded by a sharp increase in the noise level with up to 60-100 pulses/hour or more, while the normal background level is 5-20 pulses/hour. Kagan and Lavrov (1966) carried out seismo-acoustic investigations in the Yunkom pit (Central Donbass coalmine) using three geophones installed at a depth of 2-3 m in the coal seam. They found that the seismic noises were located at a distance of up to 16 m ahead of the face. However, most of the seismic noises were located within 2-10 m of the face.

Long-term observation of the seismo-acoustic activities for seams prone to rock bursts showed that some sections of the seam have higher noise levels than others (Ivanov, 1966). This may suggest that the occurrence of rock bursts in worked coal seams can be characterized into zones.

Observations on the Andreevskii seam (the 596 m horizon) of the Yunkom pit were carried out for more than two years. The face advanced 600 m in this period, during which six high noise zones were observed having a total length of 197 m, and widths ranging from 8 to 47 m. More than 20 bursts were located within these noisy sections. A zone 47 m long was found confined to a fault. Similar phenomena were found on the 476 m horizon. Zones 2-5 m long were found to be caused by periodic sagging of the roof rocks. The distances between these zones were about 12-15 m corresponding to the spacings of natural sags in the main roof. This observation suggests that the occurrence of anomalous noise in a periodic manner may be due to:

1. Changes in the properties of the coal or its strength due to structural change.
2. Change in pressure near the face.

This phenomenon is known in mining as "periodic weight" (Sinha et al., 1972). It is caused by caving and sagging of the main roof which does not always take place with each unit of face advance.

Boiko (1966) carried out an experiment to find out the relationship between the distribution of normal stress and noise level in the abutment pressure zones. The experiment was carried out in a number of burst-prone seams in the Yunkom pit. Stress measurements in the vicinity of the coal face were carried out using an elastic pressure gauge in a borehole 8-10 m deep, in advance of the face. Simultaneously, measurements of the noise level in the corresponding part of the seam were recorded using a seismometer. The results of the pressure measurements and hourly noise level at different positions of the face, were plotted together in Figure 1.4.1 to show the relationship between them. In all observations where a normal noise level was observed in the coal seam, the maximum stress was at a depth of 3-6 m ahead of the face. This indicates that the redistribution of the stress in the rocks took place smoothly and without sudden jumps. However, a high

noise level was observed corresponding to a sudden increase of the maximum stress at a depth of 1-2 m ahead of the face. This phenomenon represents a potential rock burst danger. The experiment showed that the noise level of the seam increases with rock pressure and that the position of the maximum stress in the seam varies with respect to the face position. This confirms Ivanov's observation concerning the zonal characteristics of the coal seam with respect to rock burst occurrences.

Since 1957 the seismo-acoustic research station of the Donets Economic Council has been engaged in measuring the noise level in seams worked out at the Yunkom pit (Ivanov and Parshikov, 1966). It has been found that the noise level in the dangerous seams being mined under or over previous workings increases ten times as soon as the seam passes outside the protected region. According to the safety regulations in the U.S.S.R. "the protective effect is lost when the face of an under-protected seam advances a distance equal to twice the interseam distance toward the abandoned face of the protective seam". However, further observations showed that as long as the face of the protecting seam was in advance of the protected seam face, the noise level remained normal. In 1961-1962 measurements were carried out in the Kamenka seam, which is protected by the Mazur seam where a pillar of 30 m in length was left (Figure 1.4.2a). The interseam separation was 49.5 m. The noise level rose from 0.1 pulses/hour to 10 pulses/hour when the working face in the Kamenka seam had passed 4 m below the pillar. Subsequent advance of the face below the pillar made the noise level increase as follows: 18 pulses/hour after 10 m; 32 pulses/hour after 16 m; and 80 pulses/hour after 19 m, and it then fell to zero 4 m before the face emerged from the pillar zone. The lag and lead anomaly of the noise level, as the working face entered and emerged from the pillar zone, were probably due to the fact that the pillar was partially crushed at the ends. A similar observation was made during the working of the Derezovka and Andreevskii seams (Figure 1.4.2b). The vertical interseam separation was 60 m. The Andreevskii seam was protected by working in the Derezovka seam. The noise level of

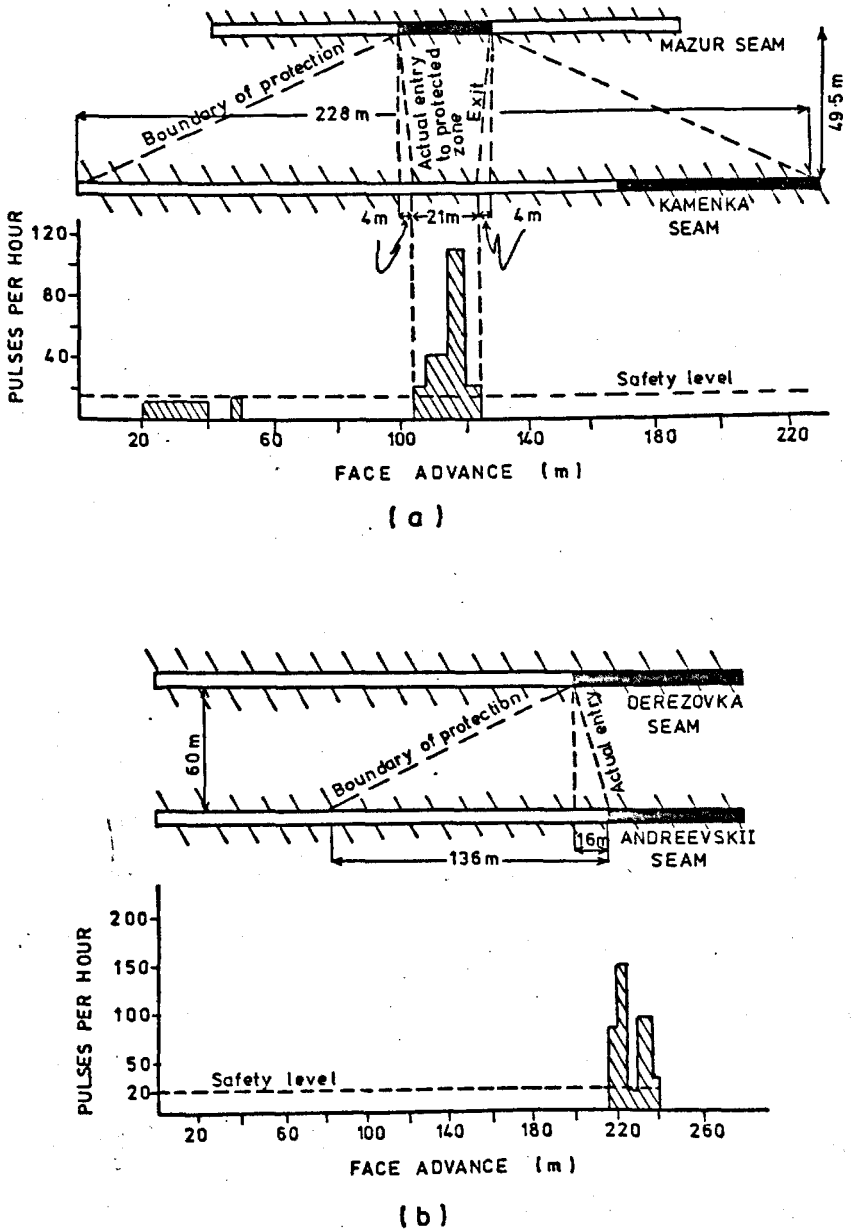

Fig. 1.4.2. Diagram showing the effect of protective region of old workings on the occurrence of seismic noises generated by a deeper current working. (a) The mine workings in the Kamenka seam protected by old mine workings in the Mazur seam. When the Kamenka face passed under the pillar in the Mazur seam the protection effect is lost and a sudden increase in the number of seismic pulses occurs. (b) The mine workings in the Andreevskii seam protected by old mine workings in the Derezovka seam (after Ivanov and Parshikov, 1966).

the Andreevskii seam during mining was 2-5 pulses/hour, which was normal for this seam. When the working face of the Andreevskii seam passed outside the protective influence of the Derezovka seam, it coincided with a sudden increase in the noise level up to 300 pulses/hour. Two bursts of 200 and 300 tons of coal occurred in the face at this time. It was also noticed that the face of the Andreevskii seam was 16 m in advance of the protective seam face when the increase in the noise level started.

In the Donbass coal field, the drilling of horizontal and rising boreholes has been found to be the most effective safety measure against rock bursts. Mirer (1966) determined the relief effect of a rising borehole by using seismo-acoustic methods in two seams in the Yunkom pit. The examined seams were the Bezymyannyi seam with a thickness of 0.7 m and the Zolotarka seam which ranges from 0.44 to 0.65 m in thickness. During this experiment the face passed through four rise boreholes of 0.25-0.3 m in diameter and 30 m in length, and was there accompanied by a low seismo-acoustic activity level. It has been noticed that the noise level started to fall at a greater distance from the boreholes than that at which it began to rise. This may indicate that the maximum pressure rapidly shifted deeper into the solid coal as the face traversed the borehole. Also, at the same time, in front of the boreholes, the face passed through a zone which had suffered disintegration.

The distance from the borehole to the point where the noise level started to fall was taken as the mean for the four boreholes, and was found to be equal to 3.38 m. In the same way, the mean distance from the borehole to the point where the noise started to rise was found to be 0.88 m. The sum of these two values represents the overall relief zone for a rising borehole in the Zolotarka seam, which is equal approximately to 4 m. The relief zone for the Bezymyannyi seam was found to be about 2 m. This is because the ratio of the borehole diameter to the thickness of the Bezymyannyi seam was less than that in the Zolotarka seam.

Petrosyants and Gorbachenko (1969) conducted an experiment using a seismo-acoustic method to determine the stability of the rocks above a mine working in the Fizkul'turnik mine. The experiment was carried out by transmitting artificial pulses through the rocks between two boreholes. Two 1.8 m deep boreholes were drilled in the roof of the mine working for this purpose. A vibration source was placed in one borehole and a receiver in the other. Both transducers were at the same level and were moved simultaneously along the boreholes as wave amplitudes were measured. It has been found that low transmitted wave amplitudes coincided with fissure zones, while a sudden increase in the amplitude occurred when the transducers passed into solid rocks.

1.5 Mining induced seismicity in the Upper Silesian Coalfield, Poland

Earth tremors in Poland occur particularly in the Silesian region, where they are associated with the complex geological and tectonic structure of the Upper Silesian coalfield. Some of the tremors have caused severe damage on the surface, while rock bursts have occurred frequently and constitute a considerable hazard in the coal mines of the region.

Two hypotheses have been suggested in attempting to explain the occurrence of earth tremors in the Upper Silesian mines.

1. The tremors are of tectonic origin caused by tectonic forces still active in the area.
2. The tremors are caused by mine workings, and are generated by the disturbance of the equilibrium strata pressure by mining operations.

Until 1898 it was believed that the tremors in the coal field were caused by the occurrence of rock bursts in the working mines or by the fall of rock masses in old workings (Janczewski, 1955). However, in 1898 a strong tremor was felt over a large area and caused damage on the surface. Inspection of the mines in the vicinity of the area showed no evidence for

the occurrence of a rock burst. Therefore, some investigators tried to explain the cause of the tremors by "terrestrial phenomena". From that time the origin of earth tremors in the coalfield has been a matter of debate. Many writers, especially in the first half of this century, supported the concept of a tectonic origin for the Silesian tremors. Some writers accepted both of the two theories, although they considered one of them as being the more important. At present most investigators believe that the Silesian tremors are mainly caused by mining operations, although they do not rule out that some may be of tectonic origin.

Investigators have chosen different approaches in order to determine the origin of the earth tremors in the region, and to support one of the two theories. From the literature of the Upper Silesian earth tremors, it can be inferred that three main approaches have been used.

(i) The determination of the depth of the tremor sources:

Difficulties in determining the depth of the earth tremor foci have made the selection of the correct hypothesis from the above two hypotheses very difficult. The occurrence of earth tremors at great depths would indicate tremors of tectonic origin while the occurrence of tremors at mine levels would suggest tremors of mining origin. Janczewski (1950) studied some of the tremors and rock bursts which occurred in the years 1948 and 1949. He calculated the depth of foci of some large tremors from macro-seismic and micro-seismic data. He found that the depths ranged between 4 and 10 km. Later he revised the calculated depths to between 5 and 12 km (Janczewski, 1956). He concluded that these tremors were natural earthquakes with a shallow focus and considerable intensity. Some of these tremors were accompanied by strong or even violent rock bursts in the nearest mines. He described one such tremor which occurred on the 6th September, 1949 and was recorded as far away as Prague. At the same time, a severe rock burst occurred at a depth of about 400 m within the mine and

was felt at the surface within an epicentral distance of a few kilometres. He commented that if the tremor focus had lain at the same position of the rock burst (400 m) then the vibration produced at the surface would have been far greater than that felt. Therefore, he concluded that the tremor was that of a natural earthquake occurring at a depth of several kilometres and that the rock burst occurred immediately after and as a result of the earthquake. Wierzchowska (1962), however, advocated that the earth tremors in the coalfield were due to mining operations. She suggested that the large estimated depths found by Janczewski were due to an error in calculation arising from ambiguity and uncertainty in the interpretation of the seismograms. She suggested that if the rock bursts were triggered by tectonic earth tremors, then two seismic sources, superimposed on one another or occurring within a very short time interval, would exist on the seismograms. Examination of the recorded tremors showed no single case of this kind. This she believed indicated that the seismic source was the rock burst itself.

Using four seismographs situated in a vertical line with one at the surface and the other three at different depths, Kulpinski (1966) hoped to determine the tremor hypocentres and rock burst foci more precisely. In a period of more than one year in 1965 and part of 1966, 110 tremors were located. Kulpinski found that most of the tremors were clustered in the vicinity of the active mine workings.

(ii) Calculation of the energy release :

Budryk (1955) propounded that the frequent occurrence of rock bursts in the area is due to both the presence of thick coal seams beneath massive sandstones and the triggering effect of natural earth tremors. He suggested that small natural tremors which have insufficient energy to cause damage at the surface, affect the weak parts in the underground mines causing a momentary concentration of stresses in the rocks which exceeds the elastic

limit of the coal. Consequently a rock burst occurs which sometimes has catastrophic effects. Budryk reported that 10,000 tremors were recorded between 1930 and 1941, a third of which were detected in the mines. He therefore suggested that not only were the large tremors, accompanied by rock bursts, of tectonic origin, but the small ones also.

Gibowicz (1963) analysed 160 tremors recorded between 1948 and 1959 at epicentral distances between 2 and 80 km. He computed the energy released and the magnitude of each tremor. He was able to determine the repetition frequency of the tremors; that is the frequency of occurrence of the tremors in relation to the values of their magnitude or energy. This follows the frequency-magnitude formula given by Richter (1958). The value of $\underline{b}$ was found to be equal to 0.9 which is in general agreement with that of other natural seismic regions of the world. It was also found that an average of about 155 tremors with magnitude, M_L, from 2 to 3.6 occurred annually in the region, while the average amount of seismic energy released per year was about 9.3×10^9 J. The seismic energy released by an earthquake represents only a few percent of the total amount of earthquake energy (it was found with underground nuclear explosions that the seismic energy radiated is only a few tenths of a percent of the total explosive energy). Gibowicz estimated that the total energy of the largest seismic event in the coalfield had a value of about 10^{12} J. Gibowicz concluded from the analysis of the energy and frequency of the tremors that local natural earth tremors were occurring in the area as well as those of mining origin.

Wierzchowska (1962) refuted this argument by suggesting that the elastic energy concentrated in the mine rock mass, as a result of mining operations, can be sufficiently large so as to cause these very large tremors. Znanski (1959) showed that the kinetic energy which could be liberated during a violent failure of the virgin coal surrounding the mine face could bring about a seismic event of magnitude equivalent to that of

a tectonic earth tremor. He gave two examples of large rock bursts which occurred in the East and West German Potash mines. One of them was felt on the surface over an area 20 km in radius, and recorded at many distant European seismic stations, up to an epicentral distance of 2,000 km.

(iii) Statistical observations:

This approach was based on the comparison and analysis of seismograph data and the occurrence of phenomena accompanying rock bursts and tremors.

Neyman (1955) pointed out that earth tremors in the Silesian coalfield could be of tectonic natural origin, as well as due to mining operations. He noticed that the most frequent and violent rock bursts always occurred when a new seam was first being mined. During the extraction of the next seam the rock bursts occurred less frequently and were smaller, due probably to the release of stress as a result of the extraction of the first seam. Neyman (1964) carried out statistical studies of the occurrence of earth tremors and rock bursts in the coalfield. He found that 11,528 tremors were recorded by the seismic stations between 1955 and 1960. Only 915 of these were reported as rock bursts in the mines. The largest tremor released about 10^{10} J of seismic energy. The daily distribution of tremors and rock bursts showed that most of them occurred during working times, with a peak of incidence during blasting times. He also noticed that in the period between 1956 to 1963, 12 large tremors occurred immediately after blasting. These tremors were felt at the surface and recorded by many seismograph stations. He suggested that this indicated a close causal relationship between mining operations and the occurrence of tremors, since it was unlikely to be coincidental. At the same time, Neyman did not exclude the possibility of the occurrence of the occasional natural tectonic tremors. These tectonic tremors may initiate rock bursts, but only in the highly stressed rocks.

Wierzchowska (1962) argued also that earth tremors in the coalfield are not of tectonic origin, but are due to mining operations. She also did not exclude the occurrence of a few natural earth tremors. She based her evidence on the macro-seismic and micro-seismic analysis of earth tremors and also on the observations of phenomena accompanying rock bursts and tremors in mines and their effects on the surface. Her synthesis of the evidence on which her conclusions were based are as follows.

1. The abrupt fall-off of earth tremor intensity with epicentral distance indicated that the earth tremors originated at little depths, and probably at the same level as the mine workings. Macro-seismic observations showed that the largest tremor was never felt at an epicentral distance greater than 10 km.

2. The occurrence of many tremors and rock bursts, some of them very large, at the same time or shortly after blasting suggested that they were caused by mining operations.

3. The regions of occurrence of the largest tremors were also the regions of the most powerful rock burst occurrence. Since the rock burst intensity is directly proportional to the magnitude of the stresses concentrated in the mining strata as a result of mining operations; this suggests that the coincidence of the seismic regions with those of rock bursts is evidence for the existence of a relationship between the intensity of the tremors and the magnitude of the concentrated stress in the mines of a given region. Consequently, this indicates that the occurrence of tremors is due to mining operations, otherwise their intensity in different regions would not follow the intensity of the rock bursts. However, this can be interpreted to suggest that the tremors and the rock bursts were of tectonic origin.

4. Tremor and rock burst occurrence in certain parts of the seam known to be rock burst-prone ceases with the cessation of mining activity

in that part of the mine. After mining operations start again, tremors and rock bursts recommence. This indicates that the tremors are of mining and not tectonic origin since if they were of tectonic origin they would not be affected by interruptions in mining operations.

5. The occurrence such as cracking noise, the snapping of coal from faces and floor heaves before the occurrence of a rock burst in the mine indicates that the stresses in the strata have reached a critical state. This can be interpreted to suggest that the occurrence of the tremors and rock bursts were due to increasing stress in the mine and not due to tectonic origin.

6. It has been found that the intensity of tremors in the mine, particularly in the vicinity of the rock bursts, was higher than that at the surface and other parts of the mine. This indicates that the tremors were not of tectonic origin, because if they were of tectonic origin, particularly if the tremor did not cause a rock burst, the tremor should be felt with the same intensity throughout the whole mine. Moreover, if the tremor initiates a rock burst, the tremor should be felt at least a few moments before the occurrence of the rock burst.

A summary of different opinions concerning the origin of earth tremors in the Upper Silesian Coalfield has been presented above and it is possible to conclude that these tremors were most probably due to mining operations in the coalfield.

1.6. Mining induced seismicity in Britain

In British mines, major rock bursts have always been rare, and those that do occur usually occur in coal mines.

Davison (1924) studied mining induced earth tremors. He indicated that these tremors occurred entirely or partially due to mining operations. He gave many examples about tremors frequently felt in mining districts, particularly in Cornwall, the South Wales Coalfield and around Manchester. He

reported others felt near Sunderland and other places on the magnesian limestone of the Durham Coast. He mentioned that some of these tremors were accompanied by noise.

In the South Staffordshire coalfield, where the coal seams are thick, the problem of rock bursts has been a serious feature in the mine, particularly in those at great depth (The South Staffordshire and Warwickshire Institute of Mining Engineers, 1932-33). These bursts caused coal to break out suddenly from the faces and sides of the roadways, crushing coal pillars, crushing and throwing out supports and lifting the floor. Most of the bursts were "pressure bursts" as described by Phillips (1944-45) (see Section 3.2.1).

In May 1930 a committee was established to investigate and determine the factors which caused rock bursts in the South Staffordshire, Warwickshire and Cannock Coalfields. It was found that the most important factors affecting the occurrence of rock bursts in the South Staffordshire coalfield were the depth, geology and the mode of mining (The South Staffordshire and Warwickshire Institute of Mining Engineers, 1932-33, 1945-46). Thick coal seams had been worked successfully in South Staffordshire at shallow depth with few rock bursts and roof control problems. At greater depths (about 730 m), however, the rock bursts became very serious. As a consequence of the great depths and coal thickness, a large amount of compressional strain energy was created which was the main reason for pressure bursts. It could also be that the working of these thick seams without proper supports have led to irregular settlement. Consequently, large masses of strata may have suddenly broken and appeared as rock bursts. The committee also indicated that the coal seam was softer than the roof and the floor, hence the coal seam would be the first to yield under pressure. However, since the seams are composed of interbedded soft and hard coal, violent rock bursts can occur (within harder coal). The committee found that most of the rock bursts

occurred during the driving of headings, particularly when two roadways approached each other. It was noticed that the number of rock bursts increased with increases in the rate of excavation. Also, when the extraction approached a fault the rock bursts became more frequent and violent. The committee gave many examples of the occurrence of rock bursts and tremors in the South Staffordshire thick coal seams.

At Hickleton colliery, near Doncaster, a series of rock bursts occurred in October 1964 when face 324 of the Parkgate seam was passing under a coal pillar left in the overlying Barnsley seam (Shepherd and Kellet, 1973). At that time the face had advanced 338 m. The seam lies at a depth of 900 m. The face advanced a further 165 m before another series of rock bursts took place. The third series of rock bursts occurred during the working of a coal pillar 5.5 m wide left between this panel and another old panel (panel 322). These rock bursts caused large amounts of coal to blow out from the face, and displaced the supports and machines. After that it was decided to stop production in this face. All the rock bursts were located near the righthand end of face 324 (on the abutment stress zone of a previous 322 panel).

It was decided that a new face (face 325) advancing parallel on the left side of panel 324 would be opened. Therefore it was decided to carry out stress measurements ahead of the face. Several strain gauges were deployed in advance of the face in order to determine the build-up of stress at a point in the solid as it approached and passed by the face. It had been observed that a zone of high stress in the buttress zone of the face was encountered as the face advanced. Therefore, it may be deduced that the rock bursts occurred when this zone of high stress was aggravated by adding another zone of high stress from the side abutment due to the presence of an adjacent old mined-out area.

In Scotland, Mashkour (1976) carried out a seismic investigation in the Monktonhall colliery in the Midlothian coalfield in order to determine the sources of earth tremors and rock bursts whose occurrence in the area have been reported since the early 1960's. He used two seismic networks of large and small aperture. The mine workings were carried out at a depth of 900 m. The seismic velocities of the strata and their thicknesses were determined by seismic refraction, and a borehole logging survey in the area. The accuracy of the location was determined from the seismic location of two known blasts underground. It was found that their epicentres and foci lay within ± 200 m of their actual positions.

In the period from 1969 to 1974, a total of 121 seismic events were recorded on the Scottish Low Lands Seismic Network (LOWNET) which was operated by the Institute of Geological Science in Edinburgh. The network consisted of seven vertical seismometers, one of them recording the two horizontal components as well as the vertical component. For a more accurate study of the seismic activity in the area, a small seismic network consisting of five vertical seismometers was installed on the surface around the colliery. During the seven months of observation, between December 1974 and June 1975, 227 events were located. The seismic energy released from the seismic events ranged between 10^3 - 10^6J. Most of the events were shown to be located near the active parts of the mine. Some of the events were located in old mined-out areas. Another group of tremors was located near faults or fault intersections.

Monthly distribution of the tremors showed that no tremor occurred during the months coinciding with the miners' holidays, and also during the months of the miners' strike in 1972 and 1974. The maximum number of tremors occurred in 1973 coinciding with a maximum number of reported rock bursts in the colliery. The weekly distribution of earth tremors and rock bursts showed that the least number of tremors and rock bursts occurred on

Sundays, while the most occurred on Thursdays. The daily distribution showed that the lowest number of tremors and rock bursts occurred during the shift changes, whilst the maximum incidence occurred in the middle of each shift.

Mining induced seismicity has been studied in the Trent Vale area of the North Staffordshire coalfield. This will be described in Chapter 7.

1.7 Mining induced seismicity in Canada

In Canada, mining induced seismicity associated mainly with the gold mines at Kirkland Lake. Lake Shore and Hargreaves mines are the deepest in the area and were developed at an average depth of about 2465 m below the surface.

Detailed studies of the seismic activity which took place at Kirkland Lake in the period 1938-1945 were carried out by Hodgson (1958). Correlation of the earth tremors recorded on the surface seismographs with the mine data suggested that there were two groups of rock failures. One group was observed at the Lake Shore mine but not recorded on the surface seismographs. These include some important rock falls. These bursts have released a small amount of energy which was not enough to be recorded on the surface seismograph, although some were recorded on down-mine seismographs. The second group of tremors were usually larger and were recorded on the surface seismographs but not reported in the mines. These might have occurred in the old workings of the Lake Shore mine or in adjacent mines. Hodgson also found that bursting occurred in many instances at the same time as blasting or shortly afterwards. Leaving pillars has also been shown to be a cause of rock bursts. Therefore complete extraction of the ore was recommended so that gradual and uniform subsidence of the roof may occur.

The rock bursts at Lake Shore mine were caused by the pressure effects of the superincumbent strata which was unequally distributed due to the mining operations and the presence of faults (Robson, 1946). Robson

discussed in detail this problem, particularly the mechanism of the rock bursts. He pointed out that the most important factors affecting the occurrence of rock bursts in the area are:

1. The nature of the ground: it has been shown that the ore and surrounding rock are hard, brittle, and can sustain great pressure up to the point of sudden failure, i.e. the rocks are susceptible to bursting.

2. Mining technique: during the mining some pillars were left to act as supports. If the stope extended great distances without enough support, the hanging wall would have subsided and collapsed.

3. Geological structure: the ore bodies were found in steeply dipping veins which occurred in zones of fractured rocks. As a result of these fractures a great number of large blocks of hard, brittle rocks was developed, and during mining the stress builds up along these lines of weakness and becomes a source of danger.

In the Wright-Hargreaves mine the first series of rock bursts started in 1932, and became a major problem in the later 1930's (Buckle, 1965). Between 1932 and 1964 about 227 rock bursts were located. These caused 52 injuries and seven deaths. Some other rock bursts were not located. Those mostly involved remnant pillars in old mined out areas. Again, most of the rock bursts have been noticed as occurring during or shortly after blasting. It has also been noticed that the frequency of the rock bursts increases proportionally with deepening of the mines.

In August 1964 two strong rock bursts occurred. The magnitude of the second one was estimated to be between 4.5 and 5 on the Richter scale. It was reported at Blue Mountain station in Oregan and at Tonto Forest station in Arizona at distances of 2832 km and 2912 km respectively from Kirkland Lake. The source of the events was the shaft pillar section where severe damaged occurred and two miners were killed. Buckle believed that these rock bursts were initiated by the movement of strike fault at the bottom of the shaft. Many small rock bursts followed these two events for about two days.

In the Crowsnest Pass coalfield, Alberta, Milne and White (1958) carried out two experiments using three seismographs to study the rock bursts which were occurring in the coal mines, and to determine their relationship with the local earthquakes in the area. Again they found that one group of events was reported in the mines but not recorded on the surface, while the other group was recorded on the surface but not reported in the mines. The authors established that there was no relationship between the rock bursts and the natural earthquakes, and there was no indication of an increase in the number of rock bursts after an earthquake.

1.8 Mining induced seismicity in the Kolar gold field, India

By the beginning of this century rock bursts in the Kolar gold field mines had become serious and have been one of the major mining problems of the field ever since. The bursts may be small, affecting one isolated development, or large, causing damage over hundreds of feet in many levels (Taylor, 1962-63). The reef is of quartz and dips 40° W near the surface to 85° W at greater depths. It is bounded by highly metamorphosed hounblende schists. The reef and its surrounding rocks are faulted by a number of large and small faults and are intruded by dolerite dykes and pegmatites (Crowle, 1931).

Seismic investigations of the rock bursts in the field began in 1912 using a Wiechert Seismograph (Isaacson, 1961). Crowle (1931) studied thoroughly the rock burst phenomenon in the field. He mentioned that about 13,000 shocks were recorded every year between 1912 and 1930. Some of them had been felt on the surface at a distance of up to 24 km. He classified the rock bursts in the region as follows.

(a) The small local bursts: These caused little damage and occurred throughout the area, but more frequently in recent mines.

(b) The pillar bursts: These were due to sudden failure of pillars, particularly in extensively mined areas deeper than 150 m. They were less

frequent but stronger than group (a), and sometimes caused serious damage to the workings.

(c) Bursts in fault zones: These occurred in the vicinity of faulted zones. Their frequency and intensity depended on various factors, such as depth, and the nature and extent of the excavation near the fault zone.

(d) The heavy shocks or quakes: These were mainly due to failure of the rock walls. Usually they were severe and caused extensive damage.

Isaacson (1957) described in detail the instruments and the methods which have been adopted to investigate the problem of rock bursts in the region in order to find ways of combating them. These methods generally consisted of measuring underground stress and strain, and determining their relationship with the rock bursts. Several instruments and methods were used to measure the underground stress. It was found that the pressure encountered was greater than expected from the weight of the overburden rocks only. This indicated the existence of high inherent stress in the area, possibly produced by tectonic processes or metamorphism. Measurements of the abutment stresses induced ahead of a stope face showed that the maximum stress occurs at about 1.8 m from the face. Therefore an experiment was carried out to de-stress the face by blasting in holes 3 m deep inside the face.

Observations of the recorded rock bursts on local seismographs revealed that the frequency of rock bursts increased during blasting times (Isaacson, 1957). While observations of the rock bursts in the mines indicated that most of the recorded bursts were not observed underground (Isaacson, 1961). The occurrence of rock bursts in groups was also noticed by Isaacson. This may have been due to one burst triggering off the other.

Taylor (1962-63) studied about 125 rock bursts which occurred in the mines during the period from 1956 to 1960. He confirmed that faults and

dykes were important factors affecting rock burst occurrence. Again he found many rock bursts occurred at or shortly after blasting. The number of rock bursts showed an increase towards the weekend with a peak on Friday. This is probably due to the building up of stress as extraction continues during the week.

1.9 Mining induced seismicity in Czechoslovakia

In Czechoslovakia, rock bursts occur mainly in the deepest zinc ore mine of the Brezove Hory district (Pribram region) at a depth of about 1520 m below the surface. The zinc ore was extracted from five mines in the district, from veins dipping 82° E. These veins were mostly embedded in diabase and greywacke (Sibek, 1963; Sibek et al., 1964).

The rock bursts were first noticed in the district in 1880 when they were small in number and intensity. Since 1910 when the frequency and intensity of the rock bursts increased, accurate records of the rock bursts have been collected (Sibek, 1963; Sibek et al., 1964). In the period between 1910 and 1960 about 1,522 rock bursts were recorded. Of these, 291 were large bursts and caused heavy damage within the mine workings. The geology and the mining technique used were found to be the main factors affecting the occurrence of rock bursts. It was also noticed that the number of rock bursts increased after blasting. Mining in the region was carried out using the "cut and fill" method. In this method the veins were divided into pillars of 50 m x 50 m in size. The pillars were extracted from a lower level upwards, towards an upper level. After working each step the worked out space was filled immediately with debris. When the extraction reached two thirds of the height of the pillar, which was called "critical mining height", it became very dangerous since the remaining part of the pillar caused considerable potential energy to be accumulated in the rocks. During the mining of the remnant pillar, the limit of elasticity and strength of a part of the pillar was exceeded and violent rupture occurred which usually appeared as a rock burst.

Experiments were carried out in 1962 using the seismo-acoustic and deformation methods in an attempt to predict the rock bursts (Sibek, 1963; Sibek et al., 1964). The seismo-acoustic method was conducted by using underground geophones. It has been found that the number of impulses increased within one to five days before the occurrence of a rock burst. The deformation method was carried out by using Rheostat gauges to measure the convergence of the stope. Both vertical and horizontal convergences can be measured to an accuracy of 0.1 mm. It was noticed that a measurable amount of permanent deformation started when the limit of elasticity was exceeded and this corresponded to the occurrence of seismo-acoustic impulses. It has also been found that there was an increase in the average rate of convergence before the occurrence of the rock burst, reaching a maximum rate at the time of rock burst. After the rock burst there was a rapid decrease in the average deformation rate. Maximum convergence occurred near the position of the rock burst and vice versa. Finally, the authors concluded that the possibility exists to prevent the rock burst danger; firstly by adopting a suitable plan of mining; and secondly by predicting the occurrence of rock bursts using the seismo-acoustic method.

Holub (1966) studied the rock bursts recorded in the period from 1962 to 1965, for three mining regions in the neighbourhood of Pribram. These were the Bytiz and 9.Kveten mines, and the mines of the Brezove Hory district. Among the recorded rock bursts in the mines of the Brezove Hory, four intensive rock bursts occurred in 1962. They were also reported in the mines, where three of them caused some rock falls from the roof and the walls. The seismic energy released by the largest rock burst was 10^7 Joules.

The rock bursts in the Bytiz and the 9.Kveten mines started when the workings reached a depth of about 700 m. 36 rock bursts occurred in the Bytiz mine, while 7 occurred in the 9.Kveten mine. The energy released from these rock bursts ranged between 10^5 and 10^8 Joules.

Rock bursts in Czechoslovakia also occur in the coalfields. During the period between 1918 and 1972, 251 rock bursts were reported in the bituminous coal district of Ostrava-Karvina (Sebor, et al., 1976). The coal seams lie at a depth of about 1200 m. Recently the intensity of the rock bursts has increased, while their numbers have increased also to about 30 per year. Rock bursts also occur in the coal mining area of Kladno district (Sibek et al., 1964; Sebor et al., 1976). The thickness of the coal seams range from 6 to 8 m, and lie horizontally at a depth of about 500 m. The overlying strata consist of claystones, sandstones and conglomerates. The floor consists of clayey rocks. A seismic network consisting of four seismic stations about 1500m apart was installed over the mining area. About 15 weak shocks were recorded daily. Most of the tremor foci were located in the overlying sandstone. The largest tremor had an energy of about 10^6 Joules.

Prediction of the rock bursts in this district has been made. It has been noticed that during regular mine extraction there exists a linear relationship between the energy of the large rock burst and the time elapsing until the occurrence of the next event.

1.10 Mining induced seismicity in the Ruhr Coalfield, West Germany

In some mines of the Ruhr Coalfield in West Germany, the occurrence of rock bursts due to excessive stress concentrations in the vicinity of working areas was quite common. Between 1946 and 1976, 68 rock bursts occurred at different depths in the Ruhr coalfield (Leiteritz, 1978).

Cete (1977) indicated that magnetic tape recordings of the seismic activity have been obtained since 1956. The Ruhr district seismic network consists of three seismic stations. However, expansion and modernisation of the network is now being carried out due to extensions of the mining area. The new seismic network will consist of a large scale network as well as a small network.

In order to determine the zones of stress concentration in the coalfield mines, Baule and Rao (1979) monitored the seismo-acoustic activity in the coalfield using underground geophones installed in the roadways around the panels, in a number of mines. The co-ordinates of the sources were computed initially using a constant velocity model. Later the data for a group of events (approximately 10 events on a given day) whose sources were found to be clustered in the same area, were processed together with the velocity as an additional unknown. The value of the obtained velocity was also assumed to represent the velocity applicable to the other events occurring that day. The accuracy of the seismic locations was determined by locating blasts whose co-ordinates were known. It was found that most of the event sources lie within 40 m ahead of the working face, and that their distribution pattern indicates zones of stress concentration. Very few sources were located in the goaf.

Baule and Rao also carried out an experiment in one of the coal mines to determine the influence of de-stressing on seismo-acoustic activity in the seam. De-stressing operations were conducted from 17th November to 20th November, 1976 by drilling 25 m long holes from the base road into the seam. It was found that the events occurring during the de-stressing were encountered at the ends of the corresponding de-stressing holes in the seam. The maximum number of seismic events occurred on the 18th November, while no seismic event occurred on the 20th November, the last day of de-stressing. This indicated that the seam was apparently relieved of the excessive stress.

1.11 The characteristic features of mining earth tremors

1.11.1: From the above summary of mining induced seismicity in different parts of the world, some general points concerning the characteristic features of mining earth tremors, and the application of micro-seismic techniques to this problem can be inferred.

The characteristic features of mining earth tremors are summarized in the following points, and an attempt is made to compare them with natural seismic events.

1. The most important feature of mining tremors is the abrupt fall-off of their intensity from the epicentre to the boundary of the disturbed area. This indicates that their foci are shallow. This feature was observed and noted by Davison (1924) in British mines, by Weiss (1938) in Witwatersrand gold mines, and by Wierzchowska (1962) in the Upper Silesian coalfield.

Davison (1924) noted that the disturbed areas due to mining tremors were mostly circular or slightly elongated. The long axis of elongated disturbances was mostly parallel or nearly parallel to dykes or faults in their immediate neighbourhood.

In the literature there is little information about the intensity of mining earth tremors at the epicentre. However, as will be seen in Chapter 7, one mining earth tremor has occurred in the North Staffordshire coalfield with maximum intensity 6 on the Modified Mercalli Scale, and local magnitude M_L, of about 3.

2. As described in this chapter, most mining earth tremors have local magnitudes, M_L, ranging between -0.5 and + 3.5. However, the largest mining induced earth tremor reported by Buckle (1965) in a Canadian gold mine reached a magnitude estimated to be between 4.5 and 5. Thus mining earth tremors can be very large and reach a size comparable with natural earthquakes.

3. In the case of most mining tremors, the intensity is greater in the mine than on the surface. The greatest intensities are usually observed in the immediate vicinity of rock bursts. In contrast, Davison (1924) suggested that the intensity of a natural earthquake is usually much weaker in the mine than on the surface. However, Bath (1973) has suggested that

whether or not the intensity is weaker in the mine than on the surface has not been established reliably.

4. Davison (1924) indicated that the shock of mining tremors consists of one or two pulses of vibrations followed, sometimes, by a brief thud such as that produced from the fall of a heavy body onto the floor. He suggested that the average duration of the shock was about two seconds, while for a natural earthquake it ranged from three to six seconds.

5. The existence of a prominent S-phase for mining tremors in the Witwatersrand gold mines, led Gane et al. (1946) and Logie (1951) to conclude that the original release of energy at the focus bears a closer resemblance to that of a natural earthquake than to that of an explosion. The latter gives rise mainly to compressional waves and a very small proportion of shear waves.

6. It has been found that the frequency-magnitude distribution of mining earth tremors follows the frequency-magnitude formula given by Richter (1958) which also applies for natural earthquakes (see sections 1.5, 3.4.1 and Chapter 7).

1.11.2: Both macro-seismic and micro-seismic techniques have been used to investigate mining induced seismicity. Many different investigative methods and strategies have been used in the many different case histories described in this chapter. From the collective experience of the investigations described, the following general points concerning the use of microseismic methods in the study of mining induced seismicity can be listed.

1. Tremors generated by rock bursts, bumps, etc. can be recorded at considerable epicentral distances using conventional natural earthquake observation instruments.

2. Since the occurrence of a tremor is unpredictable, it is necessary to record the output signal of the seismometer networks continuously.

3. For the accurate location of seismic events, a seismic network of small aperature must be deployed within the mining area.

4. The local seismic network should be deployed so that the seismic events are well located in both epicentral position and depth, i.e. there must be a wide variation in range and azimuth of the seismic stations from the epicentres.

5. For more accurate depth determinations of hypocentres, a three dimensional seismic network is preferable.

6. For hypocentral location of the seismic events, the travel time from the source to at least four seismometers should be used in the calculation.

7. For accurate location, the output from all seismometers should be recorded with a common time code, on common graphic paper or magnetic tape.

8. The accuracy of the seismic location is limited by the accuracy with which the velocity structure of the area is known.

9. For more accurate locations an anisotropic velocity model is required.

10. The accuracy of the seismic location is limited by the precision with which the arrival times of the seismic waves at the seismometers can be determined.

11. Because of the short distances between the tremor foci and the local network seismometers, accurate timing to at least 0.01 second is required.

CHAPTER 2

MINING INDUCED STRESS, STRAIN AND ENERGY RELEASE BY MAKING AN UNDERGROUND EXCAVATION

2.1 Introduction

Without understanding the distribution of mining induced stress and strain and their role in mining induced seismicity, it is difficult to find the causes of mining earth tremors and to interpret their actual mechanisms. The intention of this chapter is to give some general knowledge about mining engineers.

If the ground is not subjected to any kind of tectonic movements (folding, faulting, etc.) before an underground opening is made, the rock mass is in equilibrium in its virgin state. The ground at any point at depth is subjected to a pressure equal to the weight of the superincumbent strata.

When an underground opening is made, the ground on the sides, and above and below the opening is deprived of its natural supports. Consequently the rock mass around the opening is no longer constrained. Therefore the equilibrium is destroyed and the rock masses around the opening tend to deform towards the opening. This situation leads to the redistribution of strata pressure around the opening. The mode of mining plays an important role in this new distribution of strata pressure, and consequently on strata control.

2.2 Theories of rock pressure and strata movement

The theories of rock pressure and strata movement are closely related. The former deals with the phenomena of underground stresses, while the latter attempts to explain the consequent movement and the ultimate settlement of the strata. The movement is the physical manifestation of the

stresses developed within the strata as a result of mining operations. Rock movements include deformation of the rocks in the vicinity of an excavation, rock bursts, rock falls and surface subsidence.

Various theories based mainly on underground observations of strata behaviour surrounding the excavation have been put forward in order to explain the distribution of mining induced stresses, and consequently to try to interpret the phenomenon of rock bursts.

In general these theories can be grouped into two main categories:

1. The Pressure dome theory

Observations of the cavities and tunnels in the rocks, which often remain stable without artificial supports, have led to the dome concept (Denkhaus, 1964). The principle of this theory is that the pressure is arched over the excavation and bridges between two abutments.

Crowle (1931) and Dinsdale (1937) advocated the pressure dome theory to explain the rock burst phenomenon in mines. They suggested that when an underground excavation is made, the natural support for the layers above, below, and at the sides of the opening is removed. The layers are therefore fractured and deform towards the excavation, thus removing the support from the next layer and so on. As these fractures proceed outwards from an excavation, a dome-like area of fractured rocks is developed. The fractured rock inside the dome is decompressed (intradosal ground), but a high stressed zone is created around the dome in the solid rocks (extradosal ground). Ultimately this high pressure exceeds the elastic limit of the rocks in the extradosal ground causing them to fail. As the excavation goes on, pressures are concentrated on the ribsides and on isolated pillars or remnants causing the formation of many small pressure domes. Failures of these pillars result in two or more small pressure domes meeting to form a very large dome, thus causing further stress concentration on the abutments. For the footwall, the dome is smaller than for hanging wall, and this might be due to the

gravity effect which assists the breaking of the rocks in the hanging wall. The extent and pressure effect of the dome increases as the depth and the excavation increase.

Dinsdale (1937) considered the length of the roadway and modified the idea of a dome by using an arch.

2. The cantilever theory

Stratification of the rocks has led to the concept of treating the strata as a series of beams or plates overlying each other. The principle of this theory is that the immediate roof stratum detaches itself from the overlying strata and acts as a beam or cantilever over the goaf (Denkhaus, 1964).

Sinclair (1936) and Joseph (1938) advocated this theory to explain the pheonomenon of rock bursts in Witwatersrand gold mines. As the excavation is made in almost horizontally layered deposits, the strata of the unsupported roof will sag under the effects of their own weight and the superincumbent pressure. The sagging layers act as beams or cantilevers. The deflection of each beam depends upon its thickness and its elastic deformation modulus. The process of sagging proceeds upward decreasing in each succeeding layer, until finally a short beam is reached. This beam represents the apex of what appears as an arch or dome if the points in a vertical plane at which the sagging ceases at both ends of the beam (abutments) are joined. As a result of sagging of a layer, the next layer above it transmits its own weight and the weight of the above layers which it supports to the nearest point of contact between it and the lower stratum. Therefore, each sagging layer creates a compressive stress on the layer below it at the points of support (abutments). Consequently, if a large number of layers act as a beam, high compressive stress will be concentrated on the abutments. If the concentrated stress exceeds the strength of the supports, failure will occur.

The sagging increases as the depth and the excavated area are increased. As the excavation increases the hanging layers (beams) begin to fracture producing small rock bursts. The fractured layers may then act as cantilevers supported at one end on the face, while the other end is free.

In the case of an inclined excavation, another force exists. This force is the tangential pressure of the roof which is augmented in stratified deposits by the natural tendency for the rock mass to drag down or sag on the line of dip. This will lead to the development of a greater pressure on the support on the down dip side, causing more shearing and greater tendency to burst (Sinclair, 1936).

From above, it can be inferred that the two theories do not contradict each other. Rather, they represent two versions of one universal theory. Both theories suggest that roof sagging is the main cause of the rock bursts. Both recommend the setting up of adequate supports in the excavated area as soon as the excavation is made in order to prevent or reduce roof sagging and consequently reducing rock burst incidence.

2.3 Mining induced stress in the case of longwall , and rooms and pillars extraction

From the point of view of strata control, mining methods can be carried out in two general ways (Whittaker, 1974):

1. Partial extraction without caving of the roof (rooms and pillars). In this method the strata pressure is redistributed in such a way that it is taken by the remaining pillars.

2. Longwall extraction. In this case the roof strata behind the face are allowed to cave in, causing the strata pressure to be shifted to the waste region and abutments.

2.3.1 Stress distribution in the case of pillars

During mining, pillars are usually left for various reasons such as preventing or reducing surface subsidence or preventing water infiltration. In general the pillar needs to be of sufficient size to remain stable.

The pillar supports the strata immediately above it as well as some of the strata which cantilever over into the surrounding openings. Thus in a typical room and pillar layout, assuming that the overburden pressure is uniformly distributed over the pillars, Hoek and Brown (1980) show that the average stress imposed on a pillar is given by the following formulae:

$$\sigma p = \rho g H \left(1 + \frac{Wo}{Wp}\right) \left(1 + \frac{Lo}{Lp}\right) \quad \text{... Rectangular pillar} \qquad 2.3.1a$$

$$\sigma p = \rho g H \left(1 + \frac{Wo}{Wp}\right) \quad \text{... Long pillar} \qquad 2.3.1b$$

where σp is the average vertical pillar stress,

Wo is the width of the opening,

Lo is the length of the opening,

Wp is the width of the pillar,

Lp is the length of the pillar,

ρ is the average density of the rocks = 2537 Kg/m^3,

g is the gravitational acceleration ≃ 9.81 m/sec^2,

H is the depth below the surface.

Hoek and Brown also calculated the average pillar stresses for other kinds of pillars.

The stress distribution within the pillar is not uniform. Hoek and Brown also calculated the values and distribution of the major and minor principal stresses around a pillar. They presented a number of diagrams showing the distribution and magnitudes of the principal stresses,

normalized to the average vertical pillar stress, in a rib pillar having different ratios of pillar height to pillar width (Fig. 2.3.1).

Fig. 2.3.2 shows the distribution of the overburden pressure within the pillar. The figure shows that at the sides of the excavation a de-stressed zone occurs since the coal is fractured in this area and suffers little lateral constraint. Inside of the pillar edge, into the solid rock, the stress increases gradually and the pressure peak (abutment pressure) occurs at about 1-10 m from the side of the pillar. This abutment pressure represents the failure strength of the coal under the prevailing conditions. The broken coal in the area between this pressure peak and the side of the roadway is called the "Yield Zone" (Wilson and Ashwin, 1972). The coal in the region inside the pillar is relatively undisturbed, and still follows the laws of elasticity since it has not passed the yield point. It is surrounded on all sides by the "yield zone" which tends to constrain it. This central region is called the "pillar core" and it has an average stress lower than the peak abutment pressure. In the case of a large pillar, the average stress in the pillar core drops to the value of the overburden pressure. In the case of a small pillar, the core stress may rise to the value of the abutment peak stress. If the pillar core stress exceeds the abutment pressure a breakdown in the cohesion of the pillar core occurs since it is beyond the elastic limit. However, the broken pillar can still withstand high stress as a result of the lateral constraint offered by the fractured rocks in the ribs of the pillar to the broken rocks inside the pillar. Wilson and Ashwin suggested that the strength of the pillar core is increase because of the confining constraint afforded by the yield zone. The increase in pillar core strength is proportional to the confining stresses according to the equation:

$$\sigma = \sigma_0 + \sigma_3 \tan\beta \qquad 2.3.2$$

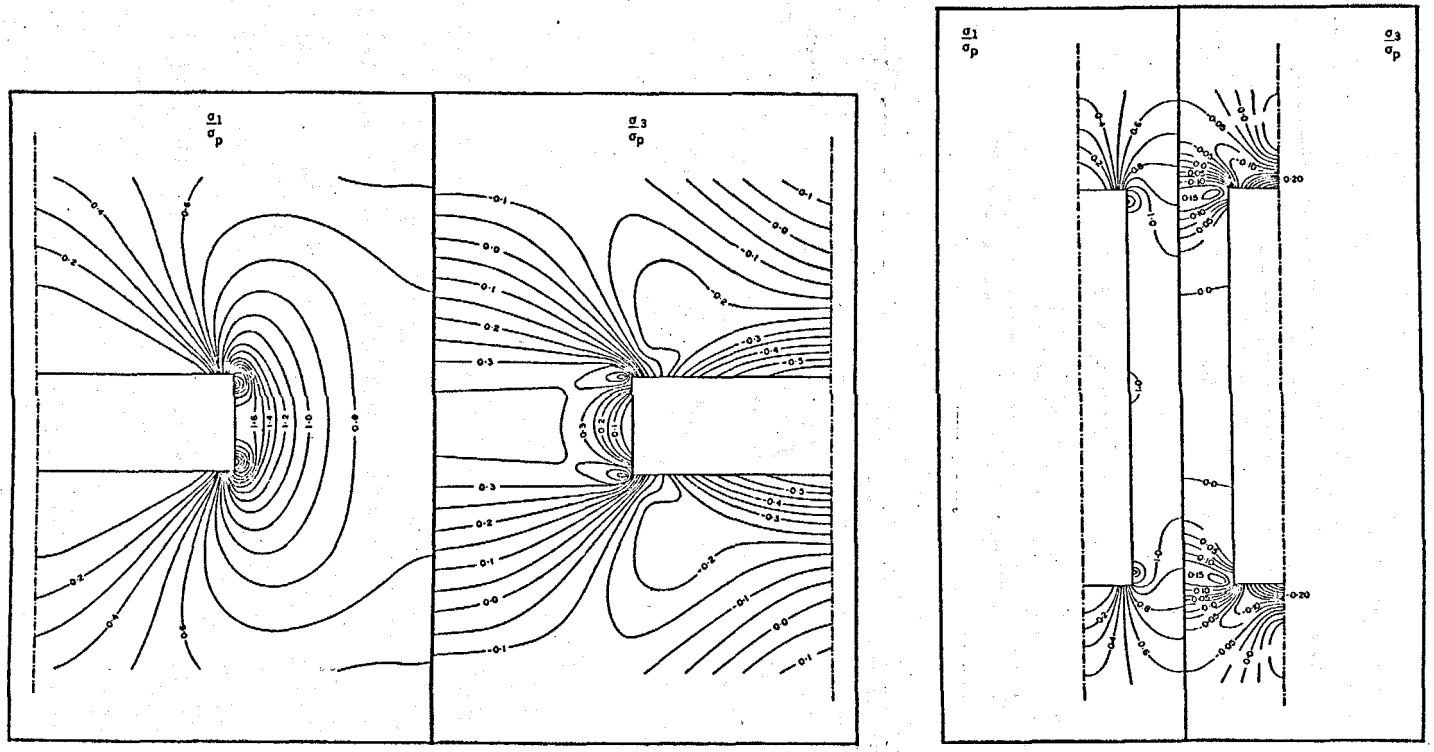

(a) (b)

Fig. 2.3.1. Principal stress distributions in a rib pillar defined by a ratio of pillar height to pillar width of (a) 0.25 and (b) 4.0 respectively. The contour values are given by the ratio of major and minor principal stresses to the average vertical pillar stress. (After Hoek and Brown, 1980).

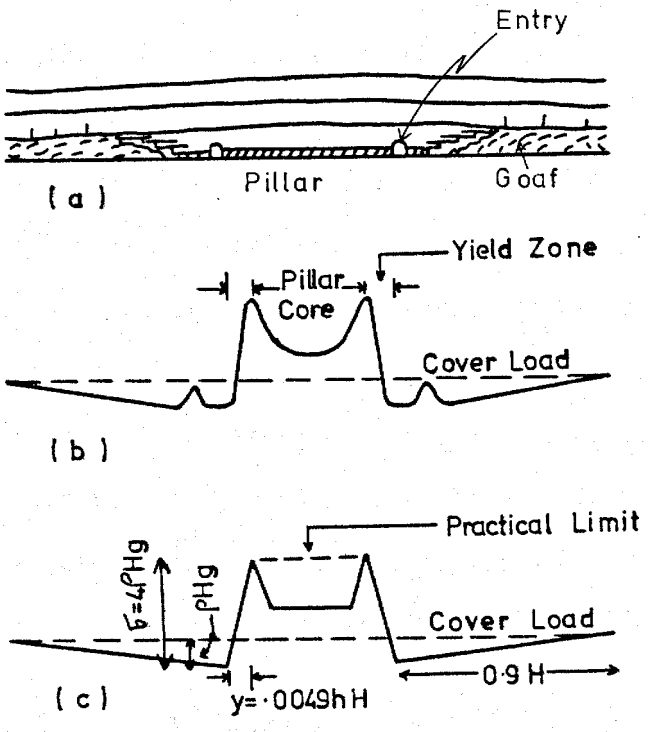

Fig. 2.3.2. Stress distribution across pillars and adjacent goafs.

(a) Section across pillar.

(b) Probable stress distribution.

(c) Hypothetical stress distribution.

(After Wilson and Ashwin, 1972).

where σ = the stress needed to cause failure, or flowage if the rock is already fractured (i.e. the strength of rocks in confining conditions).

σ_0 = the unconfined compressive strength, or the inherent strength. If the rock is broken $\sigma_0 = 0$.

σ_3 = the confining stress.

β = the average slope angle of the curves of σ versus σ_3. For British Coal Measures $\tan\beta = 4$.

This suggests that at depth the stress required to cause failure or flowage in the coal measure is about four times the confining pressure, regardless of their unconfined strength or state of fracture. Wilson and Ashwin further suggest that in the case of a lithostatic virgin state of stress, i.e., both vertical and horizontal stresses are equal, the maximum yield strength (i.e. the maximum vertical abutment pressure) is given by:

$$\sigma_{max} = \sigma_0 + 4\,\rho gH$$

or

$$\sigma_{max} = 4\,\rho gH \quad \text{in case of fractured rocks.} \qquad 2.3.3$$

where ρ = the average density of the rock,

H = the depth below the surface,

g = the gravitational acceleration.

Observations have shown that the value of the peak abutment pressure ranges between 3 and 5 times the superincumbent pressure.

The authors showed that the distance of the peak abutment pressure (Y), Figure 2.3.2, from the rib side can be expressed by the formula:

$$Y = 0.0049\,hH(m) \qquad 2.3.4$$

where h is the excavation height in metres, and

H is the depth below the surface in metres.

This indicates that if the pillar width is less than 2Y, the pillar has no centre core. In this case the pillar is unstable. Wilson and Ashwin were able to infer the required width of the pillar by equating the strength and the average pressure subjected to different types of pillars. Whittaker (1974) indicated that underground observations showed that pillar strength depends on the pillar materials and the size and shape of the pillar. The pillar fails if the overlying pressure (P) exceeds the pillar strength. The ratio of the pillar strength to the pillar loading pressure gives the safety factor (S):

$$S = \frac{\text{strength of the pillar}}{\text{pillar loading pressure}}$$

Observations of a number of stable and collapsed pillars showed that most of the stable pillars have a safety factor of more than 1.3 (Whittaker, 1974). During the determination of the safety factor, local mining conditions should be taken into consideration. Creep and natural weathering can weaken the pillar strength. Undermining a seam containing pillars can also promote or accelerate pillar collapse.

2.3.2 Stress distribution in the case of longwall face

The longwall mining method is used extensively in the working of stratified deposits, particularly in the European coalfields. This method can be applied in a variety of geological conditions and at great depth. It has been found that this method is very reliable in places where the roof and floor of the coal seam are not strong.

The longwall face usually ranges between 50-300 m in width, while the length of the panel ranges from 300 m to more than 1,000 m. Generally, in this method, the extracted region behind the face is allowed to cave in.

Mining using the longwall method results in a redistribution of the strata pressure in such a way that low-stressed and high-stressed zones are created, as shown in Figure 2.3.3 (Whittaker, 1974). High pressure zones are developed in the solid rocks surrounding the excavation, while a

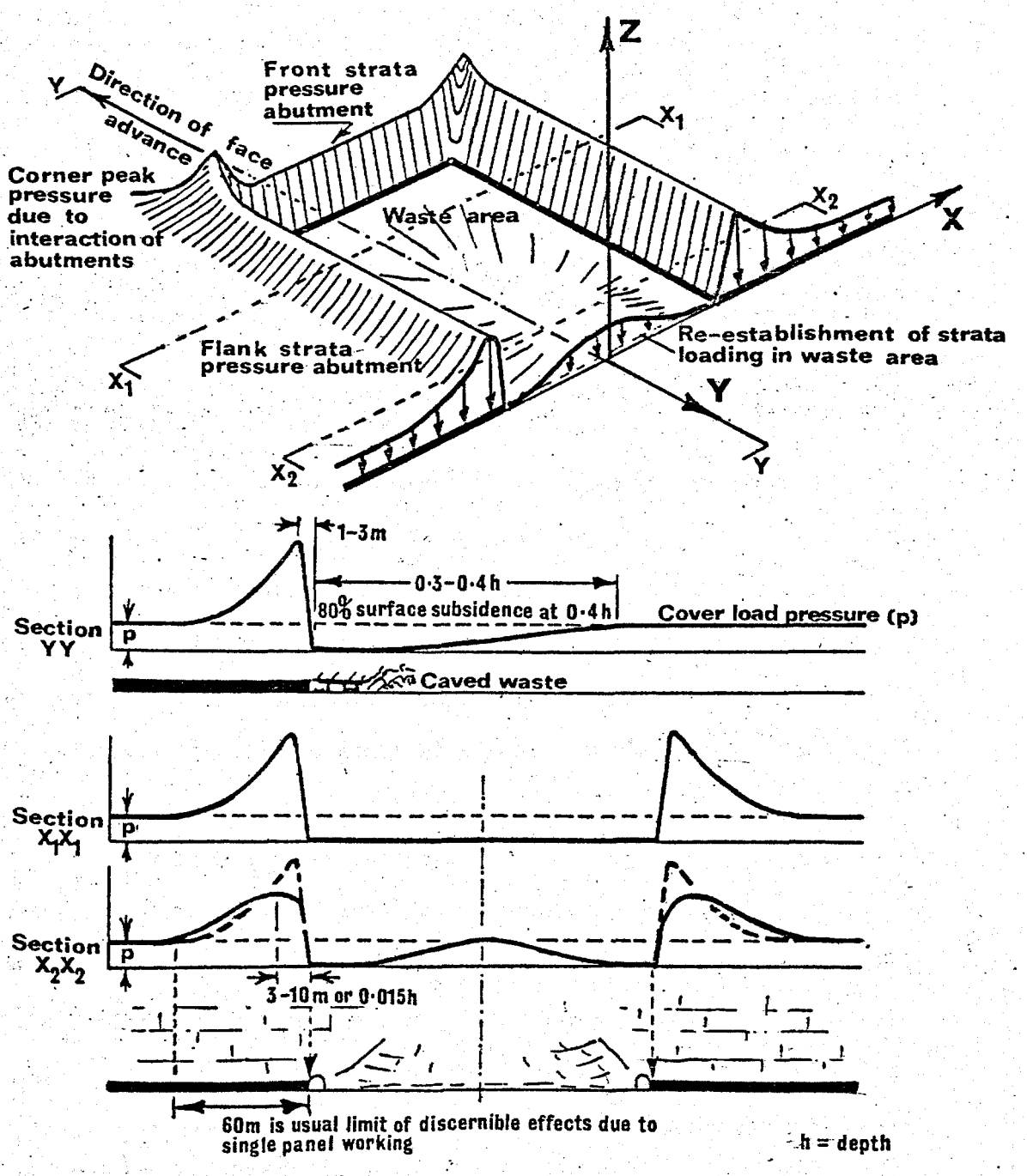

Fig. 2.3.3. Stress distribution around a longwall face. (After Whittaker, 1974).

de-stressed zone is created behind the face as a result of the extracted coal and breaking of roof strata.

Wilson and Ashwin (1972) showed that the vertical stress applied to the waste is directly proportional to the distance from the face. The load, after reaching a minimum immediately behind the face, increases slowly and continues to increase, as the overlying strata collapse and compact, until it reaches the value of the overburden pressure, after which it remains constant, i.e. there is no rear abutment pressure. The point in the goaf at which the vertical stress reaches the overburden stress is equal to 0.3 times the depth. Before this distance is reached, the load which is not taken by the waste is thrown onto the face. Some authors (Spruth, 1951; Alder et al., 1951) have indicated that another abutment pressure exists behind the face in the goaf. This is called the rear abutment pressure. However, Shepherd (1973) pointed out that "It has now been shown conclusively that the concept of a rear or back abutment is untrue and this also is the view of workers abroad".

The front abutment pressure (ahead of the face advance) exerts its peak pressure 1-10 m ahead of the longwall face. However, Peng (1978) indicated that this abutment pressure is first felt at distances as far as 150 m ahead of the face. This pressure abutment plays an important role in inducing coal bursting. The strength of the coal and the surrounding rocks plays an important role in determining the magnitude and position of the peak pressure. Spruth (1951) and Shepherd (1973) pointed out that in the case of sandstone roofs the abutment pressure occurs at a greater distance ahead of the face, compared to that in the case of mudstone roofs. This is because sandstone is a relatively rigid rock and yields little before breaking, causing a more uniform distribution of pressure, whereas mudstone is flexible and yields greatly before it fractures. Figure 2.3.4 shows a diagramatic comparison between the relative position of the peak

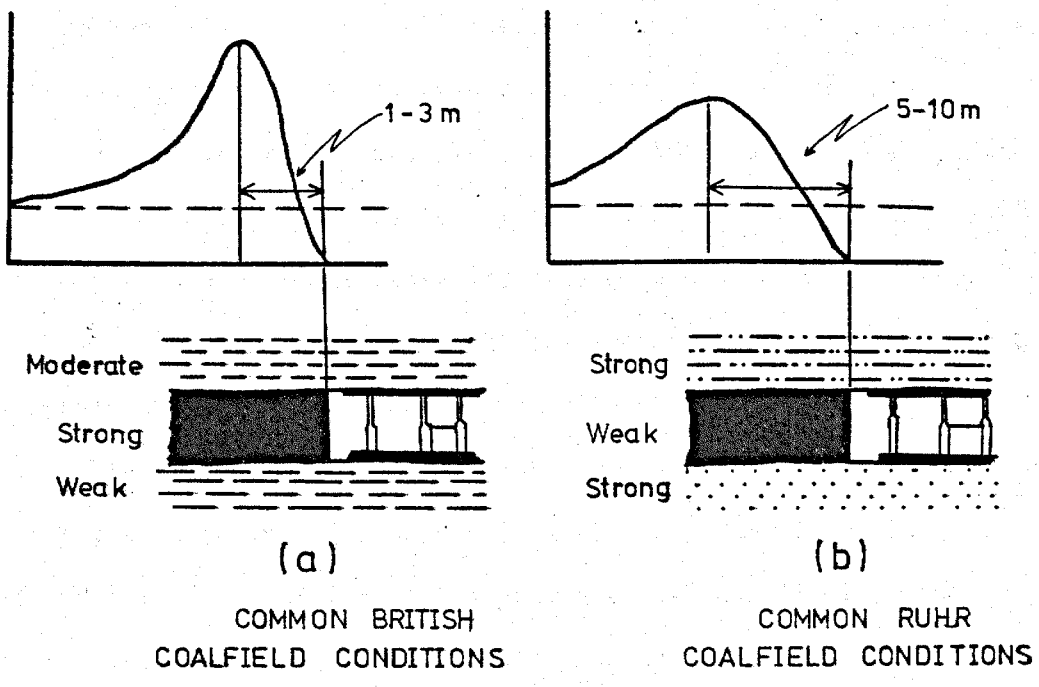

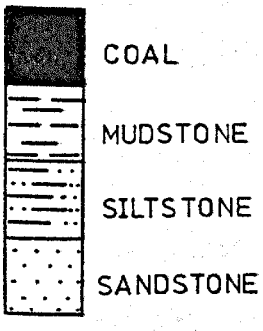

Fig. 2.3.4. Diagrammatic comparison between the general position of the front peak abutment pressure for British and Ruhr (West Germany) coal measures rocks (after Whittaker and Pye, 1975).

of the front abutment pressure for two different geological conditions, representing British and West German (Ruhr coalfield) coal measures (Whittaker and Pye, 1975). Ruhr coal measures are generally composed of a strong silty-sandstone roof, a relatively weak and friable coal seam which is underlain by a strong sandstone. This combination results in a reduction in the pressure intensity near the face line. It was found that the peak of the strata pressure abutment generally lies at a distance of between 5 m and 10 m ahead of the face. British coal measures, on the other hand, generally consist of a mudstone roof of moderate strength, a relatively stronger coal, and a much weaker seat earth forming the floor. This situation causes a concentration of pressure intensity near the face line. It has been found that the position of the pressure peak usually lies about 1-3 m ahead of the face. The value of this peak pressure is usually equal to about 4 to 5 times the overburden pressure.

Along the two sides of the panel, abutment pressure is also developed; this is called the flank abutment pressure (section X_1 X_1, Figure 2.3.3). As the face advances further, and with the elapse of time, the entry ribs in the goaf area yield. This may cause a reduction in the flank pressure abutment, and the transfer of the peak pressure further into the solid (section X_2 X_2, Figure 2.3.3).

For British coal mining conditions, the value of the peak pressure in the longwall rib sides has been estimated to be about four times the overburden pressure, while the distance of this peak from the rib side is equal to about 0.015 times the depth.

The front and flank abutment pressures are superimposed at the corner of the advancing face due to their interaction, and together form the corner peak pressure (Figure 2.3.3).

2.4 Strata deformation around a longwall face

Farmer and Altounyan (1980) have measured the deformation ahead, above and to the sides of a longwall face in a number of mine workings. A typical example is shown in Figure 2.4.1. The deformation is presented in terms of vertical strain contours. It is shown that compressive strains occur ahead of the face within the front abutment, and that they decrease as the distance from the face increases. The large tensile strains above the worked area indicate fracturing of the caved rock. Laboratory tests suggest that in the relatively unconfined conditions existing above the worked area a tensile strain greater than 0.25% is indicative of rock fracture.

2.5 The effects of interaction from multiple workings

In British coalfields, mining in virgin areas is becoming increasingly uncommon (King, et al., 1972). Many coal faces encounter interaction at least once during their working life.

Interaction is a term used to describe the pressure effects produced by one underground working upon another. An equally important aspect is the effect of mass displacement of strata on an underground opening (King et al., 1972). Holland (1958) indicated that "stress concentration in an overlying or an underlying seam may be reflected in a bed being mined ..... Whether or not the stress concentrations will have a serious effect depends on the distance between beds as well as the cover on the beds, and to a lesser extent, perhaps, on composition of the rocks between the beds concerned". King et al.,(1972) suggested that the sources of interaction are:

1. Stress field changes due to old or current workings.
2. Triggered interaction due to the changes produced by current workings upon old workings.
3. Active strata displacement in other workings due to current workings.

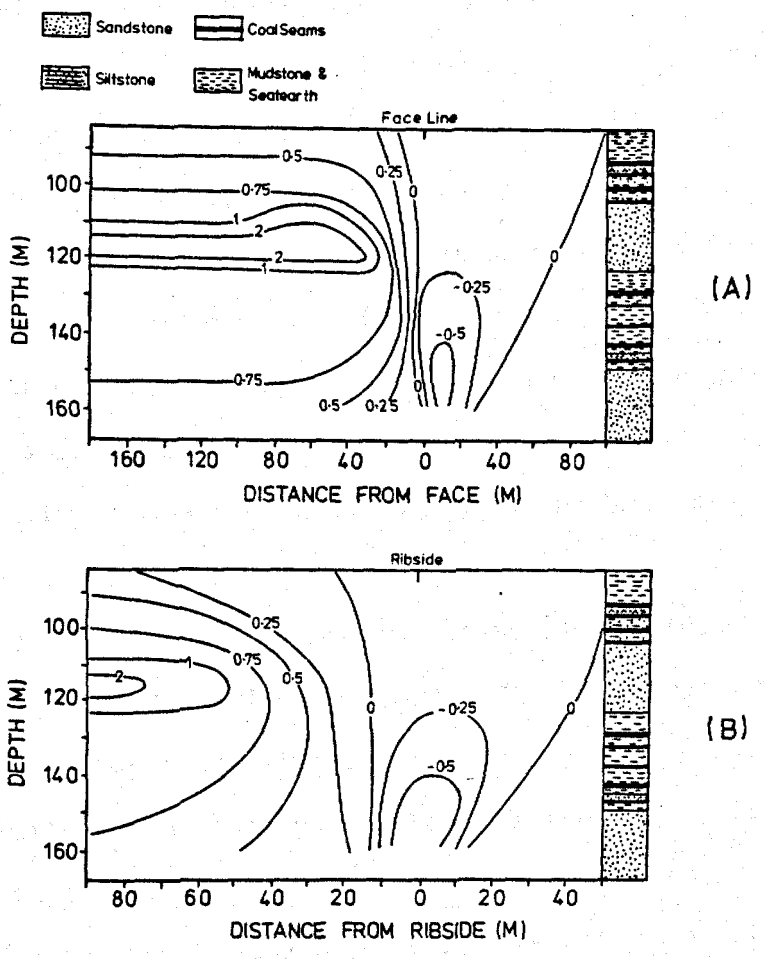

Fig. 2.4.1. Vertical strain contours above a longwall face.

(A) Vertical section along the panel.

(B) Along the face.

Contour units are % strain - tensile positive.
(After Farmer and Altounyan, 1980).

Interaction from other workings often have a marked effect on the stability of existing roadways and coal faces. It can affect underground workings in such a way that:

(a) Closure in the working areas, particularly in the roadways would increase as a result of abnormally high strata pressures. Strata control in these areas consequently becomes very difficult.

(b) The natural strength of the strata declines as a result of this high pressure. Remnant pillars in a previously worked seam result in the strata immediately above and below the pillar being subjected to a high compressive stress, while the regions to the side are under lateral tension due to rock fracture. This situation results in vertical fractures in the strata immediately above and below the pillar (Whittaker, 1974). These fractures have a tendency to run in a direction parallel to the longer axis of the pillar. Therefore, during the extraction of the next seam, locating roadways in these high pressure zones must be avoided since this tends to cause high convergence.

(c) Interaction arises when an active subsidence trough of a lower working face affects a higher working face. This mostly occurs when several seams are simultaneously mined.

During the extraction of the non-initial seam, it has been found that the best method is to locate its face over or under the old goaf. Location of the active face in this de-stressed region will result in good strata control on both the face and the gates. Figure 2.5.1 shows some examples of composite longwall working layouts as suggested by Whittaker and Pye (1975).

2.6 The effect of stress on rock fracture

Many authors discuss the problem of mining induced stresses assuming that the rocks behave elastically.

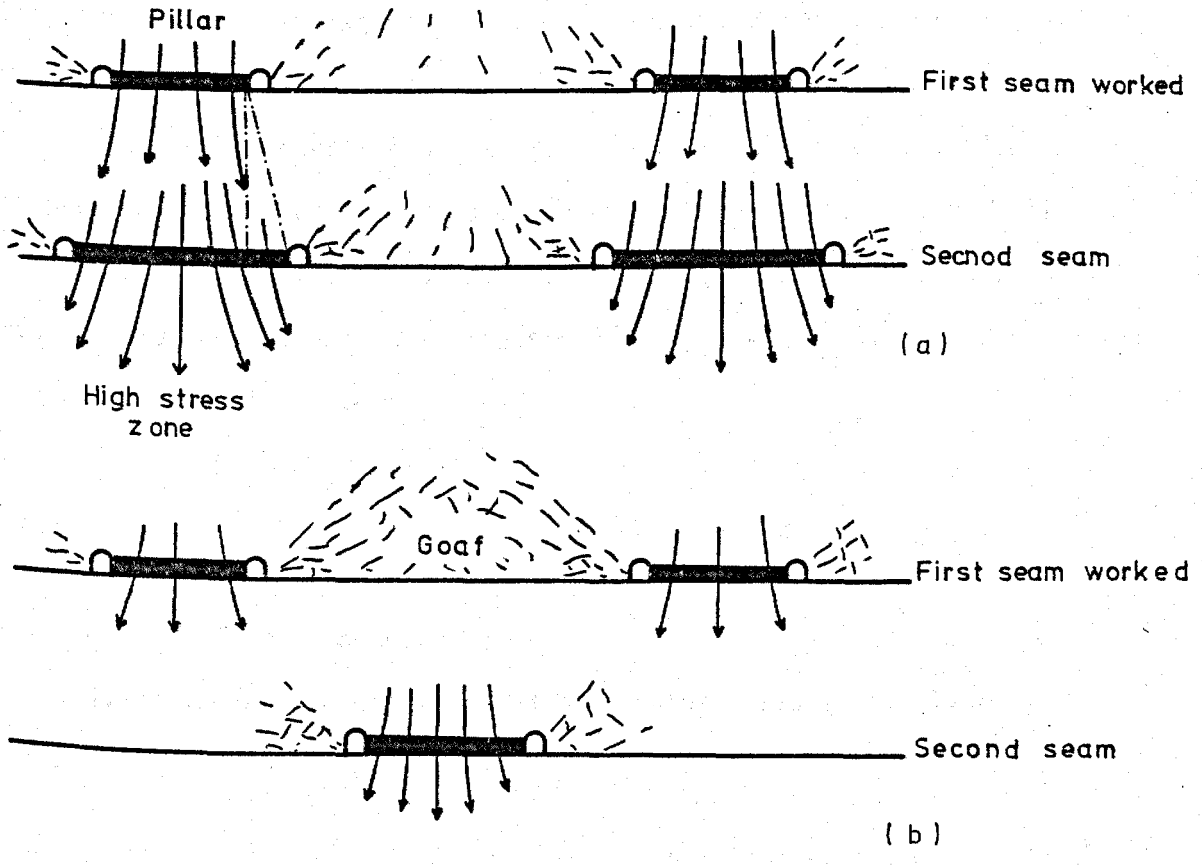

Fig. 2.5.1. Composite layout of longwall workings showing the best position of the current mine workings (2nd seam) with respect to old mine workings in an adjacent seam.

(a) Working in descending order, pillars increasing with depth.

(b) Working below existing pillar, gates sited in the low-stressed zone.

(After Whittaker and Pye, 1975).

If the strata are horizontal before mining at depth, the strata overlying a coal seam are subjected to a vertical pressure equal to the weight of a column of overlying material (Hudspeth and Phillips, 1932-33; Shepherd, 1973). In Figure 2.6.1, zone A shows a cube of material in a virgin area subjected to a vertical force P_1 which compresses and expands the cube, parallel and at right angles to the force action respectively. The cube remains in an equilibrium constraint condition under the effects of the two lateral forces P_2 and P_3. These two forces act parallel and perpendicular to the coal face respectively. Under these conditions (virgin state):

$$P_2 = P_3 = \frac{P_1}{m-1}$$

where m = Poisson's number.

The difference between vertical and horizontal stresses is given by

$$P_1 - \frac{P_1}{m-1}$$

During mining the lateral constraining pressure ahead of the face changes as the face advances. The lateral forces P_2 and P_3 are gradually reduced. P_3 ultimately becomes zero as shown in zone B, and it may even become tensional (zone C) due to roof bending. Consequently, the coal deforms towards the excavation. In this case

$$P_2 = \frac{P_1}{m}$$

and the stress difference increases to

$$P_1 - \frac{P_1}{m}$$

The reduction in the lateral stresses results in an increase in the vertical strain with a consequent increase in coal deformation towards the excavation.

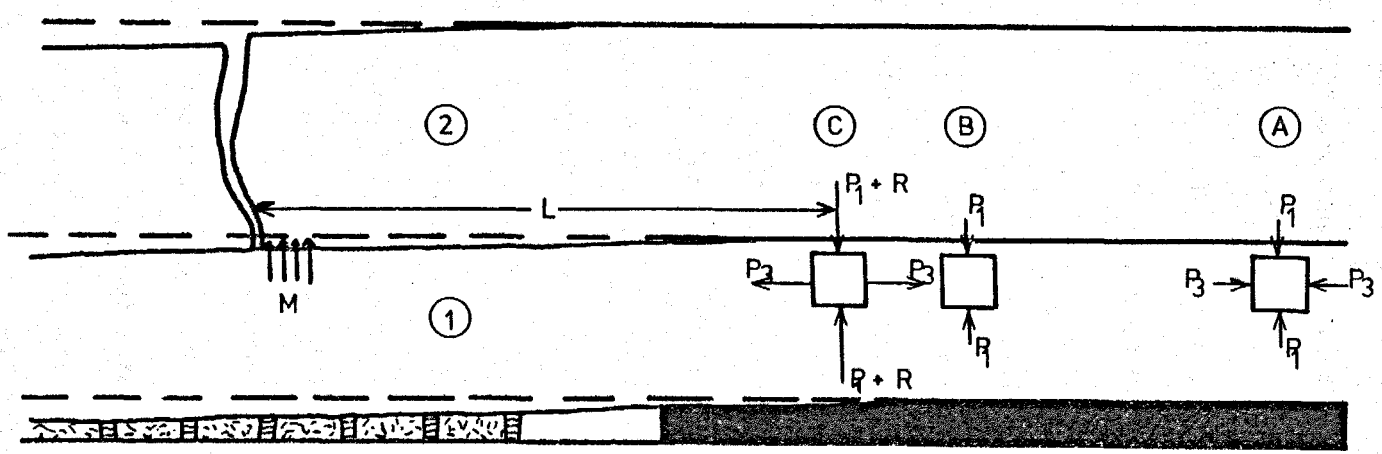

Fig. 2.6.1. Vertical section through coal face and goaf, illustrating the action of strata pressure in three different places (A, B and C) in front of the coal face. (After Hudspeth and Phillips, 1932-33).

The deformation produced as a result of the reduction of P_3 with the consequent increase in stress difference (shear stress), may influence the development of induced shear failures in the rocks ahead of the face. Assuming that the value of $P_3 = 0$, as in Zone B, the maximum stress difference will be equal to P_1. The value of P_1 is about 22 kN/m^2 per metre of depth. This value is insufficient to cause fractures in coal measure rocks, and so indicates that other forces must account for most of the fractures in the coal measure rocks. As we have seen from the previous sections, during mining a very high abutment pressure is developed in the rocks ahead of the face. This abutment pressure is represented by (R) in Zone C. In this zone the total vertical stresses are represented by $P_1 + R$. Therefore, the increases of the vertical pressure from P_1 to $P_1 + R$, with or without reduction in P_3, may result in a stress difference (shear stress) sufficient to cause shear fracturesin the rocks ahead of the face. The shear fractures take place along two intersecting planes, hading in opposite directions. Shepherd (1973) indicated that once the coal is extracted, the backward hading fracture must be controlled, because the rock blocks formed by these fractures may cause convergence, roof falls and cavities.

Hudspeth and Phillips (1932-33) showed that the magnitude of induced stress (R) (in Figure 2.6.1) depends on the amount of roof sagging and on the span (L) to the nearest adjacent effective support (M), such as a pillar, packing or powered support. The shorter the distance to the adjacent supports the less the roof sags, and consequently the smaller the value of (R). This is because if the roof strata are strong, such as bed (2) in the figure, they can act as beams or cantilevers (see Section 2.2). Therefore, the presence of supports such as (M) will result in a reduction of (R). Hudspeth and Phillips suggested that due to the inevitable existence of a certain span of unsupported strata, it is impossible to reduce the induced stress (R) to zero.

2.7 The application of elastic theory to analyse the movements in the rock mass around an ideal longwall stope

The elastic theory assumes that a large mass of perfectly elastic and homogenous material contains a void in the form of a slit of negligible thickness and indefinite extent. A lithostatic virgin stress state is also assumed (Ryder and Officer, 1964).

A model based on the theory of elasticity has been developed by Cook (1962) to illustrate the behaviour of the rock mass in the vicinity of a deep level tabular excavation (stope). This model was applicable to the Witwatersrand gold mines where quartzite surrounds the stope (see Section 1.2).

A stope of 610 m span and 0.9 m high at a depth of 2,440 m below the surface was investigated seismically. The failure of the quartzite was found to be consistent with the Coulomb failure criterion. This is defined by:

$$q_c = s + fp$$

where q_c = the maximum shear stress on the failure plane.

s = the shear cohesion.

f = coefficient of internal friction.

p = normal stress on the failure plane.

He used elastic theory to calculate the magnitudes and directions of the principal stresses around the stope in which the seismic investigation was made. He assumed in the calculation that the quartzite around the stope was strong and behaved elastically. The stress field solution is presented in Figure 2.7.1.

Cook applied the failure criterion for quartzite to those theoretical stresses, and found that the quartzite fails in a small region around the stope. If q is the shear stress on any plane and q_c is the maximum shear stress defined by the failure criterion for the same plane, wherever

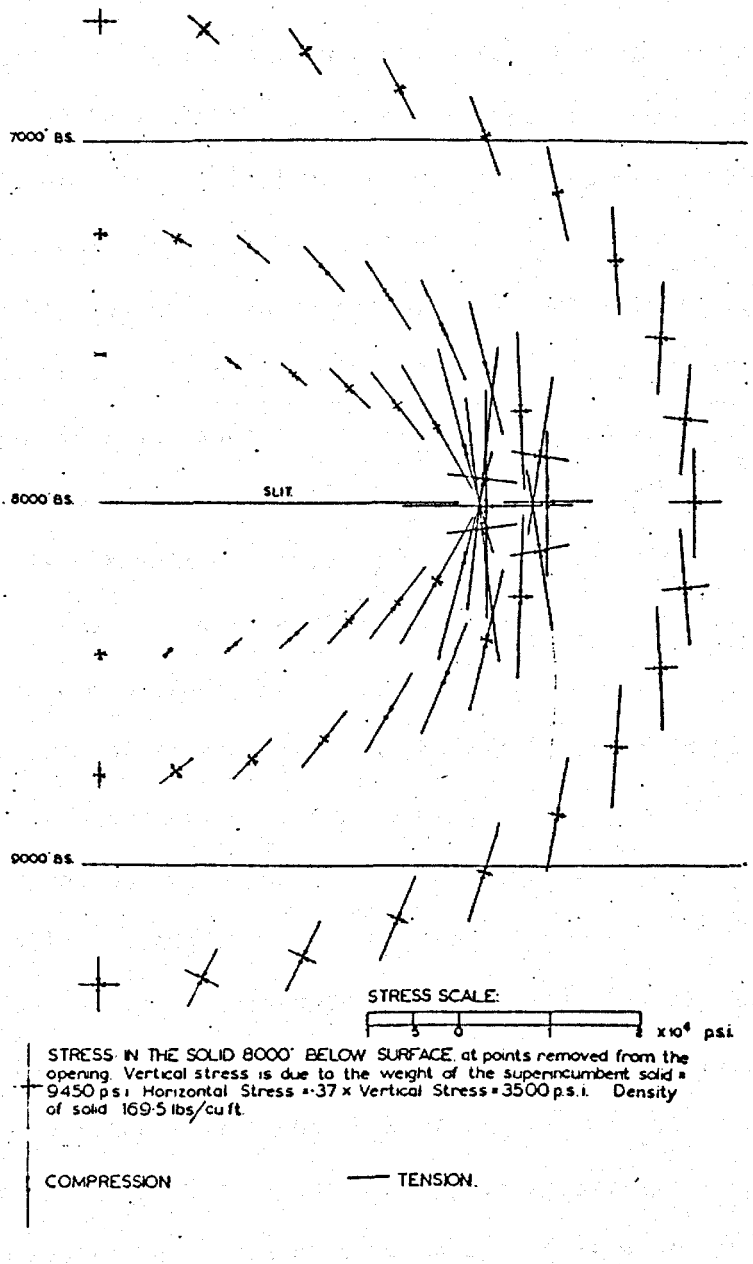

Fig. 2.7.1. The magnitudes and directions of the principal stresses along one half of a horizontal slit in an elastic body subject to gravity. (After Cook, 1962).

$(q/q_c)_{max.}$ exceeds unity, failure must occur. The seismic investigation showed that most of the failures occur in the region predicted by the model.

Ryder and Officer (1964) used a model based on the theory of elasticity, calculated theoretically the movements induced in the solids as a result of mining in a dipping stope. The theoretical calculations are presented on graphs. By using these graphs it is possible to obtain the absolute movement at any given point in the solid. They showed that due to the action of primitive stresses (vertical and horizontal) on the dipping stope, two components of stress will exist; the normal stress P and the shear stress Q. As a result of applying these two stress components on the stope, three components of movement induced by mining in the solid are predicted by the elastic theory as shown in Figure 2.7.2.

1. A horizontal movement (U) in the X-axis directed towards or away from the stope centre line.
2. A perpendicular component (W) in the Z-axis directed normally towards the plane of the stope.
3. A ride component (V) in the Y-axis moves down dip and up dip in the hanging wall and footwall respectively.

Ryder and Officer (1964) and Cook et al. (1966) measured the vertical displacement in the rock mass surrounding an excavation by precise levelling of a number of accurate benchmarks spread along tunnels running through the rocks in the vicinity of the excavation. The benchmarks were fixed at the ends of 2.44 m long holes drilled into the tunnel roof. It was noticed that rock movements started well ahead of the working faces and that the movement increased as the span of the excavation increased (Ryder and Officer, 1964). Figure 2.7.3 shows a comparison between the observed and calculated elastic theory displacements along a tunnel in the hanging-wall of two longwall stopes. It was found that there was a good agreement between the observed and calculated movements. The good correlation led

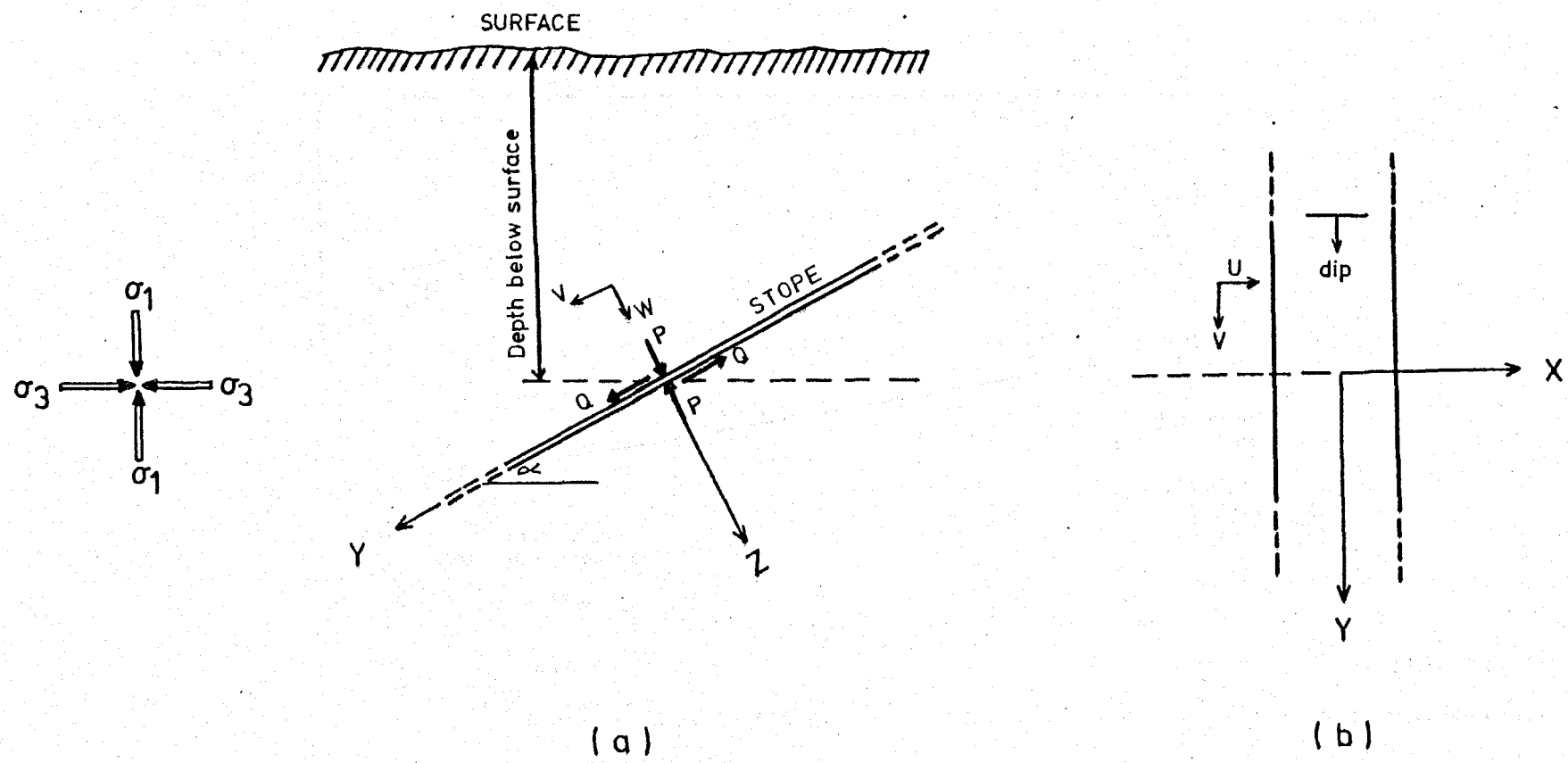

Fig. 2.7.2. Induced components of movements in the solid rocks as a result of the action of lithostatic stresses on a dipping stope.

(a) Dip section. (b) Plan view.

(After Ryder and Officer, 1964).

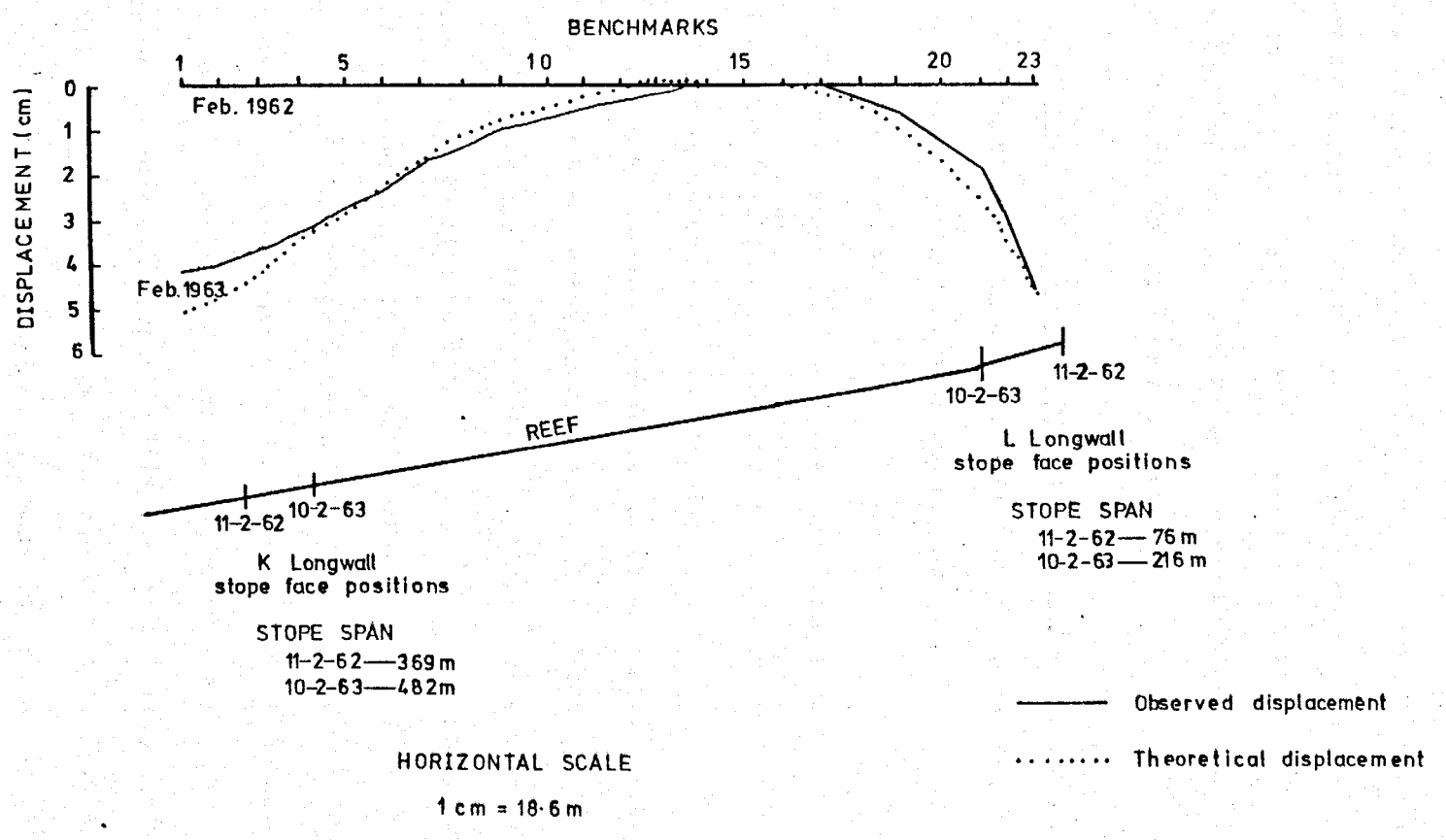

Fig. 2.7.3. Comparison between observed and calculated elastic theory displacements, along tunnel 58 in the vicinity of the K and L longwall stopes (Witwatersrand), relative to benchmark 15 from February 1962 to February 1963. (After Ryder and Officer, 1964).

Ryder and Officer to conclude that deformations in the rock mass induced by mining may be described or predicted in terms of elastic theory. The theory may also be used to calculate the stresses and the energy distribution around the excavation. Such calculations may be used to make a correlation between rock failures and mining induced stresses, strains, and energy distribution in the mines and consequently may provide greater understanding of rock failure mechanisms.

2.8 The energy released by making an underground excavation

Since rock bursts are the result of a violent release of energy, a study of energy change during mining may be useful in understanding the mechanism of rock bursts.

In an underground stope, the rocks immediately surrounding the excavation are fractured but the rock mass behind these fractured rocks is solid and tends to behave elastically.

The work done in the deformation of an elastic material is equal to the area beneath the stress-strain curve (shaded area in Figure 2.8.1a). During unloading the strain follows the same curve and this work is recovered from the elastic strain energy. When a load is applied to a plastic material, however, it may deform continuously and it will not recover its original shape after unloading (Figure 2.8.1c). Therefore the work done in this deformation is dissipated within the material.

When an underground excavation is made, a change in the potential energy of the rock mass occurs. This change is called the gravitational potential energy (W_G) and occurs as a result of rock displacements under the influence of the gravitational field (Cook et al., 1966). These displacements represent the amount by which the rock mass above the excavation moves toward the excavation (towards the centre of the earth). The loss in potential energy (W_G) can be expressed in terms of the superincumbent vertical pressure and the volumetric closure of the excavation.

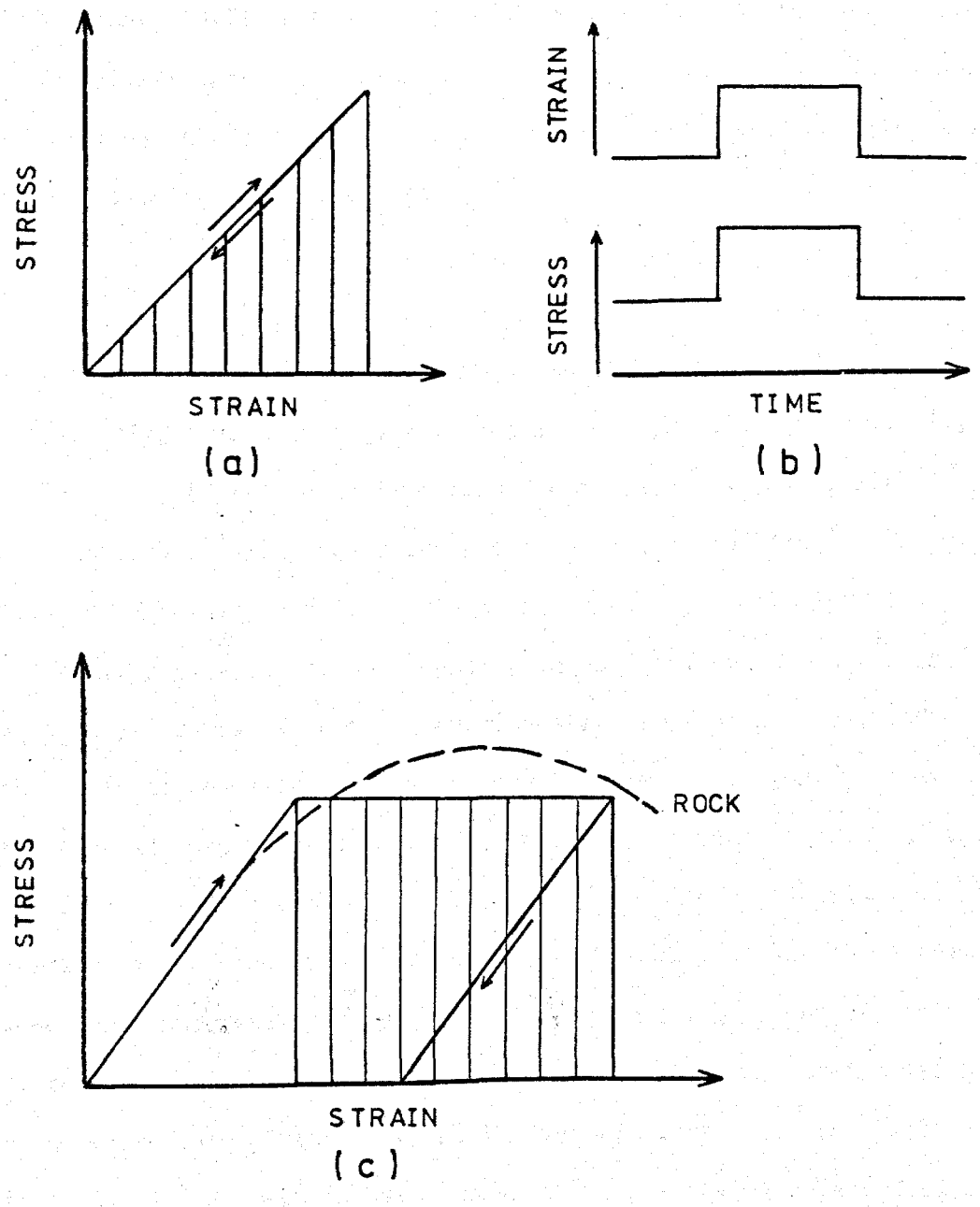

Fig. 2.8.1. (a) Stress-strain curve showing the strain energy resulting from the deformation of an elastic material.

(b) Strain-time relationship showing the instantaneous strain response of an elastic material, to changes in stress.

(c) Stress-strain diagram showing the energy dissipated in non-recoverable deformation of an ideal elastic material.

(Caption and diagram after Cook, 1963).

$$W_G = VP \qquad 2.8.1$$

where V is the volumetric closure.

P is the overburden vertical pressure.

Part of this energy will be stored as strain energy (W_S) in the surrounding rocks, which significantly increases the stress in these rocks. The other part (W_R) will be released. However, the released and stored energies must satisfy the following relationship:

$$W_G = W_R + W_S \qquad 2.8.2$$

The non-elastic behaviour of the rock mass results in greater displacement and, consequently, greater energy release, ie. $W_S \leq W_R \leq W_G$ (Cook et al., 1966). The energy (W_R) is usually released non-violently and is either dissipated through crushing the rocks and supports, or by plastic flow of the fractured materials, and is mostly transformed eventually into frictional heat. The rate at which the energy can be dissipated non-violently depends on many factors, such as excavation size, rock properties, and depth below the surface. However, the energy may be released violently, that is, it is transformed into kinetic energy and manifests itself as rock bursts, sometimes causing severe damage. Cook (1962) from his seismic study of the Witwatersrand earth tremors, showed that a small amount of strain energy is released, without damage to the stope during blasting. However, the blasting does not release all the excess strain energy. At other times failures occurred intermittently releasing seismic energy between 1.36×10^3 J to 1.36×10^5 J which is small compared to the energy released by a large failure. The largest failures released up to 1.36×10^9 Joules of seismic energy and usually caused damage in the mine and occurred in the form of a rock burst. Those failures releasing less than 1.36×10^5 J of seismic energy rarely caused damage. During rock failures part of the stored strain energy (W_S) is also released.

Cook (1963) calculated the energy released for a long and narrow horizontal slit-like excavation in an elastic material as being given by:

$$E = \frac{4p^2S^2}{3G} \qquad 2.8.3$$

where E = total excess energy per unit length.

p = vertical overburden pressure.

S = half span of the excavation.

G = modulus of rigidity.

The rate at which this energy is released as the span of the excavation is increased is given by:

$$\frac{dE}{ds} = \frac{8p^2s}{3G} \qquad 2.8.4$$

Therefore, the total energy release and the rate of energy release are both functions of the stope geometry and overburden stress. Figure 2.8.2 shows the relationship between the rate of energy release and the span of a long-wall stope at depths of 1524 m and 3048 m (5,000 ft. and 10,000 ft.), with three possible values of maximum closure. Line A represents the rate at which energy is dissipated non-violently, and 1c represents the critical excavation size, where the two rates become equal. The graph shows that the rate of energy release increases sharply as the span increases, while the rate of non-violent energy dissipation is nearly constant. The rate of energy release augments as the span increases until the span reaches a point where complete closure occurs at the centre of the excavation, after which the rate of energy release approaches a constant value (Cook et al., 1966). The graph also shows that the rate of energy release is a function of depth (i.e. increasing pressure).

Statistical observations in mines have shown similar relationships between mine geometry, depth, and the rock burst incidence. It has been

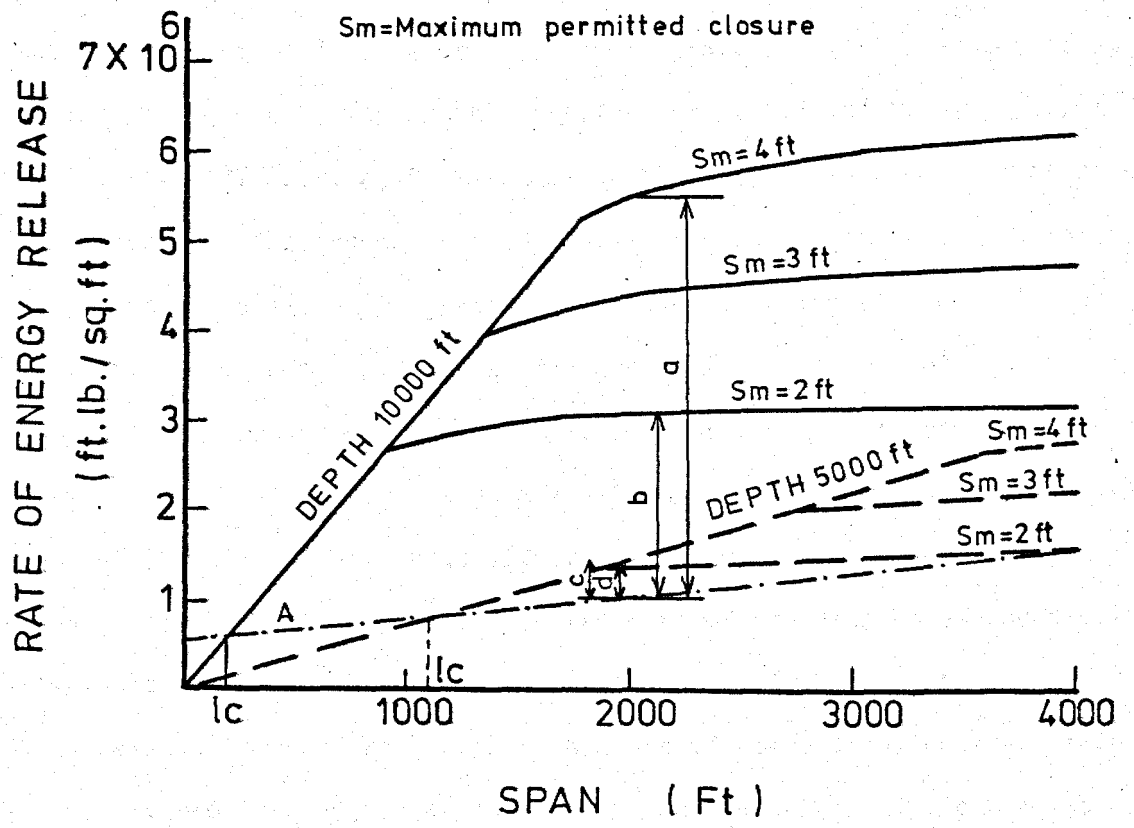

Fig. 2.8.2. The relationship between the rate of energy release and the span of a longwall stope, in which maximum closure is limited to 2, 3 and 4 ft., at two different depths. Line A represents the rate at which energy is dissipated non-violently. The difference in length between lines a and b, and c and d represents the difference in the energy release due to the effects of 2 ft. waste filling in a 4 ft. high stope. (After Cook et al., 1966).

found in the mines that the frequency of rock bursts increases both as the excavated area becomes large and deeper (see Chapter 3).

From the above it can be inferred that for a given depth, there exists a critical excavation size below which no rock burst should occur, while beyond this size, rock burst incidence increases rapidly as the excavation is enlarged (Cook et al., 1966). This critical size decreases with increasing depth. Below this critical size, all energy is dissipated non-violently. Therefore, Cook suggested that "the existence or otherwise of the rock burst hazard depends on whether the geometrical rate at which energy must be released, is greater or smaller than the rate at which energy can be dissipated non-violently as the excavation is enlarged".

It has been found that the incidence of rock bursts greatly increases wherever the excavation surrounds a small abutment. Figure 2.8.3 shows the effect of the size of pillar at different depths on the rate of energy release. The broken line represents the rate of non-violent energy dissipation. It can be seen that when the pillar size is small, the rate of energy release is much greater than the rate of non-violent energy dissipation. This provides a good explanation of why rock burst incidence increases during the extraction of remnant pillars (see Chapter 3).

Cook et al. (1966) finally concluded that by reducing the rate of energy release, it is possible to minimize the rock burst hazard. Reduction of the energy release can be achieved by reducing the stope closure, and by adopting methods of mining which ensure the most uniform rate of energy release. Such methods of mining include extraction along a regular line and the avoidance of leaving small pillars. Although total stope closure can be reduced by keeping the stope height as small as possible, there is a practical limit below which the stoping height cannot be reduced. The reduction in closure can be achieved by:

(1) Leaving solid supporting pillars between the panels

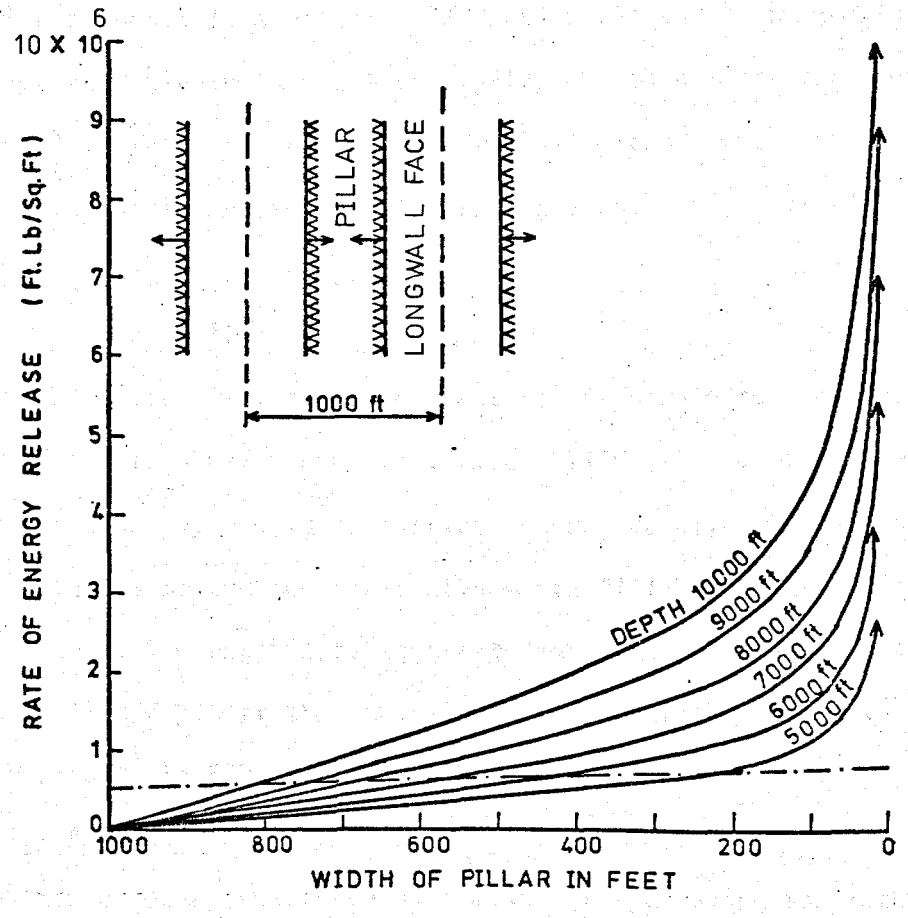

Fig. 2.8.3. The relationship between pillar size (formed by the approaching of two longwall faces) at different depths and the rate of energy release. The broken line represents the rate of non-violent energy dissipation. (After Cook et al., 1966).

This method is carried out by the extraction of long parallel panels of equal span, separated by solid pillars of equal width spaced at regular intervals. The extraction can be carried out along faces either parallel or perpendicular to the long axes of the panels.

It has been found that the released energy increases linearly and uniformly when the faces advance in the direction of long axis of the panel. However, with advances in a direction perpendicular to the long axis of the panel, the energy release is small initially, and then increases greatly (non-linearly) in the final stages of the panel extraction. Therefore the first method is considered to be safer from the rock burst hazard point of view.

(ii) Waste filling (stowing)

For the waste filling to be effective, it should reduce the closure of the excavation to a maximum extent. The filling should offer the maximum possible resistence and should be carried out as rapidly as possible. Theoretical studies have shown that while waste filling is very effective in reducing the rock burst hazard at great depth, it will only combat the hazards at shallow depth if the excavation is exceptionally large. This is illustrated clearly in Figure 2.8.2.

(iii) Roof caving

Caving has been considered as a method for reducing the rock burst hazard in Witwatersrand gold mines. However, no definite conclusion has been obtained regarding its adoption. Caving may help to prevent rock bursts in two possible ways:

1. The fractured rock masses in the caved area may be regarded as waste filling.
2. More freedom of strata movement may enable more energy to be dissipated non-violently.

CHAPTER 3

ORIGIN AND MECHANISMS OF ROCK FAILURES

3.1 Introduction

Rock failures induced by mining are generally referred to as rock bursts, rock falls, bumps and bounces. The term rock burst is most used, however rock bursts in coal mines are often called bumps (Osterwald, 1970). Blake (1972) defined the rock burst as "a sudden rock failure characterized by the breaking up and expulsion of rock from its surroundings, accompanied by the violent release of energy". This definition suggests that rock bursts occur only on free mine faces. However, Hodgson (1958) suggested that "the term rock burst should be extended to include any sudden release of rock strain energy, whether or not it is accompanied by evidence in the mine". Morrison (1947) also defined the rock burst as "that phenomenon which occurs when a volume of rock is strained beyond the elastic limit and the accompanying failure is of such a nature that accumulated energy is released instantaneously".

The lack of clear definitions of many terms used in rock burst studies had led to considerable confusion among mining engineers. A survey of the literature showed that many investigators used the term rock burst to refer to failures occurring on and deep inside the face (Weiss, 1938; Hodgson, 1953; Dunrud and Osterwald, 1965; Cook, 1962; Hodgson, 1958; Mashkour, 1976). This suggests that most writers do not distinguish the failure (strain energy release) from its effects (shock wave, noise, mine damage, etc.).

In this study the term "rock failure" is used to refer to all kinds of rock failure (and associated strain energy release) except when failure occurs on a free face (or surface) when the term "rock burst" will be used.

3.2 The Origin of Rock Failures

The origin of rock failures can be classified mainly into three categories.

3.2.1 Rock failures (rock bursts) originating in the vicinity of an excavation

In general the effect of these rock failures can be observed in the mine. The rock failures in this zone can be divided into three groups:

(i) Rock failures (rock bursts) originating in the fractured rocks immediately surrounding the excavation: As explained in Chapter 2, an excavation at depth is surrounded by a zone of fractured rocks (intradosal ground). These fractured rocks are de-stressed in the sense that they are relieved of stress due to the weight of the overburden. However, these fractured rocks are not entirely unstressed. Cook (1962) indicated that these fractured rocks can sustain certain stress levels without slipping, and that they provide some support to the unfractured rocks behind them. Roux and Denkhaus (1954) and Hill and Denkhaus (1961) called the system of stress in these fractured rocks the "Voussoir Arch". They indicated that some rock bursts may originate in these fractured rocks and they called them "intradosal bursts". They are a local collapse of the voussoir arch and they usually occur where the hanging wall tends to become unstable as a result of the presence of faults, dykes or other disturbances in the mined-out area. During enlargement of the stope or in reclamation operations, intradosal bursts may also occur as a result of the sudden adjustment of the voussoir system (Denkhaus, 1964). Roux and Denkhaus (1954) gave an example of this kind of burst. They showed that in one instance a rock burst occurred in two roadways in an area

being reclaimed. They reported that the side walls and hanging wall of the two roadways collapsed violently. In each roadway a thickness of about 1.2 m of the hanging wall and a thickness of about 0.9 m of rock from each side were forced into the excavation. However, they pointed out that the intensity of the rock burst was low compared with the extent of damage it caused. Weiss (1938) also indicated that some rock bursts occur in the immediate fractured walls. He called these rock bursts "strain bursts". They were small bursts which affect the immediate walls only and include splinters of rock which fly from the faces, flake off and slab off suddenly. Weiss suggested that these rock bursts cease when mining operation stops. Rice (1935) explained that a rupture of a cantilever bed extending over the goaf may produce a shock burst. The mass of rock falling upon a lower layer which previously had subsided may deliver a blow transmitted as a shock wave, although the distance through which the mass falls may be less than a foot.

(ii) Rock failures (rock bursts) originating in the abutment: These are the most common and severe rock bursts in the mine. They affect the solid rock as well as the immediate fractured walls. As discussed in Chapter 2, beyond

the boundary of the fractured de-stressed zone, the ground is solid and subjected to high stress (abutment pressure zone). These abutments can be inside the walls of an excavation or inside the walls of pillars. As the excavation is enlarged, the stress distribution in the abutment continuously changes and the condition can arise where the stress at any particular instant exceeds that which the rock can withstand. Consequently, the rock fails either gently or violently depending on the state of stress. The literature is full of examples about the occurrence of rock bursts during the driving of headings or roadways through these abutments (The South Staffordshire and Warwickshire Institute of Mining Engineers, 1945-46). Phillips (1944-45) recognised two kinds of rock burst which commonly occur in this zone; pressure bursts and shock bursts.

(a) Pressure bursts: These are those which occur due to sudden failure of the rock under the influence of the excessive energy gradually accumulated within it due to the application of an increasing external pressure induced by mining, or to energy inherent in the rock under the influence of pre-mining forces. This type of burst corresponds to that occurring when a pillar of coal is overloaded and then fails in an explosive manner.

The strain energy (W) stored in an unconfined body of rock subject to compressive stress can be described as:

$$W = \frac{1}{2} \cdot \frac{P^2}{E} \cdot V \qquad 3.2.1$$

where P = the compressive force per unit area.

E = Young's Modulus.

V = the volume of the body subjected to compression.

This equation suggests that depth, thickness of the worked seam and the low elastic modulus of the coal in compression compared with the other coal measure rocks have an important effect on the liability of a coal seam to

produce bursts, and also upon the severity of these bursts. In the case of a constrained body subjected to confined forces, the stored strain energy (W) can be defined as:

$$W = \frac{V}{2E}\left\{P^2 + 2\left(\frac{P}{m-1}\right)^2 - \frac{2}{m}\left[\frac{2P^2}{m-1} + \left(\frac{P}{m-1}\right)^2\right]\right\} \qquad 3.2.2$$

where m is the Poisson's number.

Phillips pointed out that m for all rocks decreases with increasing pressure, and that for most of the coal when perfectly constrained by stresses up to 211 kg/cm^2, the value of m reaches 2. The coal inside a large pillar (pillar core) is constrained. Thus according to equation 3.2.2 no additional energy can be stored if m becomes 2. Near the free surfaces of the pillar sides where the lateral forces are not effective, the stored strain energy is given by equation 3.2.1. Therefore, pressure bursts usually occur in pillars or remnants of certain limited dimensions where lateral constraint is not effective, and in the highly stressed boundary pillars of coal faces. It is possible that the boundary pressure burst can be followed by another burst which would destroy the remaining portion of the pillar.

(b) Shock bursts: These are those caused by the sudden application of strain energy accumulated not in the coal bed but in a superjacent strong bed of rock, i.e. the sudden application of an external load. Phillips used the cantilever theory to explain the occurrence of this type of burst. This type of burst is produced in mines having strong strata which are able to sustain a considerable span above the excavation and which produce an upward bending force (counter force) over the coal ahead of the face. Abrupt failure of these beds result in the sudden reversal of these forces producing an impact or blow to the immediate roof and seam which is the immediate cause of the burst. The impact is often of sufficient intensity to cause the coal seam to burst into the roadway, to crush pillars, to

induce the floor to lift, and sometimes to bring down the roof. The occurrence of this phenomenon has been explained diagrammatically (Figure 3.2.1) by Holland (1958), though he indicated that its existence has never been proved. If the pillar remnant in Figure 3.2.1a fails suddenly, part or all of the load it supported is instantly transferred to the pillar at A and may produce a high impact stress that might cause a shock bump at A. In Figure 3.2.1b the stress at C increases as the span of the cantilever increases due to mining. If the span becomes long, a pressure bump may occur at C. If the cantilever fails suddenly, the stress at C is decreased, but a high impact stress may occur in area B and could result in a shock bump in this area.

Phillips pointed out that the amount of stored strain energy (W) produced by the bending forces in a bed spanning the excavation loaded by its own weight and that of the overburden strata is given by:

$$W = \frac{M^2 l^5}{40EI} \qquad \text{for a cantilever} \qquad 3.2.3$$

$$W = \frac{M^2 l^5}{1440EI} \qquad \text{for a fixed beam} \qquad 3.2.4$$

where l = the beam or cantilever length

E = the elastic modulus in bending

M = the load per unit length

I = the moment of inertia $= \frac{BD^3}{12}$ where B and D are the width and thickness of the bed respectively.

From these equations it can be seen that the stored strain energy in the bed varies as the fifth power of the span, i.e. if the span is doubled, the elastic strain energy will increase 32 times. The most interesting feature is that the cantilever beam stores 36 times as much energy as a similar beam suspended at both ends, provided the span length of both beams is the same. This indicates the importance of avoiding long roof spans and, if

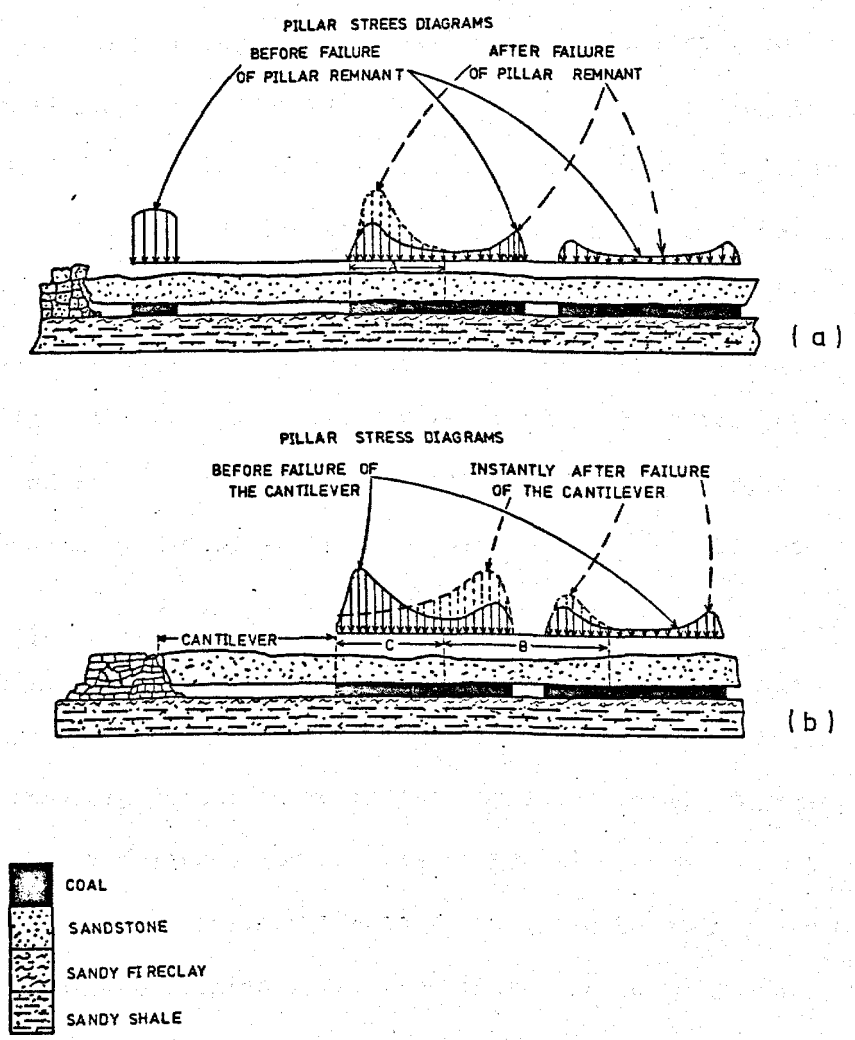

Fig. 3.2.1. Impact stress in coal beds.

(a) In the case of a beam suspended at both ends.

(b) In the case of a cantilever suspended at one end.

(After Holland, 1958).

these are inevitable, there should be adequate roof support provided in order to prevent or reduce rock bursts.

(iii) Rock failures (rock bursts) originating in the floor: If a strong floor of limited thickness is underlain by a weak soft layer, this soft layer tends to squeeze out from beneath the sides of the excavation when subjected to high pressure, and an upward thrust will develop against the immediate overlying strong bed. Consequently, this strong bed will fail, which sometimes occurs suddenly and violently so appearing as a rock burst (Peng, 1978). This kind of rock burst has been observed in the South Staffordshire, North Staffordshire and Lancashire coalfields (The South Staffordshire and Warwickshire Institute of Mining Engineers, 1945-46). In the Kolar gold field, Crowle (1931) noticed that the footwall, when it bulged upwards into the excavation, was often sheared at short intervals along the rigid edges of the stope faces, producing moderate rock bursts and forming planes of weakness at right angles to the plane of the reef.

3.2.2 Rock failures (rock bursts) originating far away from the excavation

In general the effect of these rock failures cannot be observed in the mine since they are located deep inside the solid rock. However, the sources of these rock failures can be located by seismic monitoring techniques. In some mines the seismic events are located in places far away from the excavation (see Section 1.2). In Witwatersrand gold mines, McGarr et al. (1975) used ten underground seismometers to locate the source of the seismic events. They found the tremor foci located in the quartzite hanging wall at about 200 m above the reef (with a location error of about ± 30 m). Tests on samples from the hanging wall and footwall quartzites, revealed that Young's Modulus is higher and Poisson's ratio lower in the hanging wall than in the footwall, while the strength of the hanging wall quartzite is about 1.4 kb higher than the average strength of the footwall quartzite. This suggested that the seismic events tended to occur in the stronger

hanging wall quartzite where the rock is capable of storing a great amount of elastic strain energy before failure.

Correlation between the incidence of rock bursts in the mine and earth tremors recorded by a seismic network in many mines have shown that the number of recorded earth tremors were far greater than the reported ones (see Sections 1.2 and 1.5). In the Kolar goldfield, 13,000 tremors were recorded annually while only 0.6% of this figure was reported as rock bursts (Weiss, 1938). Even assuming that some small rock bursts may have occurred in the abutments and produced no visible effect in the mine, or that they occurred in old and inaccessible parts of the mine where they could not be observed, the number of tremors still remains far higher than the possible number of rock bursts. This indicates that most of the earth tremor sources were located in the solid rock and probably far away from the excavation.

Weiss (1938) explained the occurrence of rock failures in the solid rock remote from the excavation or in pillars as a result of the accumulation of large amounts of elastic strain energy due to the elastic hysteresis of the rocks and the increase of pressure. He explained that during mining the stresses are continuously changing, increasing and decreasing, but owing to elastic hysteresis no complete release of the stresses is possible within the time scale involved in mining. If the stress increases and decreases repeatedly at intervals which are much shorter than that required for the dissipation of the residual stresses, then due to hysteresis after a certain time the stresses reach values higher than the critical strength of the rock. Eventually the rocks fail, causing partial release of the stresses. The stresses however do not disappear immediately after the rock failure, but are reduced to just less than the critical value. Therefore a further slight increase of stress by some other contributing factors will upset the temporary equilibrium and a rock failure occurs again. Weiss

called the rock failures occurring in the solid rocks crush bursts. However, this explanation seems to be more logical for the occurrence of rock bursts in the abutment zone (Section 3.2.1) which may be he considered as being far away from the excavation.

3.2.3 Rock failures occurring as a result of fault-slips

Opinions differ as to whether movements along pre-existing fault planes cause rock failures, or rock failures cause movements along fault planes. Consequently, different opinions exist as to whether the presence of faults in the mine increases or decreases rock burst incidence (Lama, 1967; Leiteritz, 1978).

In general it is believed that mining in the vicinity of a fault or faults is more liable to greater failures. This is because movements occur more frequently near a fault or faults than elsewhere due to the additional stress result from tectonic origin and/or the concentration of the mining stresses along the fault. Many observations in mines confirm this (Robson, 1946; Isaacson, 1961; Taylor, 1962-63; Osterwald and Dunrud, 1965).

Davison (1924) indicated that sliding of a rock mass along a fault generates vibrations similar to that produced by rock bursts. The seismic focus is then a portion of the fault plane. From his observations of mining earth tremors in Britain, he showed that most of these tremors occurred in areas where the mining took place near a known fault or faults, and that the foci of these tremors were on the down throw side at depths near the mine level. He also noticed the migration of the tremor epicentres along or parallel to some known faults. These observations led him to conclude that the tremors were caused by small fault slips triggered by the mine workings. He suggested that as a result of coal extraction the overlying rock subsides due to the removal of support. Near a fault or faults, the subsidence may take place by a series of fault-slips each of which might give rise to a rather strong shock. The disturbed area would be small with a circular or slightly elongated shape.

Janczewski (1956) in his study of the Upper Silesian earth tremors, noticed that some large tremors were characterized by their location along one inclined plane. He suggested that this plane may represent a major fault cutting across the crystalline basement. He also found that the tremors in the coal field released more energy in the S-phase than in the longitudinal phase. This also indicates that these tremors were due to sliding movements along the fault plane. Crowle (1931) observed evidence of movements along a fault plane known to hold isolated pockets of water in two separate instances in the Kolar goldfield. In one instance "the fault had been intersected by a drive, 1830 m below surface, ten days before a burst occurred in the vicinity of the fault in an adjoining property, a considerable distance away from the level. The fault was dry when passed through and remained dry until a few hours after the burst, when a considerable amount of water entered the level from the fault plane". Crowle also noticed in the goldfield that the major axis of the damaged area as a result of extensive ground movements is always nearly parallel to the lines of the intersection of the reef with the larger faults in the area.

Peperakis (1958) and Osterwald and Dunrund (1965) gave many examples of the correlation between faults and the occurrence of rock bursts in the Sunnyside mines, Utah. Peperakis reported that in one instance the rock bursts first started as a tunnel face approached to within about 9 m of a dip fault. No further disturbance was noticed as soon as the face penetrated the fault.

In contrast, however, many observations have shown the reverse effect with the occurrence of rock bursts decreasing in faulted areas (Holland and Thomas, 1954; Holland, 1958; McGarr, 1971; Leiteritz, 1978). Some authors believe that faults usually release the excessive stresses and so the area intercepted by faults should be less prone to bursts. This opinion might seem logical since the fault not only releases the energy

but also causes crushing of the rock in the surrounding area. Consequently these rocks should not be able, subsequently, to accummulate high amounts of elastic strain energy. Therefore, overall, the presence of faults should not favour the occurrence of rock bursts (Lamal, 1967; McGarr, 1971).

Holland and Thomas (1954) and Holland (1958) from their study of coal mine rock bursts in some American coalfields, showed that some rock bursts occurred in areas disturbed by faults. However, the absence of these faults in other areas where rock bursts have occurred indicated that the presence of faults do not necessarily contribute to the occurrence of rock bursts. Leiteritz (1978) stated that in the Ruhr coalfield (West Germany) most of the rock bursts occurred in mining areas where there is little faulting, and the events were largely reduced in more faulted and highly fissured ground. He indicated that in the case of a reverse fault, rock bursts occur more often in the lower block than in the upper block. The same phenomenon was observed in the Upper Silesia coalfield (Lama, 1967). This may be because during faulting the upper throw block is crushed more than the lower block.

3.3 The mechanisms of earth tremors based on the analysis of first motions

Any sudden disturbance or displacement in rock results in the energy being radiated throughout the surrounding rocks in the form of seismic waves. Consequently a great deal of information about rock failures has been obtained from studies of their associated seismic waves. This is based mainly on analysing seismic wave first motions, which corresponds to the elastic radiation from the onset of seismic events, at large distances (Knopoff and Gilbert, 1960).

Volumetric expansion or volumetric collapse causes the surrounding rocks to move outwards or inwards respectively. It follows that the first arrival of a P-wave will be detected at the surface as either compression

(anaseismic) or dilatation (kataseismic). P-waves generated from an explosion inside the earth push the surrounding rocks outwards on a spherical surface, and the seismographs at the surface will detect these waves as an upward push and record it as an upward (anaseismic) first motion. If the source of the detected P-waves is a fault, the first P-motion will be recorded in a simple pattern at the surface depending on the direction in which the P-waves left the fault. The radiated first motion pattern will form a four-fold symmetry about the centroid of the failure, of alternating compressions and dilatations.

The orientation of the fault plane (strike, dip and dip direction) can be determined graphically from the data of the signs of the first motion of the P-wave and by using the stereographic projection technique. In an ideal fault-plane solution where the seismic network surrounds the seismic focus, two quadrants each of compression and dilatation are obtained. The solution consists of two orthogonal planes, separating the polarity quadrants, called the nodal planes. One of these is the fault plane which must be determined using supplementary geological and geophysical information about the area.

Characteristic fault-plane solutions correspond to three fundamentally different types of faults, namely, wrench faults, normal faults, and reverse faults are shown in Figure 3.3.1. By comparing the fault-plane solution of any seismic event with the characteristic solution given in this figure, the type of fault can be determined.

Gane et al. (1952), working in the Witwatersrand gold mines (Section 1.2), studied the first motions of P-waves in order to determine the focal mechanism of the earth tremors. They suggested that the predominant recorded downward (kataseismic) movement of the P-wave first motion indicates that the initial movements must be inwards toward the focus. However, they considered it to be rash to interpret the kataseismic first

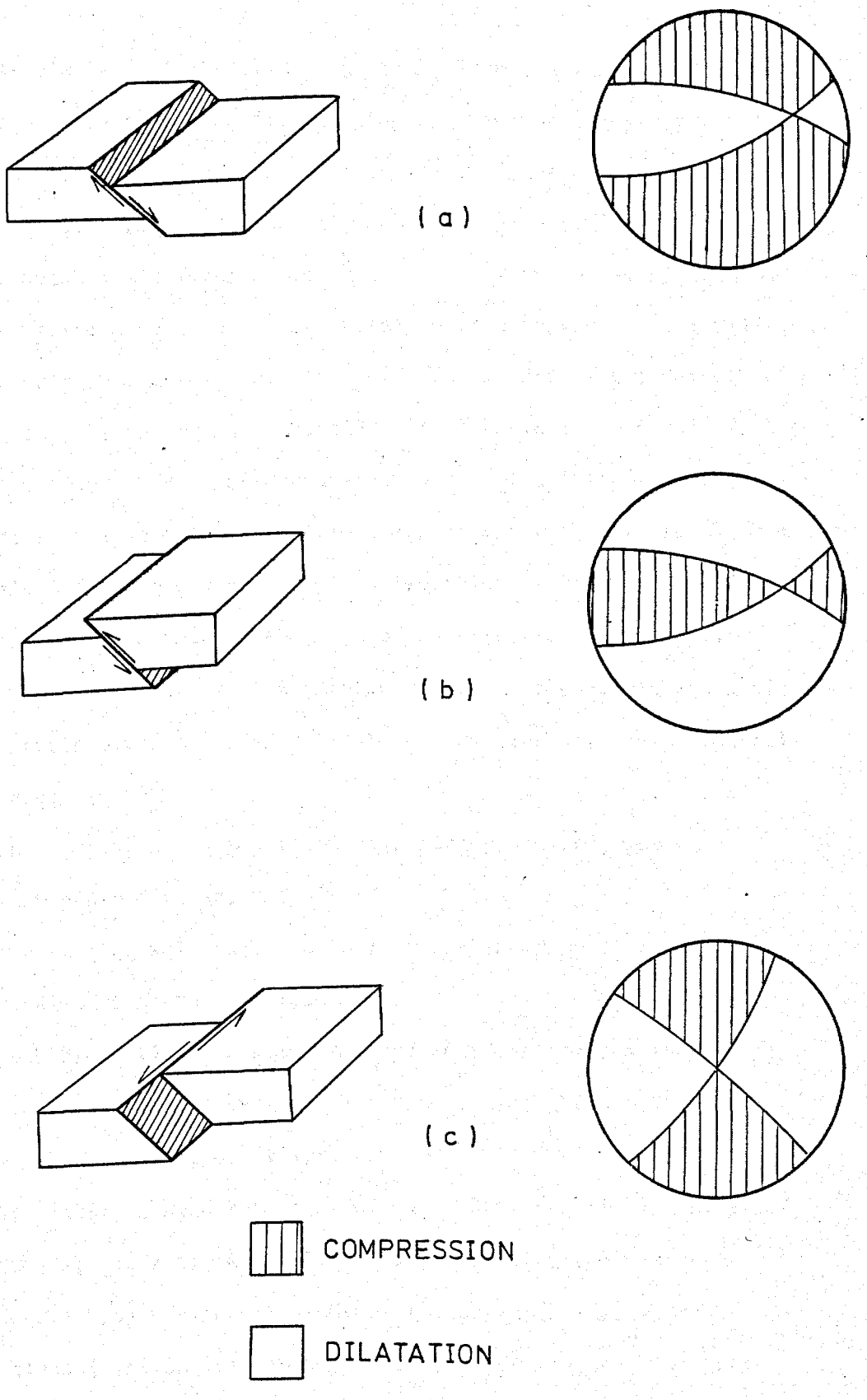

Fig. 3.3.1. Fault-plane solutions for three typical fault movements.

(a) Normal fault.
(b) Reverse fault.
(c) Wrench or strike-slip fault.

motion as a simple fall of the overyling strata into the excavation under the influence of gravity. They defined the first motion as that occurring within a few milliseconds from the absolute start of the event at the focus, i.e. the first motion related to the elastic movement associated with the failure. The kataseismic first motion could arise from the absolute downward movement of the hanging wall as a result of the failure of the pillars and other supports in compression. This kind of failure is typical of pressure bursts. The authors also concluded that failures in simple tension or in tension due to bending is an uncommon form of initial failure. They suggested that in such a case of failure the unbroken rock will spring upwards in vertical tension giving an upward (anaseismic) first motion at the surface. They indicated that in the case of shear failure both types of first motion were obtained. In the opinion of Gane two possible modes of shear failure could give kataseismic first motions over a large epicentral area. These are:

1. The hanging wall, supported in shear by pillars, moves down dip and shears the pillars.
2. The hanging wall shears at a face working down dip, so tending to close the stope.

Cook (1962) noticed in Witwatersrand that most of the energy released was contained in the vertical shear component which may suggest that shear was the mechanism of failure.

Hodgson (1958) showed that most of the tremors in the Kirkland Lake mines, Canada, generated kataseismic longitudinal seismic waves.

Mashkour (1976) during his study of the earth tremors at Monktonhall colliery, Scotland (Section 1.6) found three types of tremor. The first group produced kataseismic first motion at all stations. He suggested that these which are pressure bursts, and always occur when the face enters an abutment pressure of another worked out area, could arise from the downward

movement of the hanging wall. The second group of tremors at Monktonhall colliery generated anaseismic first motions. He considered these to be shock bursts produced by the failure of rocks in tension due to bending where the unbroken rock springs outwards giving anaseismic first motions. However, it is known that the energy released when the rock fails in tension is less than the energy released when the rock fails in compression (Osterwald and Dunrud, 1966; Kusznir et al. 1980b). Gane et al. (1952) also mentioned that failure in tension is an uncommon form of failure in mines. This may suggest that the Mashkour interpretation may be incorrect since he did not discuss the distribution of seismometers with respect to the position of the tremor foci. It could be that the tremors which generated only anaseismic first motions occurred within a small arc of azimuth with respect to the position of the seismometers, so that they recorded only anaseismic first motions.

The third group of tremors, which had the lowest incidence, arose from the fracture of the rocks in shear and generated both kinds of first motion.

3.4 Factors affecting rock failures

Rock failures in coal mines have occurred in several places under diverse geological and mining conditions. The factors affecting rock failures are variable and their relationship is very complicated. It is difficult to determine the absolute effect of one separate factor on the incidence of rock failures. However, knowledge of the various isolated factors can be attained from statistical analysis of the rock burst data obtained from underground observations.

In general, the factors can be classified into two categories: Artificial or controllable factors. These are:

1. The mode of working.
2. The rate of face advance.

Natural or uncontrollable factors. These include:

1. The physical properties of the rock.
2. The nature of surrounding rocks.
3. Depth.
4. The existence of dykes and faults.
5. The presence of folds.
6. Pore pressure and moisture.

3.4.1 Artificial or controllable factors

1. The mode of working

The mining method is undoubtedly one of the most important factors affecting the occurrence of rock failures. Improper mining methods can induce a very high stress in localized areas, such as pillars and headings (see Chapter 1).

Statistical studies in the Upper Silesia coalfield showed that 76.3% of rock bursts occurred in headings or roadways, 10.5% at the slicing faces, 9.4% at longwall faces, with 3.8% associated with other cases (Lama, 1967).

A comparison of various extraction methods showed that 74.7% of the rock bursts were associated with the room and pillar extraction technique. This may be because in this method a great number of preliminary headings are required. Longwall systems contributed about 22.1% and the rest about 3.2% (Lama, 1967). Lama indicated that with the room and pillar technique, the occurrence of rock bursts per 100,000 tons of coal produced was 5.1 times greater than that in the longwall system. Holland and Thomas (1954) stated that longwall mining has been advocated as a means of preventing or reducing rock bursts in coal mines. They found that in room and pillar mining, more than 67.6% of the rock bursts occurred on pillar line points. Taylor (1962-63) indicated that for the period 1900 to 1938, 30% of the rock bursts which occurred in the Kolar gold field were pillar bursts, 27% were development excavation bursts, mostly in shafts, 10% were

area bursts, and the remaining 33% could not be classified accurately. In recent years, 10% of the rock bursts were pillar bursts, 7% were development bursts, and the rest were in stopes or stope abutments.

In general, however, it has been found that the extraction of pillars (a) and the excavation of large areas (b) were the major source of tremors.

(a) Pillar or abutment size: Nearly all writers on the subject agree that pillars are the most prominent source of rock failures (Crowle, 1931; Holland and Thomas, 1954; Neyman, 1955; Hill and Denkhaus, 1961). When an underground excavation is made, the stress and the strain energy per unit volume increase in the surrounding rocks. In the case of a pillar surrounded by excavations on nearly all sides, the stress and the strain energy are more highly concentrated. As the pillar size is reduced, the stress in the pillar increases until the strength of the pillar is exceeded and the pillar fails (see Section 2.3.1). Weiss (1938), Pretorius (1964), Cook et al. (1966) and Blake (1972) found that during pillar extraction, the stress ahead of the face increased, and this caused rock bursts. When the highly stressed abutment becomes small it may be completely fractured (de-stressed) and therefore becomes progressively less prone to bursting. Figure 3.4.1 shows the influence of the type and size of the abutment on rock burst incidence. The rock burst incidence increased with decreasing abutment size, until an abutment area of slightly less than 1672 m^2 (500 square fathoms) was reached, thereafter it decreased until the pillar was completely extracted.

However, leaving proper pillars may reduce the number of tremors in the mines, as has been found by McGarr and Wiebols.(1977). They studied the effect of pillars on the seismicity and overall seismic deformation in the Witwatersrand mines (Section 1.2). Ten underground geophones deployed in a region of about 3 km in extent and ranging in depth from 1.8 to 3.3 km were used to monitor the tremors over a period of 100 days in 1972. The mine faces in two regions were bounded by strike pillars. These pillars

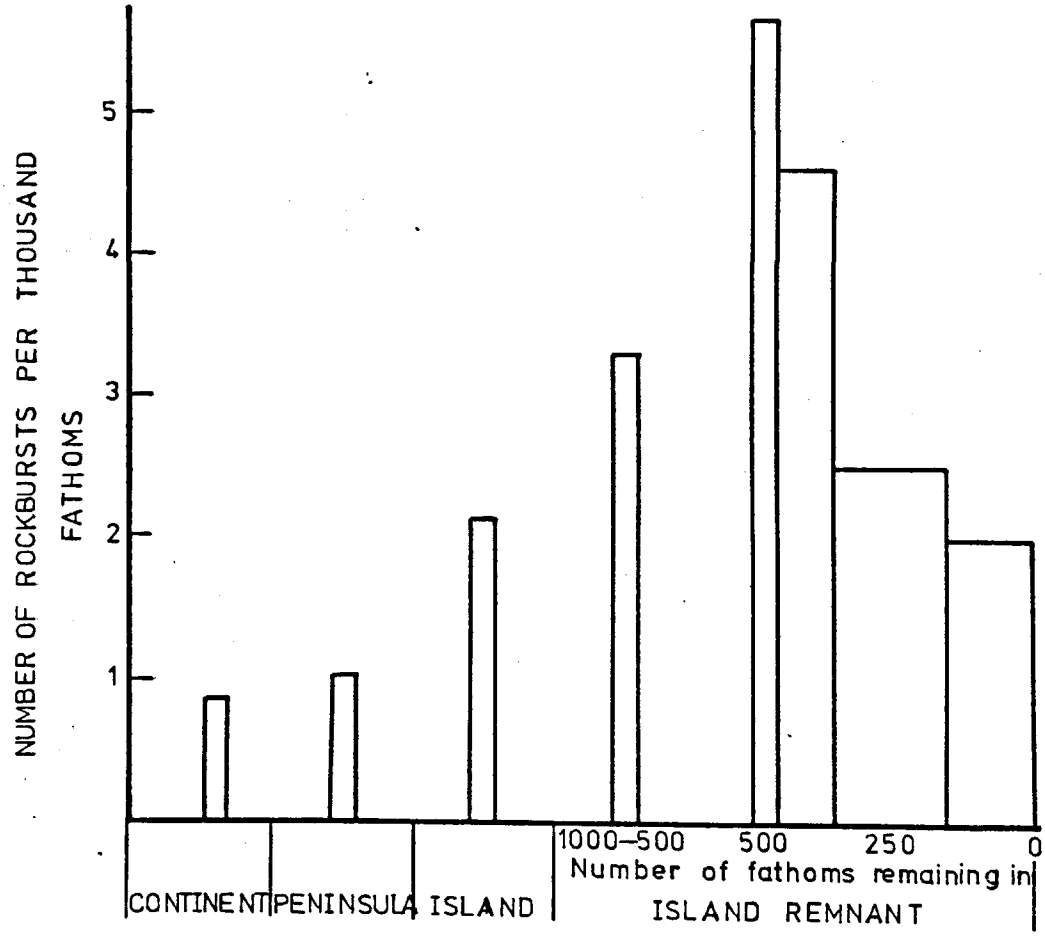

Fig. 3.4.1. The variation in rock burst incidence for various abutment types. Also shown is the influence of the size of abutment on rock burst incidence, in the case of island remnant. (After Pretorius, 1964).

were left unmined in order to prevent stope convergence and to help in the problem of strata control. In the third region the faces were far from any pillars. During the experiment 450 tremors were located. Most of the foci were located near the active faces, while seismic gaps occurred in the stabilizing pillars. It was found that the distribution of tremor hypocentres in the two regions bounded by the pillars were less intensive than in the third area. The magnitude-frequency distribution of the tremors in the three areas using equation 7.4.1 (Richter, 1958) gave b values nearly the same for the three areas, indicating, according to the authors, that b values are stable in relation to changes in position and mine geometry. Values of the constant a were lower in the areas bounded by the pillars. The seismicity level, S, per unit volume of rock mined, was defined by McGarr and Wiebols as:

$$S = 10^{a}/\Delta vm \qquad 3.4.1$$

where Δvm is the volume of rocks mined in a particular region. Using this equation, it was found that the number of tremors per unit volume of rock mined in the area affected by the pillars was about 40% of the number in the area not affected by the pillars. They also found that the pillars prevented about 60-75% of the convergence that would have occurred in their absence.

(b) Excavation size: As already described in Sections 2.2 and 2.8, as the excavation size increases the pressure on the abutments and the amount of energy released increases and consequently rock failures increase.

In the Witwatersrand, a relationship between the number of rock bursts per thousand fathoms versus the stope span (the distance between opposite faces on strike) is shown in Figure 3.4.2 (Pretorius, 1964). The number of rock bursts increased with the stope span until a maximum value of approximately 1.4 rock bursts per thousand fathoms was reached at a span

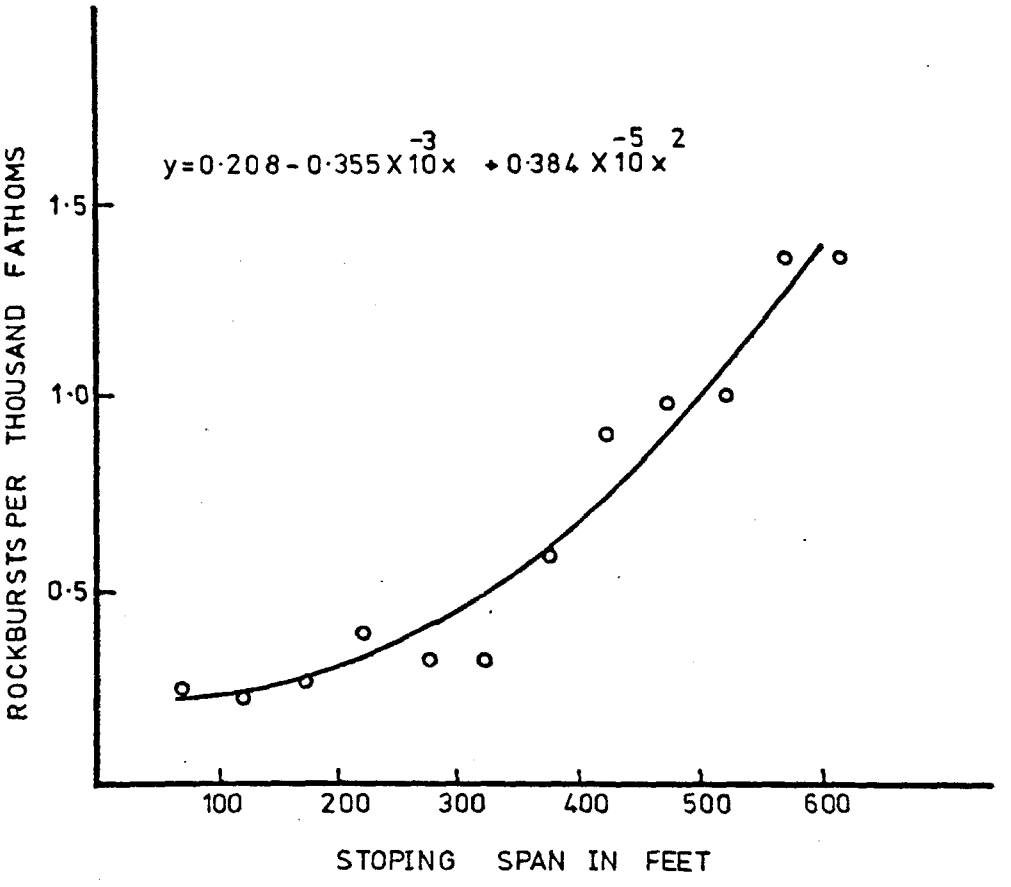

Fig. 3.4.2. The influence of stoping span, in a typical longwall face, on the rock burst incidence. (After Pretorius, 1964).

of approximately 183 m (600 ft). Thereafter the number of rock bursts decreased to a level of 0.9 rock bursts per thousand fathoms for a span of more than 274 m (900 ft). For greater spans no significant changes in the incidence was noticed. This may suggest that the size of the remaining abutment is the main geometrical controlling factor at this stage rather than the excavation size.

In the Kolar goldfield, Crowle (1931) reported that the rock bursts usually started when about 60% of the reef had been extracted from a given area. The depth of workings in this case was about 1520 m below the surface.

2. The rate of face advance

In the Witwatersrand gold mine it has been found that an increase in the rate of face advance up to a certain value results in a decrease in rock burst incidence. Above this rate the incidence increases again (Cook et al., 1966). (This initial reduction in rock burst incidence may be a false reduction, because when a rock burst occurs on the face it causes a delay in production). The rate of face advance beyond which the rock burst incidence starts to increase as the rate of advance increases depends on the size of the abutment. Cook suggested that beyond a certain rate of face advance, varying between about 4.6 m/month for small abutments to 7.6 m/month for large abutments, the incidence of rock bursts increases as the rate of advance increases.

In the Kolar goldfield, Crowle (1931) noticed that reducing the rate of pillar removal resulted in fewer rock bursts. Therefore, he suggested that during the extraction of pillars, the face should be advanced slowly giving time for the development of fractures of the rock inside the pillar face, and consequently of the releasing pressure. The same phenomenon has been observed in the South Staffordshire coalfield (The South Staffordshire and Warwickshire Institute of Mining Engineers, 1945-46).

Hodgson and Joughin (1967) discussed the effect of the rate of face advance in terms of the spatial rate of energy release during excavation. They carried out experiments in two mines at different depths in the Witwatersrand gold mines. They found in both mines that seismic activity and the incidence of violent rock bursts were a function of the spatial rate of energy release as the excavation is enlarged. They suggested that the conditions in the mines are considered to be good if the energy release rate is less than 10^7 J/m^2, and if it is less than 10^6 J/m^2 the problems arising from rock failures are negligible.

3.4.2 Natural or uncontrollable factors

1. The physical properties of the rock

It has been accepted that the physical properties of rocks have a bearing on the incidence of rock bursts (Mukherjee and Singh, 1964). The stress conditions in the rock at fracture is defined as the ultimate strength. Different types of material have different strengths. If the rock is subjected to pressure which exceeds its strength, the rock fails, releasing its stored strain energy. The quantity of energy released depends upon the volume of the fractured rock and upon the energy released per unit volume of rock which has failed.

If a coal measures shale which is naturally soft, is subjected to stress, it will yield comparatively easily and slowly. Consequently, very little or no strain energy can be accumulated. The release of stress in this type of rock takes place slowly during crushing of the rocks and continuously through the whole process of loading. Therefore this kind of rock is not associated with rock bursts. The harder and more brittle rocks, such as sandstones and quartzites can sustain very high values of stress before yielding, and therefore have the ability to accumulate great amounts of energy. When the stress exceeds their strength they fail suddenly, releasing their energy which is manifested as rock bursts. This indicates that

the susceptibility of coal to bursts depends on its ability to accumulate elastic strain energy. The susceptibility of coal to bursts can be expressed by an energy index (W_E) according to the formula given by Peng (1978):

$$W_E = \frac{Ee}{Ep} \qquad 3.4.2$$

where Ee = the elastic strain energy accumulated in the coal.

Ep = the permanent strain energy.

If $W_E > 5$ the coal is severely liable to bursts.

W_E is 2-5 the coal is slightly liable to bursts.

$W_E < 2$ the coal is not liable to bursts.

Sebor et al. (1976) reported about experiments carried out on rock samples to determine the susceptibility of the rocks to bursting. The method determined the ability of the rock to accumulate strain energy during a loading cycle, and the way of releasing this energy after reaching the ultimate strength. As a result of these tests, the rocks were classified into three categories:

1. Rock non-susceptible to rock bursts: These rocks do not release any, or only a very small amount of seismic energy at their ultimate failure, and the emission of seismic impulses continues during the entire loading cycle.

2. Rock susceptible to induced bursting: These rocks release a considerable amount of energy at their ultimate failure. However, emission of seismic impulses occurs during the whole loading cycle. In this type of rock an "induced rock burst" can occur as a consequence of sudden stress increases, such as those caused by blasting, adjacent rock burst or tectonic earthquake.

3. Rocks susceptible to spontaneous rock bursts: These rocks release a great amount of energy at their ultimate failure, and the emission of seismic impulses is minimal during the loading cycle. This is typical of burst-prone rocks.

2. The nature of surrounding rocks

The term "surrounding rocks" should be taken to mean the rocks in the roof and floor. Observations in many mines have showed that burst-prone coal seams were mostly overlain by a strong massive rock stratum such as sandstone, siltstone or conglomerate (Phillips, 1944-45; Holland and Thomas, 1954; Shepherd and Kellet, 1973). The presence of strong overlying strata does not necessarily mean that rock bursts will occur. A weak stratum sandwiched between the coal seam and the strong strata, and the presence of a soft floor bed, will gradually dissipate the applied stress by the yielding of the weaker strata, and consequently insufficient energy will be accumulated to develop a rock burst (Phillips, 1944-45; Peng, 1978). However, Rice (1935) indicated that the presence of the strong massive strata does not necessarily need to be immediately above the seam, and that it could be as far away as 10-15 times the thickness of the coal bed. Phillips (1944-45) suggested that the role of the strong roof beds lie in their ability to span the excavation which results in the transmission of excessive pressure onto the coal face or pillar and leads to rock bursts. He gave an example about the influence of strong roof strata on the occurrence of rock bursts in the Springhill mine, Nova Scotia, Canada.

In Britain major rock bursts have been experienced in the Parkgate seam at Barnborough in Yorkshire, where a thick, predominantly massive sandstone, overlies the coal seam (Phillips, 1944-45; Shepherd and Kellet, 1973). In the Ruhr coalfield, West Germany, it has been found that seams with overlying and underlying sandstone were very prone to bursts, while seams with no roof and floor sandstones were mostly free from rock bursts (Leiteritz, 1978).

Where the floor is very strong, the bursts may be more frequent and violent (Rice, 1935; Phillips, 1944-45; Peng, 1978). If the floor is softer than the pillars, the pillars are likely to punch into the floor

resulting in the dissipation of the energy stored in the pillars. Hill and Denkhaus (1961), showed in the Far East Rand, Witwatersrand gold mines, that rock bursts were relatively infrequent. This is because the footwall consists of shale, and as the stress increases ahead of the faces, the shale yields gradually by plastic deformation. Therefore the stress cannot accumulate in sufficient amounts to produce rock bursts. The thickness of the strong floor may play an important role in the occurrence of rock bursts, as explained in Section 3.2.1.

3. Depth

As explained in Chapter 2, the vertical pressure exerted on the coal faces and ribs or pillars is proportional to the height of the overburden. The deeper the coal seam the higher the pressure, which may exceed the rock strength and consequently increase the incidence of rock failures. For each particular coal field, there is a minimum depth for the occurrence of some mining peculiarities, such as rock bursts, roof falls, floor heaving, and pillar failures. This minimum depth depends upon the lithological and structural geology in the field (such as the presence of massive sandstones, faults, and dykes). Rice (1935) reported that coal bursts occur when the depth is 300 m or more. In the Donets Coal Basin, Russia, the natural condition of the mine starts to deteriorate at a depth of 500-600 m. In the Kizel Coal Basin, deterioration starts at 600 m, while in the Kuznetsk and Karaganda Coal Basins it is at about 400-500 m (Krasnikovsky and Baranovsky, 1963). At Springhill, Nova Scotia, the rock bursts begin at a depth of about 550 m, and in Upper Silesia at about 230 m.

In the Witwatersrand gold mines a linear relationship was found to exist between rock burst incidence, the size of the excavated area, and the depth below the surface (Cook et al., 1966). Cook carried out experiments to determine the relationship between rock burst incidence and the size of the excavated area (in an area far away from faults, dykes, etc.) at

different depths (Figure 3.4.3). An empirical formula relating the incidence of rock bursts to the excavation size and depth below the surface was obtained.

$$Y = - 0.0731 - 0.0294X - 0.00393X^2 + 0.549 \times 10^{-6} X^3H \qquad 3.4.3$$

where X = percentage of the excavation in a 1,000 ft. radius

H = depth below the surface (ft.)

and, the number of rock bursts per thousand fathoms = Y if $Y > 0$

= 0 if $Y \leq 0$.

4. The existence of dykes and faults

It has been found that rock burst incidence for stopes in the vicinity of dykes and faults was always higher than for those remote from them (see Chapter 1). Observations in the Witwatersrand gold field have shown that as the stope faces approached dykes and faults, the incidence of rock bursts increased, Figure 3.4.4 (Hill and Denkhaus, 1961). They indicated that when the stope face reached a distance of 15 m from the dyke, the incidence of rock bursts increased rapidly. It was also noticed that the incidence of rock bursts was greater in the case of thick dykes than in the case of thin ones. Cook et al. (1966) indicated that the effect of the dykes and faults was more obvious when they were in small abutments (such as remnants or island abutments) (See Section 3.2.3).

It is believed that dykes cause a concentration of stresses in the surrounding area, consequently the frequency of rock bursts increases (Lama, 1967). He stated that "the rise in temperature, metamorphism and re-crystallisation of rocks occurring near the dykes have an effect of increasing the inherent energy and homogeneity of the rock mass".

5. The presence of folds

Peng (1978) stated that when a regional horizontal stress causes strata to fold, secondary local stresses are induced in the neighbourhood of the anticline and syncline. Tensile stress is generated at the crest

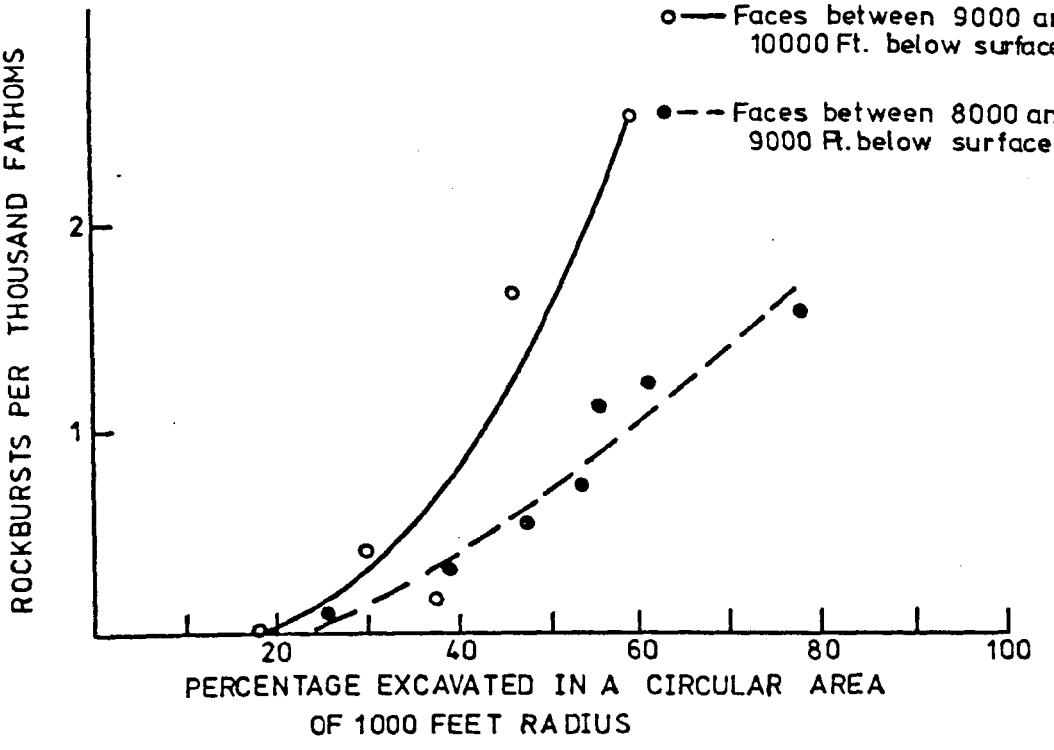

Fig. 3.4.3. The relationship between rock burst incidence and the relative excavation size at different depths in the Witwatersrand gold mines. (After Cook et al., 1966).

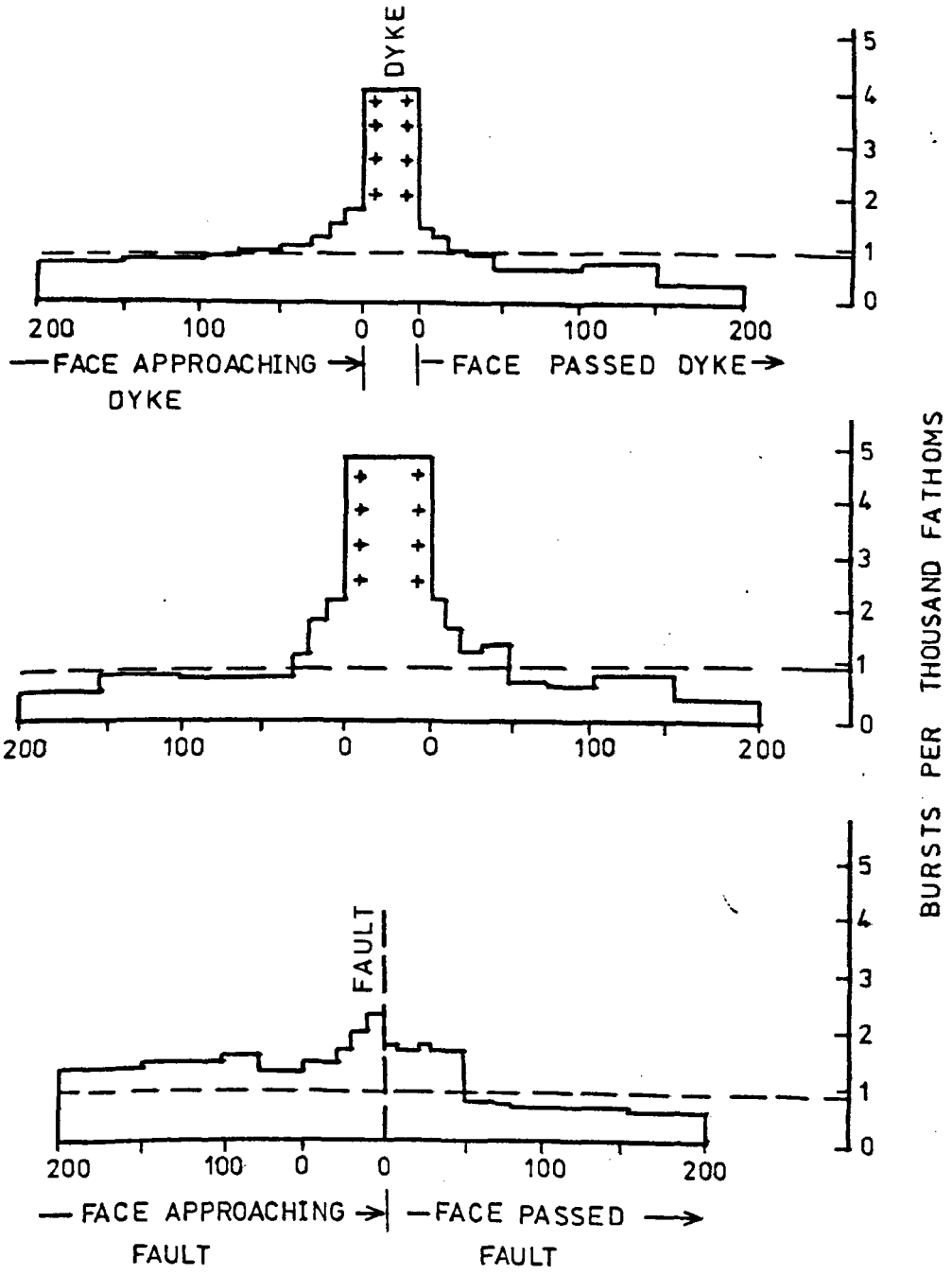

Fig. 3.4.4. The effect of dykes and faults on rock burst incidence in the Witwatersrand gold field. (After Hill and Denkhaus, 1961).

of the anticline creating tension joints. In the synclinal area, local compressive stress occurs in the trough, which develops shear joints. Lama (1967) also indicated that the syncline is associated with very high stresses. He gave examples of the occurrence of rock falls and bursts during mining in a synclinal area. He reported that cross-cuts driven at the base of small synclinal folds were very difficult to maintain and as they passed through the synclinal region the trouble ceased.

In the Upper Silesia coalfield, Neyman (1955) noticed that the rock bursts occur less frequently and less severely in the mines situated in the main anticline. He explained this as being due to the anticlinal shape of the uplift, the presence of numerous faults, and the shallower depth of the seam than in the syncline, which did not favour the accumulation of elastic strain energy inside the seams.

6. Pore pressure and moisture

Beneath a flat homogeneous ground surface, the ground water will form a level water table, below which all the pores are saturated, and above which they are only partially so. The water table might be close to the surface or be at a depth of several hundred metres below it. This will depend on the relative values of rainfall, permeability, and local topography. The pore pressures beneath the water table rise hydrostatically with depth, assuming all pores are inter-connected by highly permeable paths, and above the water table they will be approximately zero. Variation in rainfall results in fluctuations in the water table height, and this will consequently affect the value of pore pressures.

It has been found that the most important effect of the pore pressure upon the mechanical properties of the rocks is to reduce the frictional resistance of the sliding block (Hubbert and Rubey, 1959). The reduction of friction is achieved by reducing the normal component of effective stress which correspondingly reduces the critical value of

the shear stress required to produce faulting. According to Hubbert and Rubey, for porous fluid-filled rocks the Mohr-Colomb criterion for failure must be modified to the form:

$$\tau_{crit.} = \tau_0 + (\sigma - P) \tan\phi \qquad 3.4.4$$

where $\tau_{crit.}$ is the critical shear stress required to cause failure.

τ_0 is the initial shear strength of the rock when the effective normal stress is zero.

σ is the normal stress.

P is the pore pressure.

$\tan\phi$ is the coefficient of internal friction.

$\sigma - P$ is the normal effective stress.

In addition to the effects of internal fluid pressure in reducing the effective stress, the pore fluid without pressure (moisture) can have a significant influence upon the strength of rock (Bell, 1975; Hoek and Brown, 1980). It has been found that the strength of samples of shale and sandstone was reduced by a factor of 2 from oven dried to saturated specimens.

In many places seismic activity has been related to the filling of large reservoirs (Simpson, 1976; Gupta and Rastogi, 1976). The activity ranges from micro-earthquakes to destructive earthquakes. Simpson (1976) and Beale (1981) indicated that the occurrence of reservoir induced seismicity is related to the water height and, to a lesser extent, the water volume. On the other hand, the filling of many other large reservoirs has not been accompanied by increased seismicity. Simpson (1976) suggested that the filling of a large reservoir creates stresses which are superimposed on a pre-existing tectonic stress regime. Whether or not seismicity is generated, depends on the way in which these stresses interact within the tectonic, geological and hydrological environments. The reservoir changes

the stress regimes in such a way that it increases the vertical stress due to the weight of the water mass (the load effect), and decreases the effective stress (and therefore strength) due to increasing pore pressure (the pore pressure effect).

The significance of pore pressure changes in generating induced seismicity has been clearly shown for the cases of seismicity related to high pressure fluid injection (Raleigh et al., 1976; Healy et al., 1968). In these cases where any loading effect is minimal, the seismicity can be properly explained by the reduction of effective stress due to increased pore pressure as described by Hubbert and Rubey (1959). Simpson (1976) indicated that the increases in pore pressure involved in the cases of fluid injection (a few hundred bars) are much higher than those created by a deep reservoir (1 bar/10 m height of water, or a few tens of bars). Simpson also indicated that in the cases where fluid injection has triggered earthquake activity (Denver, Rangely, Matsushiro), injection has taken place into, or very near, a fault zone.

As indicated above, the association between fluid injection and seismicity has been well established. Less well known are the relationships between seismicity and fluid extraction, particularly with regard to petroleum production (Yerkes and Castle, 1976). Yerkes and Castle reported two certain cases of faulting and seismicity associated with oil extraction in the U.S.A.; the Goose Creek oil field, Texas, and the Wilmington oil field, California. The earthquakes of Goose Creek oilfield occurred in 1925 and were closely associated with surficial displacements along steeply dipping faults that were localised along the margins of the subsidence area. In the Wilmington oil field, eight separate seismic events, occurring between 1947 and 1961, were accompanied in each case by subsurface faulting within the oil field. Yerkes and Castle attributed the faulting and seismicity associated with oil extraction to differential compaction at depth caused

by reduction of the reservoir oil pressure and attendant increase in effective stress. Differential compaction leads not only to differential subsidence and centripetally directed horizontal displacement, but to changes in both vertical and horizontal strain regimes.

The effect of pore pressure on generating mining induced seismicity has not been described or investigated to date. Mining induced seismicity differs from reservoir induced seismicity in that reservoir induced seismicity is generated or triggered due to changes in the stress fields resulting mainly from filling the reservoir, while mining induced seismicity is generated due to changes in the stress fields resulting principally from differential elasticity between the artificial excavation and the surrounding rocks. The magnitude changes in the stress field, compared with that of the virgin state, associated with mining may be several orders of magnitude greater than that associated with reservoir loading. Underground mining may be associated with water extraction from the strata overlying the working level. This will lead to the increase in effective stress and strength of the rock. Consequently the rocks will become able to withstand greater pressures before they fail. However a pronounced correlation between rainfall and rock burst incidence was noticed in the Kolar goldfield by Isaacson (1957). He explained that the seepage of water underground caused the decay of old supports in the upper level workings, or alternatively have caused the lubrication of various planes of weakness along which potential failure occurred. However, this correlation between rainfall and rock bursts could be re-interpreted as due to the effect of pore pressure. Peng (1978) also indicated that water in the mine will soften some floor rock and cause subsidence or heaving problems. He explained that the effect of moisture in a coal mine is more serious because of the abundance of shale and the cyclic nature of moisture content in the air. Weiss (1938) suggested that much of the slabbing and flaking of rocks in

the Witwatersrand gold mines were probably partly due to the moisture content acting through the fissures produced by mining operations. He suggested that if this flaking and slabbing continued, it could result in a reduction in the size of the pillars, and eventually the pillars might become unable to withstand the overlying pressure, and failure would occur.

3.5 The prediction of rock failures

One of the most promising features of the microseismic method is to forecast when and where rock failures will occur. Long ago, miners used to predict failure from natural warning signals such as creaks, pops, and snaps, which were an indication of excessive pressure in the mine. Obert and Duval (1945) pointed out that all rocks subjected to stresses approaching their ultimate strength, generate microseismic activity (rock noises). The number of microseismic events generated per unit time (the microseismic rate) increases as the time of failure approaches, i.e. increases with the applied stress. According to this concept, Hooker et al. (1974) and Leighton and Stebly (1977) suggested that the recording and analysis of microseismic activity is a useful stability analysis tool, because stable areas of a mine structure release very few rock noises at a constant rate, while unstable areas release large numbers of rock noises at varying rates.

The key to using the microseismic method in prediction lies in its ability to detect and locate precisely in three dimensions the source of the rock noises. Consequently, the area expecting rock failure can be determined by constructing rock noise source location plots. Usually seismic noises occur near the area being mined and if this area is stable, the noises do not recur at the same location on consecutive day plots, but progress with the mining. However, if the noises are generated by unstable areas, they will recur at the same location each day. By monitoring the changes in the rate of microseismic activity when the rock approaches failure, the time of failure can be estimated. During mining operations in a stable area, the total number of microseismic events released during a working shift does not change dramatically from day to day. As an area is subjected to increasing stresses or is becoming unstable, the rate at which rock noises are generated in that area increases. Prior to failure, the

rate of microseismic activity changes rapidly. Experiments have shown that failure areas generate seismic noises several days in advance of failure. Cumulative plotting of seismic events on mine maps was found to be very effective in determining where failure is going to occur. The method was conducted by adding the data from one daily plot to the next one, starting at one particular point in time. Figure 3.5.1 shows a cumulative plot of the rock noises in an area preceding the occurrence of a rock burst. It can be seen that the number of microseismic events increased daily and concentrated in one particular area although the mine workings moved. Therefore this area was considered to be a potential area of failure, and a rock burst occurred on 30th April. As we can see from Figure 3.5.1a, the failure area becomes evident nearly four weeks prior to final failure. Figure 3.5.2 shows the rock noise rate plot. It can be seen that a sharp increase in noise activity started one week before failure.

The authors suggested that by using this method, and with experience, it may be possible to predict where and when failure will occur.

The same method was used by Blake (1972) to locate the zone of impending failure during pillar extraction in the Galena mine, Idaho.

On the same basis as discussed above, the U.S. Bureau of Mines conducted experiments on controlled roofs (Leighton and Steblay, 1977). They found that there was usually a background of microseismic events emitted from the roof. About an hour before the roof failed, there was a sudden increase in the rate of microseismic events, followed by a decrease. Failure then occurred about 15 minutes later.

3.6 Preventing and combating rock bursts

The problem of rock bursts arises mainly due to the effect of the large stresses generated by mining. Consequently the methods of preventing and combating rock bursts depend basically on finding and applying ways to eliminate or reduce the additional pressures in the mine. However, these

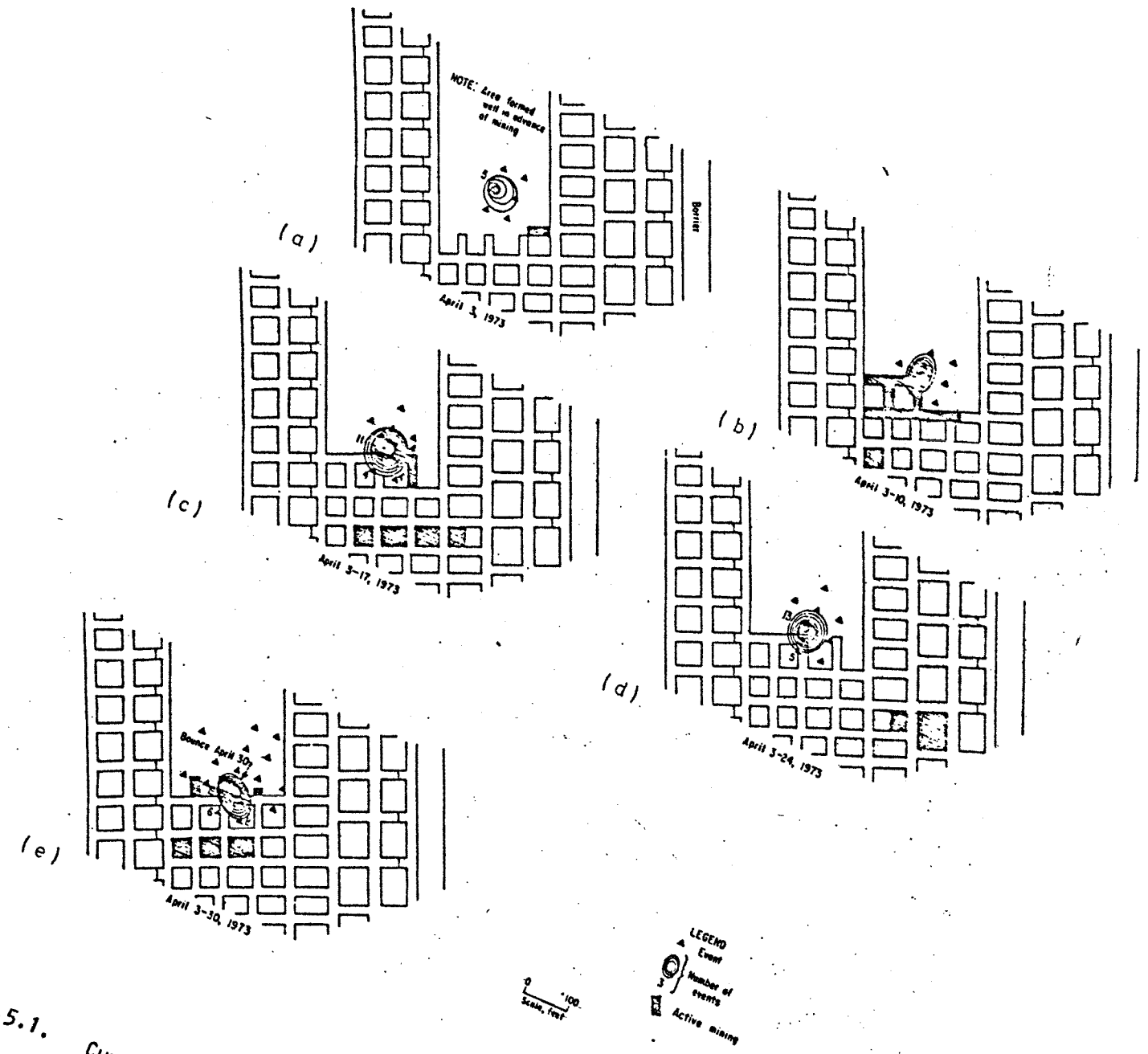

Fig. 3.5.1. Cumulative rock noise location plots showing growth of rock burst (or bounce). (After Leighton and Steblay, 1977).

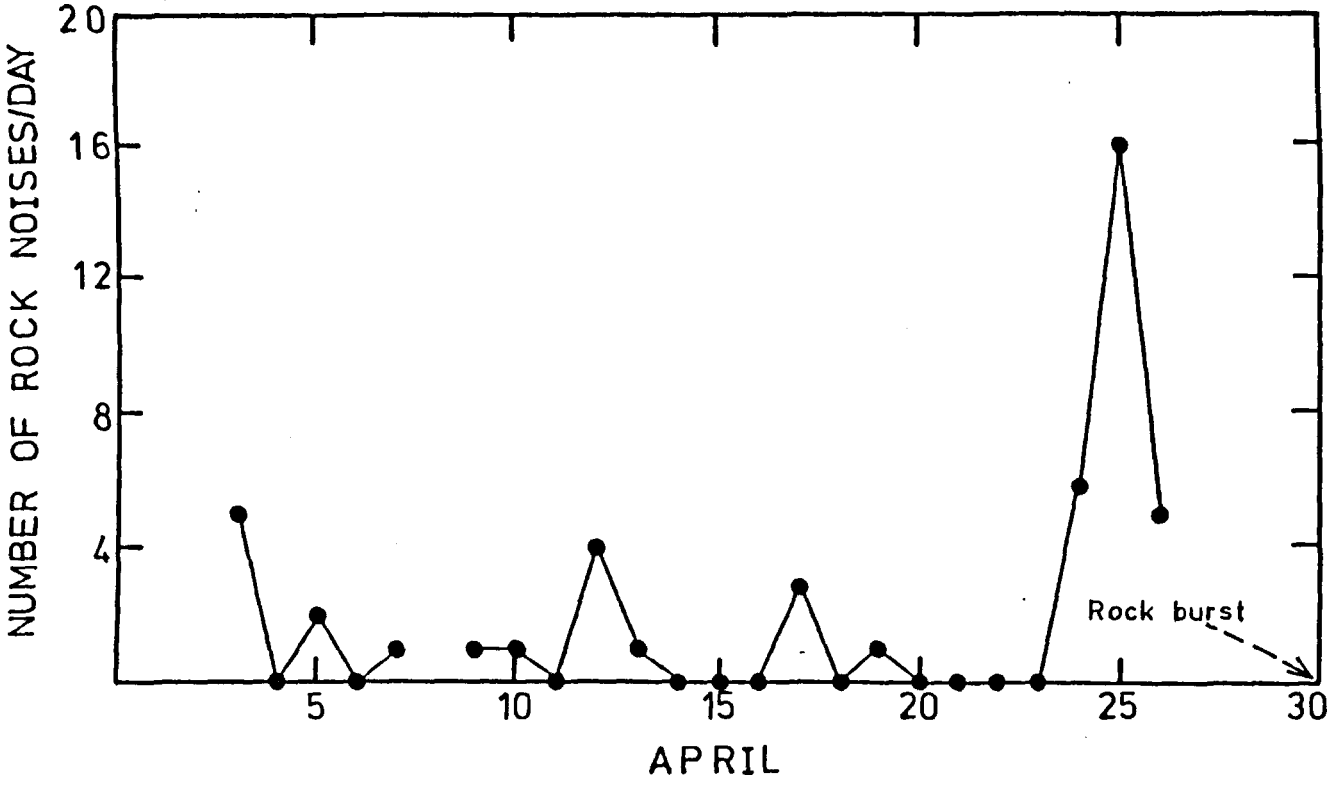

Fig. 3.5.2. Development of rock noise rate associated with the rock burst shown in Fig. 3.5.1. (After Leighton and Steblay, 1977).

methods do not entirely prevent the occurrence of rock bursts but reduce their occurrence and restrict their consequences in the mine.

3.6.1 Preventing rock bursts

Prevention usually means taking some measures aimed at preventing or reducing the occurrence of excessive pressure during mining, and consequently reducing the chance of rock burst occurrence. Most of the stress-raising factors are known and should be taken into consideration when planning the extraction of a new seam or mine. The literature contains many procedures and examples used in mines to prevent or reduce the occurrence of rock bursts. However, some general points can be deduced.

1. Planning of the mine layouts should take into consideration the effect of factors such as old workings, faults and dykes.
2. The mine layouts should provide for pillars of uniform size and shape.
3. Pillars should be recovered in a straight line. An irregular line of pillars results in excessive pressures being exerted on the protruding points.
4. In the room and pillar method, all coal should be recovered, i.e. the practice of leaving pillars in the goaf should be avoided.
5. Roof span over the goafs should be kept as short as possible by providing adequate supports or allowing the roof to cave in.
6. The use of longwall mining techniques is preferred wherever possible.
7. Reducing additional pressure by mining the panel over or under a previously mined out area in the adjacent seam.

3.6.2 Combating rock bursts

Combating means to use methods during the mining operations in order to attain controlled release of the excessive pressure already in existence in some parts of the mine, or to safely trigger the rock burst (Peperakis, 1958; Krawiec and Stanislaw, 1977). Different methods are used.

1. Shock blasting: Basically this method involves drilling a series of boreholes perpendicular to the face prone to bursts and blasting them with the intention of stimulating rock bursts or shattering the rocks. The shattered rocks cannot store high energy and the high stresses are pushed back further inside the face. Therefore the face can be advanced for some distance without any danger. This method is used in the Witwatersrand gold mines (Hill and Denkhaus, 1961), in Czechoslovakian coal mines (Sebor et al., 1976) in Polish coal mines (Krawiec and Stanislaw, 1977), and in U.S. coal mines (Peperakis, 1958; Talman and Schroder, 1958).

2. Injection of water: It has been found from experiments that the tendency of a coal seam to burst decreases with its increasing moisture content (Krawiec and Stanislaw, 1977). For this reason the injection of water under great pressure is widely used in Polish coal mines. The water is injected through boreholes driven perpendicular or parallel to the burst-prone face.

3. Drilling de-stressing holes: This method is usually conducted by drilling vertical or horizontal holes through the seam in order to break the coal and relieve the stress. This method is used in Russian, West German (see Chapter 1), and in Czechoslovakian coal mines (Sebor et al., 1976).

CHAPTER 4

THE NORTH STAFFORDSHIRE SEISMIC NETWORK

4.1 Introduction

In North Staffordshire, earth tremors which are known locally as "goths or bumps" have occurred occasionally since the latter part of the last century (Davison, 1919). In early 1975 some small tremors were felt by the local residents in the Trent Vale-Hanford area, in the south of Stoke-on-Trent. Westbrook (1977) recorded some of these tremors using a three component set of seismometers operated on behalf of the National Coal Board (N.C.B.)

On the 15th July, 1975 a strong temor occurred and was felt over an extensive area of Stoke-on-Trent causing some damage to buildings in the Trent Vale-Hanford area. The intensity of this tremor was 6 on the Modified Mercalli Scale, and of local magnitude, M_L 2.8, as estimated by the Institute of Geological Science (I.G.S.) Lownet seismic network (Kusznir et al., 1980a). Analysis of the macroseismic survey carried out by the Global Seismology Unit of the I.G.S. suggested that the depth of this tremor was less than 1 km, and consequently at the same level as the mining operations which were being carried out in this area. The Ten Feet coal seam was being mined at a depth of about 900 m. This tremor was the largest one in a series of tremors which had been felt in the area throughout early 1975 and continued to be felt until August 1977 (Westbrook, 1977; Kusznir et al., 1980a).

On the same day another tremor occurred and was felt in the Knutton-Silverdale area to the west of Stoke-on-Trent. However, the occurrence of earth tremors in this area died away during autumn 1975 (Westbrook et al., 1980).

The frequent occurrence of earth tremors in the Trent Vale area suggested that they may be connected in some way with the extensive mining operations conducted in the area (see Chapter 7). However, further investigations were necessary before this relationship could be established.

4.2 Stoke-on-Trent seismic network (S.O.T. network)

Following the event which occurred on 15th July, 1975, and in response to public concern, the Global Seismology Unit of the I.G.S., with the co-operation of the Department of Geology, Keele University, installed a seismic network in Stoke-on-Trent. The objective of the network was to monitor seismic activity in the area and to try to find the cause and mechanism of these tremors. The network was originally designed to provide accurate locations for tremors in the Trent Vale-Hanford and Knutton-Silverdale areas (Westbrook et al., 1980).

The monitoring network consistedof five vertical component seismometers deployed in the Stoke area in a square array having an interior station, and diameter of about 8.3 km and encompassing the mine workings in the Trent Vale area. The three dimensional co-ordinates of each seismic station, the station delay times (see Section 4.6), the Amplifier/Modulator gain, and the amplification are shown in Table 4.1. The seismic stations were named according to their location. Keele station (K) measured north-south and east-west horizontal components in addition to the vertical component.

Figure 4.2.1 shows the position of the seismometer stations, the recording station, the mine workings during the monitoring period and the major structural features in the area. It can be seen that most of the active mine workings are located outside the boundary of the network. Each of the seismic stations contained a short period seismometer (with a natural period of 2 seconds) and Amplifier/Modulator, and were housed in a pit with a concrete base built for this purpose, or in outbuildings with a concrete floor. The latter facilitatedrapid installation of the network following

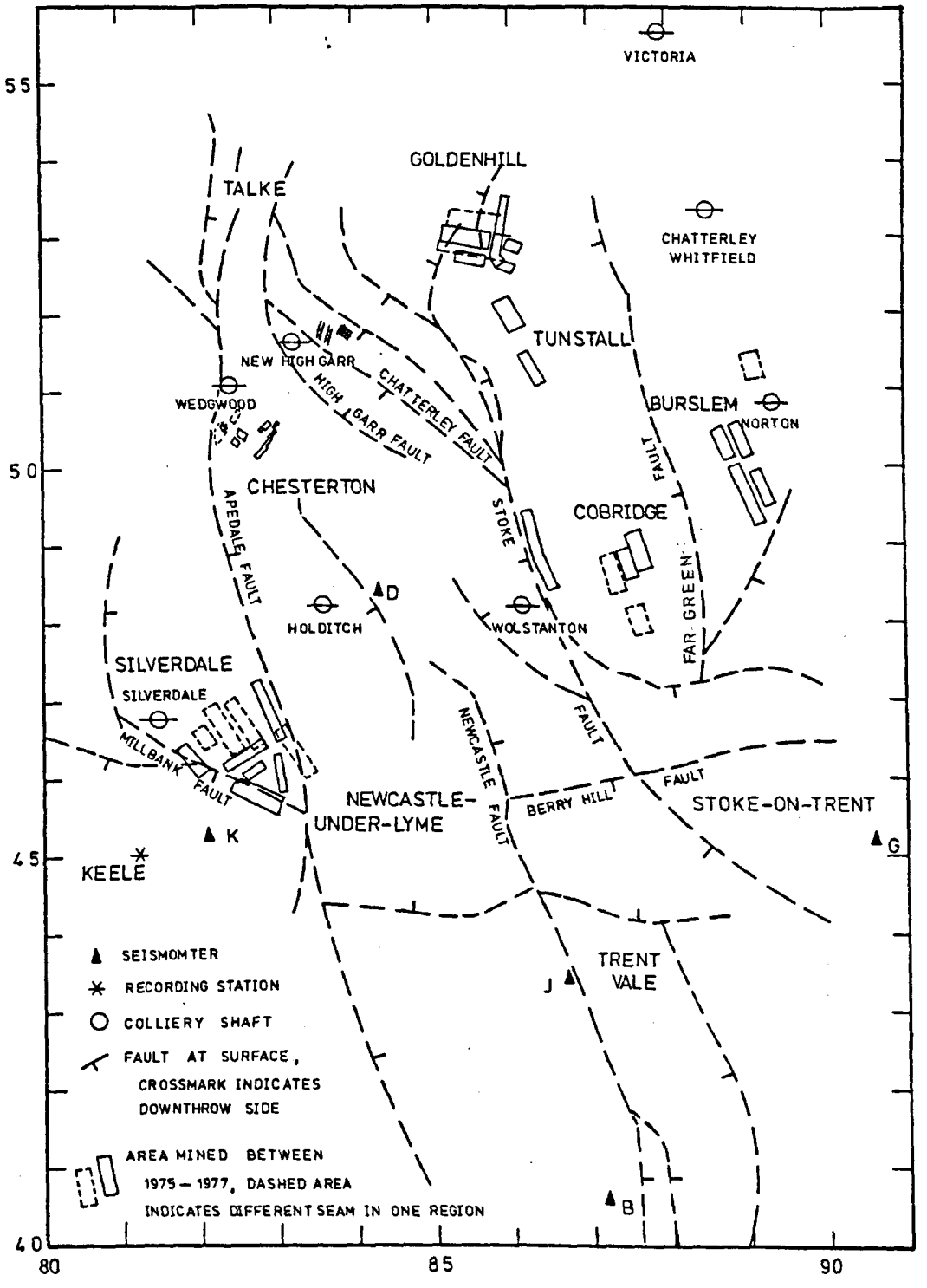

Fig. 4.2.1. Map showing the positions of the active mine workings, major surface faults, seismometer sites, seismic recording station and the colliery shafts in the northern part of the North Staffordshire Coalfield.

Table 4.1

The co-ordinates, delay time and amplification of the seismic stations

Station Name	Code	Northing (km)	Easting (km)	Height above O.D. (km)	Delay Time (sec)	Gain of A/M	Amplification
Dimsdale	D	48.41	84.34	0.155	+.015	5	120
Keele	K	45.25	82.15	0.203	-.010	5	120
Greenhill	G	45.25	90.63	0.189	-.004	4	48
Saint Joseph	J	43.45	86.78	0.125	-.010	4	48
Barlaston	B	40.60	87.23	0.130	+.016	4	48

the event of 15th July, 1975. The electrical output signal from each seismometer, proportional to the velocity of ground movement, was amplified, converted to a frequency modulated tone, and then transmitted via a U.H.F. radio transmitter or via cable to the central recording station at Keele University. At Keele the seismic data from all the seismometers were recorded on a 14 track, half inch magnetic tape with a common time code. The three-component set of seismometers at Keele station (K) were connected to the main recorder by military field telephone cables. The other four stations were telemetered to the recorder via a line of sight U.H.F. radio link.

The advantages of radio-linked stations are that their seismograms are recorded on the same tape, with a common time coding, saving tapes and making the handling of the recorded data more convenient. Another advantage is that the distance between the seismometer and the recorder can be increased up to 100 km. For a land line the transmission may be effective up to 10 km if the Amplifier/Modulator is powered by a separate battery, or up to 3 km if it is powered from the central recording site through the data line.

The use of magnetic tape allows considerable flexibility in processing the recorded data, e.g. choosing different pass-band filters on playback to obtain the most convenient record.

During the installation of a seismic network, several considerations must be taken into account. These are:

1. The geometry of the seismic network should be such that the earth tremor hypocentres can be well defined in both epicentral position and depth, i.e. there must be a wide variation in range and azimuth of the stations from the epicentre.

2. The seismometer sites should be chosen so that noise from various non-seismic sources, such as traffic, wind and machinery are minimal.

3. The seismometers should be installed as close as possible to bed rock to ensure good coupling between the seismometers and the ground.

4. The seismometers and the tape recorder must be secure from theft and damage.

5. The recording site should be chosen to provide easy access for frequent visits. (The recording station for the S.O.T. seismic network was near the Department of Geology, Keele University).

4.3 Instrumentation

Instruments may be divided into those forming part of the detection/tape recording system, and those of the play-back system. Figure 4.3.1 shows a typical layout of the seismic network, detection/tape recording instruments, in the field. The play-back system was used entirely separately to replay the recorded seismic data and to produce visual seismic records.

4.3.1 The detecting instruments (seismic stations)

The instrumentation at each station consisted of a vertical seismometer, an Amplifier/Modulator unit, and a U.H.F. radio transmitter.

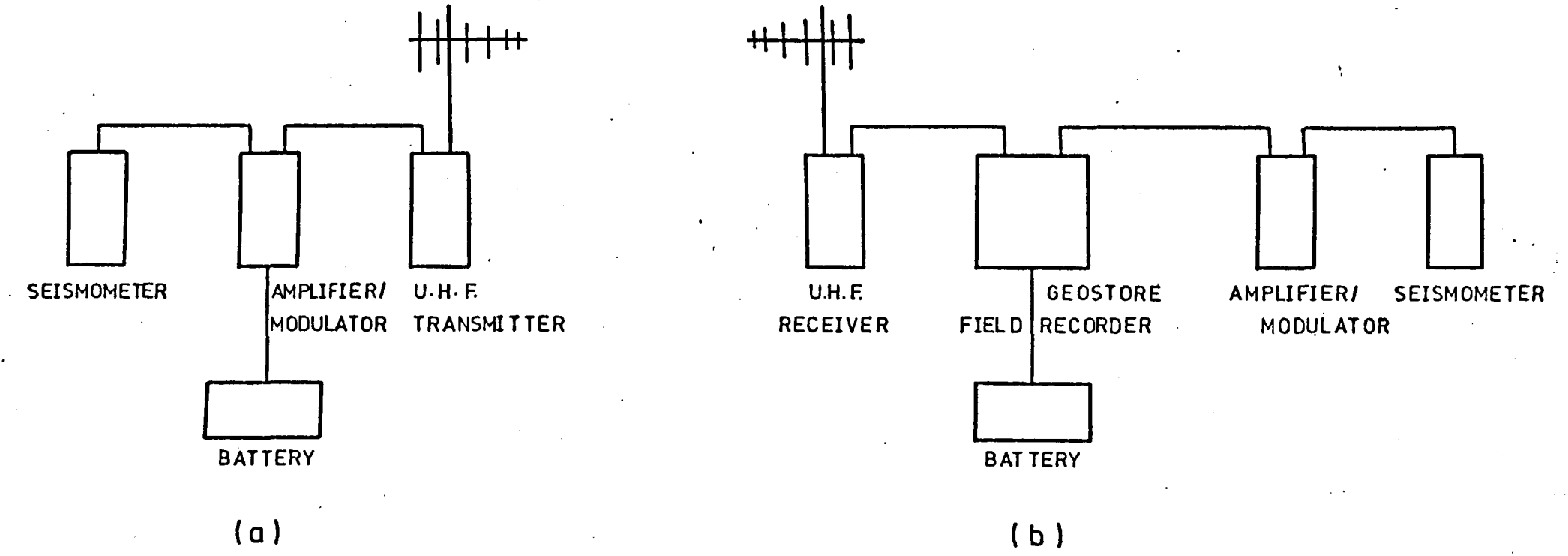

Fig. 4.3.1. Typical layouts of the seismic network, detection and recording system.

(a) Radio-linked outstation.
(b) Cable-linked outstation.

(i) Seismometer: Willmore MKII short period seismometers with a natural period of 2 seconds were used to detect earth tremors. The device consists of a magnet suspended by a spring set to move only in the axial direction and a coil fixed to the instrument's case. When in use, the case is firmly fixed to the ground. Provided that the coupling between the seismometer and the ground is good, relative motions between the magnet and the coil occur as the seismometer frame vibrates in sympathy with the ground motion, so inducing an E.M.F. in the coil. The electrical output from the seismometer is directly proportional to the ground velocity. The natural period of the oscillation can be adjusted within the range of 0.6 to 3.0 seconds with the instrument in a vertical position, and to 5 seconds when it is installed horizontally. The sensitivity of the instrument is approximately 5.7 volts/cm/sec. when fitted with a 3,300 ohm coil. The instrument has the ability to detect ground movements of the order of 10^{-7} cm.

(ii) Amplifier/Modulator Unit: This is used in conjunction with a seismometer at the seismometer site (in the field). The function of this unit is to amplify and to then convert the seismometer output signals to a frequency modulated signal (centre frequency 676 Hz) suitable for line or radio transmission and direct recording onto magnetic tape. The unit has ten switched gain ranges, such that ± 40% frequency deviation is produced by an input voltage of 0.25 mV at gain 10 to 250 mV at gain 1. The ground motion is therefore represented by deviations in the frequency of the carrier wave signal. The optimum gain setting can be selected depending upon the site noise level and the expected seismic wave amplitude. The unit is usually supplied by a direct current carried over the data lines from the recording station, or in the case of a radio link station, through a separate power supply.

(iii) U.H.F. Transmitter: When a radio link station was used, the output signals from the Amplifier/Modulator were fed to a small U.H.F.

transmitter. The cable also carried the power required to operate the transmitter. The transmitter was housed in a metal can attached to an aerial mast with a multi-element Yagi antenna directed towards the central recording station.

4.3.2 The recording system

The recording equipment consisted of four U.H.F. receivers, a magnetic tape recorder, a radio receiver, and a field test box.

(i) U.H.F. Receiver: The radiated signals from the outstation were received by a U.H.F. receiver via another multi-element Yagi antenna installed at the site of the central recording station at Keele University. The signals were then fed to the recorder through a multi-core armoured cable.

(ii) Magnetic Tape Recorder: The tape recording unit used was a Racal-Thermionic Geostorefield recorder. It is housed in a weatherproof aluminium cabinet which can be operated in a wide range of environmental conditions. The recorder has been designed to record frequency modulated data over a long period with very low power consumption. It accepts FM input signals with a centre carrier frequency of 676 Hz, and maximum linear deviation of ± 40%.

The recorder has 14 tracks, 11 of which are available for data. Two provide flutter compensation to improve the signal to noise ratio, while the other one carries the time code. It has an internally-generated and crystal-controlled time encoder having an accuracy of better than one second per week. The time encoder produces a train of pulses at intervals of one second recorded on channel 2 in accordance with Vela Uniform Code, with a one minute time frame. An external check facility has also been included whereby a radio time signal can be recorded on one data channel. The time signals can be recorded continuously or intermittently, controlled by an option switch.

The recorder is used with 2400 ft (731 m) of half inch (12.5 mm)

magnetic tape wound on an 8 inch (20.3 cm) spool. It has three recording speeds, 15/640, 15/320 and 15/160 inch/sec., giving maximum recording times of 680, 340 and 170 hours respectively using bidirectional recording. Bi-directional recording can be used only if not more than five data channels are being used. Conductive marks are used to provide end-of-tape and auto-reverse signals. Each recording speed has a particular bandwidth frequency. The recorder requires a 12 volt power supply (normally a standard car battery). Facilities are available for changing batteries without disturbing the recording or the time code.

(iii) Radio Receiver: A short wave radio receiver was used to receive the MSF time signals transmitted from the Rugby radio transmitter. The received signals were fed into the recorder through the radio input terminal to be recorded continuously on channel 14, after being amplified and frequency-modulated. This recorded time signal is used as an absolute time check.

(iv) The Field Test Box: This was used to monitor the frequency-modulated tone of each channel and to verify correct functioning of the equipment.

4.3.3 The playback system

To recover the seismic events detected by the seismometers and recorded on the central recording station, the tape must be played back and the frequency modulated signals must be demodulated and displayed in a visible form. The playback system consistedof two parts:

(i) The playback unit: This was a 14-channel Racal Store reproducer. The signals are demodulated and flutter compensated on replaying. The output is 1.2 v for full ± 40% frequency deviation. Seven tape speeds were available from 15/16 in/sec. to 60 in/sec. The instrument was fitted with a four digit counter and reset button. The counter indicates the length of the tape used in feet.

(ii) The Jet Pen or Chart Recorder: An eight channel Siemens Jet Pen Recorder was used to obtain the visual transcriptions of the tape data. The output signals from the playback unit were fed into the jet pen on which the signals were reproduced in a visible form on paper. The ink trace is made by directing a fine jet of ink at a moving paper chart. The jet pen has variable gains and paper speeds. Headphones were also connected to the store 14 output in order to listen to the seismic events.

4.4 The seismic network operation

The network was operated for two years in the period between September 1975 to September 1977. The recording equipment was operated 24 hours a day during most of the monitoring period, except for brief periods when the tapes were being changed.

Since the seismometers were sited in urban areas, a low signal to noise ratio was expected. The gain of the Amplifier/Modulator was set at different levels at each seismometer site (see Table 4.1). During the data processing, the noisiest records were obtained from the seismometer sited at Greenhill (G). The tapes were recorded at 15/320 inch/sec. to give a maximum recording time of one week. However, sometimes the speed was reduced to 15/640 inch/sec. to give a longer recording time, particularly during holidays. The frequency response for these two speeds are 32 Hz and 16 Hz respectively as shown in Figure 4.4.1. A log was kept containing the tape number, date and time of changing the tape, the tape recording speed, the stations and time channel numbers, the date and time of battery change, and the faults or maintenance to the network during the recording life of each tape. This log book was used during the data processing for checking.

Data on about ten tapes recorded early in 1976 and having a total recording time of up to two months were lost due to the cross-interference of the output signals from three stations, K, D and G. Further data were lost from about twelve tapes recorded during 1975 and early 1976 having a

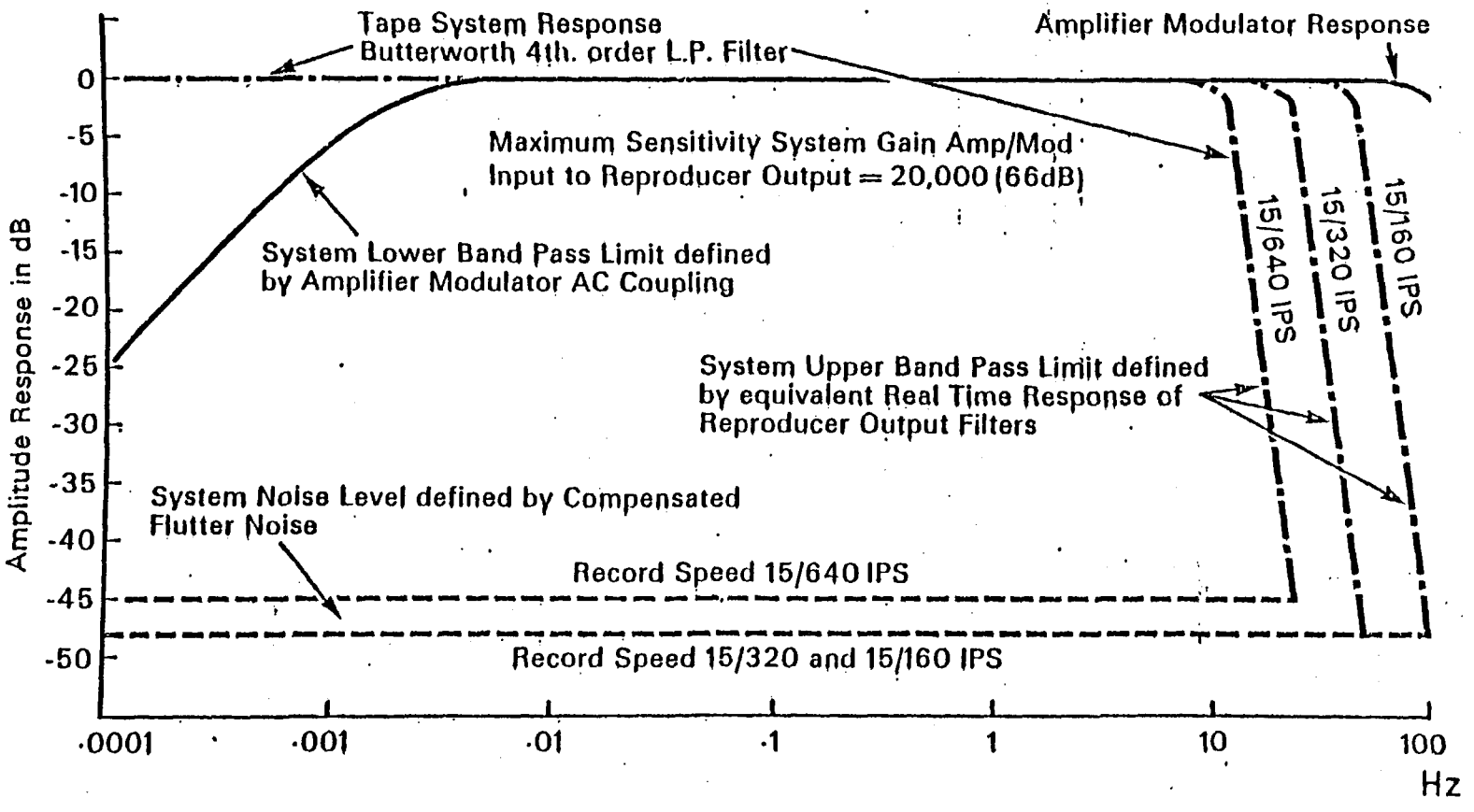

Fig. 4.4.1. Overall Geostore system frequency response (excluding seismometer). (Taken from Racal-Thermionic Limited).

total recording time of about two and a half months, due to the interference between two stations; either K and D or D and G. However, about 20 events were identified on these latter tapes at four stations only. The output signal from D station was the most powerful, overlapping signals from the K or G stations. An attempt was made to separate the D station output signals from the output signals of K and G stations. However, the attempt failed due to both signals having the same frequency.

4.5 Data analysis

The recorded magnetic tapes were initially played back at about 40 times the speed of the original tape recording, using a relatively slow jet pen paper speed to produce visual records. The visual records were used for rapid identification of local seismic events. An event can be easily distinguished from any other nearby non-seismic source, such as lorry noise or small quarry blasts. The seismic events were usually recorded at three or more seismic stations, while noise was usually recorded on the nearest seismic station only.

The date, the number of the tape, the paper page number, the approximate tape length position, and the approximate location (i.e. north or south of Stoke) of the identified seismic events were listed in a file. The identified events were then played back at slower tape speed and faster paper speed to give more detailed records of the events. Since the jet pen has only 8 tracks, each seismic event was replayed twice to give two records. One record showed the seismic data obtained from the five vertical seismometers. The other one showed the Keele (K) three-component set siesmograms. Great care was taken to eliminate errors caused by the alignment of the jet pens.

The arrival times of the seismic waves were then measured and the polarity of the p-wave first arrivals were identified. The maximum amplitude and the frequency of each seismic wave were also measured.

4.6 Determination of the local velocity structure

The seismic velocity structure for the Trent Vale area, as determined by Westbrook (1977) was used initially to locate the seismic events in the northern part of the coalfield. The velocity structure for the Trent Vale area was determined initially from sonic logs in boreholes drilled for the N.C.B. in the area. It was found that the velocity increased linearly with depth (Westbrook et al., 1980). This velocity structure was later revised by using the joint hypocentre determination (JHD) method. The method involves the relocation together of a group of seismic events located in the same region, with the velocity structure treated as extra unknown parameters (Westbrook et al., 1980). For further checking a 45.5 kg explosion was detonated at a known time and in a known position. Treating the shot as an unknown tremor, Westbrook obtained a solution, using the velocity parameters derived from the JHD which placed the hypocentre within 110 m of the shot and at a depth of 300 m below it. However, using the known co-ordinates and origin time of the shot, the velocity parameters were revised and local delay times assigned to each station (see Table 4.1). The preferred local velocity structure in the Trent Vale area is 3.2 km/sec. at O.D. with a linear increase in velocity with depth of 1.2 km/sec/km.

Using the above velocity structure to locate the seismic events occurring in the northern parts of the coalfield, it was found that the seismic events were distributed mainly in five different areas (areas A, B, C, D and E). Therefore to locate the seismic events in these areas more accurately, the local velocity structure in each area needed to be determined more precisely. Due to the inability to detonate any calibration shots in these urban areas, the joint hypocentre determination (JHD) method was used to determine the velocity structure in each particular area. By using this method, the following velocity structures (Table 4.2) were obtained.

Table 4.2

The local velocity structure in different parts of the coalfield

Area Name	Code	Velocity at O.D. (VD) km/sec.	Gradient Velocity (GV) km/sec/km
Cobridge	A	3.194	1.067
Wolstanton	B	3.853	0.992
Silverdale	C	3.301	0.980
Tunstall	D	3.956	0.660
Chesterton	E	5.452	0.587

The velocity parameters for the first four areas are very similar to the velocity parameters for the Trent Vale area. These velocity parameters may represent the actual velocity structure in these areas. For area E, the velocity at datum is very high compared with the other areas, while the gradient velocity is relatively lower. This is probably due to a lithological anomaly in this area.

An alternative model was examined assuming a two layer velocity structure with a simple horizontal refractor. Although the model gave good hypocentral location for the test shot in the Trent Vale area, it was not used for the location of the seismic events. The solution put the refractor at a relatively shallow depth of about 200 m below the O.D. The geological information in the area suggests that there is no major lithological discontinuity at this depth (see Chapter 5). At the same time also, the structure of the area is more complicated than can be represented by two layers with a horizontal or even dipping refractor.

The velocity of S-waves (Vs) in the northern part of the coalfield was determined from an estimate of the ratio Vp/Vs, using the method

described by Francis et al. (1977). An estimate of Vp/Vs was obtained by finding the difference Δp in any two first arrival p-times for each event, and the corresponding difference Δs in the first arrival S-times. Since the first arrival S-times for most of the seismic events in the coalfield were very difficult to determine from the same pair of seismic stations (in our case stations K and G), the differences in arrival times (Δp and Δs) were only obtained from 12 events from all the five seismic areas in the northern part of the coalfield. The differences were plotted in Figure 4.6.1 as Δs against Δp. A regression method was used to fit a straight line through these points, which gave a ratio of $\frac{Vp}{Vs} = 2.075$. This value corresponds to a Poisson ratio of about 0.35. This value is relatively high but probably represents the true value. The area has been extensively excavated for many centuries, consequently the rocks are greatly fractured. At the same time, the lithology of the coalfield mainly consists of shaly materials which do have a high Poisson ratio. However, when the Vp/Vs ratio was determined using known high accuracy hypocentre determination in the Trent Vale area, a value of 2.03 was found, corresponding to a Poisson ratio of 0.34. This $\frac{Vp}{Vs}$ ratio gave generally lower hypocentre solution residuals.

4.7 Determination of seismic event parameters

The key to interpretation of the seismic mechanisms in mining induced seismicity is the determination of the source location of each recorded seismic event. The source of a seismic event may be defined by five parameters, namely, the latitude (or northing) and longitude (easting) of the epicentre, depth of the source (focal depth), the time of the seismic event occurrence (origin time), and the size (magnitude) of the event (Bath, 1973).

Although the various methods of locating earth tremor epicentres and foci differ in detail, they depend fundamentally upon one principle which is that the travel time of a seismic wave from the source (hypocentre) to a given point on the earth's surface is a direct measure of the distance

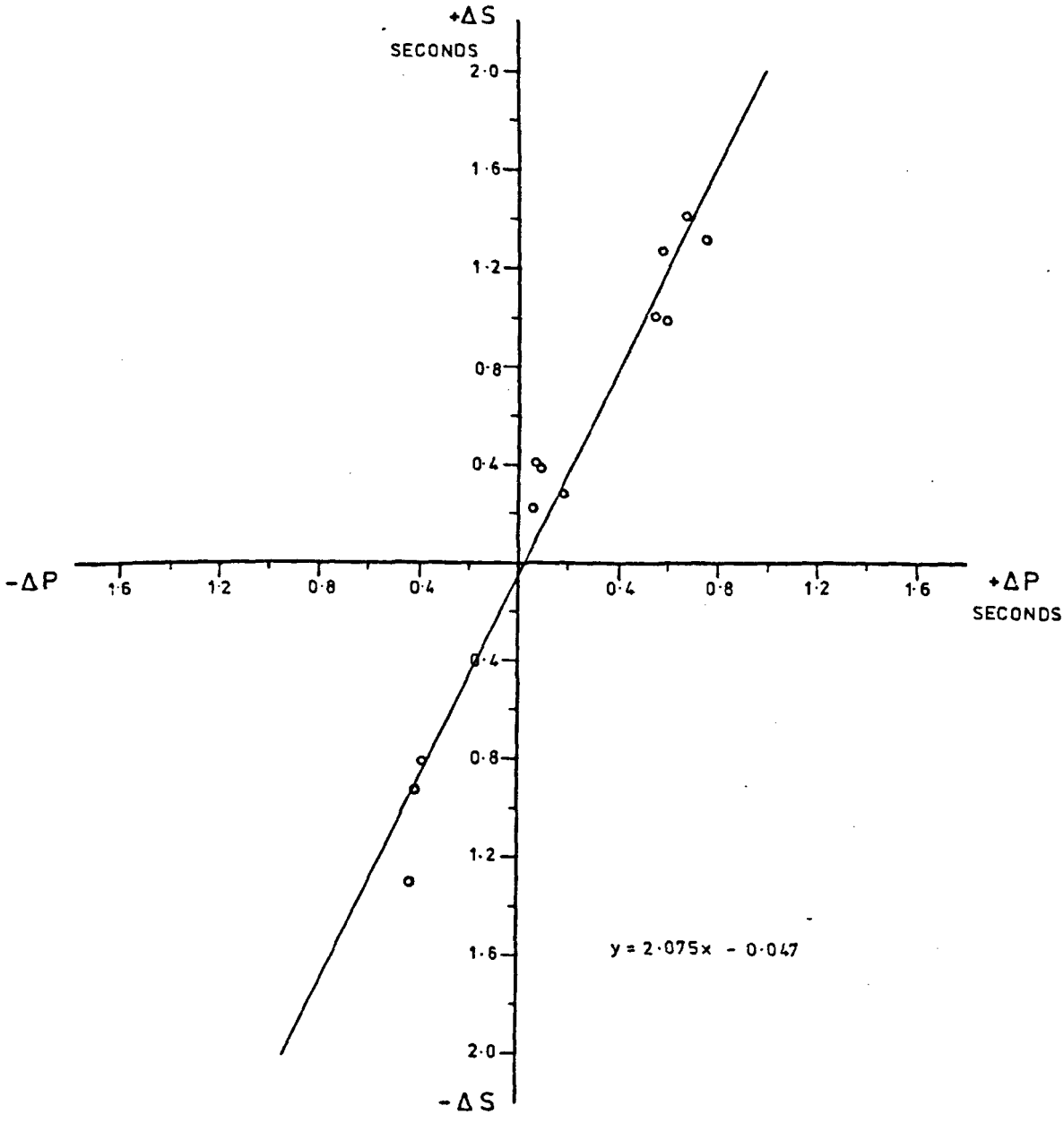

Fig. 4.6.1. Plot of S-arrival time difference (ΔS) against P-arrival time difference (ΔP). The straight line indicates that the ratio between P and S velocities is 2.075.

between the two points. The time required for the seismic waves to travel from a tremor hypocentre to the seismometer is defined as the difference between the time of the occurrence of the seismic event and the time of arrival of the seismic waves at the detecting station.

When a seismic event occurs, compressional waves (P-waves) and shear waves (S-waves) are generated in the surrounding rocks and propagate from the source in all directions. The P-wave travels with a speed of about twice that of the S-wave. Both these waves may be detected on the seismograms where the difference in their arrival times can be measured. The S-P time interval increases as the distance from the tremor hypocentre increases. If the seismic velocities of both these seismic waves are known for the media, it is then possible to calculate the distance of the seismic station from the source. This method is called the S-minus-P method, or simply the S-P method (Milne and White, 1958). Since the onset of the S-wave is mostly obscured by the train of P-waves, the S-P method is rarely used for focal parameter calculations. Computations of the seismic event parameters are usually carried out by using the fractional difference of the P-wave first arrival times at various seismic stations.

4.7.1 Graphical method

To calculate the epicentre of a seismic event we need arrival time measurements of the P-wave from at least three stations (Bath, 1973), i.e. we need three given quantities to calculate three unknown parameters (latitude, longitude, and origin time).

If a seismic network in a given area consists of three stations, A, B and C, t_1, t_2 and t_3 are the measured arrival times of the P-wave at these stations respectively. For a velocity structure with no lateral discontinuities, the bisector of the line joining any of the two stations is the foci of events which will give a zero time difference at the two stations. The lines of constant time difference between the stations are

smooth if there is a constant velocity structure, but if there is any lateral change in velocity a "kink" in the curves will result. Therefore, in areas of complicated velocity structure, it is expected to have curves with several kinks (Browitt, 1977; Banson, 1970).

Consider arrival times at three seismic stations so that $t_1 < t_2 < t_3$. For the two stations A and B, the epicentre of the seismic event must lie on a line along which the time difference t_2-t_1 is constant, i.e. the loci of constant time difference (Figure 4.7.1). Such a line is an hyperbola. A second curve having the geometrical loci of possible epicentres which correspond to a time difference t_3-t_1 can be introduced by considering the pair of stations A and C. The intersection of the two time difference curves t_2-t_1 and t_3-t_1 determines the epicentre location. This method is called the hyperbola method (Bath, 1973). In practice, the loci of constant time differences may be computed for a known velocity structure and assumed depth of focus for pairs of seismic stations in a given seismic network. A set of charts could be constructed in advance for a number of different depths of focus. The charts are usually drawn on tracing paper, so that when they are used two or more charts are superimposed over each other to give the location of the epicentre from the intersection of two or more lines of given time differences. Since the location of the epicentre in this method is determined by the intersection of two lines, the accuracy of the epicentre determination is greater if the intersection is nearly at right angles, than in the case where the intersection occurs at a more acute angle. Therefore, in order to obtain a good epicentral determination, the seismic event and stations must not be collinear (Banson, 1970). Figure 4.7.1 shows that outside the perimeter of the network the loci of equal time difference becomes almost parallel, allowing for observational errors in the relative onset data (Browitt, 1977). This results in large errors in the hypocentre determination. However, using

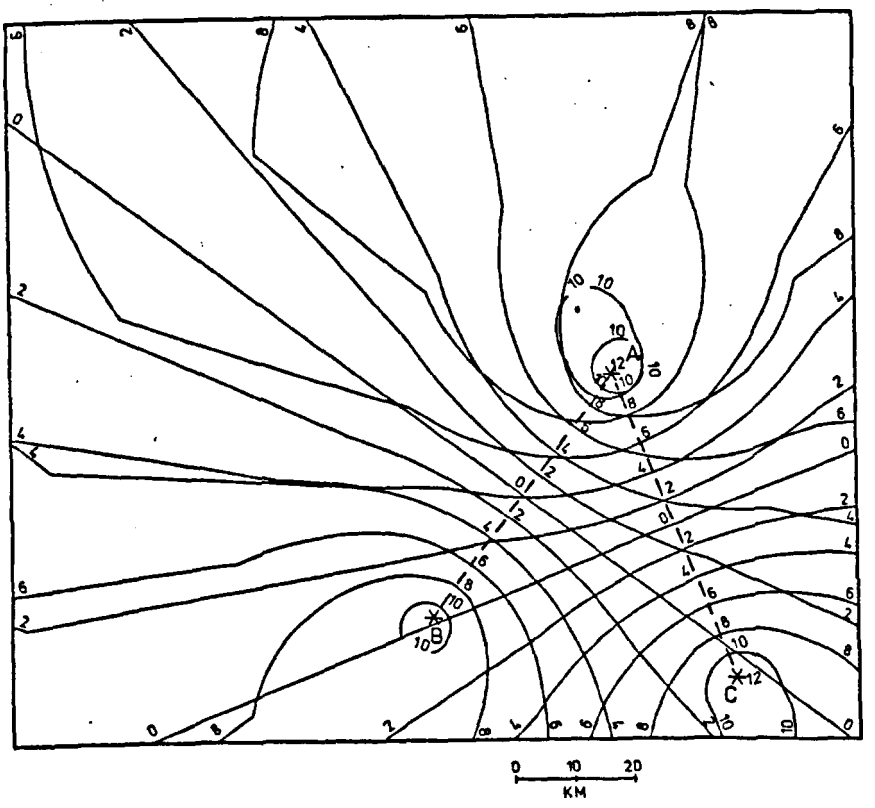

Fig. 4.7.1. Two time-difference charts obtained from two pairs of stations (stations A and B, and A and C) superimposed on each other illustrating epicentre location technique. (After Browitt, 1977).

the S-wave arrival time from at least one station can put some constraint on the solution.

If the focal depth of the seismic events is also required then the arrival time of P-waves from a fourth station is also required.

In practice, however, the graphical method of locating seismic event parameters is laborious and time consuming, and moreover inaccurate. Therefore, the epicentre and hypocentre solutions are determined analytically using a computer.

4.7.2 Analytical method

The hypcentres of the seismic events in the North Staffordshire coalfield have been located using mainly the relative differences between the arrival times of P-waves, and also using some S-P arrival times. The hypocentre location has been determined by using a computer program written by Dr. G. K. Westbrook. The program calculates the travel times for a theoretical case and compares them against the observed times, and the coordinates of the hypocentre varies until the differences between the observed and computed times become minimum (Westbrook et al., 1980). This was achieved using non-linear optimisation procedures (James and Roos, 1971), minimising an objective function which was the variance between the observed and computed times. The seismic velocity structure used in the program has a linear increase of seismic velocity with depth (Appendix 1). The depth of focus was not treated as a free variable, instead it was constrained to be less than a depth of 2 km. With no depth restraints, convergence was slow.

Initially the hypocentre for each seismic event was located individually using a single hypocentre location method (SHL) and using the seismic velocity structures obtained for the Trent Vale area (see Section 4.6). As explained before, it was found that the seismic events were located in five grouped areas.

For a particular area the JHD method was used to relocate a group of the clearest seismic events for that area. The JHD-calculated velocity

structure was then used to relocate the other events in the area.

The JHD method, as well as determining the seismic velocity structure in a particular area, improves the location of the seismic events in that area. In the SHL method the hypocentre location of an event is less reliable since in this method the program used for calculation tries to vary the hypocentre position until the residual becomes minimal and the effect on the solution of any travel time anomalies in the region, particularly on the hypocentral depth, is difficult to detect. In the JHD method which involves the joint, or simultaneous, determination of all hypocentres for a group of seismic events located in the same region, it is possible to minimize or remove statistically the effect of travel time anomalies (regional bias) between the source of tremors and the stations recording them (Dewey, 1971; Douglas, 1967).

4.8 Accuracy of the tremor hypocentre determination

The accuracy of hypocentre location may be expressed as the difference between the calculated hypocentre location and the true hypocentre location. The accuracy to which a hypocentre can be located seismically depends mainly on four principal factors:

1. The accuracy of onset times of P and S-waves

The accuracy of determining the arrival times of P and S-waves depends on the background noise at the seismometer sites and the aperture of the seismic network.

In the urban areas, background noise arises from various human activities. Such noises often tend to be the cause of serious difficulty in reading or interpreting records. In the Stoke area, the background noise imposed a detection limit of 0.4 μ/sec. (Westbrook et al., 1980). Much of the artificial noise, however, was eliminated by partially burying the seismometer in a hole on or near to bed rock, and a hard horizontal cemented surface was used for installation to ensure good seismic coupling.

The detection noise may also be reduced by reducing the sensitivity of the seismometer and also by reducing the amplification. However, there is a limit to this since the small seismic signals generated from small or distant tremors cannot be detected. The arrival times of the seismic waves in the Stoke area were determined to an accuracy of about 0.01 second for P-waves and less accurately for S-waves. The dominant frequency of the seismic waves produced by the seismic events in the area was between 10-15 Hz. Filtering was not of any great value in improving the clarity of the records since the dominant frequency of the noise and the seismic waves were similar. If an improper pass band filter is used for filtering the noise, the error in determining the onset times of the seismic waves can be more serious, and can change the polarity of the P-wave first motion (Banson, 1970).

In general, seismic records of tremors occurring close to seismic stations are characterized by wave groups of higher frequency and larger amplitude. The high frequency seismic waves are rapidly attenuated with distance leading to an increase in rise time (Cook et al., 1966). The accuracy to which the arrival time at the detecting station can be determined is greatly dependent upon the rise time of the initial seismic pulse. The rise time can be kept small if the high frequency seismic wave attenuation is reduced by shortening the distances between the hypocentre and the seismic stations, i.e. using a small aperture seismic network. Moreover, by shortening the travel paths, anomalies in the seismic velocities are also reduced. Janczewski (1950) indicated that satisfactory hypocentral solution can only be obtained for arrival times from seismic stations sited at epicentral distances no greater than 4 to 5 times the depth of the focus concerned.

However, reducing the travel path will give a short separation between the arrival of P and S-waves, consequently making the determination of the onset of the S-wave arrival very difficult if not impossible.

According to the above argument, it can be concluded that the Stoke-on-Trent seismic network is quite suitable for the study of seismic activity in the North Staffordshire coalfield as a whole, but it is too large for the precise study of seismic activity associated with mining operations in a specific longwall panel. If a precise study is required for a given longwall panel, a small array seismic network (high resolution seismic network) needs to be installed immediately above and in the vicinity of the panel. Such a network was installed in the Trent Vale area to study the seismic activity associated with panel 206 (see Chapter 7).

A study was conducted on 15 of the best recorded seismic events to determine the error in hypocentral location due to the error in determining the first arrival times of the P-wave. The 15 events were chosen from all the five seismic areas. These events were located by using the arrival times from five seismic stations and the single hypocentre location (SHL) method. Since the true hypocentre location of these events are not known, their calculated hypocentres were assumed to be the true hypocentre locations.

In this study the true arrival times for station (J) were reduced by 0.01 seconds (the error in determining arrival time), whereas the true arrival times for the other four stations were increased by 0.01 second. It was found that all the tremor epicentres were shifted in a direction towards the centre of the network, i.e. towards station (J) as shown in Figure 4.8.1a. Most of the events became shallower except for some of the events in areas E and D which became deeper.

The same experiment was repeated by reducing the true arrival times for station (K). In this case most of the tremor epicentres were moved to the north west as shown in Figure 4.8.1b. The tremor hypocentres in the areas near to the (K) station (areas C and E) became shallower, while in the other areas they became deeper.

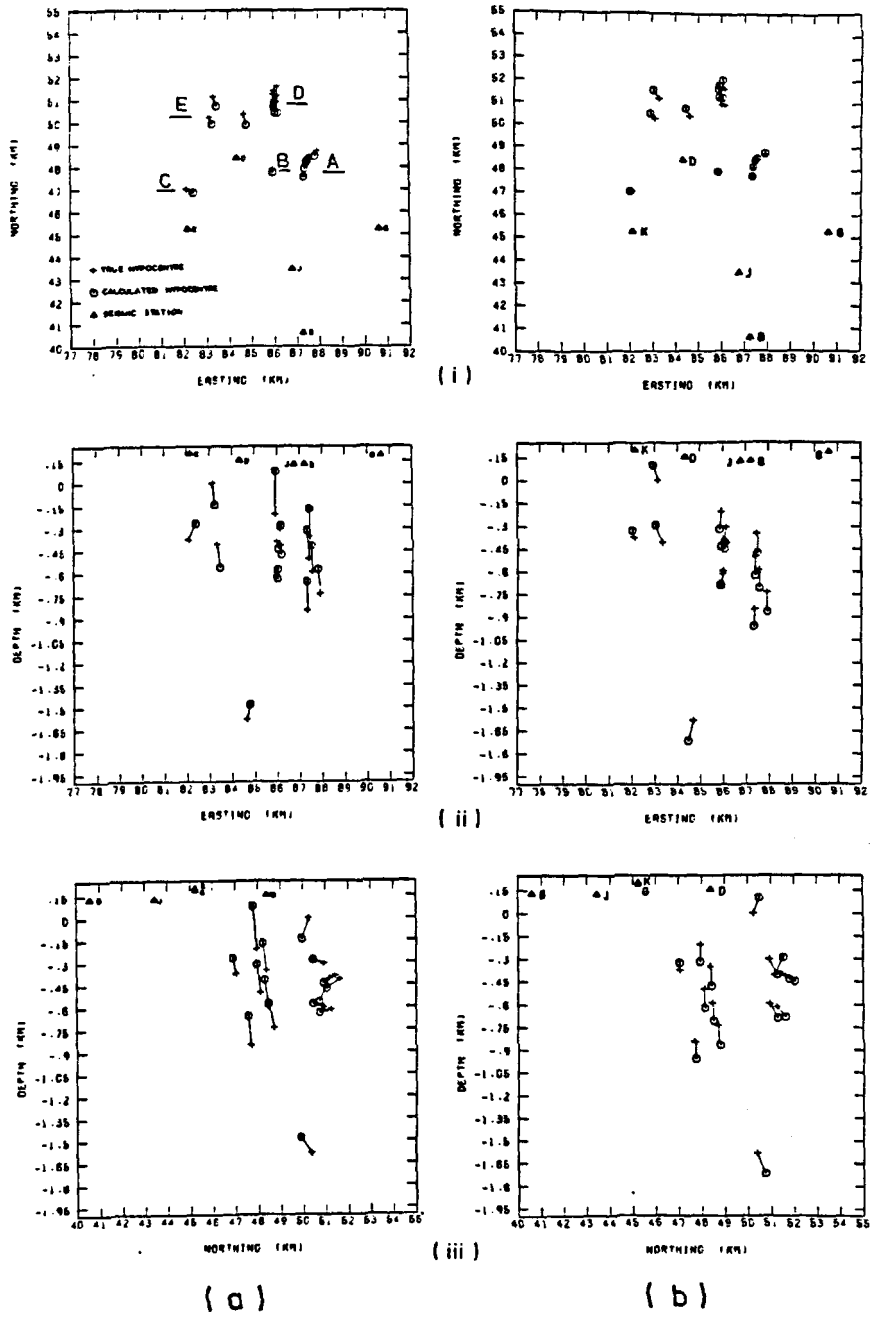

Fig. 4.8.1. Variation of calculated hypocentre due to arrival time errors.

(a) Error in J arrival time.
(b) Error in K arrival time.

(i) Plan view (ii) E-W vertical section
(iii) N-S vertical section.

The underline letters indicate different seismic regions.

In both cases the tremor epicentres were shifted to the east or west by an amount ranging between 3m and 305 m, and by 1-558 m to the north or south. The depths of the tremor foci vary by up to 192 m.

In both cases it was noticed that the tested events from areas E and D have the maximum epicentral deviation. This may be because they are situated farthest away from the centre of the seismic network.

In general, it can be seen from the figures that the epicentre deviations are greater in the north-south direction than in the east-west direction. This may be because most of the events are located within the diameter of the seismic stations in the east-west direction, while they are located north of the boundary of the network in the north-south direction.

2. Accurate knowledge of the local velocity structure

As a result of vertical and lateral variations in lithology within sedimentary sequences, seismic velocity varies widely and may also show anisotropy.

In the North Staffordshire coalfield, errors in hypocentre location of the seismic events are most probably due to a lack of precise values for the local velocity structures. Errors also arise from the assumption of an isotropic velocity structure in the area (see Section 1.3). The lateral and vertical variation of seismic velocity is further increased by the process of coal extraction which itself causes discontinuity and inhomogeneity of the rocks. In most sedimentary formations, however, the velocity of the seismic waves increases with depth due to differential compaction effects. This type of velocity structure is assumed for the North Staffordshire coalfield (see Section 4.6).

A study has been carried out in the coalfield to find the effect of velocity errors on the accuracy of hypocentre locations. An error in the velocity structure equal to ± 0.450 km/sec. for the velocity at O.D. (VD), and ± 0.290 km/sec/km for the velocity gradient (GV) were introduced. These

values are slightly higher than the average difference between the velocity structure in the four areas (areas A, B, C and D) and the velocity structure in the Trent Vale area (see Table 4.2). Hypocentres have been determined using errors in VD and GV of - 0.45 km/sec. and + 0.29 km/sec/km respectively, and also for errors of + 0.45 km/sec. and - 0.29 km/sec/km. The results are shown in Figures 4.8.2a and 4.8.2b respectively. It was found in both cases that all the epicentral events were shifted to the east or west by an amount ranging between 1 m and 781 m and by 4-522 m to the north or south. In the first case the hypocentral depths for 14 events became shallower by amounts ranging between 46m and 674 m, while only one event was relocated deeper. In the second case the hypocentral depths increased or decreased by 46-460 m. The events in areas A, C, and some events in area D became deeper while those events in the other areas were relocated at shallower depths (see Figure 4.8.2b).

Repeating the same experiment by introducing an error of + 0.45 km/sec. for VD and + 0.29 km/sec/km for GV relocated all the tremor foci at the surface, while introducing an error of - 0.45 km/sec. for VD and - 0.29 km/sec/km for GV increased the hypocentral depths by at least 1 km, relocating all the foci at depths greater than 2 km.

3. The geometry of the seismic network

The accuracy of the mathematical solution of the hypocentre is affected by the seismometer array geometry, linear or planar seismometer arrays do not give reliable source locations especially for focal depth (Leighton et al., 1972; Banson, 1970). Lilwall and Francies (1978) studied the effect of the seismic network configuration for Ocean Bottom Seismographs on the accuracy of hypocentre location. A simple network of three or four stations was examined. The geometry of the networks studied was tripartite with side of 10 km, and two quadripartite networks; a square network with side of 10 km and an equilateral triangle of the same area

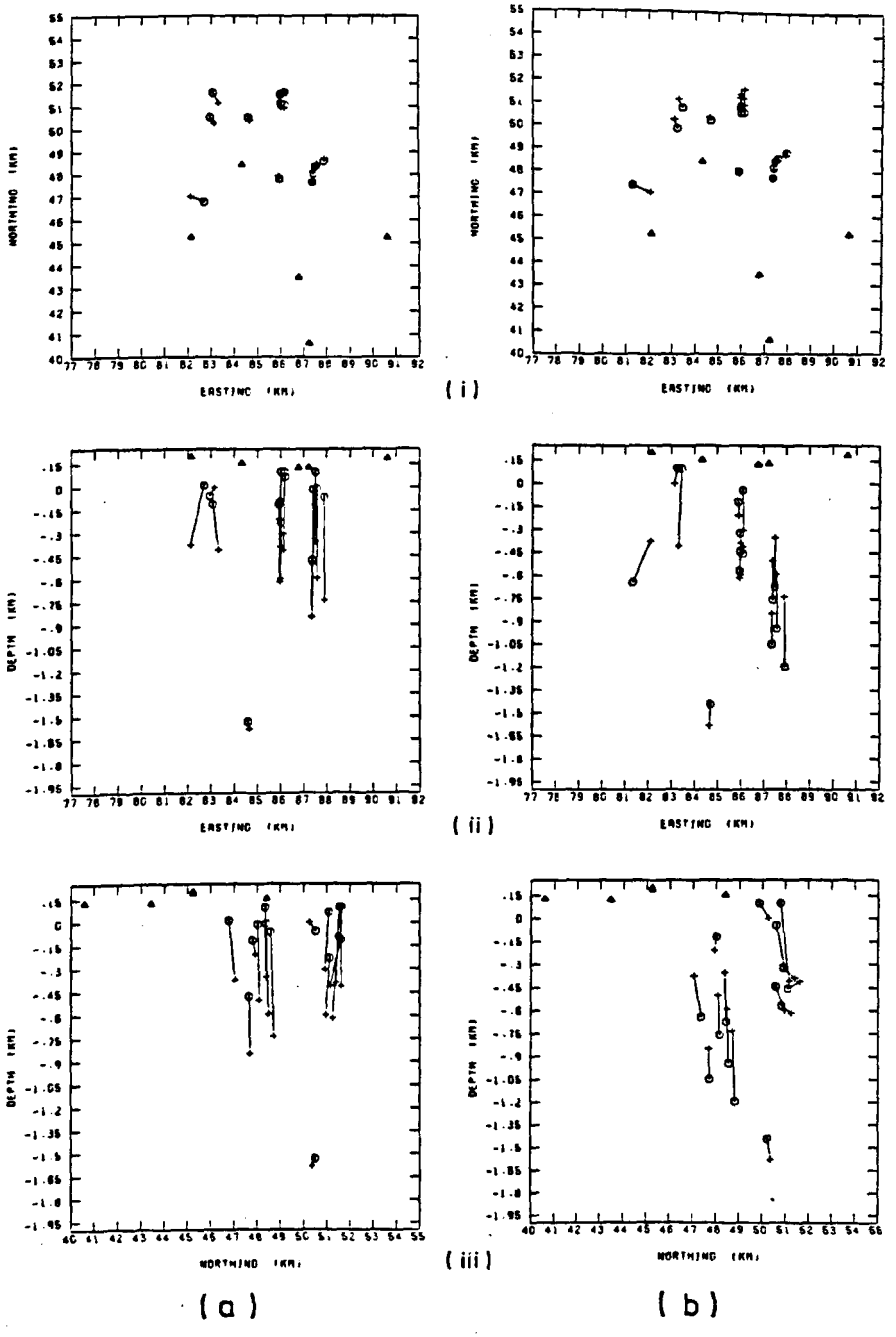

Fig. 4.8.2. Variation of calculated hypocentre due to seismic velocity errors.

(a) Errors in VD and GV of -0.45 km/sec. and + 0.29 km/sec/km respectively.

(b) Errors in VD and GV of +0.45 km/sec. and -0.29 km/sec/km respectively.

(i) Plan view (ii) E-W vertical section (iii) N-S vertical section.

(For legend see Fig. 4.8.1.)

with the fourth station at the centroid. The study was carried out for simulated events at a depth of 1 km. Simulated arrival time data for P and S-waves were obtained by calculating the travel times from hypocentre to the stations and then adding normally distributed errors. The velocity structure used to compute the travel times was a two gradient structure. For each network the mean errors in depth and epicentre were computed. Figure 4.8.3a shows the mean epicentre errors for the three networks, while Figure 4.8.3b shows the mean depth errors for the same networks. It was found that the tripartite array has poor depth control in its interior and optimum depth control outside the triangle near the seismometers, while the epicentre errors were least at the centre of the network and increase outwards. The same results were obtained for the square network and probably for all networks with no interior stations. Browitt (1977) indicated that an event giving only time difference close to zero (i.e. located in the middle of a network with no interior station) does not yield information required to determine its depth from first arrival times alone, although its epicentre can be determined accurately. Therefore, he suggested that for good depth control there must be some stations close to the epicentre and others further away. Lilwall found that the triangular quadripartite network has the best epicentre anddepth control at its centre (Figure 4.8.3a(ii) and b(ii).

The geometry of the Stoke-on-Trent seismic network is more or less a square array with an interior station (see Figure 4.2.1). Consequently, according to Lilwall and Francies' experiments the errors in depth and epicentre are least for those events located inside the network or at its border, and the errors increase for those events located outside the network.

4. The number of seismic stations

The precision of hypocentre determination increases with the increase in the number of seismic stations used to give arrival times (James et al.,

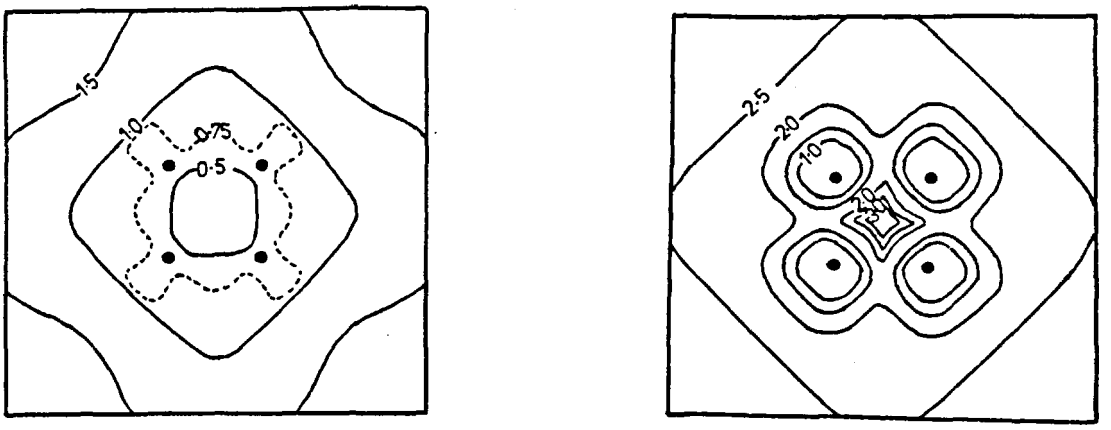

(i) Square quadripartite network side 10 km

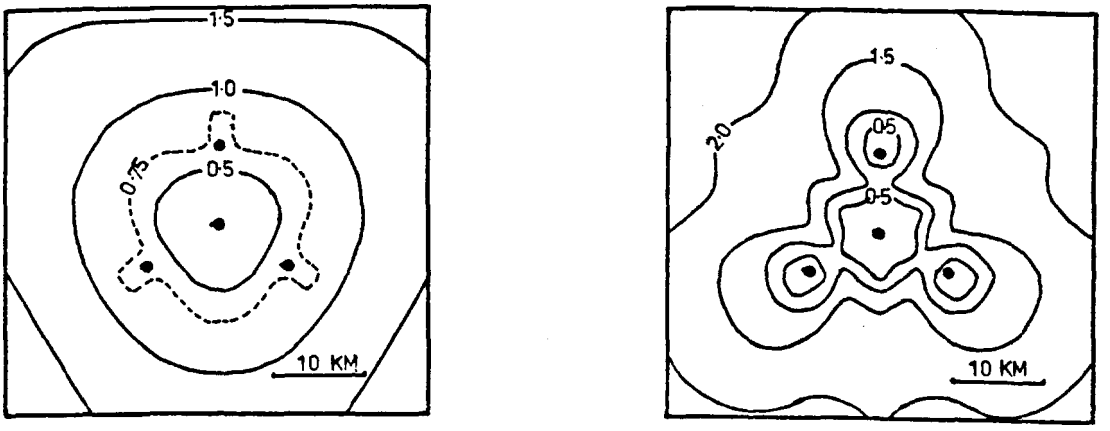

(ii) Triangular quadripartite network

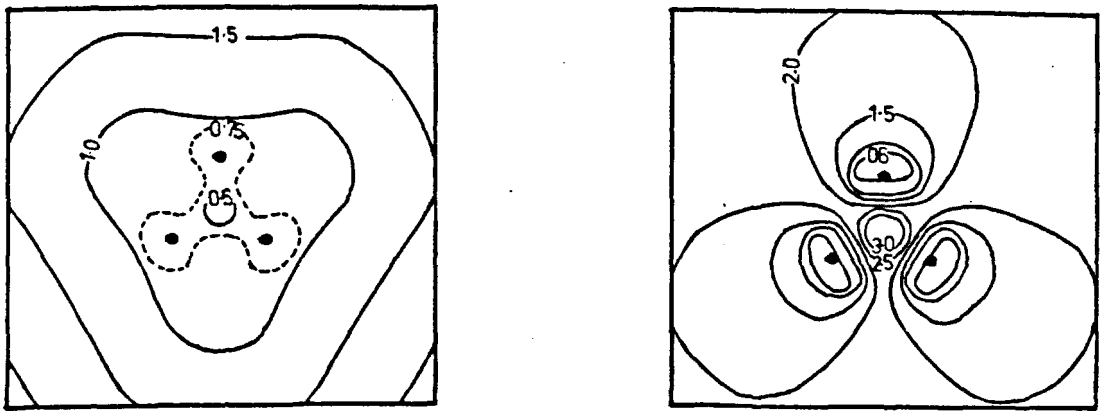

(iii) Tripartite network side 10 km

CONTOUR = 0·5 km

(a) (b)

Fig. 4.8.3. The effect of a seismic network configuration on the accuracy of hypocentre location.

(a) Mean epicentre errors in km.
(b) Mean depth errors in km.

(After Lilwall and Francies, 1978).

1969; Leighton and Duvall, 1972). James et al. (1969) were unable to determine the minimum number of seismic stations required in a network for stable calculation. However, they suggested that, in general, nine or more stations are required for good solution and the event must be well within the network. Leighton and Duvall (1972) found that the addition of information from only one seismometer can improve the solution by about 50%.

For the Stoke-on-Trent seismic network, a study was conducted on the same 15 seismic events mentioned previously to find the effect of omiting the information from one seismometer on the hypocentre calculation. In general, it was found that removing any station changes the position of the hypocentre. Moreover, subtracting the information from one or more stations can change the geometry of the seismic network significantly, which may itself lead to the variation in hypocentre determination. This was very obvious in this study. It was found that removing station G or K produced the greatest change in the epicentral positions of the tremors as shown in Figure 4.8.4. The epicentral shift is particularly significant for the tremors in areas E and D. The tremor epicentres in area E were shifted towards the east by as much as 990 m when station K was removed, and to the south by up to 2,700 m when station G was removed. The tremor epicentres in area D shifted westwards by up to 290 m and to the south by as much as 1,250 m when station G was removed. This is probably because removing station G changes the geometry of the network from a square network with an interior station to a nearly linear geometry with the seismic events in area D along its extension. The same situation also occurred for the tremors in area E when station K was removed. At the same time removing station K or G shortened the network diameter in the east-west direction markedly, consequently the epicentre determination accuracy in this direction was reduced.

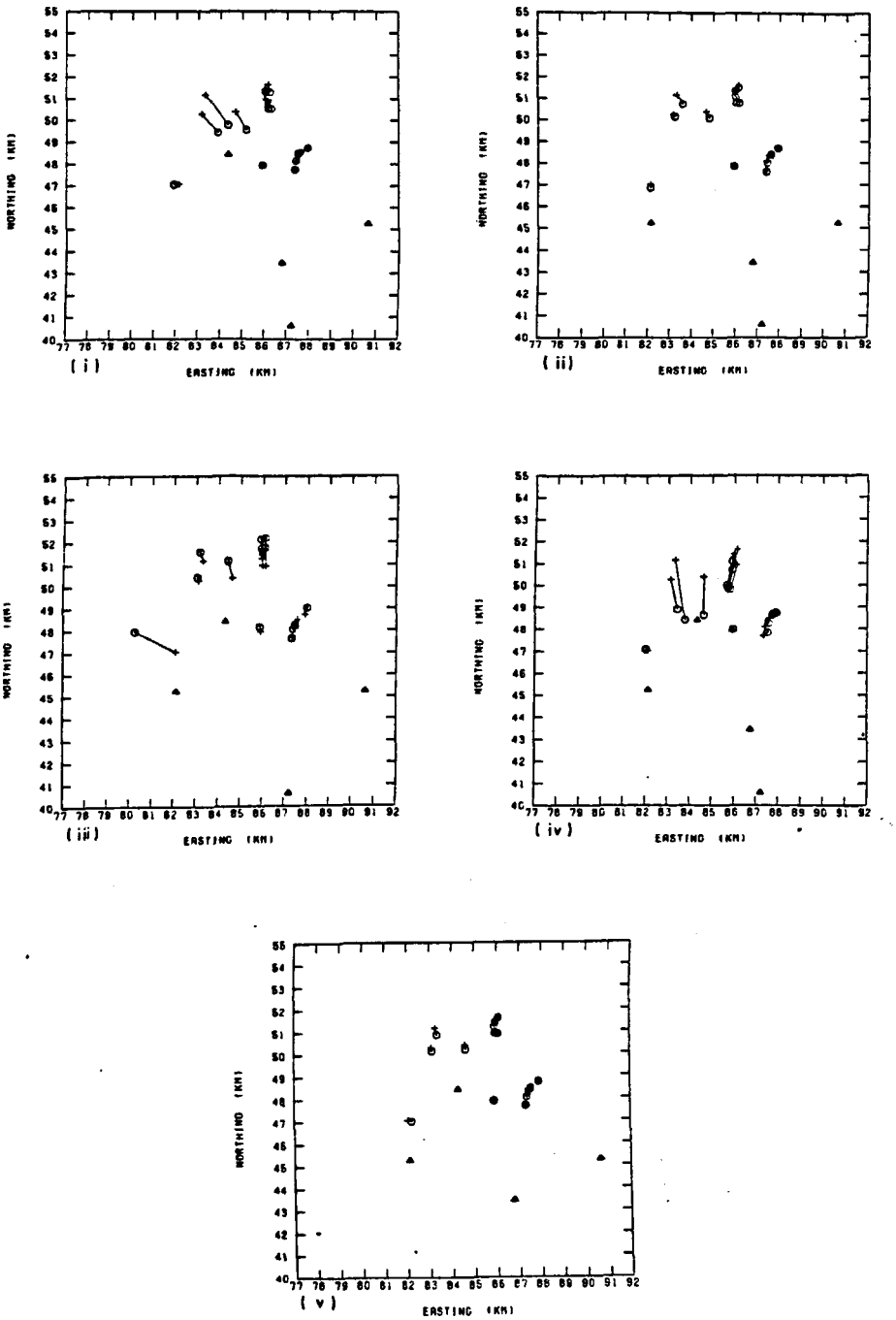

Fig. 4.8.4. Variation of calculated hypocentre due to omission of one seismometer.

(a) Plan view.
(b) E-W vertical section of tremor hypocentres.
(c) N-S vertical section of tremor hypocentres

(i) K seismometer omitted.
(ii) D seismometer
(iii) J seismometer
(iv) G seismometer
(v) B seismometer

(For legend see Fig. 4.8.1).

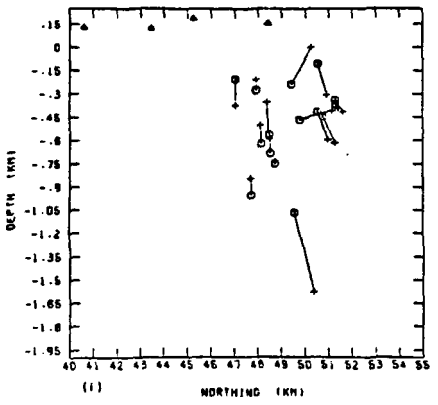
DEPTH (KM)
NORTHING (KM)
(i)

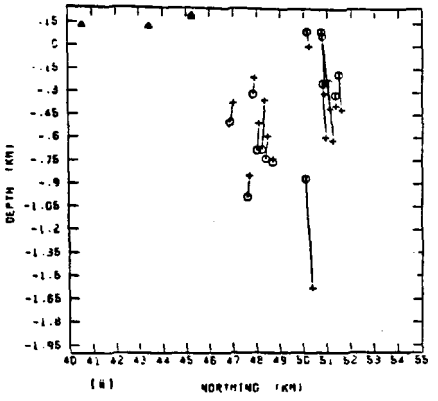
DEPTH (KM)
NORTHING (KM)
(ii)

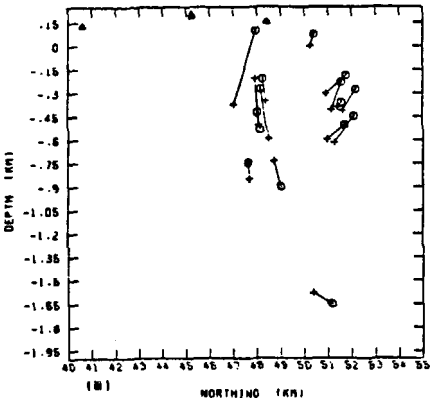
DEPTH (KM)
NORTHING (KM)
(iii)

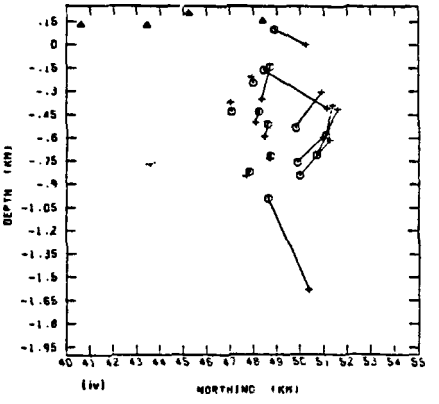
DEPTH (KM)
NORTHING (KM)
(iv)

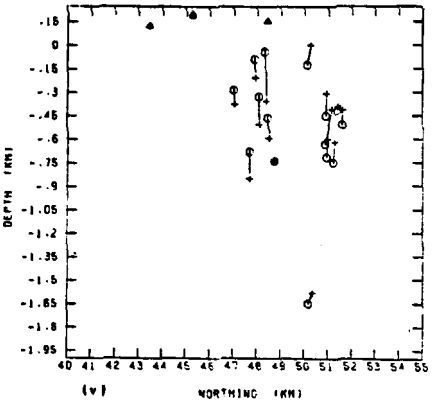
DEPTH (KM)
NORTHING (KM)
(v)

(c)

The minimum change in epicentral position occurred when station B was removed. Cancelling this station also resulted in minimal change in the hypocentral depth (see Figures 4.8.4a (v), b (v) and c (v)). This may be because this station is located far away from the tremor locations. Hence, removing this station had less effect on the hypocentral depth than the others. Also, removing this station did not change the network geometry in such a way that produced great effect on the hypocentral determination. The maximum difference in the hypocentral depth occurred when the data from station D was omitted (Figures 4.8.4a(ii), b(ii) and c(ii)). The depths of the tremor foci were increased or decreased by up to 710 m. As we can see from the figures, nearly all the events are located in the vicinity of this station. Consequently, removing this station had the greatest effect in their depth determination.

Another factor which may have an effect on the hypocentre determination is the errors in station co-ordinates. This error was considered negligible for the Stoke-on-Trent seismic network.

From these error studies it can be concluded that the error in hypocentral location (in both epicentral position and depth) introduced by any or all of the four tested parameters may be about ± 500 m. The errors in hypocentral determination are generally higher for the tremors located in areas E and D than the other areas.

4.9 The determination of the seismic events' local magnitude

Magnitude is a quantitative empirical scale used to measure the size of earthquakes instrumentally.

In general, magnitude determination depends upon the maximum amplitude of a seismic wave that a given earthquake produces at a specific epicentral distance. Richter (1935) first constructed a scale for measuring the size of southern Californian earthquakes quantitatively. Before the construction of this scale the intensity scale was used to estimate the

power of an earthquake in a particular region. Richter plotted the logarithm to the base 10 of the recorded trace amplitude for a group of southern Californian earthquakes recorded on Wood-Anderson seismographs against their epicentral distances. Curves were then drawn through the points corresponding to each earthquake. These curves were shown to be roughly parallel. These curves were then combined into a single composite curve passing through an arbitrarily selected point. This point defines the "standard shock" and was chosen so that the calculated amplitude of registration at an epicentral distance of 100 km is 0.001 millimetres. Richter defined his Local Magnitude Scale as the logarithm to the base 10 of the maximum seismic wave amplitude (expressed in thousandths of a millimetre) which the standard Wood-Anderson seismometer would register at an epicentral distance of 100 km. The local magnitude scale (M_L) can be expressed by:

$$M_L = \log_{10} A - \log_{10} A_0 \qquad 4.9.1$$

where A = the recorded trace amplitude (in mm) for a given earthquake at a given epicentral distance, as recorded by a Wood-Anderson seismometer.

A_0 = the amplitude for a particular earthquake selected as a standard.

The value of log A_0 for a particular epicentral distance can be read off from the composite curve. These values are also listed in a table as a function of epicentral distance given by Richter (1958). Richter did not specify the type of seismic wave to be used, the only condition was that the wave chosen be the one with the largest amplitude.

However, the application of the Richter Local Magnitude Scale to measure the size of the North Staffordshire coalfield tremors raises four major problems.

1. The amplitude response (amplification) of the S.O.T. network is not the same as that of the standard Wood-Anderson seismograph used by Richter. Therefore a correction factor is needed to convert the maximum amplitude observed by the S.O.T. seismometer to the amplitude that would have been recorded on a Wood-Anderson seismograph.

2. The S.O.T. seismometer measured the ground velocity, while the Wood-Anderson seismograph measured the ground displacement. Therefore the measured ground velocity needs to be converted to ground displacement.

3. The S.O.T. seismometers measured the vertical component of ground movement. Only at the Keele (K) station were there horizontal component seismometers. The seismic waves obtained from these horizontal seismometers were frequently saturated. Since the Wood-Anderson seismograph measures the horizontal component of ground movement, a correction factor relating vertical to horizontal ground motion must be used.

4. Richter applied his scale to the southern California region. The A_0-epicentral distance relationship applies therefore for California and cannot be assumed to apply in North Staffordshire.

An empirical formula considering the previous four factors and based on the Richter magnitude scale has been deduced to measure the local magnitude, M_L, for the seismic tremors in the coalfield. The formula is:

$$M_L = \log_{10} V + \log_{10} f - \log_{10} V_0 \qquad 4.9.2$$

and

$$\log_{10} f = \log_{10} a + \log_{10} b + \log_{10} c \qquad 4.9.3$$

where V is the maximum trace amplitude (in volts) of the ground velocity measured on the record.

V_0 is the attenuation of the ground velocity with distance in the Stoke area, i.e. the amplitude of standard earth tremors in the Stoke area. This is equivalent to the Richter A_0 term.

f is a correction factor dealing with the first three problems discussed above, and which includes:

a for the conversion of the response of the S.O.T. seismic network to that of the Wood-Anderson seismograph.

b for the conversion of the ground velocity to ground displacement.

c for the conversion of the vertical seismometer to a horizontal seismometer.

To compute the local magnitude, M_L, for the seismic events in the North Staffordshire coalfield, the maximum amplitude (in volts) and its time period (in seconds) of the seismic waves were measured from the record obtained from station B. This station is the farthest station from the seismic region. The ground velocity in mm/sec. corresponding to the maximum amplitude on the record was calculated. It was found that 1 mm/sec. ground velocity produced 17.5 volts on the record. This, of course, depends on the seismometer response, the gain of the Amplifier/Modulator, and the Store 14 response. The ground displacement in millimetres corresponding to the maximum amplitude on the record was computed assuming the seismic waves are a pure sine waves, by using the formula:

$$V_{max.} = A_{max.} \cdot 2\pi \cdot \frac{1}{\tau} \qquad 4.9.4$$

where $V_{max.}$ = maximum ground velocity (mm/sec).

A_{max} = maximum amplitude of ground displacement (mm).

τ = time period for maximum amplitude (sec).

It was found that 1 mm of ground displacement produced $110.3/\tau$ volts on the jet pen record, i.e. the amplification of station B is equal to $110.3/\tau$.

Constants a and b may be combined to give a single correction factor, such that

$$\log_{10} f = \log_{10} \frac{G_{WA}}{G_{ST}} \qquad 4.9.5$$

where G_{WA} = 2800 mm/mm = amplification of the Wood-Anderson seismograph.

$G_{ST} = \frac{110.3}{\tau}$ volt/mm = amplification of the S.O.T. seismic network.

Constant $\underline{c}$ has been assumed to be one.

The accuracy of measuring the time period is about 0.02 sec. for those maximum amplitudes measured from body waves, while the accuracy is about 0.05 sec. for those measured from surface waves. These errors produce a maximum error in magnitude of about 0.2.

The attenuation problem has been dealt with by plotting $\log_{10} V_0$ versus distance scale for the North Staffordshire coalfield, as shown in Figure 4.9.1. The figure shows the attenuation of the ground velocity with distance. The standard shock was determined by applying the established formula (equation 4.9.2) on two large earth tremors. These two tremors occurred in the region on 13th and 19th May, 1976 and their local magnitude, M_L, was determined by the I.G.S. in Edinburgh (Jacob and Neilson, 1977). It was found that $\log_{10} V_0$ at a distance of 6.3 km is equal to -2.02 volts, i.e. the amplitude for the standard shock at a distance of 6.3 km is 0.01 volts.

Unfortunately, the determination of magnitude from other seismic stations which could have provided a cross check for our local magnitude scale was not possible due to difficulty in measuring the maximum wave amplitudes and their time periods for other stations nearer to the seismic area.

Due to the different reasons mentioned above, it is expected that the error in the local magnitude scale could be about ± 0.5. Nevertheless, this scale provides a useful measure of the relative size of the seismic events within the North Staffordshire coalfield. The largest seismic event in the area was found to have a local magnitude, M_L, of about 2.5, and this explains why none of these tremors were felt on the surface.

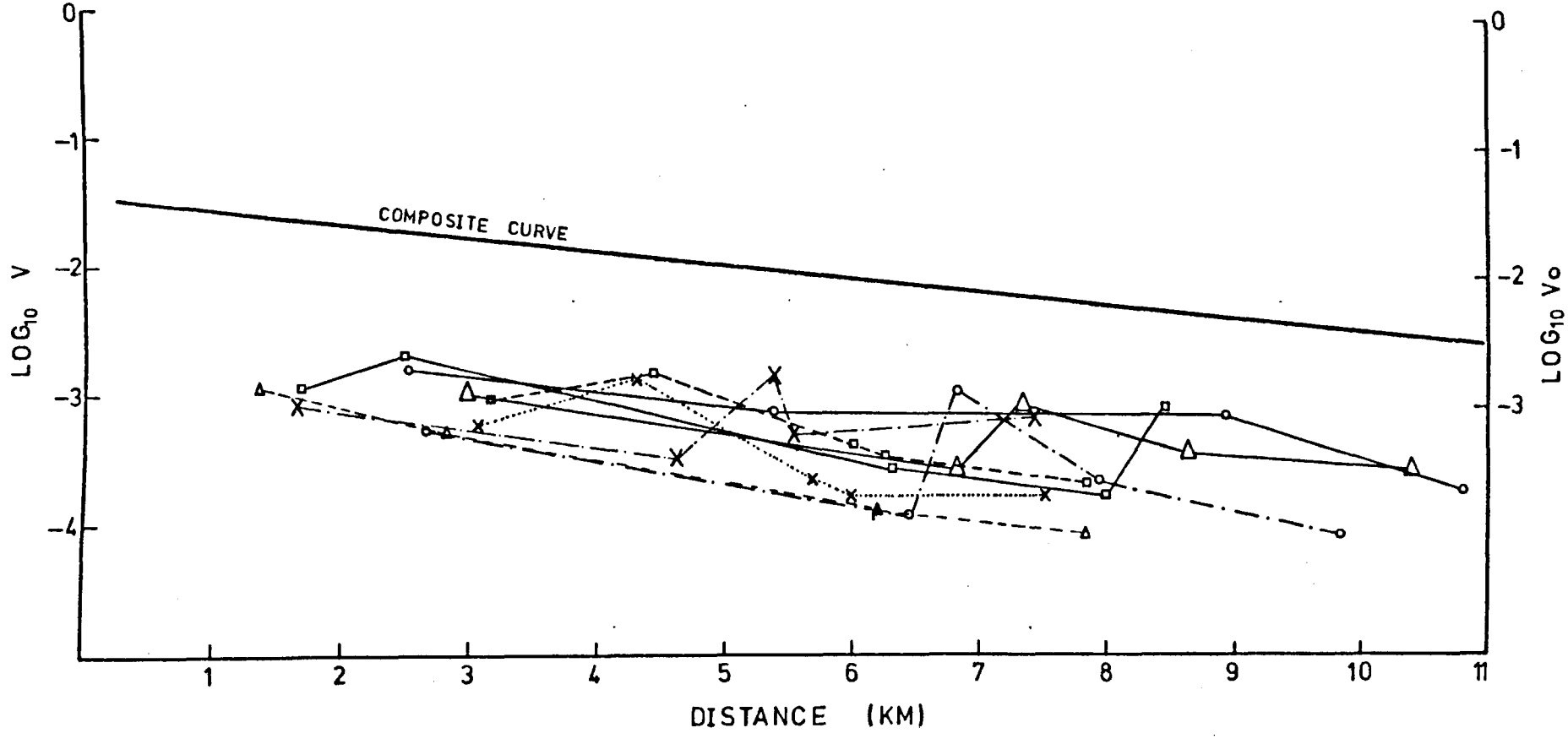

Fig. 4.9.1. Plot of logarithm amplitude ($\log_{10}V_0$) of the standard earth tremors against distance, showing the attenuation of the ground velocity in the North Staffordshire Coalfield (labelled composite curve). The figure was obtained by plotting the logarithm of maximum trace amplitude of ground velocity against its epicentral distance, for a number of seismic events. The curves were then combined into a single composite curve passing through a point chosen as the standard shock.

Although Richter did not specify the type of seismic waves used for magnitude determination, he indicated that "it would be desirable to identify the phases of each seismogram, and to compare amplitudes of the same wave or set of waves at the various distances".

The magnitude of seismic events in the area was also determined by using the largest seismic wave amplitude and its time period for body waves. However, this scale has not been used since in some records it was difficult to distinguish between the surface waves and the body waves, and so would produce an unreliable and inconsistent magnitude scale.

The seismic energy (E) released by a seismic event has been calculated from the local magnitude scale (M_L), using the following formula given by Richter (1958):

$$\log_{10} E = 9.9 + 1.9 M_L - 0.024 M_L^2 \qquad 4.9.6$$

4.10 The types of the recorded earth tremors

Four different types of records representing four different kinds of tremors were obtained by the Stoke-on-Trent seismic network.

1. The first type of records consisted of seismic waves that have low amplitudes and an average duration of about three seconds (Figure 4.10.1). This type of seismic wave may represent small tremors which originate near the detection sites. Most of these tremors were recorded on less than four seismic stations since they had relatively little energy.

2. The second type consisted of seismic waves that have relatively higher amplitude, lower frequency and longer duration than the first type (Figure 4.10.2). The arrival times of the S-wave and P-wave have a longer separation time than the first type. These represent larger and probably more distant tremors than the first type.

3. The third type have very large amplitudes and very low frequency seismic waves compared with the second type (Figure 4.10.3). The

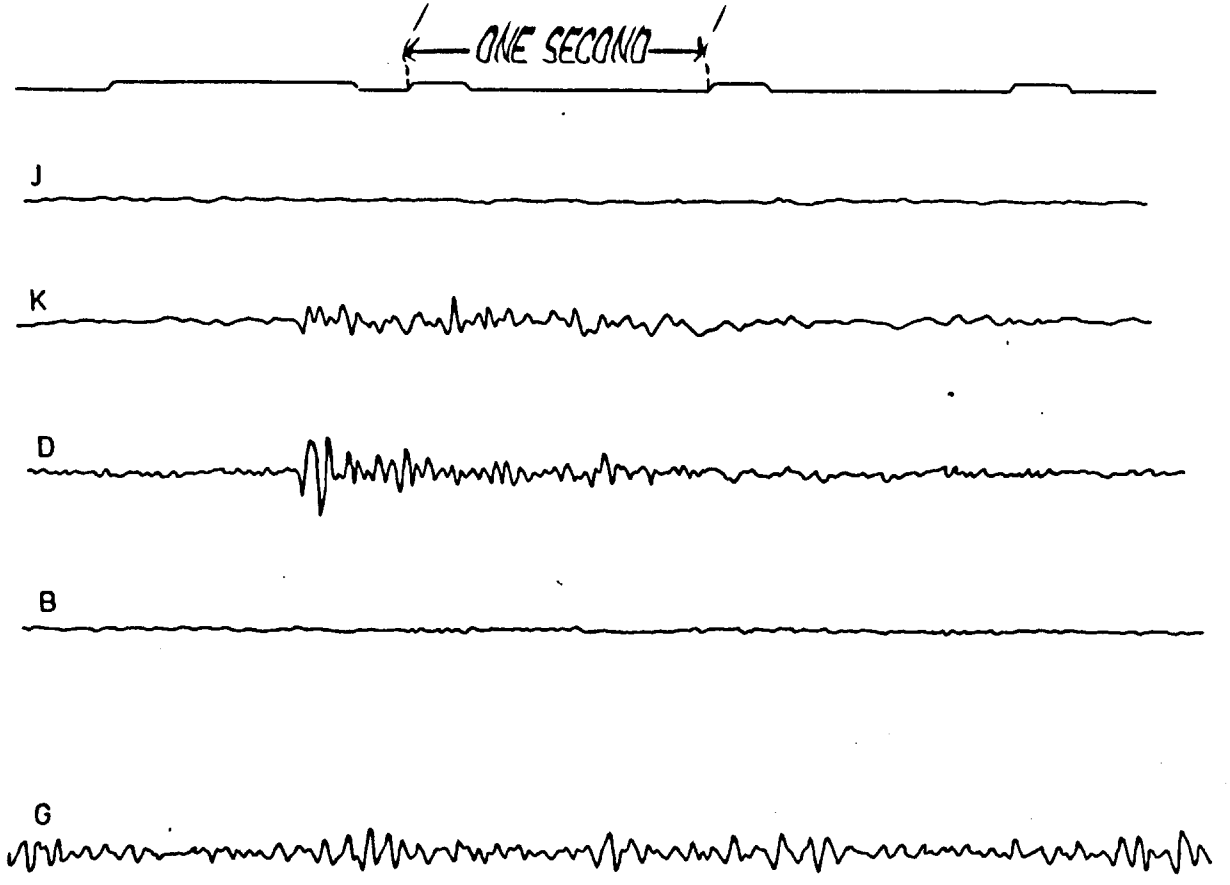

Fig. 4.10.1. Seismogram of first type of tremor recorded at 1977 6-6 06-23. Low amplitude and short duration of seismic waves probably indicate tremors which originate near the detection site. Letters designate seismometer names.

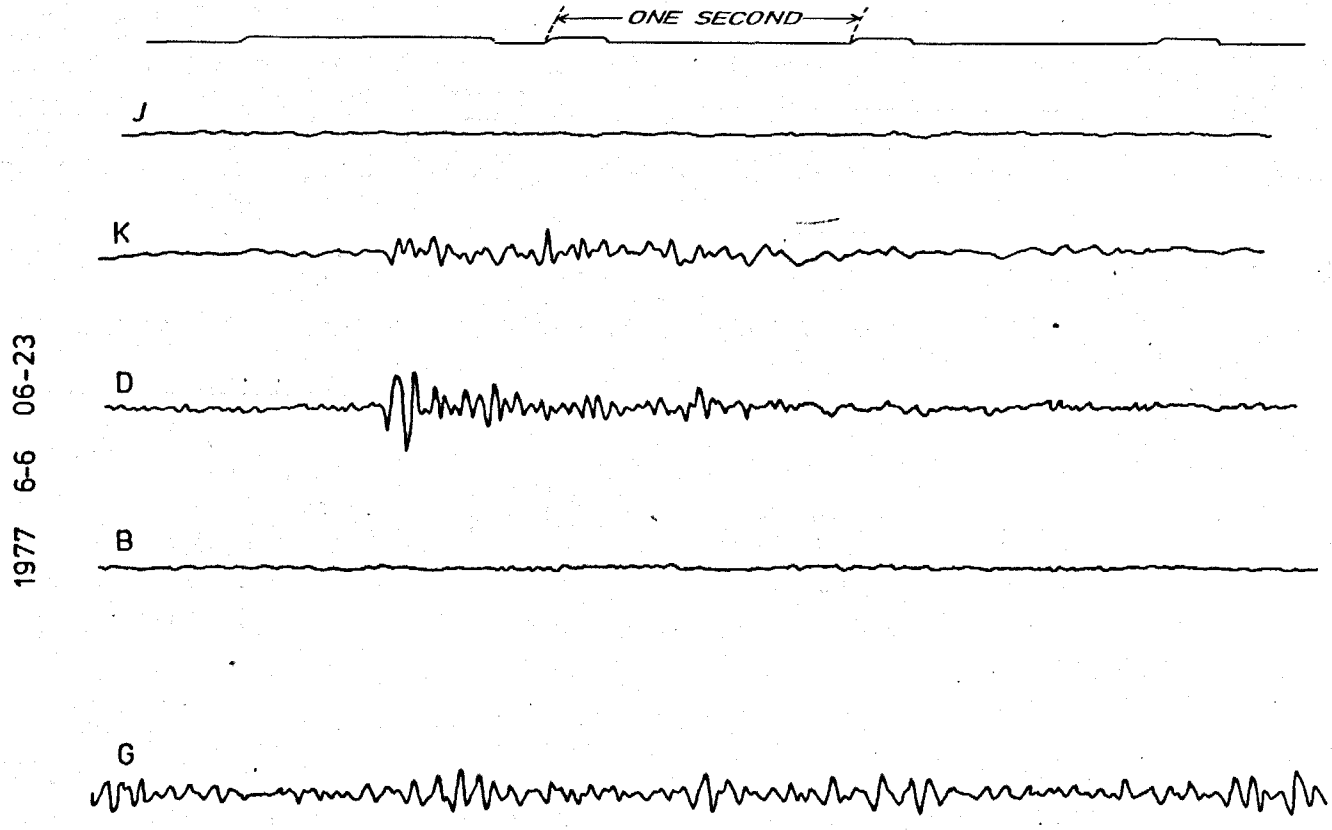

Fig. 4.10.1. Seismogram of first type of tremor recorded at 1977 6-6 06-23. Low amplitude and short duration of seismic waves probably indicate tremors which originate near the detection site. Letters designate seismometer names.

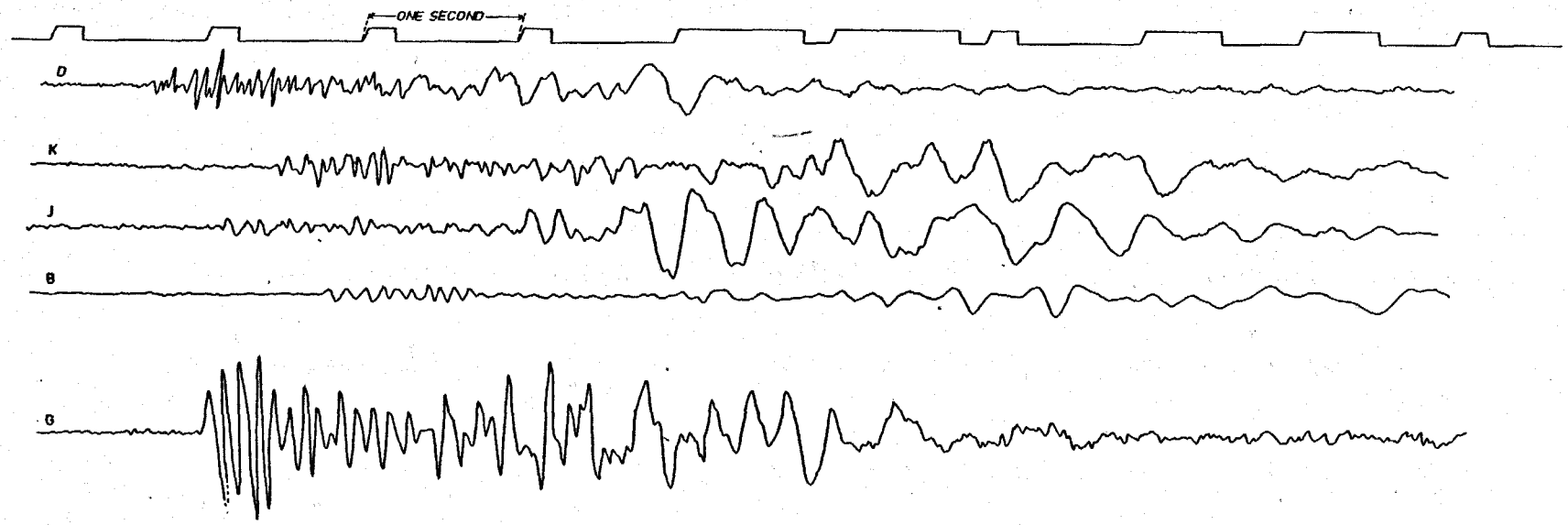

Fig. 4.10.2. Seismogram of second type of tremor recorded at 1976 10-1 20-02. High amplitude, low frequency and large duration of seismic waves probably represent larger and more distant tremor than the first type.

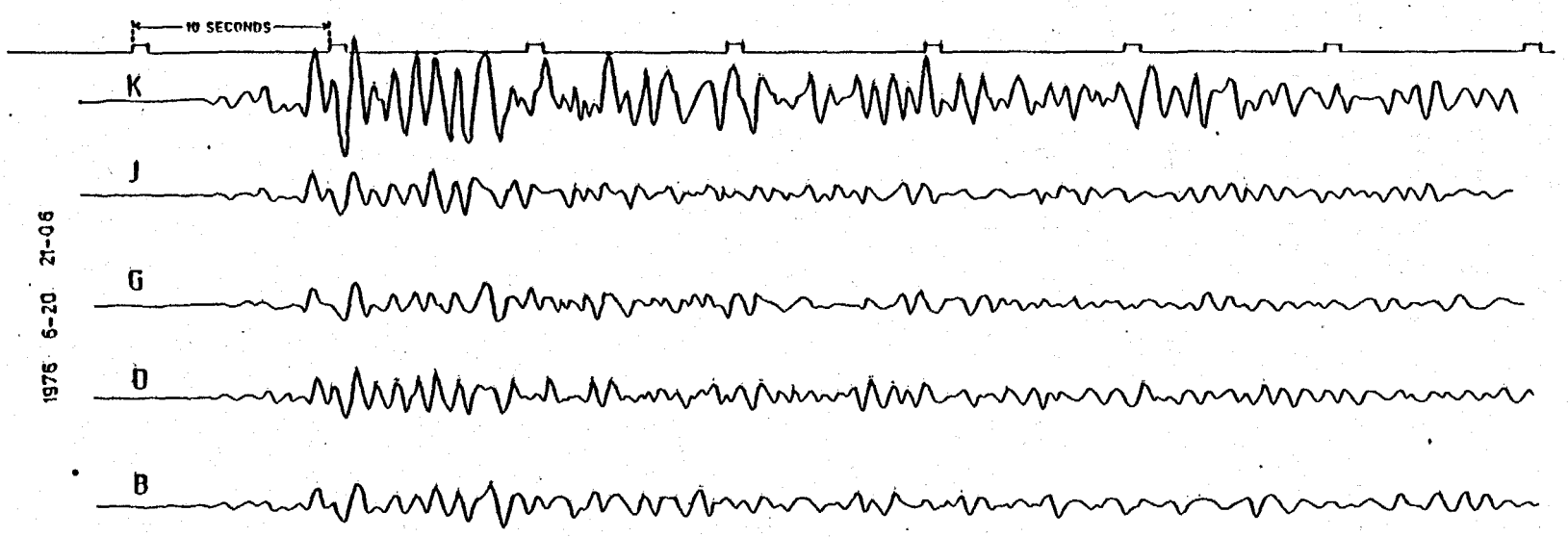

Fig. 4.10.3. Seismogram of third type of tremor recorded at 1976 6-20 21-06. Very low frequency, high amplitude and long duration of seismic waves represent regional or teleseismic events.

duration of the seismic waves lasts for several minutes. These types of seismic waves represent regional or teleseismic events.

4. A single event of this type was recorded by the network and an attempt to locate the source failed. The frequency and amplitude of the seismic waves are similar to those of the second type (Figure 4.10.4). Two prominent downward peaks can be seen in the record obtained from station K. In this station a very sharp downward first arrival followed by another prominent downward peak, less than two seconds later, was obtained. The arrival times in the other stations could not be determined. At these stations the highest amplitude seismic waves were preceded by low amplitude waves. These types of seismic waves are typical of that produced by sonic booms from jet aircraft (Goforth and McDonald, 1970).

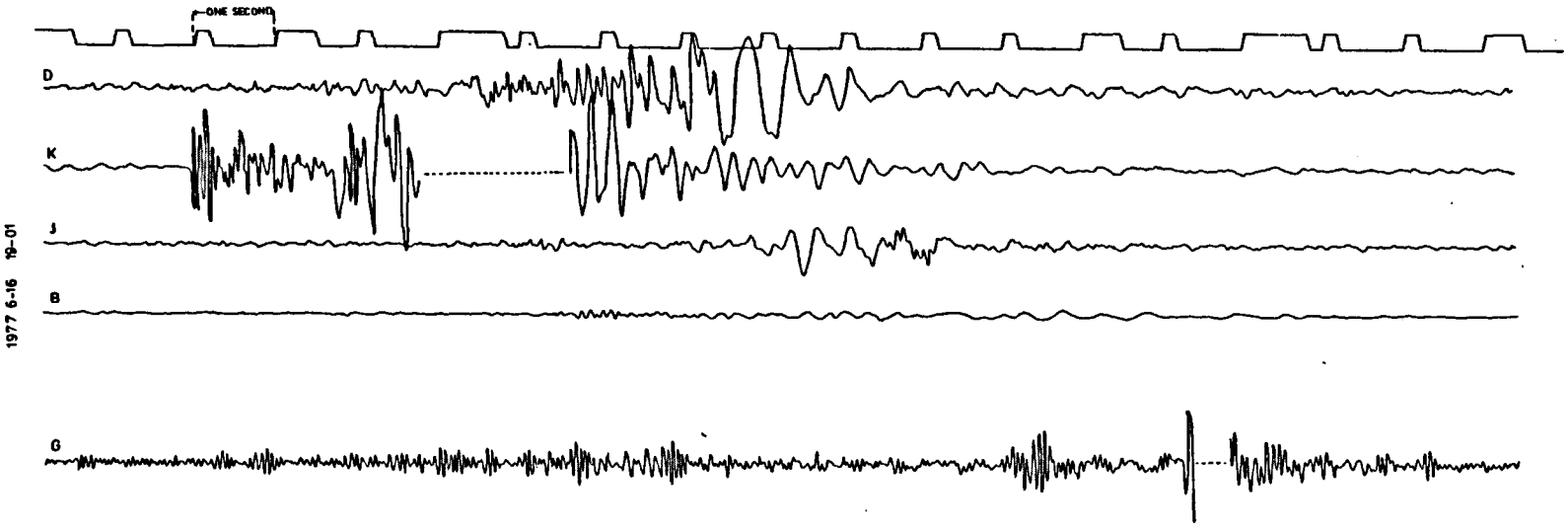

Fig. 4.10.4. Seismogram of fourth type of tremor recorded at 1977 6-16 19-01. Two prominent downward peaks can be seen in seismometer K and probably in seismometer G also, while in the other seismometers the highest amplitude seismic waves preceded by low amplitude waves. These most probably represent seismic waves produced by sonic booms from jet aircraft.

CHAPTER 5

THE GEOLOGY OF THE NORTH STAFFORDSHIRE COALFIELD

5.1 Introduction

The North Staffordshire or the Potteries coalfield lies on the western flank of the Pennines. It is roughly triangular in shape with the apex situated to the north of Biddulph, and the base to the south extending from Mucklestone in the west to Moddershall in the east. The coalfield covers an area of more than 259 km^2. In addition to coal, the region contains deposits of economic value such as iron ore and clay. The region is drained mainly by the river Trent and its tributaries.

5.2 Stratigraphy

The exposed rocks in the coalfield are mainly Upper Carboniferous sediments (Figure 5.2.1). These are surrounded by Triassic sediments to the south and west.

The Upper Carboniferous strata have been divided into two main divisions: the Millstone Grit Series at the bottom and the Coal Measures at the top. The maximum thickness of the Millstone Grit Series is over 1910 m, and for the Coal Measures, approximately 2743 m (Hains and Horton, 1969).

A characteristic feature of both the Millstone Grit Series and the Coal Measure sediments is their rhythmic deposition which led to the development of cyclothemic strata (Hains and Horton, 1969). The depositional cyclothem consists of:

one cyclothem
- seat earth
- sandstone
- siltstone
- non-marine mudstone
- marine mudstone
- coal
- seat earth

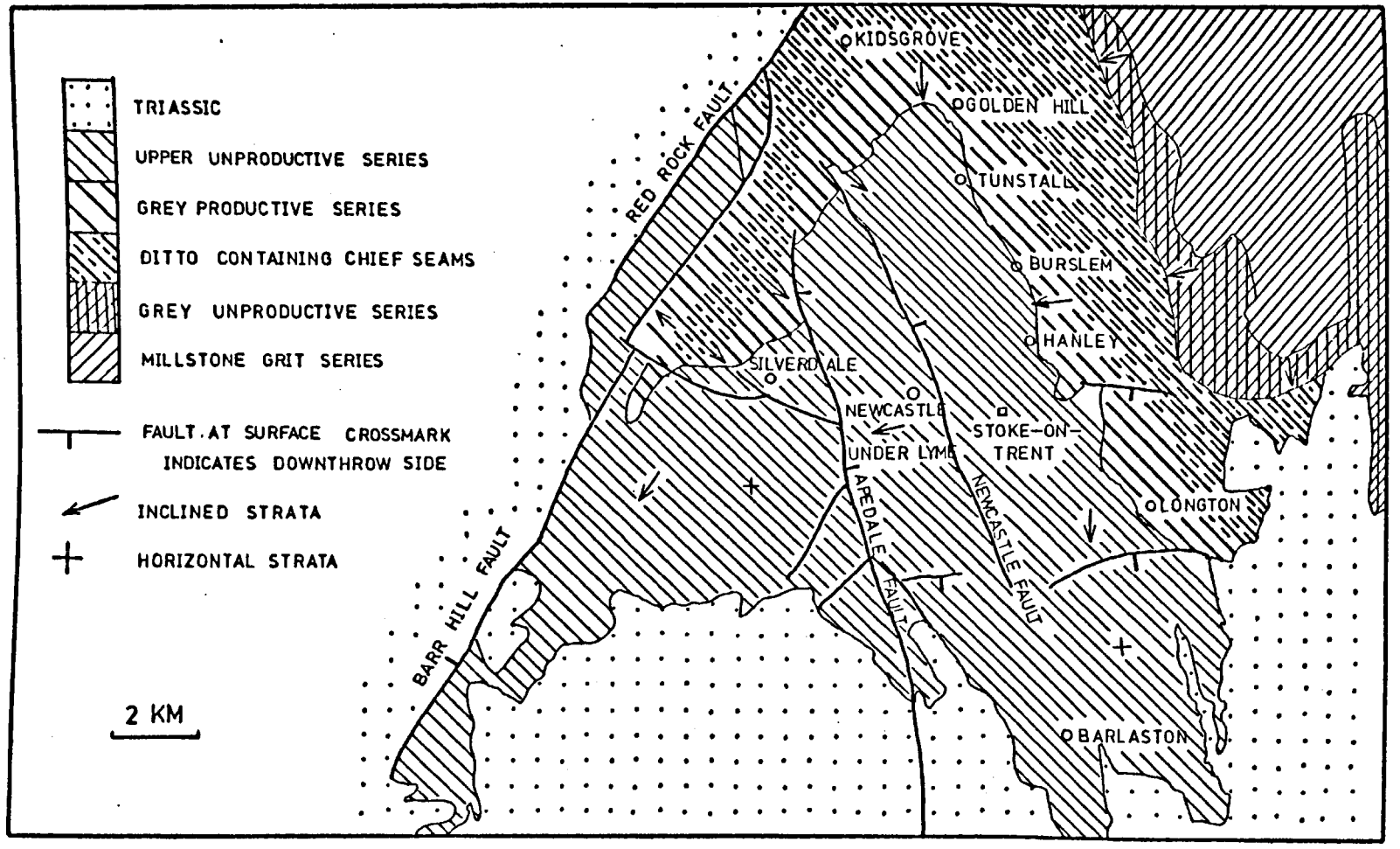

Fig. 5.2.1. Geological map of the North Staffordshire Coalfield. (After Gibson et al., 1925).

It is unusual for all the components of the cyclothem to be present; there is considerable variation in the sequence and also rapid lateral variation, particularly in the sandstones. Individual cyclothems vary in thickness, usually ranging from a few metres to tens of metres. The thickest members of a cyclothemic unit are generally the mudstones and shales (argillaceous), but massive bedded sandstone may be present. The occurrence of argillaceous rocks is often widespread and uniform and may be traceable over large areas of the coalfield. The sandstone beds are the most inconsistent members of cyclothems. They are generally lenticular in shape and vary rapidly in thickness. Most sandstones are fine to medium grained, but coarse varieties do occur occasionally and these may merge into conglomerates and breccias. In the Coal Measures, the coal seams are thicker and more frequent than in the Millstone Grit Series, while the sandstones are thinner, finer grained and less persistent.

The Coal Measures represent the chief lithology of the North Staffordshire coalfield. In the eastern part of the coalfield, the lower portions of the Coal Measures crop out and form a band bordering the central trough to the east of Longton, Hanley, Burslem, and to the north of Goldenhill (Gibson, et al., 1925). In the west, the lower parts of the Coal Measures crop out also on the eastern flank of the Staffordshire anticline. Since the syncline plunges to the south, the eastern and western outcrops coalesce northwards near Kidsgrove to form the apex of a roughly triangular area, as shown in Figure 5.2.1.

The Coal Measures have been classified into three major divisions: Lower, Middle and Upper Coal Measures (Hains and Horton, 1969). Figure 5.2.2 shows a generalized sequence and classification of the Coal Measures in the coalfield. Sharp, well-defined differences in lithological and palaeontological characteristics distinguish the Upper Coal Measures from both the Middle and Lower Coal Measures, while the differentiation between the Middle and Lower Coal Measures is very difficult (Gibson et al., 1925).

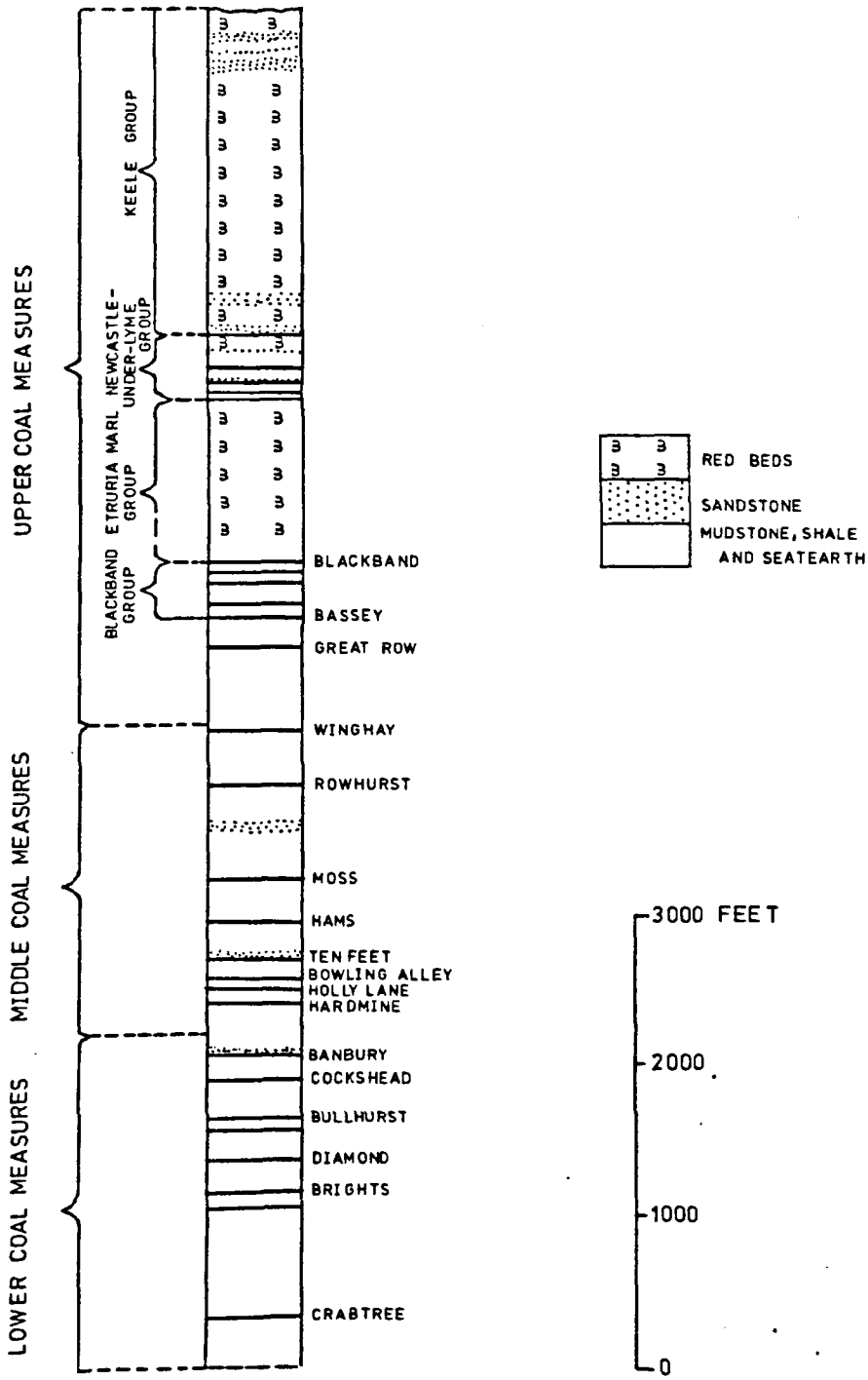

Fig. 5.2.2. General classification of the Coal Measures of the North Staffordshire Coalfield showing the succession of some important coal seams. (After Hains and Horton, 1969).

The Upper Coal Measures are the barren or unproductive Measures. They attain a thickness of about 1524 m, and their lithology consists mainly of red sandstones and marls containing bands of grey shale and grey sandstones. Seams of coal are few, thin and impersistent. They also contain many thin bands of limestone and laminated ironstone.

The Middle and Lower Coal Measures are the main productive series, and consist mainly of grey shales with coal seams and beds of grey sandstones. The coal seams constitute about 2% of their total thickness. The thickness of the individual coal seam ranges from very thin films to several metres (Hains and Horton, 1969).

The Middle Coal Measures have a thickness of about 610 m. They are characterized by the presence of many thick coal seams, particularly in their lower part, but above the Moss seam; workable seams are less common. Eight out of eleven of the seams mined during the seismic monitoring period were of the Middle Coal Measures, while the other three were of Lower Coal Measures.

The Lower Coal Measures also have a thickness of about 610 m. They consist chiefly of mudstones and siltstones. Sandstones are less common. In their upper quarter the coal seams are thicker and contain many of the best workable and valuable seams, such as the Bullhurst, Cockshead and Banbury seams, while in the lower three quarters of the successions the coal seams are frequent but generally thin.

5.3 Tectonic and geological structure of the coalfield

The coal measure deposits originally formed a thick persistent sheet of strata covering most of central England (Gibson et al., 1925). This sheet was folded and faulted by the Hercynian earth-movements, eroded and then buried deeply under Triassic sediments. Subsequent erosion has removed most of the Triassic sediments, and parts of the folded and faulted sheet (coal measures) form a number of separate coalfields in the Midlands, the North Staffordshire coalfield being one of them (Hains and Horton, 1969).

In the North Staffordshire coalfield, two major earth movements affected the carboniferous strata. These are:

1. Permo-Carboniferous movements.
2. Post-Triassic movements.

The present structured patterns of the coalfield were mainly developed during the earth movements of the Hercynain orogeny (Hains and Horton, 1969). These movements took place at the end of the Carboniferous period. The folding and faulting developed during the Permo-Carboniferous movements influenced the pattern of the Post-Triassic movements (Gibson et al., 1925; Hains and Horton, 1969). The Post-Triassic movements may have occurred along the pre-existing faults developed during the Carboniferous movements. Consequently, the amount of Post-Triassic movements along these faults cannot be determined.

The structure of the coalfield represents a broad syncline plunging towards the south-southwest. This syncline is enclosed between two anticlines (Figure 5.3.1). The Endon-Werrington anticline is to the east, and trends a little west of north, and the Western or Staffordshire anticline is on the west side running north-northeast (Gibson et al., 1925).

The central syncline encompasses the entire Coal Measure sequence, and contains the chief coal bearing strata. The syncline shows a marked asymmetry in its development. It has a steeper dip on its western side, where the outcrops are narrow, while it has a gentler dip on its eastern flank, where the outcrops are wider (see Figure 5.3.1). In the northern part of the coalfield, where the lower parts of coal seams crop out to the north of Kidsgrove, the strata are inclined at a fairly high angle, but in the southern part of the coalfield the strata gradually flatten out, and the trough structure is nearly lost. The structure of the coalfield with respect to the structure map of central England is shown in Figure 5.3.2.

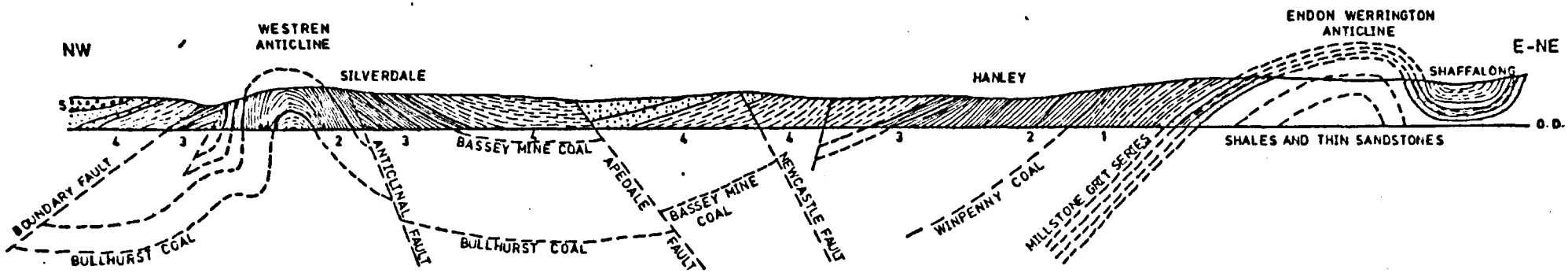

Fig. 5.3.1. General geological section across the North Staffordshire Coalfield. (After Gibson et al., 1925).

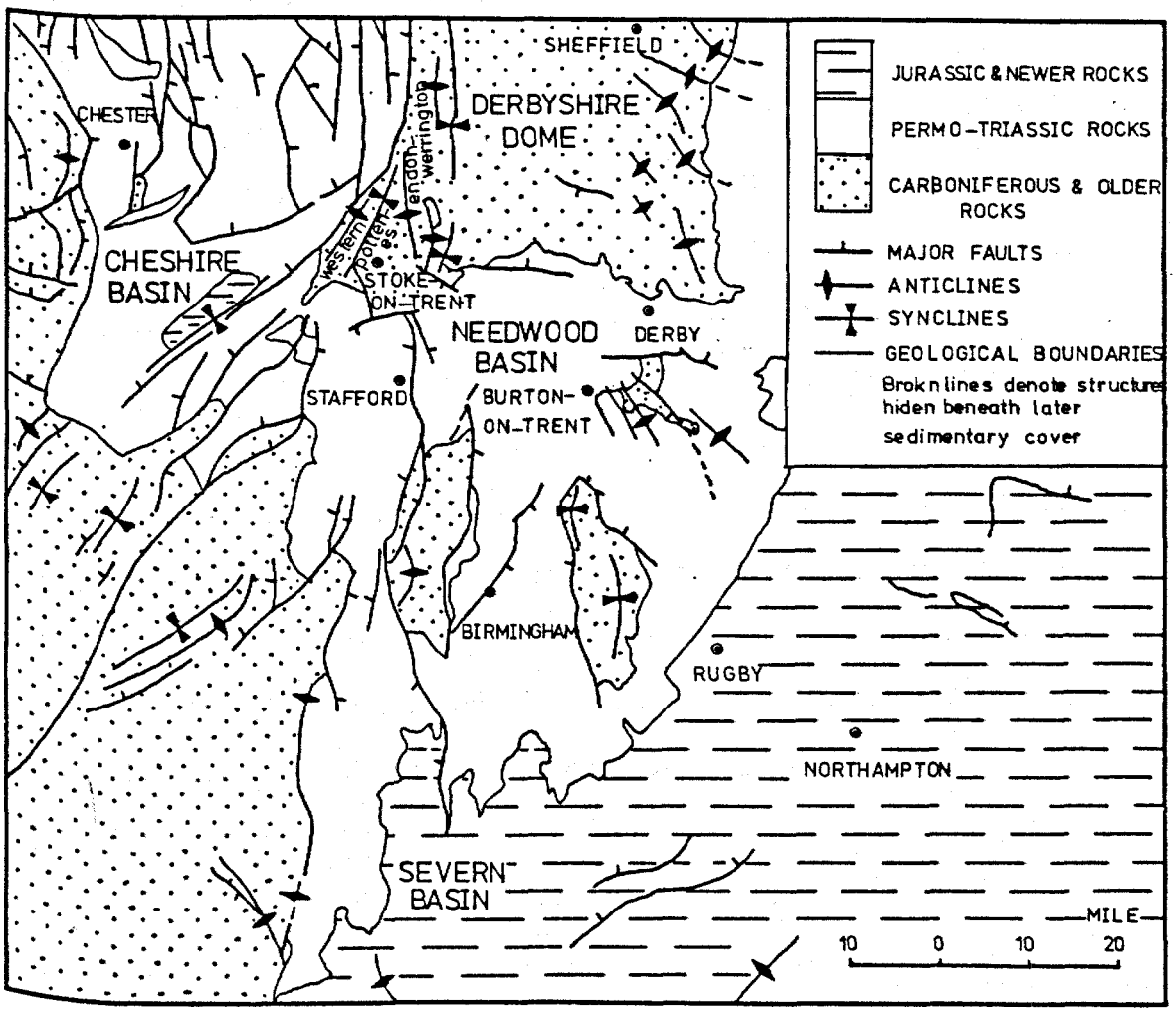

Fig. 5.3.2. The structure of the North Staffordshire Coalfield with respect to the structural map of Central England. (After Hains and Horton, 1969).

The coalfield is disturbed by numerous faults which makes an understanding of the stratigraphical succession in the coalfield very complicated. Two major sets of faults can be seen in the coalfield (see Figure 4.2.1). One set trends roughly north-south, and is the main fault set in the coalfield. The faults radiate from a focus situated at Mow Cop in the north of the coalfield. Each large fault consists of a single fracture in the centre of the coalfield, but traced northwards it divide and disappear into small fractures (Gibson et al., 1925). This radial system of faults is crossed by another system trending generally east-west. These two major sets of faults appear to have the same age. The major faults in the area were usually named according to their geographical location, their orientation or from their accompanying distinguishing structural features. All the major faults in the area are normal faults. Among the major faults are the Apedale and Newcastle faults, each well developed in the central part of the coalfield, where they have maximum throws of about 640 m and 134 m respectively. None of the faults, particularly these large ones show signs of recent movement.

In addition to these faults there are a large number of smaller subsurface faults in the area which have been encountered during mining at different levels.

The only known igneous body in the coalfield is a large doleritic dyke which penetrates the late Carboniferous and Triassic deposits and extends intermittently parallel to the Apedale fault from Butterton Park to Norton Bridge in the south of the coalfield (Gibson et al., 1925). The dyke has an average thickness of about 2.4 m. It is exposed in a quarry at Butterton Hall, and in the Hanchurch Hills it has been observed as an intrusive mass cutting across Triassic Bunter conglomerate. A borehole near Seabridge met with several intrusions at depths of 163 m and between 332 m and 344 m (Gibson et al., 1925).

According to the N.C.B. (Private communication) no igneous body has been encountered anywhere in the coalfield during mining operations.

CHAPTER 6

MINING TECHNIQUES USED IN THE COALFIELD

6.1 Introduction

Mining of coal and other ores has taken place for several centuries in the North Staffordshire coalfield. In 1850, legislation to keep mine records was first enacted in the U.K., and in 1872 the production and retention of mine plans became mandatory (Bell, 1975). However, as Bell has indicated, in areas of productive Coal Measures, even if no records of mining activities have been found, it should not be assumed that mining has not taken place.

In the North Staffordshire coalfield records of mine layouts for more than 40 coal and ironstone seams are kept by the N.C.B. showing workings which had been carried out in the area since the mid-nineteenth century. These records reveal that extensive mining has taken place under most of the North Staffordshire area at different depths. In particular it can be seen that most of the old workings followed the boundary of the coalfield (i.e. coal outcrops) on both limbs of the syncline, and eventually formed a triangular mined out area.

6.2 Mining techniques

Two general techniques have been used to extract coal; room and pillar and longwall techniques. The majority of the old mines were worked by using the room and pillar method while the recent mines have been usually worked by the longwall technique.

In the room and pillar technique, the coal in the seam is split into pillars which are subsequently extracted. During the seismic monitoring period, the coal from only one small area (area E) was being worked using this technique (by a private company having a subcontract licence from the N.C.B.)

Extraction using this method comprised two distinct operations. First a set of roadways was driven to a predetermined boundary. These roadways were then crossed by another set of roadways usually at right angles and at intervals of about 9 m to split the coal into pillars having an average dimension of about 13.5 m x 7.5 m. Then in order to maximize coal extraction from the seam, these pillars were subsequently extracted, from the goaf or the boundary backwards towards the main roadways. Cutting of the coal took place on only one shift per day (between 8 am and 3 pm). A shot was fired on the face to break the coal which was then subsequently hand cut by picks. The shot firing was usually, but not always, carried out at around 11 am and 2.30 pm to prepare the cutting for the next day. The roadways were supported by wooden legs and steel bars. Near the face the roof was supported by wooden bars. The roof in the goaf was not allowed to cave in, but was supported by 45 gallon oil barrels filled with waste and set up in rows in the goaf to prevent closure.

The longwall mining method is usually now used in coal extraction by the N.C.B. In this method the coal in a given area is extracted along a more or less continuous long working face, and usually without leaving pillars. The panels usually have lengths ranging between 250 m and 900 m, and widths ranging between about 125 m and 250 m. Two variations can be used in this method; longwall advancing and longwall retreating extraction. Both these techniques were used in the coalfield during the seismic monitoring period.

In the longwall advance technique the panel face is advanced from the main entries away towards the panel boundaries. The roadways on both sides of the panel (panel entries) are developed simultaneously and just ahead of the face. In the retreat technique the face is advanced backwards (retreated) from the rear boundary of the panel towards the main entries. The panel entries are first driven in the seam from the main entries to a

pre-determined position. These heading roadways are then connected at their rear ends by another road (cross-road) to form the boundary of the panel. The coal face is opened out at the rear end of the panel, and the coal is worked back towards the main entries.

In both these techniques the goaf is filled wholly or partially with debris (packing) or the roof is allowed to cave in fully in the goaf behind the face.

It is not known whether the roofs in the old workings were allowed to cave in or not, but in the 1960's the technique of roof caving was widely applied. In this technique the roof is supported for about 4-5 m behind the face by yielding hydraulic jacks having a canopy in contact with the roof extending to within about 1.5 m of the face. These supports not only hold up the roof, but also provide a safe space for all the necessary mining activities on the face. These supports are advanced after each cut. After the supports have moved over, the roof behind them is free to cave in, and usually does so within a matter of minutes. Since the strata when they break produce about one and a half times their original volume, only a limited height of the roof, about twice the height of coal extracted, falls and breaks up in the goaf area. The upper beds settle on the broken rock, recompressing it and a wave of subsidence is initiated which goes right to the surface.

On the face, the coal is cut mechanically by using a shearer. The height of cutting is approximately the thickness of the seam. However, up to 0.5 m of coal may be left in the roof and less than that in the floor depending on the condition of the roof and floor, especially if they are very weak or friable. Condition of the roofs were variable in different panels, but according to the N.C.B. (private communication) they were generally good. The rate of advance of the face was variable in different panels, according to local conditions, but usually ranged between less than

6 m to more than 25 m a week. The direction of face advance with respect to the seam strike was variable, but mostly they advanced along the strike (see the panel layouts in Chapter 9). The direction of cleat with respect to the face was also variable.

The mining activities were carried out 24 hours a day through three main working shifts. These shifts worked from 6 am to 2 pm, 2 pm to 10 pm, and from 10 pm to 6 am. The first two shifts were usually associated with coal extraction, while the third shift was usually used for mine maintenance. Coal extraction was carried out on working days. There was no production on Saturday although some mine maintenance took place, while on Sunday the mine was idle.

CHAPTER 7

MINING INDUCED SEISMICITY IN THE TRENT VALE-HANFORD AREA

7.1 Introduction

Mining induced seismicity in the Trent Vale-Hanford area has been discussed thoroughly by Kusznir et al. (1980a,b), Westbrook (1977) and Westbrook et al. (1980). Westbrook mainly discussed the Stoke-on-Trent seismic network and the method of locating earth tremors, while Kusznir established the relationship between mining and seismic activity, and the mechanism of earth tremors.

As already discussed in Chapter 4, the Stoke-on-Trent seismic network was installed in response to the public alarm following the earth tremor of 15th July, 1975 which shook the Trent Vale-Hanford area. This area is situated in the south of the Stoke-on-Trent conurbation (see Figure 4.2.1). The area is located between two major faults; the Newcastle and Apedale faults. Figure 7.1.1 shows a geological section drawn by Kusznir et al. (1980a) approximately north-south. The geological sequence consists of numerous coal seams occurring in a cyclical sequence with mudstone roofs and floors and with occasional intervening sandstone lenses. The seams dip to the south at about 8^{o}.

In the period between 1973 and 1977 the area was mined for coal in the Ten Feet seam by five panels (panels 202-206 in Figure 7.1.2) driven parallel to the Newcastle fault at a depth of approximately 900 m below the surface. Panels 205, 206 and part of panel 204 were mined during the seismic monitoring period (September 1975-September 1977). The face width and height of the panels were approximately 150-200 m and 2.4 m respectively. The retreat longwall extraction method was used in the extraction of panels 205 and 206. Pillars of coal were left between adjacent panels except between panels 204 and 205. The area had previously been extensively mined. The

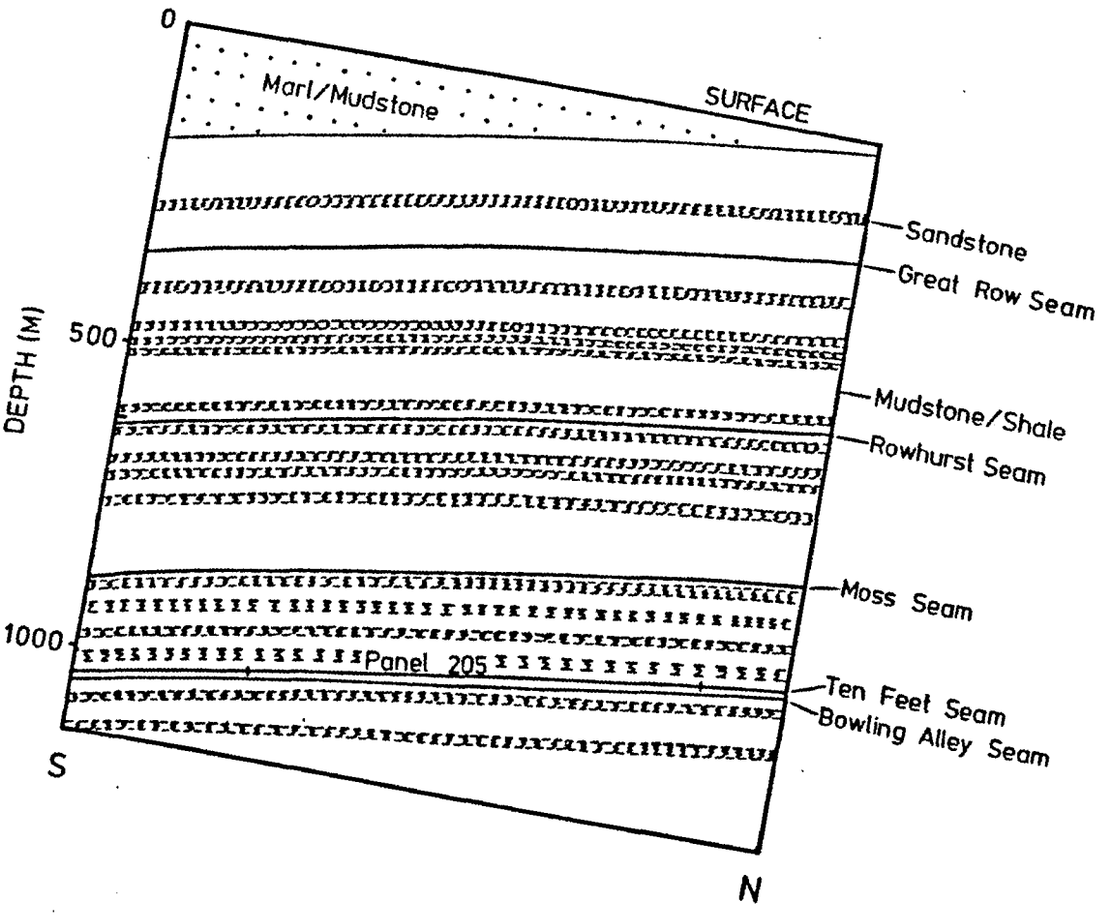

Fig. 7.1.1. General geological section along panel 205 showing major sandstone units and some important coal seams. (Taken from Kusznir et al., 1980b).

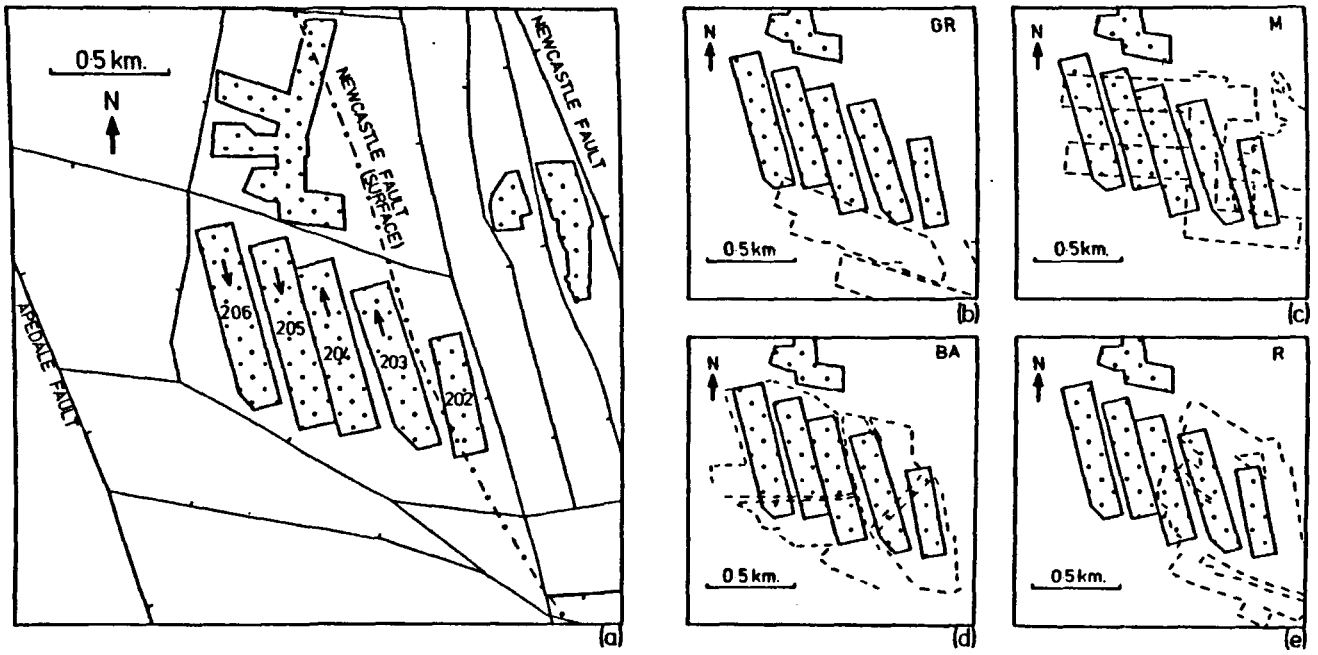

Fig. 7.1.2. Layouts of the mine workings in the Trent Vale area showing

(a) the location of the active mine workings (panels 205 and 206) in the Ten Feet seam with faults at the seam level,

(b) previous workings in the Great Row seam (GR),

(c) Moss seam (M),

(d) Bowling Alley seam (BA) and (e) Rowhurst seam (R). (Taken from Kusznir et al., 1980a).

mine workings in the Ten Feet seam are underlain by workings in the Bowling Alley seam at a depth of 15 m (Figure 7.1.2d), and overlain by workings in the Moss seam (Figure 7.1.2c) at a height of about 170 m above the Ten Feet seam. There are also previous workings in the Rowhurst and Great Row seams (Figure 7.1.2b and e) but these are considered too high above the Ten Feet seam to cause interaction problems (Kusznir et al., 1980b). Two main pillars were left in the Bowling Alley seam, one 25 m wide intersecting panels 204, 205 and 206 and the other 40 m wide intersecting panels 202 and 203. Both these pillars were affected by minor faulting. In the Moss seam there is one large pillar about 200 m wide intersecting panels 204, 205 and 206.

The mining conditions were generally good. No rock bursts were observed underground but some deterioration of access roads of panels 205 and 206 occurred when passing under or over pillars left in the adjacent seam (Kusznir et al., 1980b).

7.2 The observed relationship between mining and seismic activity

Kusznir et al. (1980a,b) have extensively described and interpreted the spatial and temporal relationship between mining and seismicity.

7.2.1 The spatial distribution of the tremor hypocentres

Kusznir et al. (1980a,b) reported that during the two year monitoring period, a total of 724 tremors were located in the vicinity of the active panels (panels 205, 206 and part of panel 204). Of these, 179 tremors occurred during the working life of panel 205 and 541 tremors for panel 206. In total, 55 tremors were sufficiently large to be felt by local residents. 39 of these occurred during the mining of panel 205, and 16 felt tremors occurred during the mining of panel 206 (Kusznir et al., 1980a). None of these tremors were felt underground. The tremor hypocentres for events which occurred during the working life of each panel were plotted in Figure 7.2.1 to show their relationship to active mine workings, previous

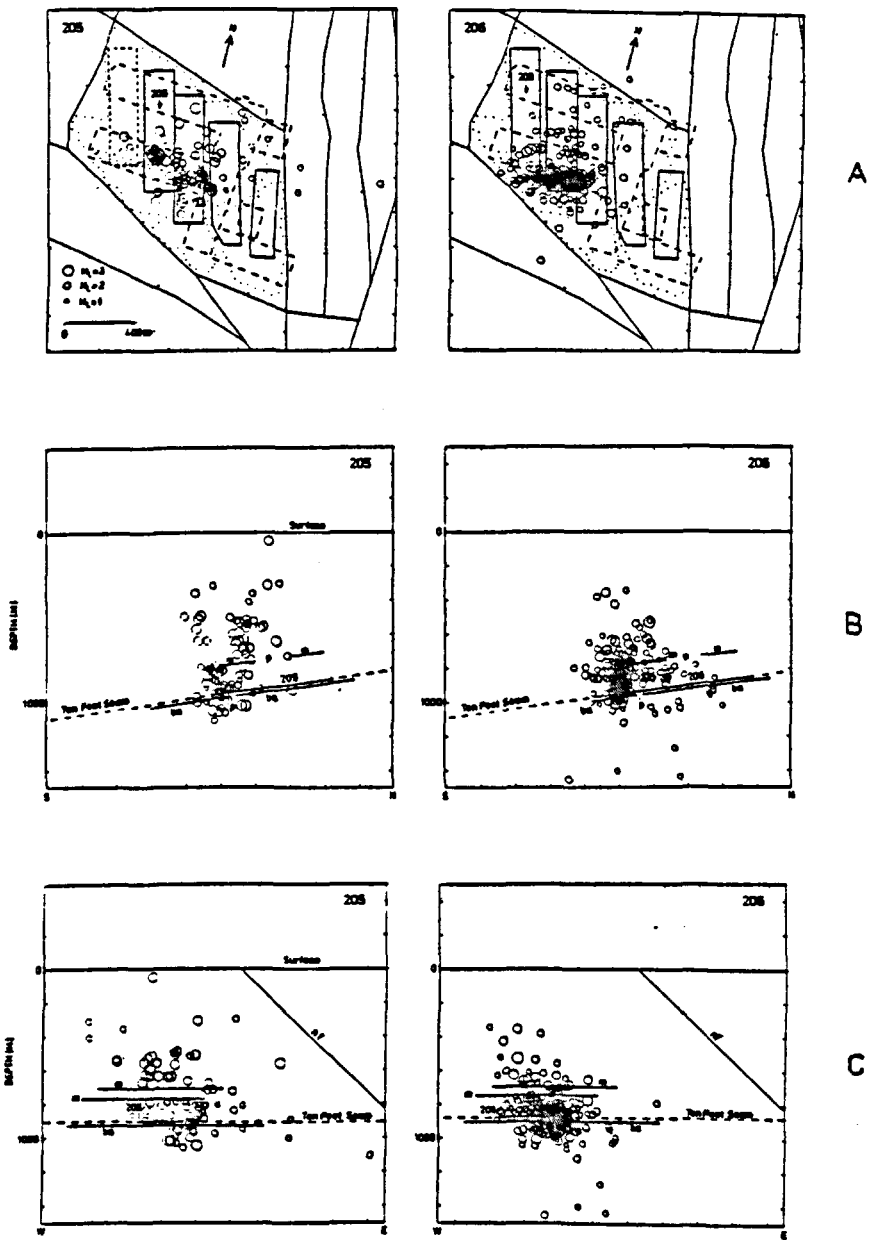

Fig. 7.2.1. The distribution of tremor hypocentres for tremors occurring during the mining of panels 205 and 206 with respect to the active mine workings in the Ten Feet seam, faults at Ten Feet seam datum, and old workings in the Moss (M) and Bowling Alley (BA) seams.

(A) Plan view.
(B) Vertical section parallel to the line of face advance.
(C) Vertical section parallel to the coal face.

(Taken from Kusznir et al., 1980b).

workings and faults in the area (Kusznir et al., 1980a). Tremor hypocentres are shown in plan and vertical sections perpendicular and parallel to the coal faces. Each event was represented by a circle whose radius is proportional to its magnitude. The accuracy of the location was estimated to be ±200 m (Kusznir et al., 1980a). It was found that most of the tremors were located in the vicinity of the active mining area and lie at depths between 400 m and 1000 m below the surface. The tremors which occurred during the mining of a particular panel are not always located immediately above or below that panel, but may be displaced slightly to the east of it, i.e. they are located above the previously mined adjacent panel. Kusznir suggested that this may be due to errors in location, or it may be a real effect. The tremor foci are well away from the nearest fault (Newcastle fault) and no relationship with any of the large or small faults has been established (Kusznir et al., 1980a,b).

For more accurate determination of tremor hypocentres, a small seismic network (T.V. network) consisting of five vertical seismometers and having an aperture of about 1.5 km was installed by Kusznir et al. (1980b) above panel 206. This network monitored the seismic activity associated with panel 206 in the period between March and June 1977. The network recorded about 50 events per day (Kusznir et al., 1980b). The two networks (S.O.T. and T.V.) combined together gave more accurate hypocentre locations which were estimated to be better than ±50 m (Kusznir et al., 1980b). Figure 7.2.2 shows the spatial distribution of the tremor hypocentres occurring during a period of about one month and located using the two networks. It can be seen that most of the events occurred above and were displaced about 200 m to the east of panel 206 (i.e. over panel 205) but all within about 250 m in depth from the working level (Kusznir et al., 1980b). It can also be seen that the larger shear type tremors (represented by solid circles) occur at the level of the previously extracted Moss seam and are

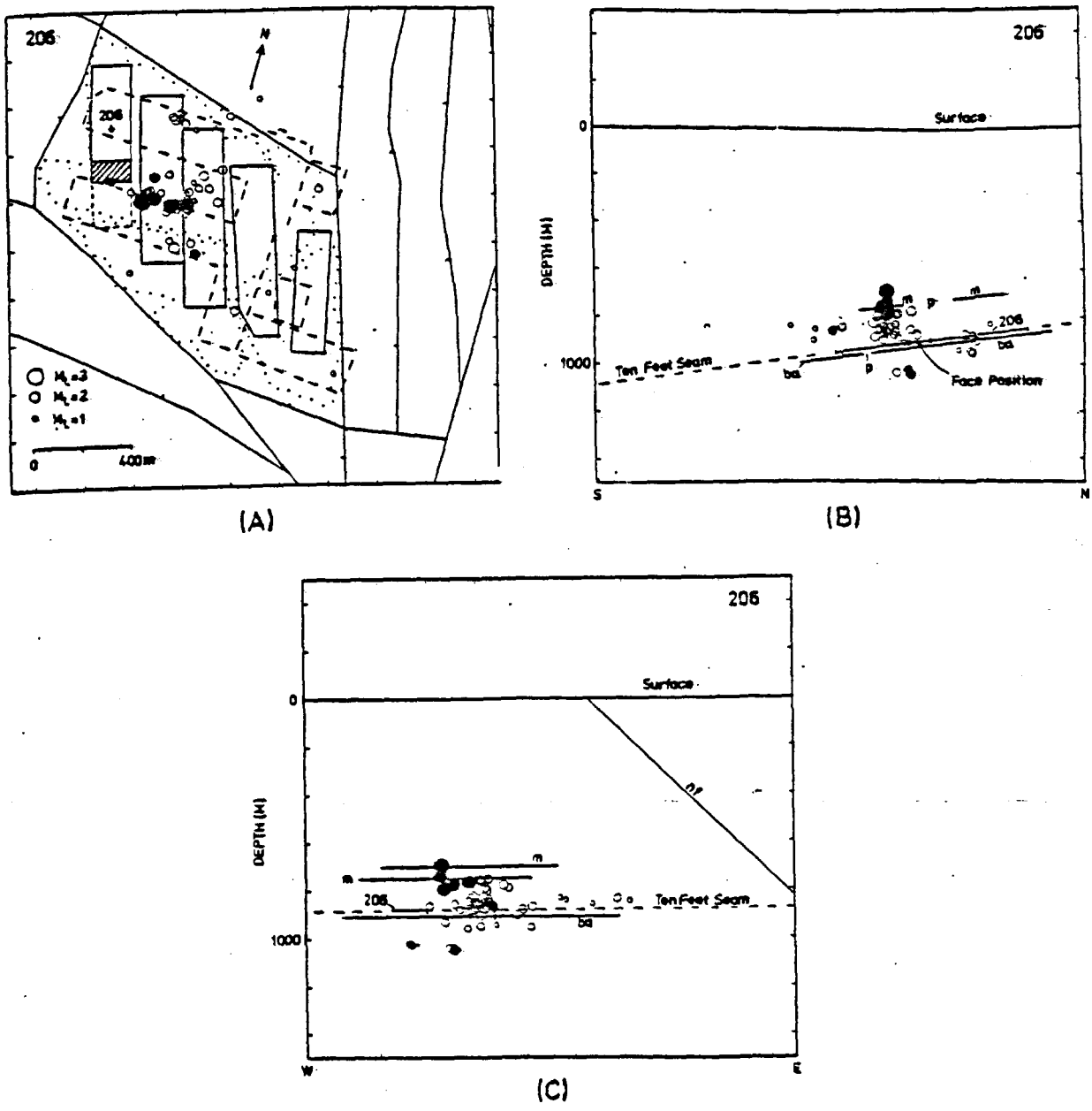

Fig. 7.2.2. Higher accuracy tremor hypocentre locations obtained during the mining of panel 206 using data from both the S.O.T. and T.V. seismic networks. Seismic events with a shear source mechanism are represented by a solid circle.

(A) Plan view, the hatached ornament represents the position of the face during the occurrence of the plotted tremors.

(B) Vertical section parallel to the direction of face advance.

(C) Vertical section parallel to the coal face.

(Taken from Kusznir et al., 1980b).

situated in the Moss seam pillar. The greater accuracy of tremor location confirms that most of the small events particularly the collapse events may occur over the previously extracted panel (in this case panel 205).

Figure 7.2.3 shows the relationship between the plan position of the tremor epicentres and the position of the working face as it advanced along the panel. The figure is drawn by plotting the horizontal position of the tremor, projected onto the line of face advance and measured from the start of the panel, against the distance advanced by the face. The figure shows that the tremors appear to migrate with the advancing face and were usually slightly in front of it. The seismic activity mainly started after the face had progressed a distance of about 250 m (Kusznir et al., 1980a,b). The figure also demonstrates that the occurrence of felt tremors were mainly associated with the passage of the Ten Feet panel face under or over the pillars of the old workings in the Moss and Bowling Alley seams. The majority of felt tremors had a shear source mechanism and local magnitudes, M_L, of greater than 2.5.

The vertical position of the tremor hypocentres were plotted in Figure 7.2.4 against the distance advanced by the face. The figure shows that those felt tremors which occurred when the Ten Feet face passed under the Moss pillar are located at a higher level than the working seam (at the level of the Moss pillar). Some of those which occurred when the Ten Feet face passed over the Bowling Alley pillar are located at the Bowling Alley pillar level. This is particularly obvious for panel 206 (Kusznir et al. 1980a). The smaller unfelt events are usually located within a height of 150 m of the level of the active panel. They had a collapse/implosional source mechanism and local magnitudes, M_L, of less than 2.5. Figure 7.2.5 shows the relationship between the depth of the tremor foci and the local magnitude. The figure clearly shows that the felt tremors are located at shallower depth. This is most probably due to the mining practice as

explained above. However it could alternatively be that the larger tremors usually have small rise times, so that the onset of the P-wave first arrivals could have been picked earlier than for weaker events. This would have caused the larger tremors to be located at shallower depths than the weaker tremors. The location of large tremors at shallower depth may have

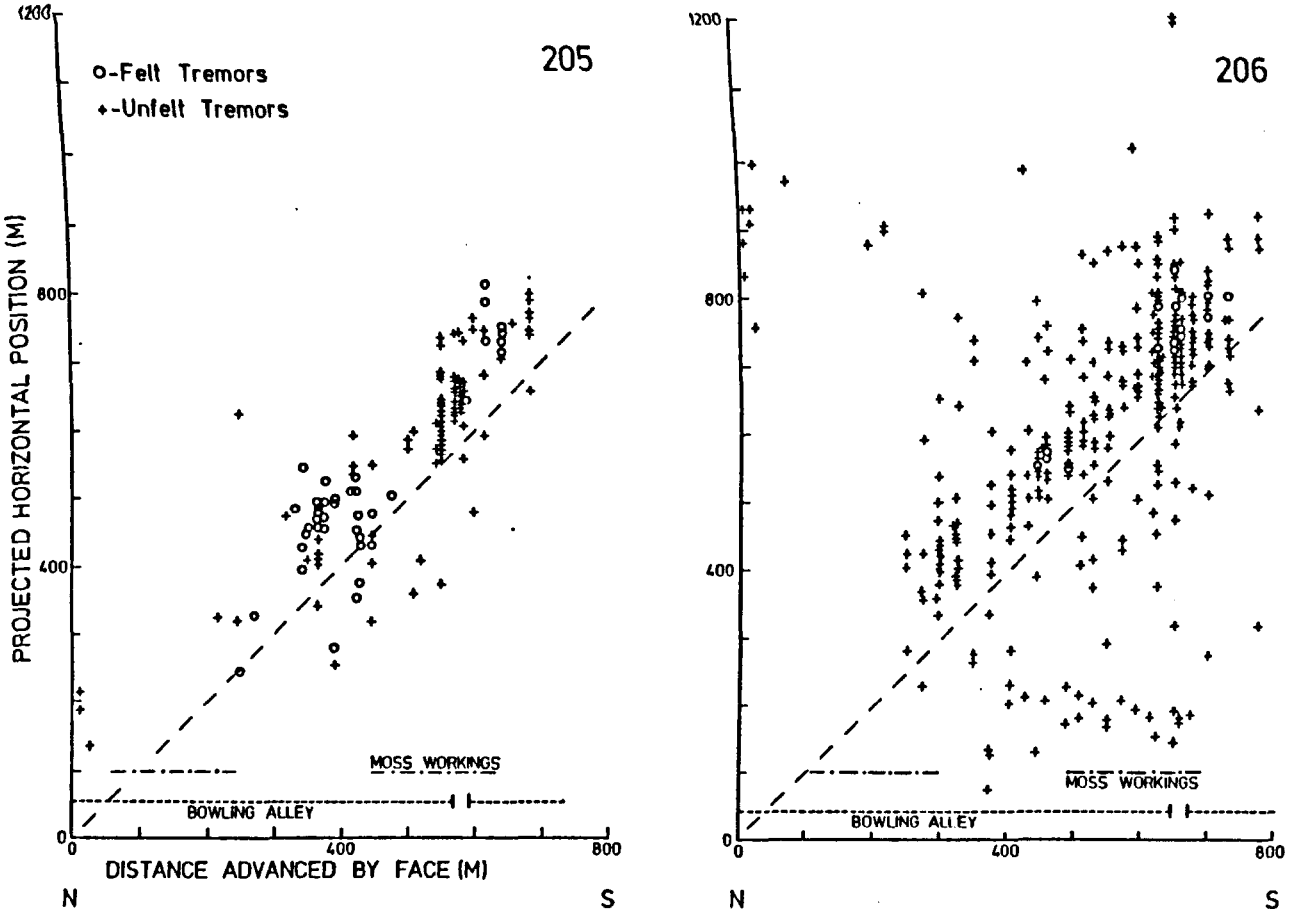

Fig. 7.2.3. Plot of the horizontal position of tremor hypocentres projected onto the line of face advance and measured from the start of the panel, against distance advanced by the face for tremors occurring during the mining of panels 205 and 206. The diagonal dashed line corresponds to the line on which tremors would plot if they occurred on the Ten Feet face. The regions where the Ten Feet face lies above or below previous Moss or Bowling Alley seam workings are also shown. (Caption and diagram taken from Kusznir et al., 1980a).

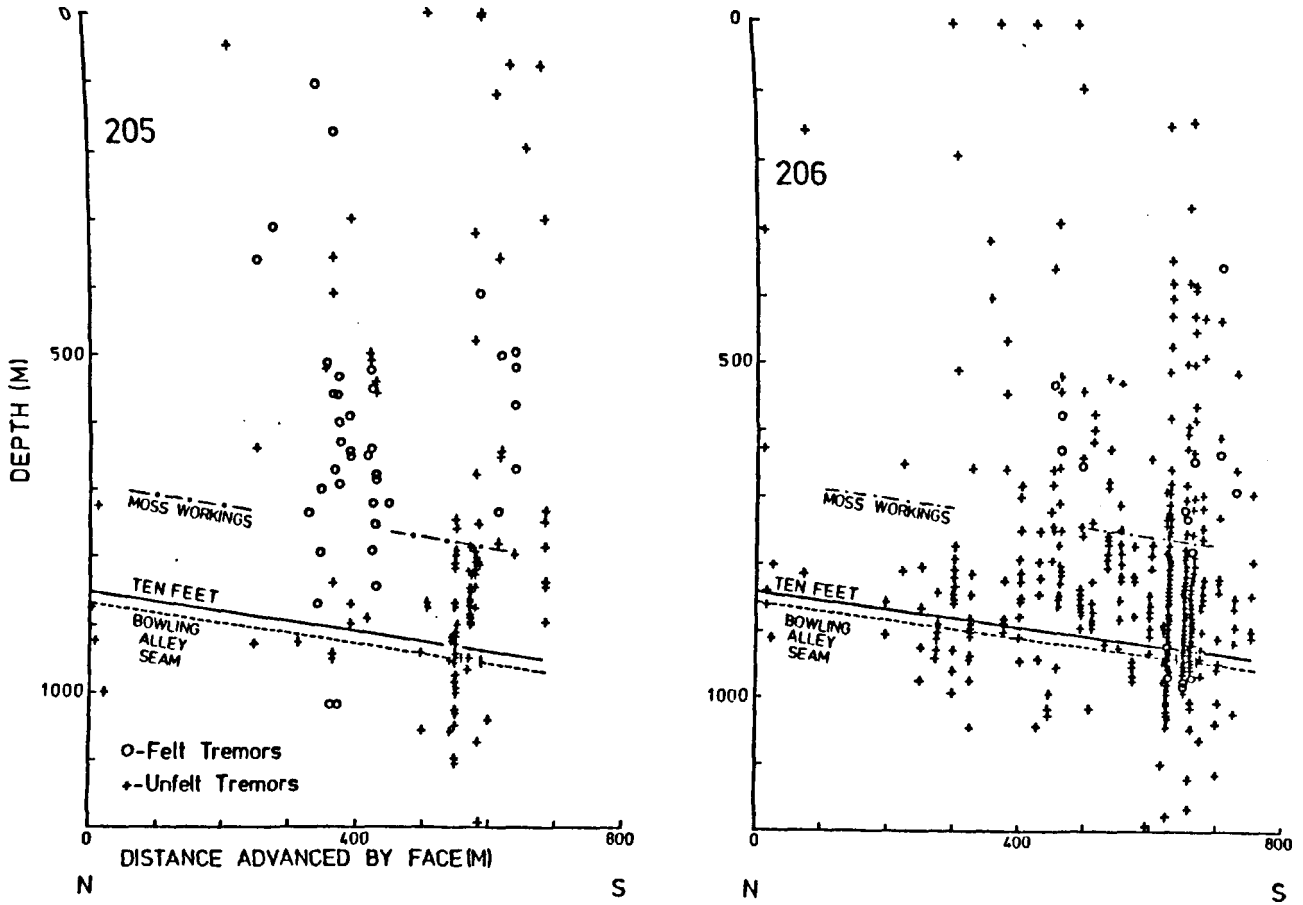

Fig. 7.2.4. Plot of the vertical position of tremor foci against distance advanced by the face for tremors occurring during the mining of panels 205 and 206. The position of the Ten Feet seam workings and previous workings in the Moss and Bowling Alley seams are also shown. (Taken from Kusznir et al., 1980a).

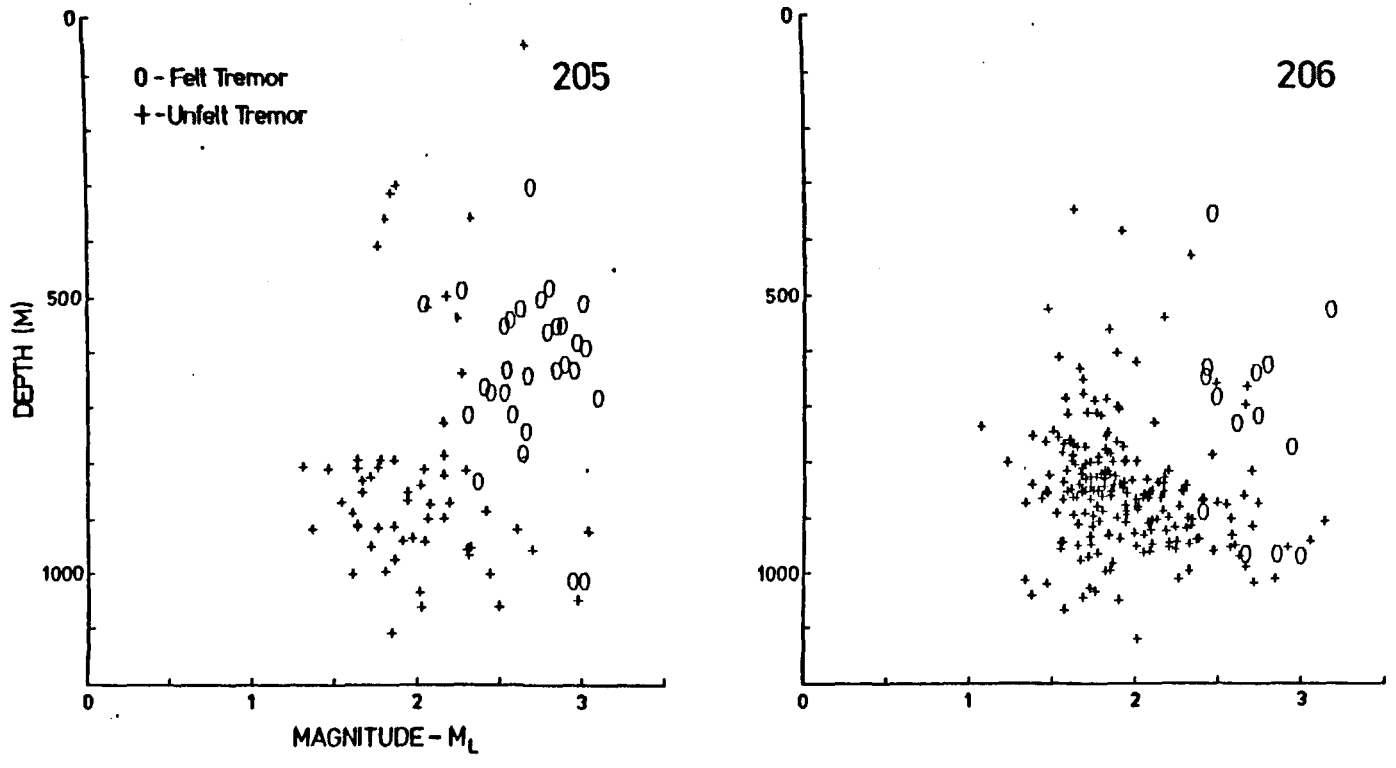

Fig. 7.2.5. The tremor depth plotted against local magnitude, M_L, for tremors occurring during the mining of panels 205 and 206. (Taken from Kusznir et al., 1980a).

led to more tremors being felt at the surface than if those events had occurred at the level of the Ten Feet seam.

7.2.2 The temporal distribution of tremors

The distribution of the total number of tremors, the felt tremors and the seismic energy released, per week and during the week, for each panel are shown in Figures 7.2.6 and 7.2.7 respectively, which were taken from Kusnir et al. (1980a). The figures show a close relationship between the mining activity (which took place between Monday and Friday) and the seismic activity. It can be seen that most of the tremors occurred during the working days of the week. The distribution of the total number of tremors per week shows that seismic activity is noticeably greater during the latter half of the lives of both panels. Westbrook (1977) pointed out that the seismic activity ceased for 12 days in late June and early July 1976 during the mining of panel 205, which corresponds to the miners' holiday. A similar relationship also existed between holidays and seismicity for panel 206 (Kusznir et al., 1980a).

Kusznir et al. (1980a,b) summarized the established relationship between mining and seismicity in the following points:

1. Earth tremors were associated with the active mining panels of the Ten Feet seam.
2. The tremors were not associated with any of the faults in the area.
3. The tremors did not start until the face had progressed about 250 m.
4. The tremor hypocentres lie adjacent to and move in unison with the face.
5. Most of the tremor hypocentres were located about 200 m to the east of the active panel, i.e. over the previous panel.

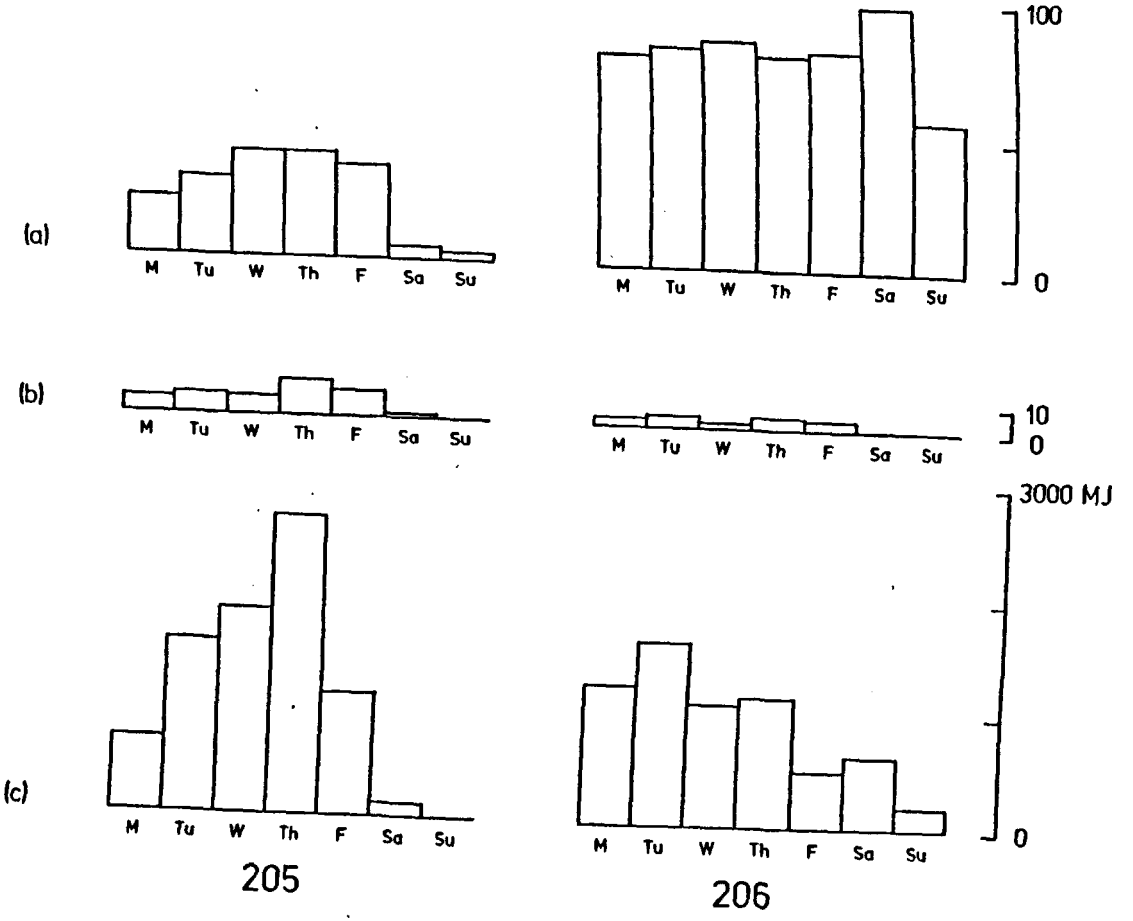

Fig. 7.2.6. The distribution throughout the week of (a) the total number of tremors, (b) the number of felt tremors, and (c) the total *seismic* energy released for panels 205 and 206. (Taken from Kusznir et al., 1980a).

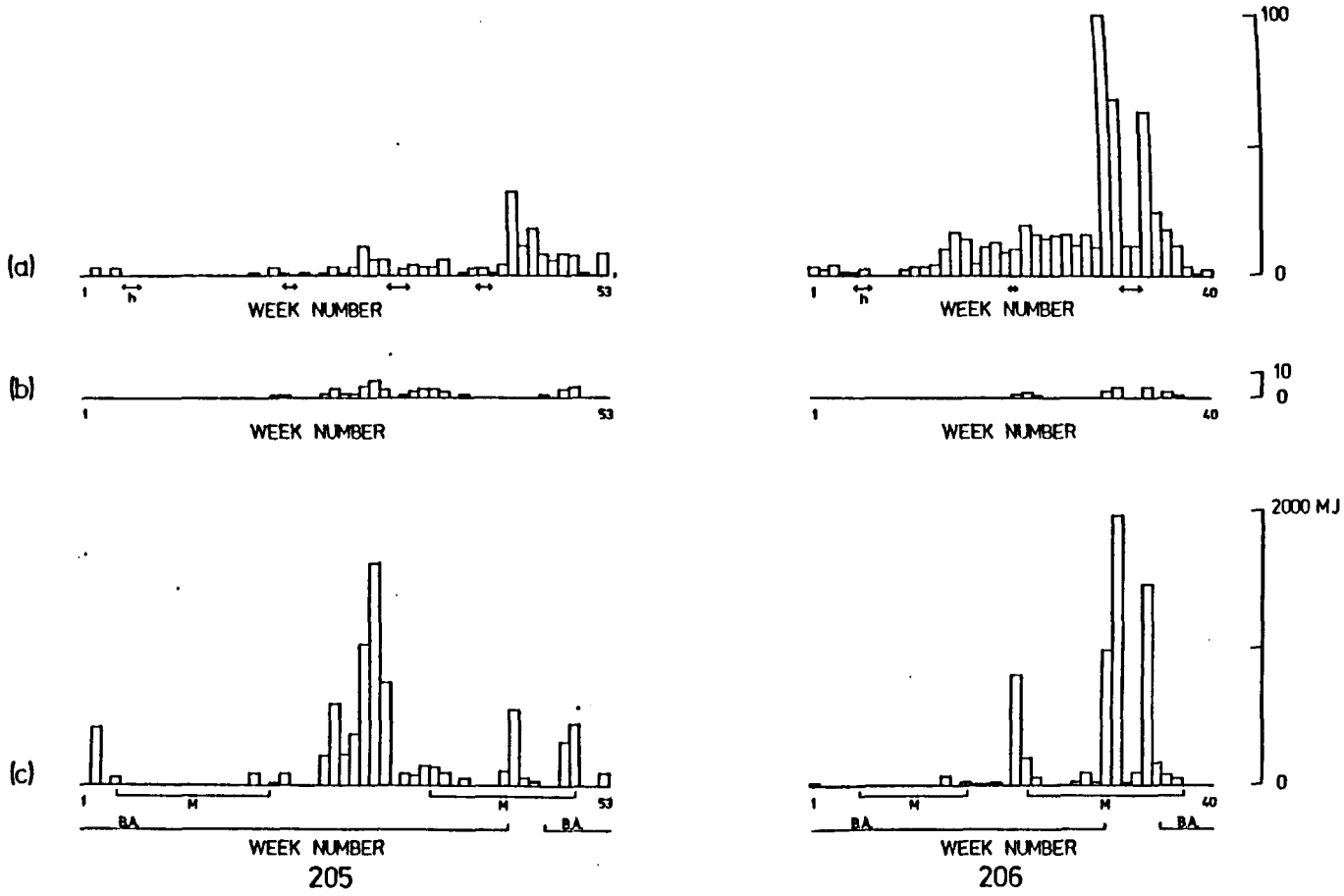

Fig. 7.2.7. Histograms of (a) the total number of tremors per week, (b) the number of felt tremors and (c) the total seismic energy release for panels 205 and 206. The periods during which the Ten Feet face was passing under or over previously extracted Moss seam (M) and Bowling Alley seam (BA) are shown. Miners' holidays are also indicated (h). (Taken from Kusznir et al., 1980a).

6. The larger tremors, particularly the felt tremors, occurred when the Ten Feet face passed under or over pillars left in adjacent previous workings.
7. Most of the large tremors, particularly the felt tremors, had a shear source mechanism, and were located in the pillars of the adjacent previous workings.
8. The smaller unfelt tremors had an implosional or collapse source mechanism, and lying usually within a height of about 150 m of the level of the active panel.

7.3 Mechanism of earth tremors

Kusznir et al. (1980b) suggested from the first motion analysis that two groups of tremors exist.

Group One: This type of tremor had magnitudes, M_L, of less than 2.5 and produced mainly kataseismic first motions. They were located within about 150 m in depth of the Ten Feet panels and usually above them. This type of tremor occurred mainly in the goaf of the previous panel adjacent to the one being mined. Some occurred in the goaf of the previous old panels in the adjacent seams. They were dilational or tensile in origin and were attributed to roof collapse above the worked areas due to the reduction of the compressive principal stress in the goaf resulting in the breaking of strata in tension due to bending. The location of the majority of this type of tremor over adjacent panels (see Figure 7.2.1) can be explained as a result of the extension of the tensile stress and strain zone already existing over the previous working, due to the working of the active panel. The stress will be at a maximum in the centre of a hypothetical beam or plate. Sandstone will be particularly able to withstand high stress. The presence of a barrier pillar such as this existing between panels 205 and 206 will reduce the stresses but only to a certain extent. Failure of the sandstone bed along a fault or sandstone lens boundary caused the release of energy.

The amount of energy released in tensile failure is far smaller than the energy released in failure by compression or shear due to the difference in material strength between compression and tension. This type of tremor is probably the inevitable and normal noise and vibration associated with the caving of strata and does not appear to constitute any form of hazard.

Group Two: This type of tremor had larger magnitudes than group one. Some of these tremors were felt on the surface. They usually gave first motions which indicated they have a shear fracture type mechanism. This type of tremor occurred mostly when the Ten Feet face passed under or over the Moss or Bowling Alley pillars. These pillars can be expected to be under heavy load. When the Ten Feet face approached such a pillar, the front abutment pressure of the face added to the pillar abutment pressure producing together a very high stressed zone which led to rock falls in shear. Shear failures can occur when the stress conditions in rock abruptly change from a state with confining stress to uniaxial stress leading to the release of great amountsof stored strain energy. The amount of energy released due to fracture depends on the rock strength, the magnitude of stresses and the size of the fracture .

7.4 Some comments on seismic activity in the Trent Vale-Hanford area

7.4.1 The mine workings in the Trent Vale-Hanford area provide a good opportunity to examine the effect on the behaviour and occurrence of earth tremors of a barrier pillar left along the panel or pillars left in adjacent seams, above or under the path of the advancing face.

As already discussed, panels 205 and 206 of the Ten Feet seam were mined using the longwall technique. Panel 205 was driven to the west of panel 204 without leaving a pillar between them, while panel 206 was mined to the west of panel 205 leaving a coal barrier pillar between them, having a width of about 40 m (Figure 7.1.2).

The frequency-magnitude relationship for seismic events which occurred during the mining of each panel has been shown to follow the frequency-magnitude distribution for natural earthquakes and can be represented by the following simple relationship given by Richter (1958):

$$\log_{10} N = a - b M_L \qquad 7.4.1$$

where N is the cumulative number of earthquakes of magnitude $\geq M_L$. a and b are constants.

The value of a varies significantly for different seismic source regions since it depends upon the period of observation, the size of the region considered and the level of seismic activity. The value of b mostly varies between 0.7 and 1.0, and depends upon the ratio of the number of earthquakes with low and high magnitudes (Gupta and Rastogi, 1976).

The frequency-magnitude distribution for the seismic events of panels 205 and 206 follow the equation 7.4.1. The following formulae were obtained graphically from Figure 7.4.1:

$$\log_{10} N = 3.1761 - 0.61 M_L \quad \text{(panel 205)}$$

$$\log_{10} N = 4.6128 - 1.19 M_L \quad \text{(panel 206)}$$

Both formulae show that there is a linear relationship between the magnitude and the frequency in the magnitude ranges between 1.7 and 2.6 for panel 205, and between 1.7 and 2.7 for panel 206. The tremors in the higher magnitude range do not fit this relationship, instead they fall below the straight line. This may suggest that a maximum magnitude exists, indicating that the rocks have an upper limit of strain energy which can be stored. The observed data in each panel were found to follow Gumbel's third statistical distribution (Gumbel, 1958; Burton, 1979) which enabled us to estimate the upper magnitude value of tremors that could have

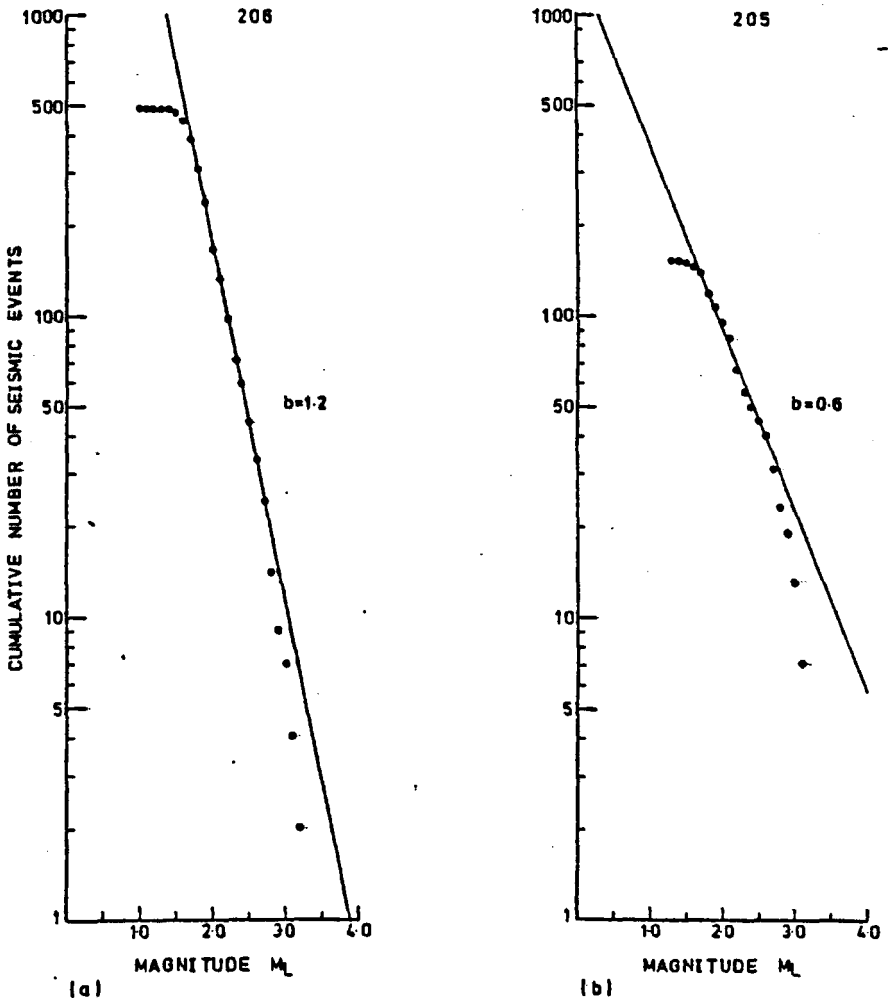

Fig. 7.4.1. Frequency-magnitude distribution for tremors occurring during the mining of panels 205 and 206.

occurred during the mining of each panel. It has been estimated that the largest magnitude (M_L) of a tremor that could have occurred during the mining of panels 205 and 206 is 3.2 and 3.25 respectively.

The total amounts of seismic energy released during the mining of panels 205 and 206 were 5.85×10^9 J and 5.18×10^9 J respectively.

McGarr and Wiebols (1977) defined the level of seismicity (S) per unit volume of rocks mined as (see Section 3.4.1):

$$S = 10^a/\Delta vm \qquad 3.4.1$$

where Δvm is the volume of rocks mined in a particular region.

The total volume of rocks mined from panels 205 and 206 were 2.97×10^5 m^3 and 2.64×10^5 m^3 respectively.

$$S = \frac{(10)^{3.1761}}{2.97 \times 10^5} = 0.005 \qquad \text{(panel 205)}$$

$$S = \frac{(10)^{4.6128}}{2.64 \times 10^5} = 0.155 \qquad \text{(panel 206)}$$

Similarly, the level of seismic energy released per unit volume of rocks mined (EL) can be calculated:

$$EL = \frac{5.85 \times 10^9}{2.97 \times 10^5} = 1.970 \times 10^4 \text{ J} \qquad \text{(panel 205)}$$

$$EL = \frac{5.18 \times 10^9}{2.64 \times 10^5} = 1.962 \times 10^4 \text{ J} \qquad \text{(panel 206)}$$

Panel 206 has a higher seismicity level per unit volume of rocks mined than for panel 205.

The ratio of the seismicity level per unit volume of rocks mined from panel 206 to panel 205 = $\frac{0.155}{0.005}$ = 31. The ratio of the energy released per unit volume of rocks mined from panel 206 to panel 205 = $\frac{1.962 \times 10^4}{1.970 \times 10^4} \simeq$ 1.0. These figures indicate that the seismic energy released per unit volume of rocks mined from both panels is remarkably the same, while we can see that the number of tremors occurring per unit volume of rocks mined from the panel affected by the barrier pillar (panel 206) is about 31 times the number of tremors occurring in the panel not affected by the pillar (panel 205). This may suggest that leaving a coal barrier pillar between, along, the active panel and the previous adjacent panel increases the seismicity level (increase a) but decreases the size, M_L, of the seismic events (increase b). The opposite happens if a longwall panel is driven along a previous old panel without leaving a pillar between them. This is also clear from observations of the total number of tremors and the number of felt tremors which occurred during the mining of each panel (Section 7.2.1).

From the above I suggest that leaving a proper coal barrier pillar, of pre-determined width, between adjacent panels is a good practice in underground mining for the purpose of reducing the magnitude of earth tremors.

Leaving pillars in the adjacent seam over or under the panel which is being mined, on the other hand, may have a different effect on the values of a and b. The faces of panels 205 and 206 retreated southwards (down dip) passing under and over pillars left in the Moss and Bowling Alley seams respectively (Figure 7.1.1). The computed a and b values in each 100 m or 200 m of advancing face are plotted in Figure 7.4.2 against the distance advanced by the face. The position of the mine workings in the Moss and Bowling Alley seams are also shown in the figure. The values were computed from the frequency-magnitude relationship of the seismic events which occurred in each 100 m or 200 m interval of the advancing face. It can be seen that as the face moved under or over pillars left in an adjacent seam, the b and a values decreasedmarkedly. The values increased as the face advanced further, reaching maximum values when the face moved under or over a previous mined out area. This is particularly clear for panel 206.

As has been discussed earlier, panels 205 and 206 retreated (down dip) passing exactly through the same pillars left in the adjacent seams. Retreating the panels down dip may have caused any competent bed, such as sandstone, present in their roofs, not to break easily, but overspan the goaf and acts as a beam or cantilever throwing its weight and the weight of the overlying strata onto the solid rocks ahead of the face (see Sections 2.2 and 2.6). This situation could be aggravated by the action of the drag which tends to concentrate more pressure on the face down dip of the seam. Therefore, when the face passed under or over a previous pillar in the adjacent seam, the front abutment pressure was increased and consequently the rocks in the pillar and ahead of the face sometimes failed violently and generated strong tremors. However, leaving a long barrier pillar along the eastern side of panel 206 may have reduced the roof sagging and consequently reduced the concentration of the pressure ahead of face 206. As a result of this the rocks ahead of face 206 may have failed relatively

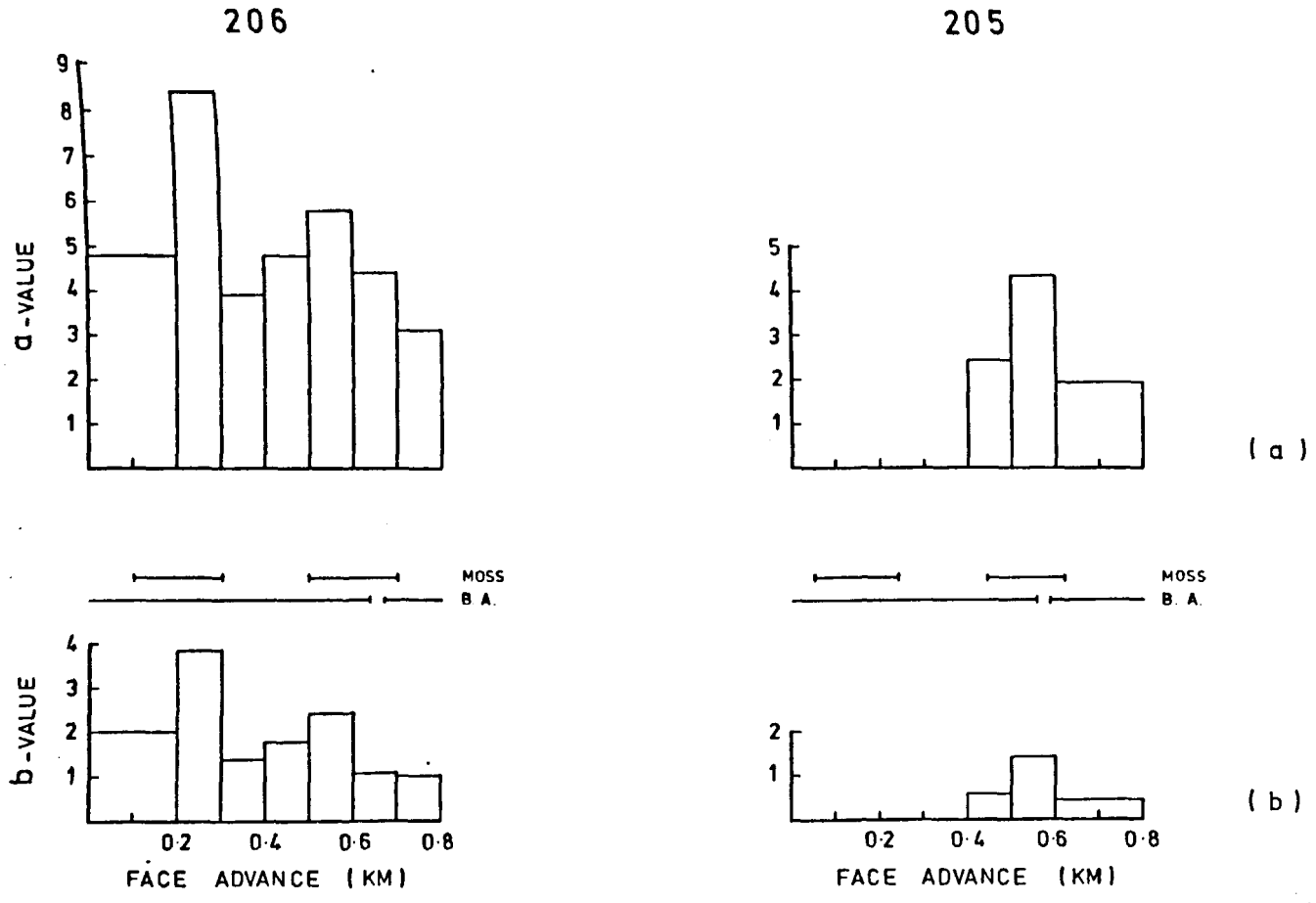

Figure 7.4.2. Histograms of (a) a-value and (b) b-value for each 100 m or 200 m of face advance, for tremors occurring during the mining of panels 205 and 206. The regions where the Ten Feet face lies above or below the Moss and Bowling Alley (B.A.) seams are also shown.

less violently releasing a more continuous sequence of small amounts of stored strain energy, so generating many small tremors. At the same time, as the face retreated southwards, the barrier pillar itself would fracture continuously due to the interaction of the flank abutment pressures for both panels 205 and 206 applied on this pillar.

From the above it can be inferred that if a pillar was left between panels 204 and 205, the earth tremors generated during the mining of panel 205 probably would have been less severe, and the stored strain energy would have been released through a large number of smaller tremors. It may also suggest that if panels 205 and 206 had been advanced northwards (up dip) it might have reduced the level and severity of the seismic activity occurring during their mining. In this case the strata in the roof could have broken and caved into the goaf more easily and consequently reduced the pressure on the panel face.

The variation of $\underline{b}$ and $\underline{a}$ values when the Ten Feet face passed under or over a pillar or goaf can be explained or interpreted in two different ways.

1. It may suggest that there is a relationship between the state of stress and the values of $\underline{b}$ and $\underline{a}$. As we have explained previously, once the face approached a pillar left in the adjacent seam the front abutment pressure of the panel face and the pillar abutment pressure were superimposed, producing together a very highly stressed zone. Consequently, the rocks in the pillar and ahead of the panel face break, sometimes violently, and appeared as tremors. As one large tremor releases more energy than many small ones, therefore, usually a few large tremors occurred. This results in a small $\underline{b}$ value and also a small $\underline{a}$ value. Scholz (1968) found, in micro-fracturing experiments, lower $\underline{b}$ values associated with higher stresses. He indicated that at a stress of about 60% of the fracture strength, new micro-fractures are developed, emitting small pulses, and as the stress is

increased the events become statistically larger producing a small b value. At low unconfined stress, Scholz found high b values. He attributed this to frictional sliding on pre-existing cracks. This may explain why the value of b is higher when the face moved over or under a previously mined out area. When a face moves over or under a previously mined area, frequent falls and sliding movements usually take place in these fractured rocks releasing small amounts of stored strain energy which in our case appeared as small tremors. This also may explain why most of the small tremors which had implosional/collapse source mechanisms were mainly located near the working level of the Ten Feet seam (see Section 7.2).

2. It may suggest that there is a relationship between the homogeneity of the rocks and the values of b and a. The rocks in the pillar are solid, while the rocks over or under a goaf in the adjacent seam are extensively fractured (intradosal ground). This means that the rocks in the pillars are less hetrogeneous than the rocks over or under a previously mined area.

In homogeneous rocks the stress is distributed more uniformly than in the case of heterogeneous rocks. If the homogeneous rock is hard it can sustain a high stress before it fails. Failures of this kind of rock usually occur suddenly and violently; this situation would also correspond to low b value. In heterogeneous rocks, localised stress concentrations occur, consequently the rocks break frequently but relatively gently, corresponding to a high b value and probably a high a value also. Mogi (1962) indicated that the frequency-magnitude relationship of elastic shocks accompanying fractures is greatly influenced by heterogeneity of the materials. He found, experimentally, that more heterogeneous rocks are characterized by much higher b values.

The position of the tremor hypocentres, for events which occurred during the working life of each panel, are plotted in Figure 7.4.3 with

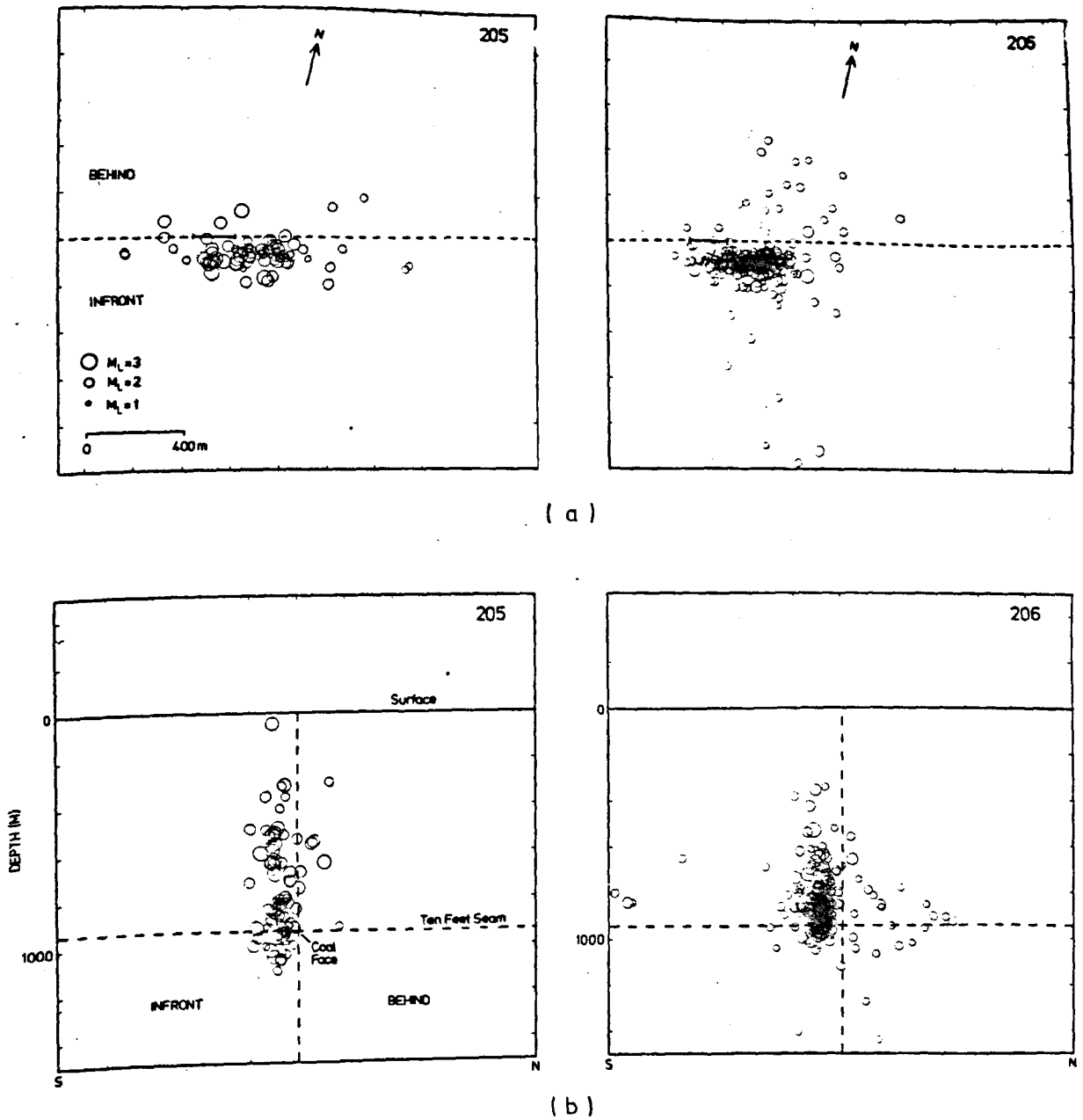

Fig. 7.4.3. Plot of tremor hypocentres relative to the position of the working face, at the time of occurrence, for tremors occurring during the mining of panels 205 and 206.

(a) Plan view.

(b) Vertical section parallel to the line of face advance.

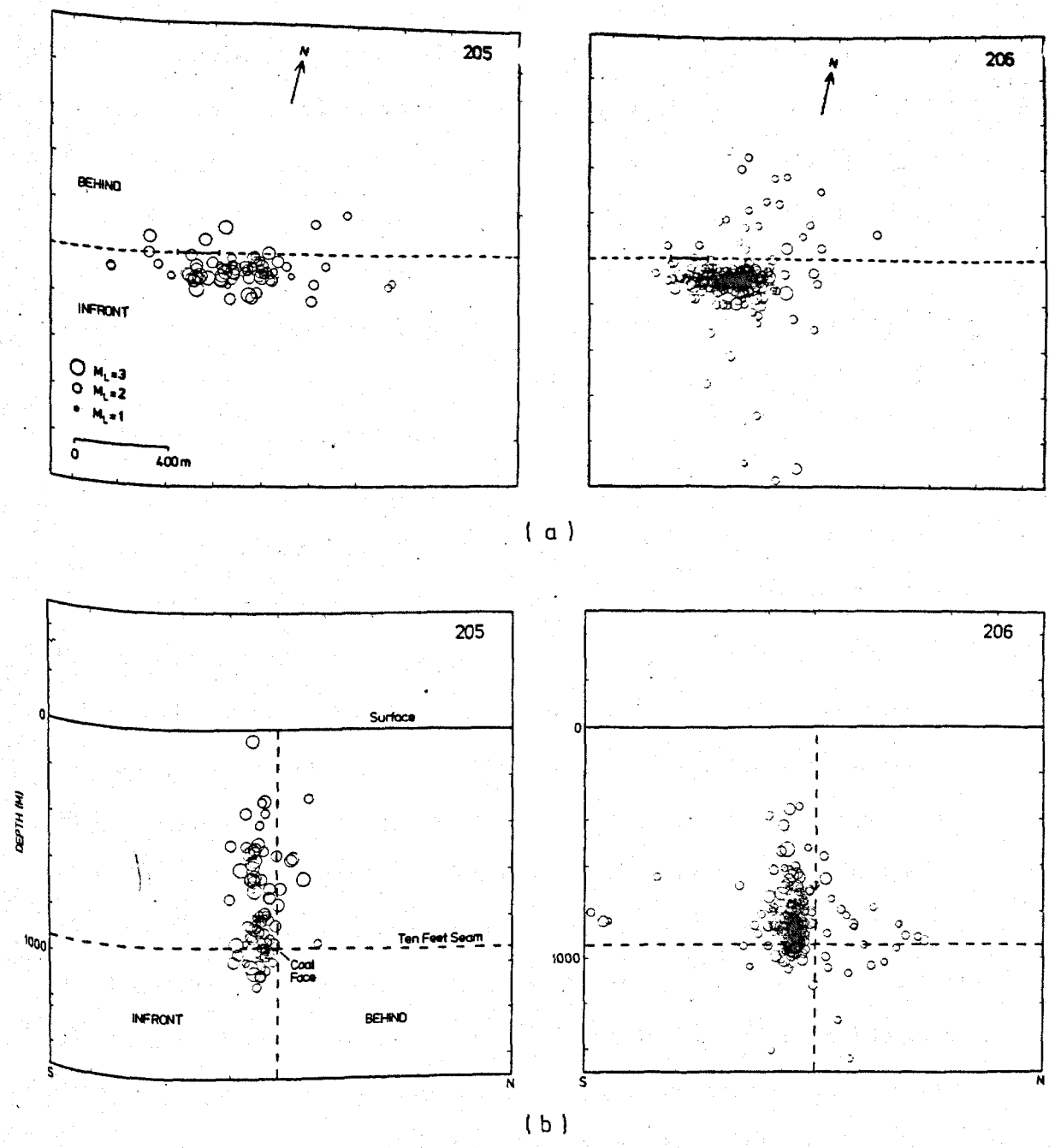

Fig. 7.4.3. Plot of tremor hypocentres relative to the position of the working face, at the time of occurrence, for tremors occurring during the mining of panels 205 and 206.

(a) Plan view.

(b) Vertical section parallel to the line of face advance.

respect to the position of the working face at the time of occurrence. Figure 7.4.3a is a plan view, while Figure 7.4.3b gives a vertical section. Most of the tremors are shown to occur ahead of the face and slightly displaced to the east (i.e. they occurred over the previously mined panel). The majority of tremors are located at the level of the face. Figures 7.4.4 and 7.4.5 show the positions and the amounts of seismic energy release with respect to the position of the coal face. Figure 7.4.4 is a plan view (corresponding to Figure 7.4.3a) while Figure 7.4.5 gives vertical sections. Figure 7.4.5a is a vertical section parallel to the coal face (corresponding to Figure 7.2.1c), while Figure 7.4.5b shows a vertical section perpendicular to the coal face (corresponding to Figure 7.4.3b). The figures were obtained by computing the amount of seismic energy released in an area having dimensions 100 m x 100 m, either in plan or in vertical section. Each area is represented in the figures by a rectangle. It can be seen that most of the energy was released ahead of the coal face and at a distance of less than 200 m from the face. Only small amounts of seismic energy were released behind the face, these being released within not more than 400 m of the face. Most of the energy was released at a depth of less than 100 m below the level of panel 206, while in the case of panel 205, most of the energy was released above the panel level and at height intervals of between 200 m and 300 m from the panel level. Figure 7.4.4 shows that in the case of panel 206 the maximum value of energy released in a unit area occurred just to the east of the face (i.e. over the long barrier pillar and over panel 205). This also helps to confirm that part of this pillar failed during the mining of panel 206 as explained above.

Figures 7.4.3, 7.4.4 and 7.4.5 indicate that in both panels the released seismic energy and the tremors were concentrated near the working coal face. This confirms without doubt that the mining operations for panels 205 and 206 generated the earth tremors in the Trent Vale-Hanford area.

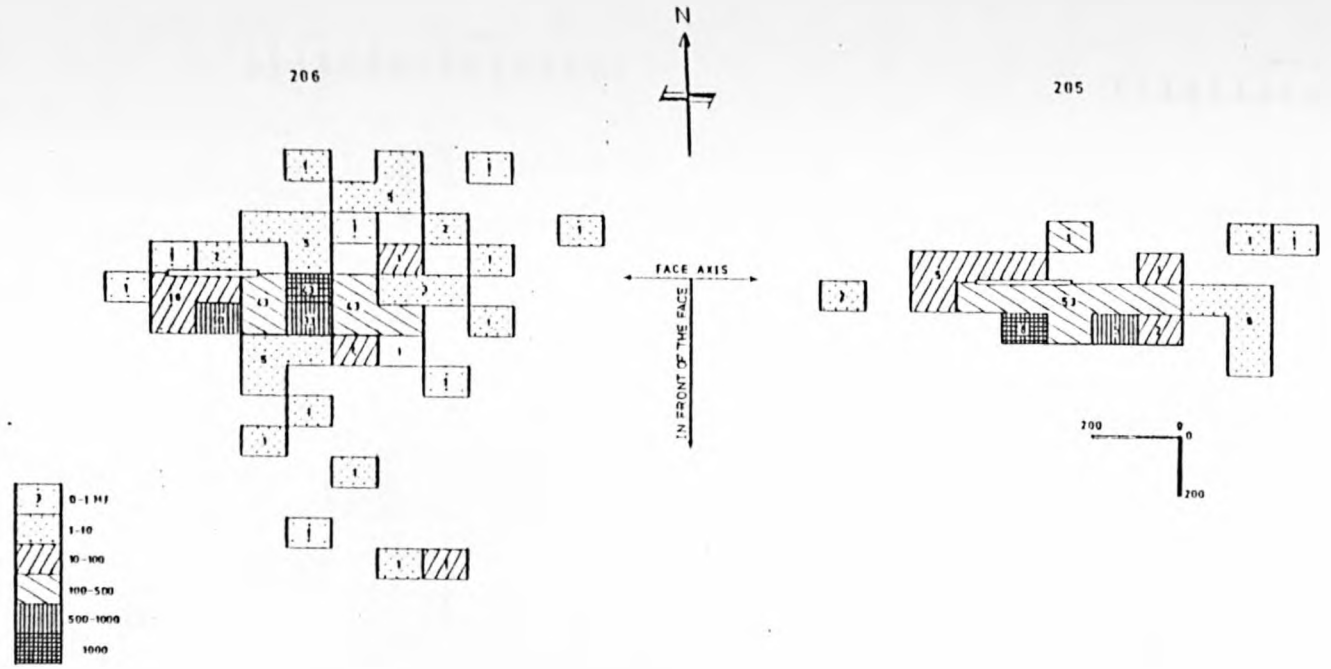

Fig. 7.4.4. Plan view showing the total amount of seismic energy released per 100 m x 100 m area (represented by a rectangle) relative to the position of the working face, at the time of occurrence, for tremors occurring during the mining of panels 205 and 206. Integers indicate the total number of tremors which occurred within the specific area.

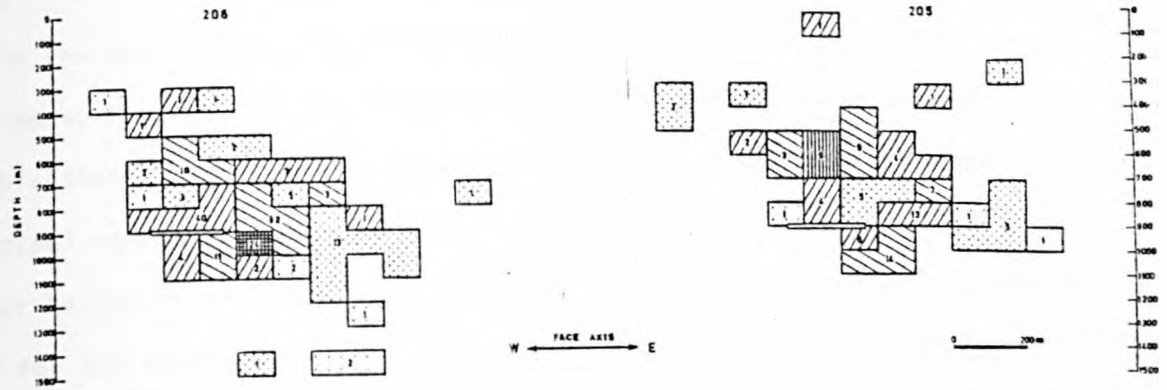

(a)

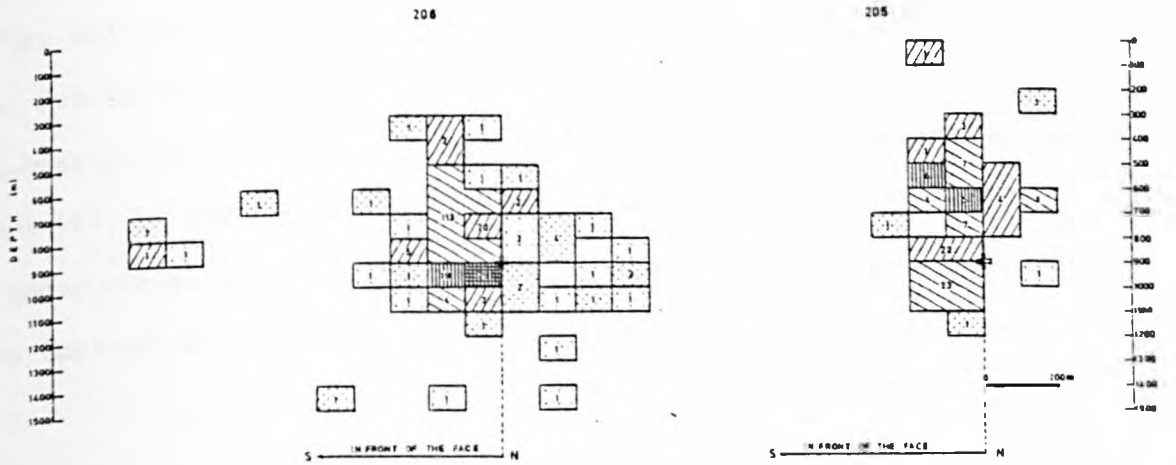

(b)

Fig. 7.4.5. Sections showing the vertical distribution of seismic energy released per 100 m x 100m area (represented by a rectangle), for tremors occurring during the mining of panels 205 and 206. The position of the panel face is also shown. (a) Vertical section parallel to the coal face. (b) Vertical section perpendicular to the coal face. (For legend see Fig. 7.4.4).

7.4.2 In order to determine the state of stress and extent of failures within the Moss and Bowling Alley pillars, before the mining of the Ten Feet seam, diagrams presented by Hoek and Brown (1980) and figure 2.3.1 in this thesis were used to estimate the values of the maximum and minimum principal stresses associated with these two pillars. The ratio of the pillar height to the pillar width is about 0.01 for the Moss pillar and 0.08 for the Bowling Alley pillar. Hoek and Brown presented a diagram with the least pillar height to pillar width of 0.25 (Fig. 2.3.1a). As we can see in Fig. 2.3.1, the ratio of the maximum and minimum principal stresses to the average pillar stress increases as the ratio of the pillar height to the pillar width decreases. Figure 2.3.1a was used to estimate the values of the principal stresses in these two pillars.

The average pillar stress, σp, in the Moss and Bowling Alley pillars prior to failure has been calculated using equations 2.3.1a and b respectively, and were found to be 46 MN/m^2 and 273 MN/m^2 respectively. Using Fig. 2.3.1a it was estimated that the lowest values of σ_1 at the edge of the Moss pillar, inside the pillar, and at the corners of the pillar, were about 184, 92 and 253 MN/m^2 respectively, while the lowest values of σ_3 at these places were about 18, 32 and 46 MN/m^2 respectively. These values were applied to the failure criterion given by equation 2.3.2:

$$\sigma_f = \sigma_0 + 4\sigma_3 \qquad 2.3.2$$

where σ_f is the compressive stress needs to cause failure.

σ_0 is the uniaxial compressive strength of the coal. Bell (1975) estimated σ_0 for strong coal to be ranging between 50 and 100 MN/m^2. Therefore, the average value (75 MN/m^2) has been used.

Wherever σ_1/σ_f exceeds unity, failure must occur. It was found that the Moss pillar must have failed at its edges and corners, but remained intact inside (i.e. it had an intact core pillar). Application of the same

technique for the Bowling Alley pillar showed that the pillar would have failed completely before the Ten Feet seam was mined. However the failed Bowling Alley pillar would still have carried a high load since the broken rocks at the edges can sustain some stress without slipping and afford some lateral constraint for the broken rocks inside the pillar (Cook, 1962; Wilson and Ashwin, 1972). Therefore, when the Ten Feet panel passed under the Moss and over the Bowling Alley pillars, interaction between the stress field in front of the panel and the stress field of the pillars occurred. Consequently rock failure in previously unfractured rocks would have occurred in front of the active panel and at the edges of the Moss pillar. Whether or not the core of the Moss pillar failed completely as a consequence of mining in the Ten Feet seam is difficult to determine. The interaction could have also caused rock slippage in the already fractured Bowling Alley pillar, and this may explain why most of the smaller tremors occurred at the level of the Bowling Alley pillar. The larger tremors were located at the level of the Moss pillar and this may be because the fracture of solid rock releases more energy than slippage within already fractured rocks.

Beale (1981) used the finite element method to estimate the magnitude and distribution of mining induced stresses around the mine openings, in particular, to examine the results of the interaction between adjacent workings. The models used were designed to investigate the mining stresses in the Trent Vale area. However, the models are limited by the assumption of two dimensional plane-strain conditions and the use of homogeneous rock properties. The models do not include the effect of rock failure and closure of the opening. Therefore the stress magnitudes presented in the diagrams and the text are not the exact values in the mine and should be treated with great caution, however they are at least qualitatively useful for the purpose of comparison. All models have been

given a Young's Modulus of 10^{10} dynes/cm^2 (10^{-7} MN/m^2) and a Poisson's ratio of 0.35.

Beale calculated the stress values and distribution around a single mine of different lengths at a depth of 1050 m, which is the depth of the Ten Feet seam below the surface. Fig. 7.4.6 shows a 100 m longwall model. It can be seen that large stresses have developed at the edges of the mine, particularly the vertical stress which reaches well above 500 bars (50 MN/m^2). However higher values of stress usually developed around the corners of the opening, but these are not resolvable by Beale's analysis since a coarse finite element grid has been used in the calculations. The 25 bars (2.5 MN/m^2) shear stress contours extend vertically to a distance just greater than the length of the mine (100 m). Horizontally the contours extend less than 50 m. With longer mine openings (200 m and 300 m in length) much larger stresses have been seen to develop around the mine. The 2.5 MN/m^2 contours extended vertically to 250 m and 400 m respectively, while the horizontal limit does not seem to have increased significantly.

Beale also used models to investigate the effect of panel interaction on the stress fields, in particular when one panel is mined under a previous pillar. Figures 7.4.7 to 7.4.9 illustrate the changing stress field whilst a face is being advanced beneath a 50 m pillar in the above seam. The interseam distance is 100 m. This situation is analogous to that existing in the Trent Vale area. When the active working lies wholly beneath one of the upper workings (Fig. 7.4.7), the stresses at the end of the active working are noticeably lower than that for a single mine (see Fig. 7.4.6). When the active face reached the boundary of the pillar (Fig. 7.4.8) the stress field surrounding the active working in this case is significantly greater than that which would be developed on its own. The shear stress field associated with the pillar is also distorted greatly, and the maximum stresses have increased by 15%. On extending

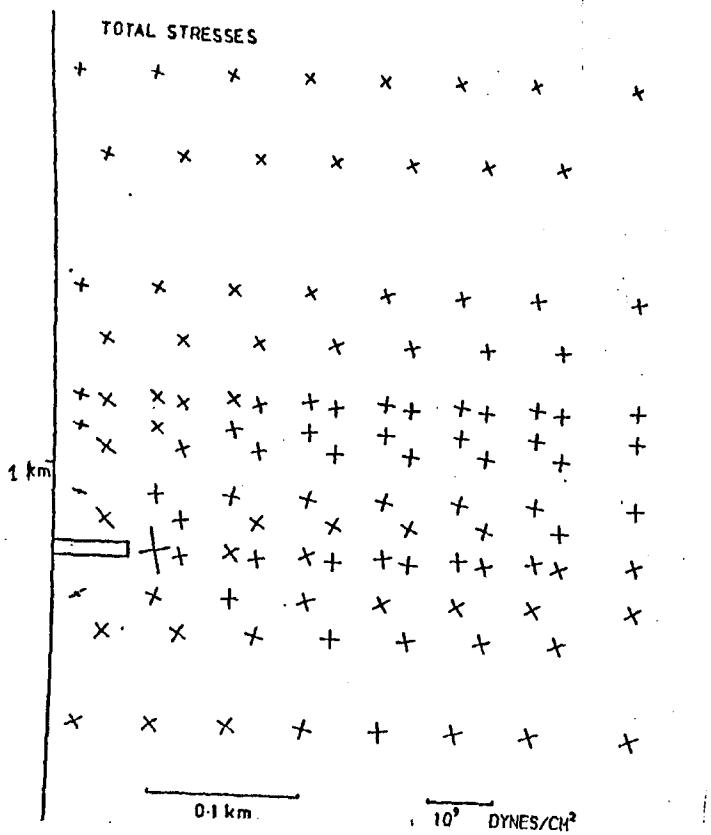

Fig. 7.4.6. Stresses induced by a mine 100 m in length. (After Beale, 1981).

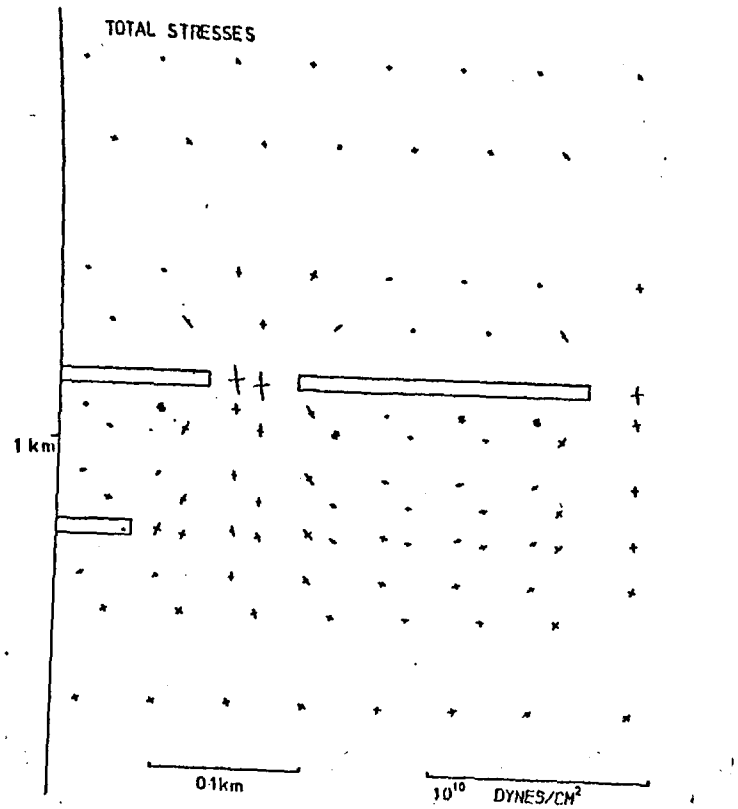

Fig. 7.4.7. Stresses induced by a 100 m length panel mined beneath a previous adjacent working of 200 m length. (After Beale, 1981).

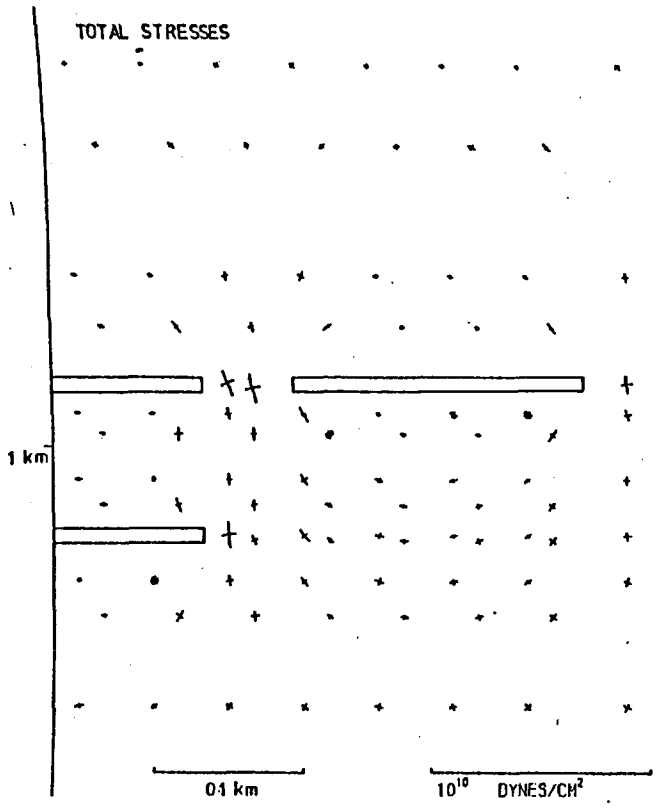

Fig. 7.4.8. Stresses induced by a 200 m length panel approaching beneath the boundary of a 50 m wide pillar. (After Beale, 1981).

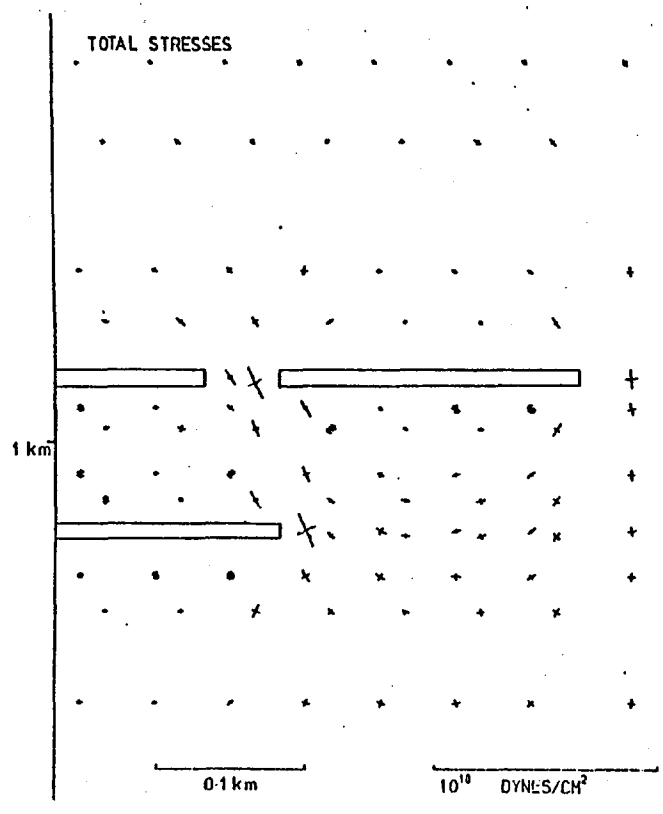

Fig. 7.4.9. Stresses induced by a 300 m length panel advancing beneath a 50 m wide pillar. (After Beale, 1981).

the face to beneath the pillar (Fig. 7.4.9) the maximum shear stresses in the pillar rise by a further 20%, and the shear stresses around the active working are 40% greater than for a single mine.

Beale finally concluded that the stress field associated with a slit-like excavation, as defined by the 25 bar (2.5 MN/m^2) shear stress, extends vertically to a distance approximately 1¼ times its length or width. He also indicated that although the stresses associated with the pillar are very great in the pillar itself, they do not have a great effect unless other workings are mined above or below it.

In the Trent Vale area the interseam distance between the Ten Feet and Moss seams is about 170 m (see Section 7.1). The length of panels 205 and 206 when they approached the Moss pillar edge were about 210 m and 300 m respectively. Therefore, according to Beale's study, interaction between the Ten Feet panel stress field (as arbitrary described by the 2.5 MN/m^2 shear stress contours) and the Moss pillar stress field would have occurred. As we indicated in Section 2.3.1, the vertical stress inside the pillar is less than the peak abutment pressure. Equation 2.3.1a suggests that the vertical stress inside the Moss pillar has a maximum value of about 2.5 times the overburden pressure (i.e. it has a value equal to the average vertical pillar stress). When the Ten Feet panel advanced beneath the Moss pillar, the maximum stress inside the pillar would have increased approximately by a maximum of about 35% according to Beale. (This value was deduced for a pillar 50 m wide and 100 m above the active working, while in the Trent Vale area the Moss pillar is about 200 m wide and lies 170 m above the Ten Feet active workings). This suggests that the Moss pillar core remained intact, since the maximum strength of the pillar core is about four times the overburden pressure (Wilson and Ashwin, 1972). Failures would have only occurred at the boundary of the pillar, since the interaction would have caused the peak abutment pressure on the pillar

edge to rise further so exceeding the strength of the rocks at the edges of the pillar as described in Figure 7.4.10.

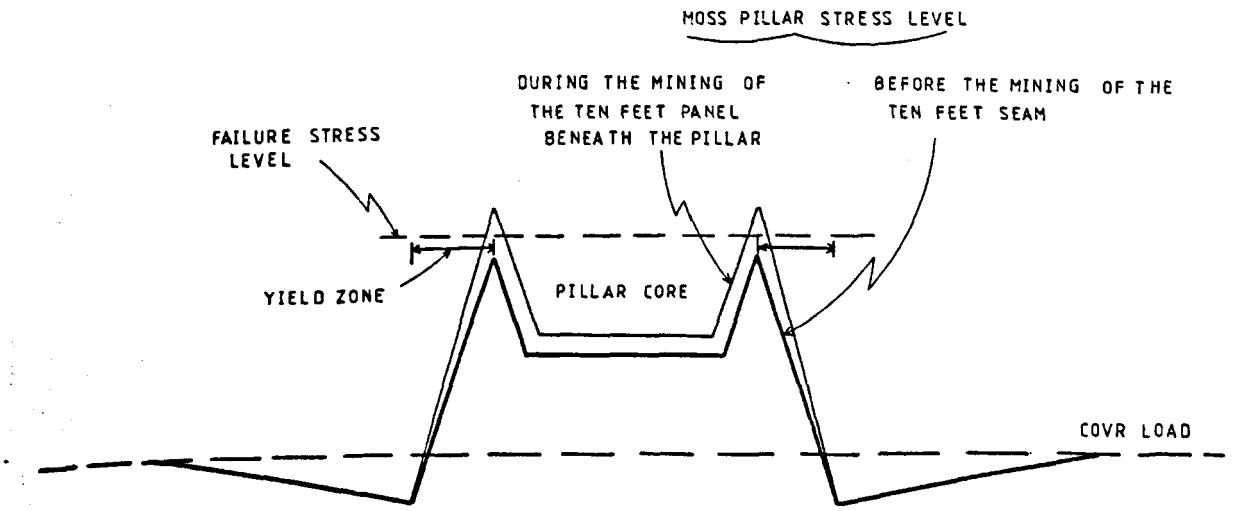

Fig. 7.4.10. Changing of the vertical stress level in the Moss pillar due to the mining of the Ten Feet panel beneath it.

CHAPTER 8

THE OBSERVED RELATIONSHIP BETWEEN MINING AND SEISMICITY IN THE NORTHERN PART OF THE NORTH STAFFORDSHIRE COALFIELD

8.1 Introduction

The Trent Vale-Hanford area, in the southern part of the North Staffordshire coalfield suffered a series of earth tremors generated by mining. Over a period of about two years, 55 earth tremors were felt and hundreds of smaller non-felt tremors were detected by the S.O.T. and T.V. seismic networks (see Chapter 7). Some of these tremors were large and caused damage to property on the surface. The northern part of the coalfield which has a similar mining activity, however, was quiet and only one tremor was felt in the Silverdale area during the same period. However, examination of the seismic records obtained by the S.O.T. network revealed that many non-felt tremors occurred in the northern part of the coalfield in regions adjacent to the active mining areas during the same period.

In this chapter, an attempt is made to find the relationship between seismic and mining activities in the northern part of the coalfield in order to establish the actual causes of the seismicity.

8.2 Seismic events recorded by the S.O.T. seismic network in the northern part of the coalfield

For the two year monitoring period, from September 1975 to September 1977, more than 300 seismic events were recorded by the S.O.T. seismic network, and found to have locations in the northern part of the coalfield. Only 98 seismic events were recorded on four or five seismometers however, so that satisfactory location of the events could be obtained. None of the recorded events were felt on the surface or underground, nor did they cause any damage to property in the area. Furthermore, according to the N.C.B. (private communication) no rock bursts were reported in the mines during

this period. This does not, however, rule out the possibility that some unobserved rock bursts could have occurred in inaccessible parts of the mine.

The local magnitude, M_L, for each event was calculated and each event is represented in the diagrams by a circle whose radius is proportional to its magnitude. The largest tremor has a local magnitude, M_L, of about 2.5, while the smallest one has a magnitude of approximately zero. The seismic energy released from each tremor was also calculated.

Appendix 2 gives a tabulated list of the dates of tremor occurrences, hypocentre co-ordinates, magnitudes, and their released energy.

8.3 Characteristics of seismic activity in the coalfield

The most prominent characteristic of the earth tremors in the coalfield is their distinctive relationship in time and space to mining activity.

8.3.1 The spatial distribution of tremors with respect to mine workings and structural geology

The location of tremor epicentres with respect to mine workings and structural geology are shown in Figure 8.3.1. It can be clearly seen that most of the tremor epicentres cluster adjacent to the mined areas, and usually are within a few hundred metres of active mine panels. Only a few events are located outside areas of mining activity. The figure also shows that the tremors are not located within all the actively mined areas, but that they were encountered within six specific areas. These areas are denoted A, B, C, D, E and F. The total number of seismic events and the total amount of seismic energy release in each area are shown in Table 8.1.

Figure 8.3.2 is a vertical section showing the distribution of tremor hypocentres with depth. Figure 8.3.2a is an E-W section, while Figure 8.3.2b is a N-S section. The majority of the foci lie between the surface and 1 km depth, i.e. within the depth range of the active mined seams.

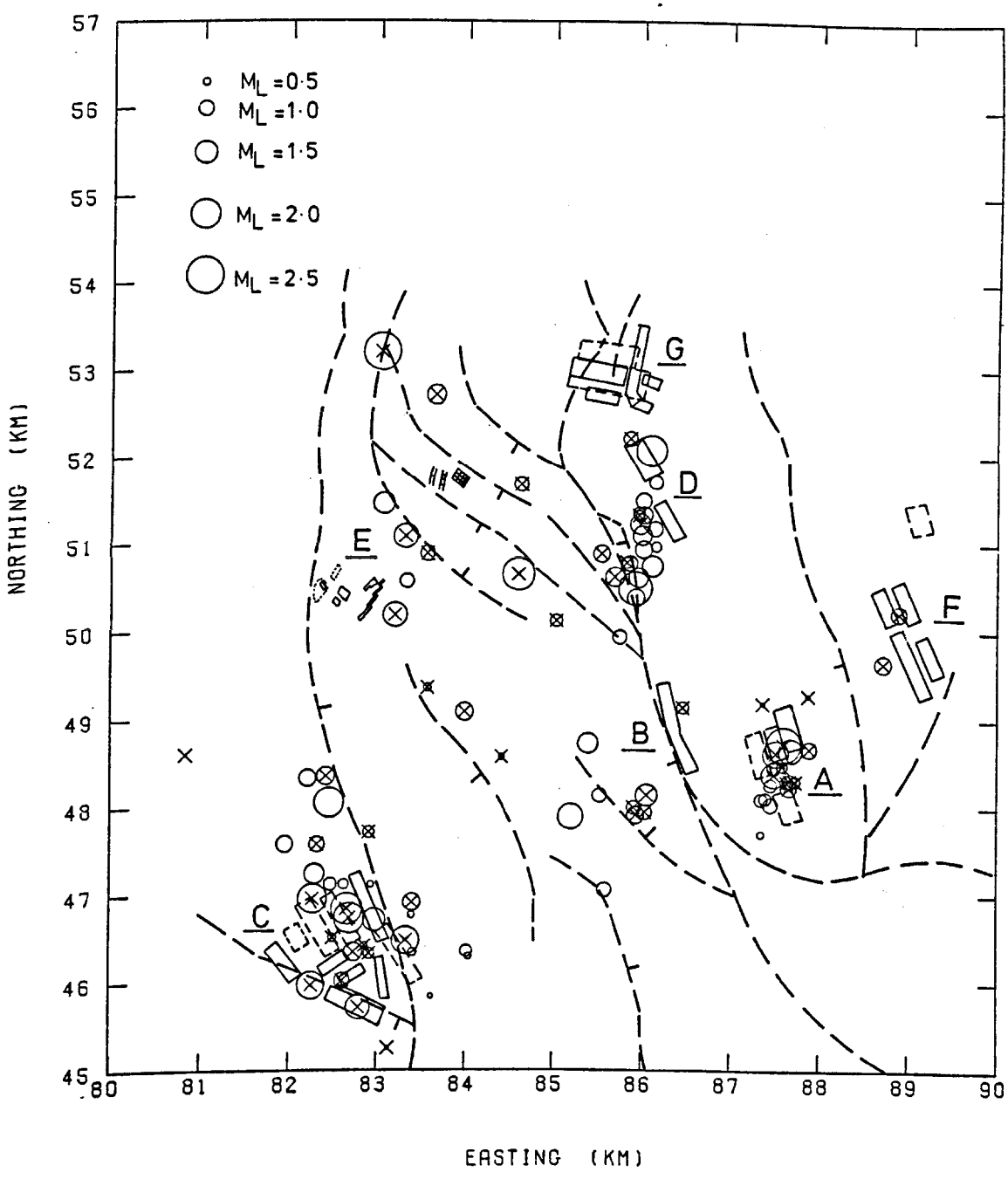

Fig. 8.3.1. Plan view of tremor epicentres for tremors occurring in the northern part of the North Staffordshire coalfield, between September 1975 and September 1977. Tremors are represented by a circle whose radius is proportional to its magnitude. Circle with a cross represent tremors with a shear source origin. Also shown are the active mine workings and the major surface faults. Letters designate the different active mining areas. (For legend see Fig. 4.2.1).

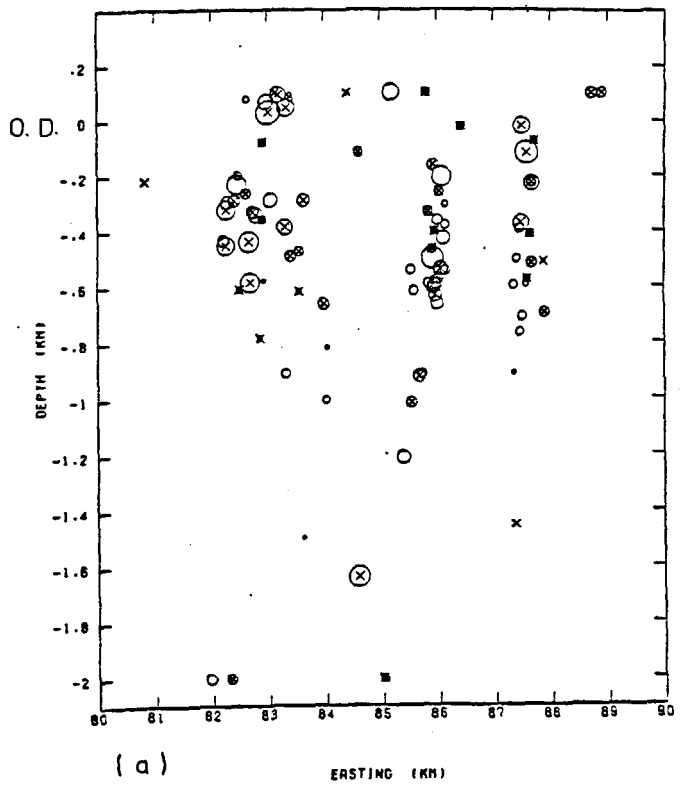

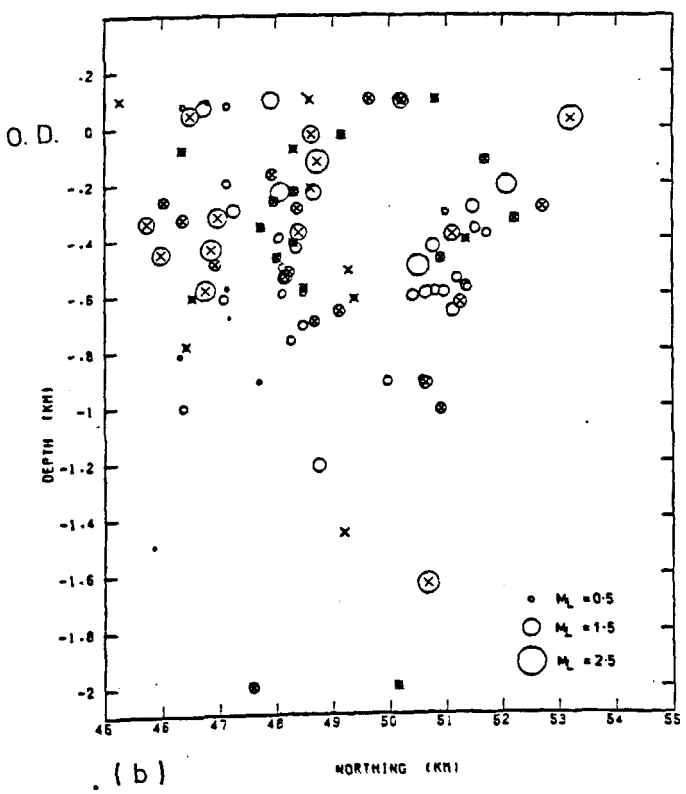

Fig. 8.3.2. Vertical distribution of tremor hypocentres for tremors occurring in the northern part of the North Staffordshire coalfield. (a) E-W section. (b) N-S section.

Table 8.1

The Distribution of Seismic Events and Energy Release in Different Parts of the Coalfield

Area	Location	No. of tremors	% of the total	No. of events with a shear origin	Total amount of seismic energy released (Joule)	% of the total
A	Cobridge	19	19.39	11	268.3×10^5	20.92
B	Wolstanton	9	9.18	5	26.1×10^5	2.03
C	Silverdale	33	33.67	19	301.5×10^5	23.51
D	Tunstall	22	22.45	7	199.4×10^5	15.54
E	Chesterton	13	13.27	11	485.3×10^5	37.84
F	Burslem	2	2.04	2	2.1×10^5	0.16
	Total	98	100	55	1.28×10^8	100

The relationship between the depth and the tremor size, M_L, is shown in Figure 8.3.3. No obvious relationship can be seen. In particular, unlike the situation in the Trent Vale area, no relationship has been obtained between the depth and the occurrence of any specific type of tremor (i.e. shear or implosional/collapse source tremors).

8.3.2 The temporal distribution of seismic events and seismic energy release

(i) Annual distribution: The total number of seismic events per year and the total amount of the corresponding seismic energy release are shown in Figure 8.3.4. The maximum number of tremors occurred during 1976, while the minimum number occurred in 1975. The distribution of events having a shear source mechanism (see Chapter 9) followed the same pattern. The number of seismic events which occurred in 1975 and 1976 do not represent

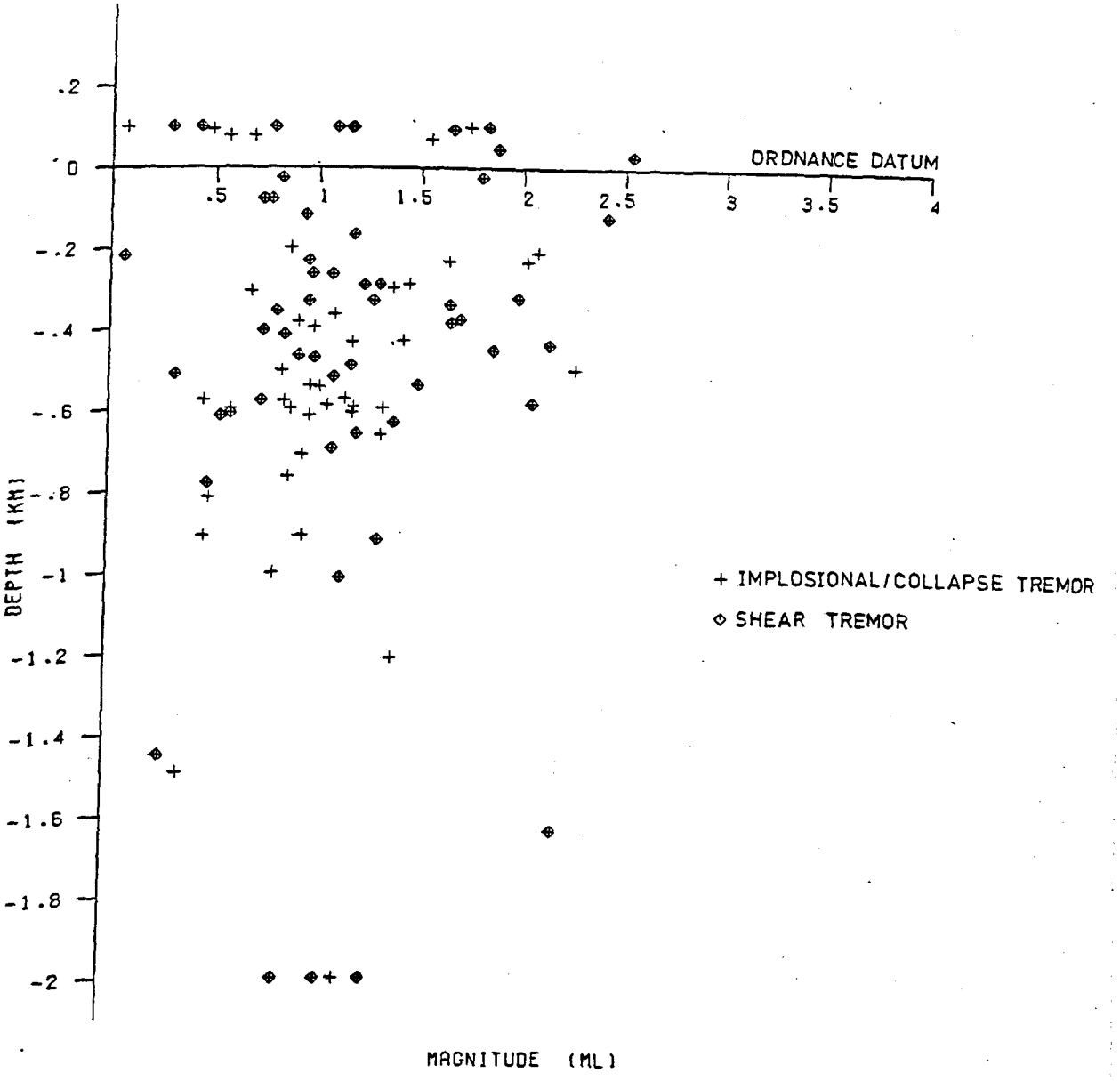

Figure 8.3.3. Plot of tremor depth against local magnitude, M_L, for tremors occurring in the northern part of the North Staffordshire Coalfield.

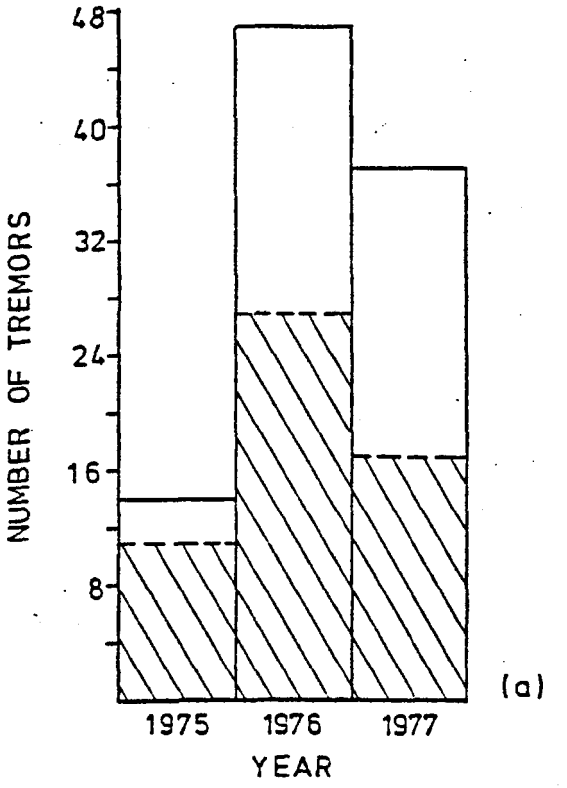

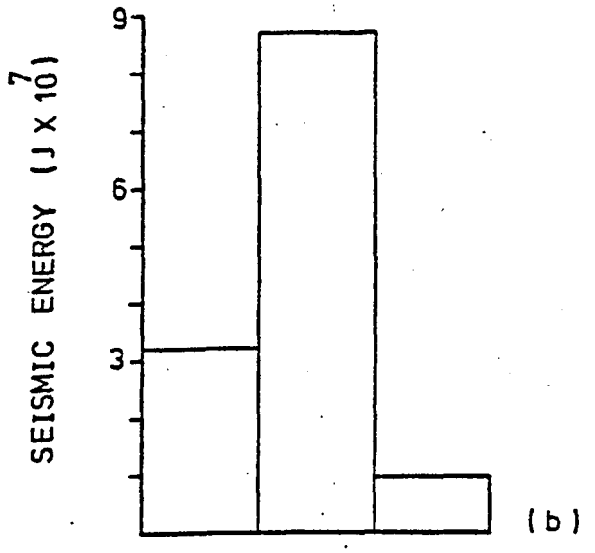

Fig. 8.3.4. Histograms showing the annual distribution of
(a) the total number of tremors (the shaded area represents tremors with a shear shource mechanism),
(b) the seismic energy release for tremors which occurred in the northern part of the North Staffordshire Coalfield.

the actual number of events since the recorded data from many magnetic tapes were lost due to cross-interference between seismic stations (see Section 4.4). The total amount of seismic energy released in 1976 was the maximum, while that released in 1977 was the minimum. The occurrence of the maximum number of tremors and seismic energy release in 1976 is most probably because 1976 represents the longest recorded time, and the largest area of coal was extracted during this year.

(ii) Monthly distribution: The monthly distribution of seismic events, the corresponding seismic energy release , and the level of coal production are shown in Figure 8.3.5. In general, the distribution of seismic events and energy release follows a cyclic pattern in each year, with minima in January and August, and maxima in June and October. The drop in seismicity and energy release in January corresponded to Christmas and New Year miners' holidays. The delay in the start of the seismic events until one month after the holidays could be due to the time required for the elastic strain energy to build up again. The drop in seismicity and energy release in July and August again coincided with holidays (the first two weeks of July). The drop in seismicity and energy release in these holiday periods may also be related to the monthly production of coal as shown in Figure 8.3.5. The figure clearly shows that the minimum coal production occurred in January and July in each year. (This figure represents the total production of the whole North Staffordshire coalfield, i.e. including the Trent Vale area).

(iii) Weekly distribution: The distribution of seismic events and energy release through the days of the week is shown in Figure 8.3.6. The relationship between mining activity during the working days of the week and seismic activity and energy release is very clear. Figure 8.3.6a shows the total number of seismic events which occurred on each day of the week, while Figures 8.3.6b and 8.3.6c show the distribution of those events

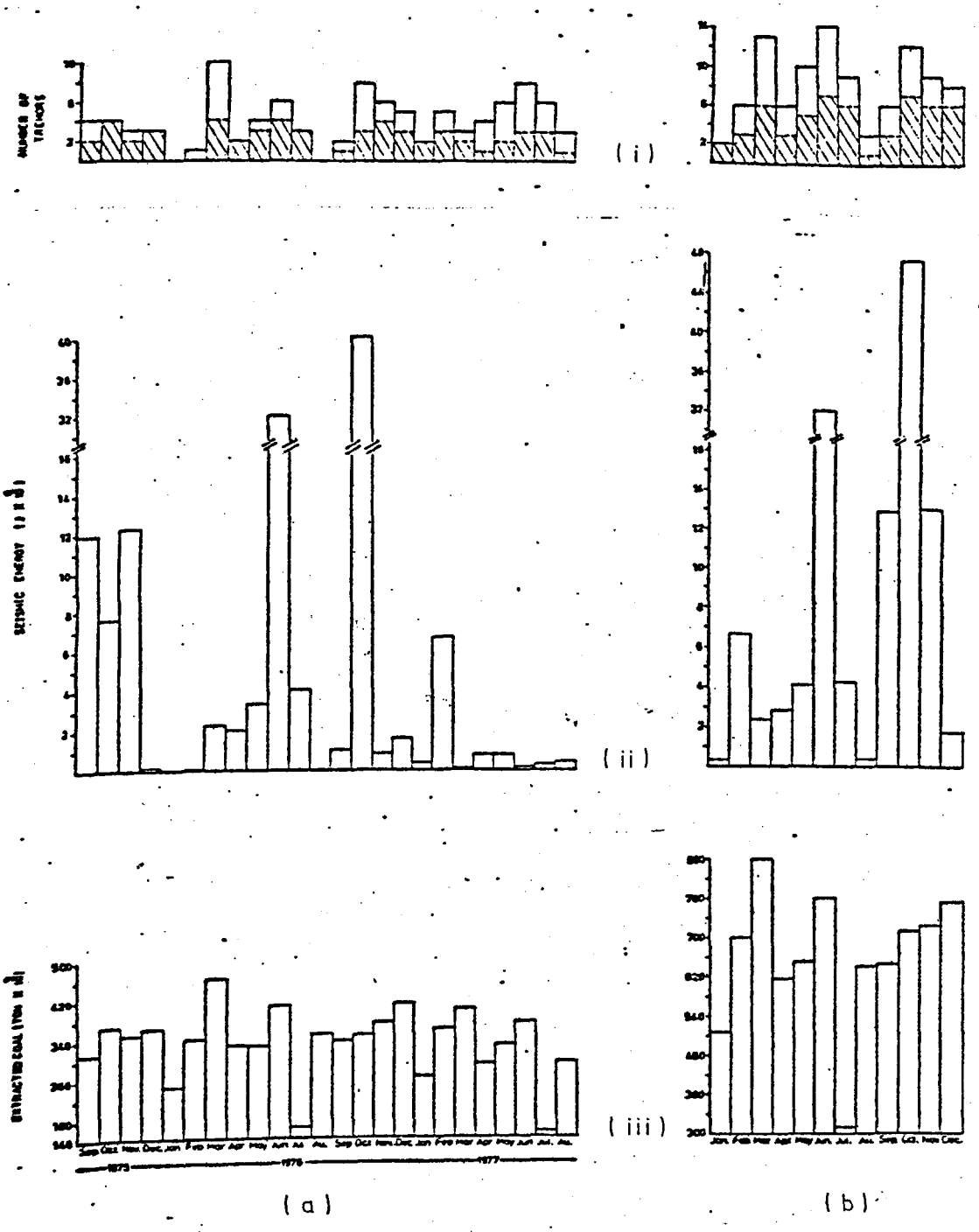

Fig. 8.3.5. Histograms showing monthly distribution of (i) the total number of tremors, (ii) the corresponding seismic energy release, for tremors which occurred in the northern part of the North Staffordshire Coalfield, and (iii) the amounts of extracted coal in the whole coalfield.

(a) Distribution per month over two year period.
(b) Cumulative monthly plot.

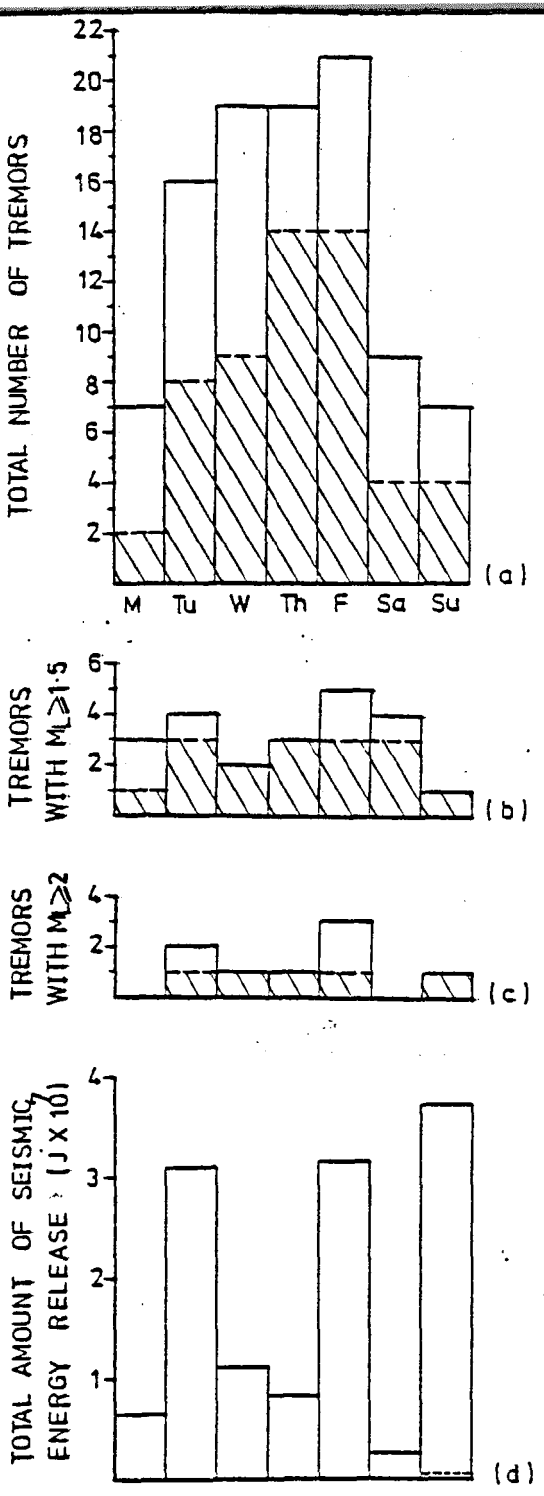

Fig. 8.3.6. Histograms showing weekly distribution of (a) the total number of tremors, (b) the number of tremors with $M_L \geq 1.5$, (c) the number of tremors with $M_L \geq 2.0$, and (d) the total amounts of seismic energy release for tremors occurring in the northern part of the North Staffordshire Coalfield. The dashed line in (d) represents the amount of seismic energy release if the seismic energy released by event 1976 10-31 15-47 is subtracted. Shaded area represents shear tremors.

with local magnitudes, $M_L \geq 1.5$ and $M_L \geq 2.0$ respectively. The figures show that the peak in seismic activity occurred on Fridays after rising continuously from Tuesdays. This might be attributed to the build-up of stress during the previous working days to its maximum value on Fridays. A marked drop in seismic activity occurred at the weekend, both on Saturdays when no actual production was carried out, and on Sundays when the mine was idle (see Chapter 6). Figure 8.3.6a shows that the minimum number of seismic events occurred on both Sundays and Mondays. The low seismic activity on Mondays, perhaps suggests a time delay between the start of production and the subsequent seismic activity associated with the mine workings, suggesting that time is needed for the stress and the strain energy to build up again after the weekend. The distribution of seismic events having a shear source mechanism follows the same pattern. Figure 8.3.6d gives the weekly distribution of the released energy, and shows a peak in the released energy on Sundays. This distribution is greatly influenced by the occurrence of event 1976 10-31 15-47, the largest event in the northern part of the coalfield, which occurred on a Sunday. This event reached a magnitude, M_L, of approximately 2.5, and released about 3.7×10^7 Joules of seismic energy. If the seismic energy released by this tremor is subtracted from the total amount of seismic energy released on Sundays, the minimum amount of released energy then occurs on Sundays (as shown by the dashed line in Figure 8.3.6d) and Saturdays respectively, while the peak is on Fridays and Tuesdays.

(iv) Daily distribution: The total number of seismic events which occurred within each hour of the day, and the corresponding seismic energy release , are shown in Figure 8.3.7. It can be seen that there is no single peak in the occurrence of seismic events, also it can be noted that no single event was recorded between 8 and 9 am. If the frequency of tremor occurrence was equal throughout the day, as might be deduced from Figure 8.3.7a, then the frequency of large tremors should be the same. However, Figures 8.3.7b

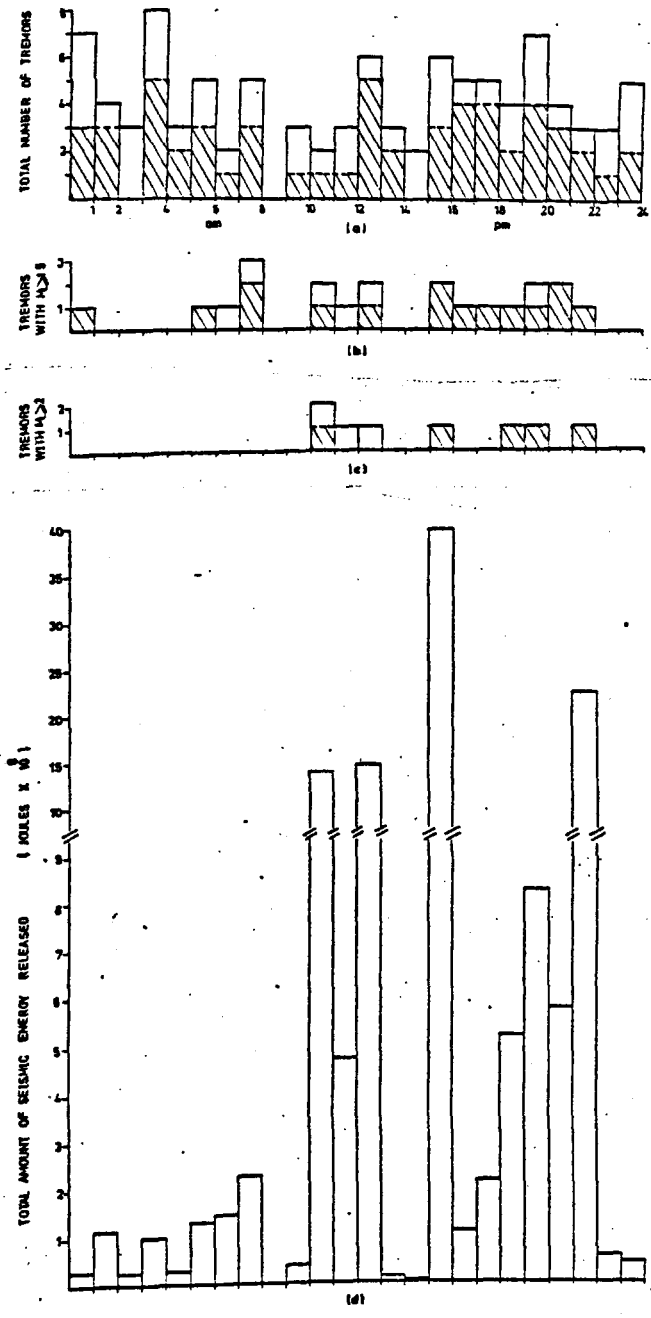

Fig. 8.3.7. Histogram showing daily distribution of (a) the total number of tremors, (b) the number of tremors with $M_L \geq 1.5$, (c) the number of tremors with $M_L \geq 2.0$, and (d) the total amount of the released seismic energy, for tremors which occurred in the northern part of the North Staffordshire Coalfield. Shaded area represents shear tremors.

and 8.3.7c, which give the daily distribution of tremors having magnitudes $M_L \geq 1.5$ and $M_L \geq 2.0$ respectively, clearly show that most of these large tremors have occurred mainly between 10 am and 10 pm.

Blake et al. (1974) indicated that as rock failure is approached, not only does the number of seismic events increase but they become more severe due to the release of progressively more energy. If this is so, then the histogram showing the total number of seismic events which occurred in each hour of the day is probably misrepresentative of the actual seismic activity during the day, since both large and small tremors are given equal weight. Thus, for a more specific quantitative assessment of the actual seismic activity, a plot showing the energy released during each hour of the day is a better guide to the level of seismic activity. Figure 8.3.7d is a histogram showing the daily distribution of seismic energy. Most of the energy was released between 10 am and 1 pm and between 3 pm and 10 pm. This can be interpreted in terms of mining activity. As already discussed in Chapter 6, mining activity was carried out 24 hours a day, through three working shifts. The first two shifts (from 6 am to 2 pm, and 2 pm to 10 pm) are mostly involved with coal production, while the third shift (from 10 pm to 6 am) is mainly concerned with mine maintenance. Figure 8.3.7d shows a marked drop in the energy released immediately after 10 pm which coincided with the end of the second production shift. During the middle of the night and the early morning when no coal extraction was carried out, the released energy was significantly low. The energy release is also noticeably low during the first half of the first production shift until about 10 am when the energy began to increase until about 1 pm when it decreased again for about two hours. The low in energy release during the first half of the first production shift may represent the time required for the energy to build up again in the rocks after the shift has started. The drop in energy release at 1 pm coincides with the shift change and the time required

for the miners in the second shift to restart production. After 3 pm the seismic energy release continued at a high level until the end of the working shift at 10 pm. The close relationship between the release of seismic energy and coal production is more clearly established from Figure 8.3.8 which is a histogram showing the daily distribution of the seismic events and the corresponding seismic energy release for those events which occurred during working days only.

The high incidence of seismic events, shown in Figure 8.3.7a, between 10 pm and 8 am (during the night and early morning) may be explained by a greater detection capability of the seismic network at night due to lower background noise. During day time the background noise increased due to the various human activities, and consequently tended to obscure the smaller events. This situation is confirmed from Figure 8.3.9 which shows the cumulative number of seismic events which occurred throughout the day. It can be seen that the detection rate of seismic events is below the average level between 8 am and 7 pm. The average seismicity level was computed using linear regression.

8.4 The frequency-magnitude relationship

The frequency-magnitude distribution for seismic events in the coalfield follows the relationship given by equation 7.4.1 which was proposed by Richter (1958) for natural earthquakes (see Chapter 7). Figure 8.4.1 shows a plot of the logarithm of the number of seismic events having local magnitudes, M_L, equal to or greater than a specific magnitude versus that specific magnitude. The values of $\underline{a}$ and $\underline{b}$ can be obtained from formula 8.4.1:

$$\log_{10} N = 2.54 - 0.82 M_L \qquad 8.4.1$$

This formula was obtained from the data shown in Figure 8.4.1. The number of tremors having local magnitudes $M_L > 2.25$ are less than that expected

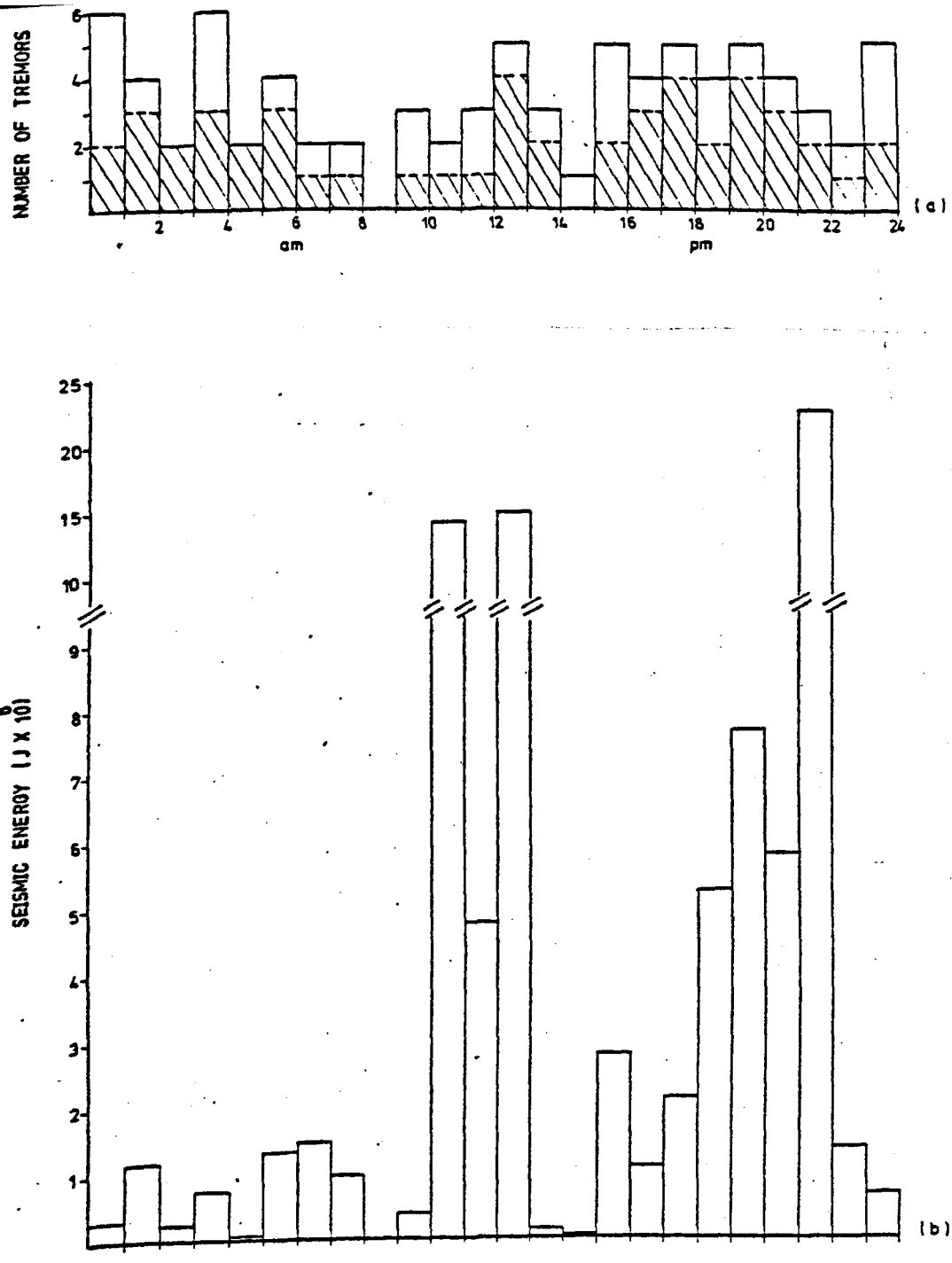

Fig. 8.3.8. Histograms showing daily distribution of (a) the total number of tremors, and (b) the corresponding seismic energy release, for tremors which occurred during working days only in the northern part of the North Staffordshire Coalfield. Shaded area represents shear tremors.

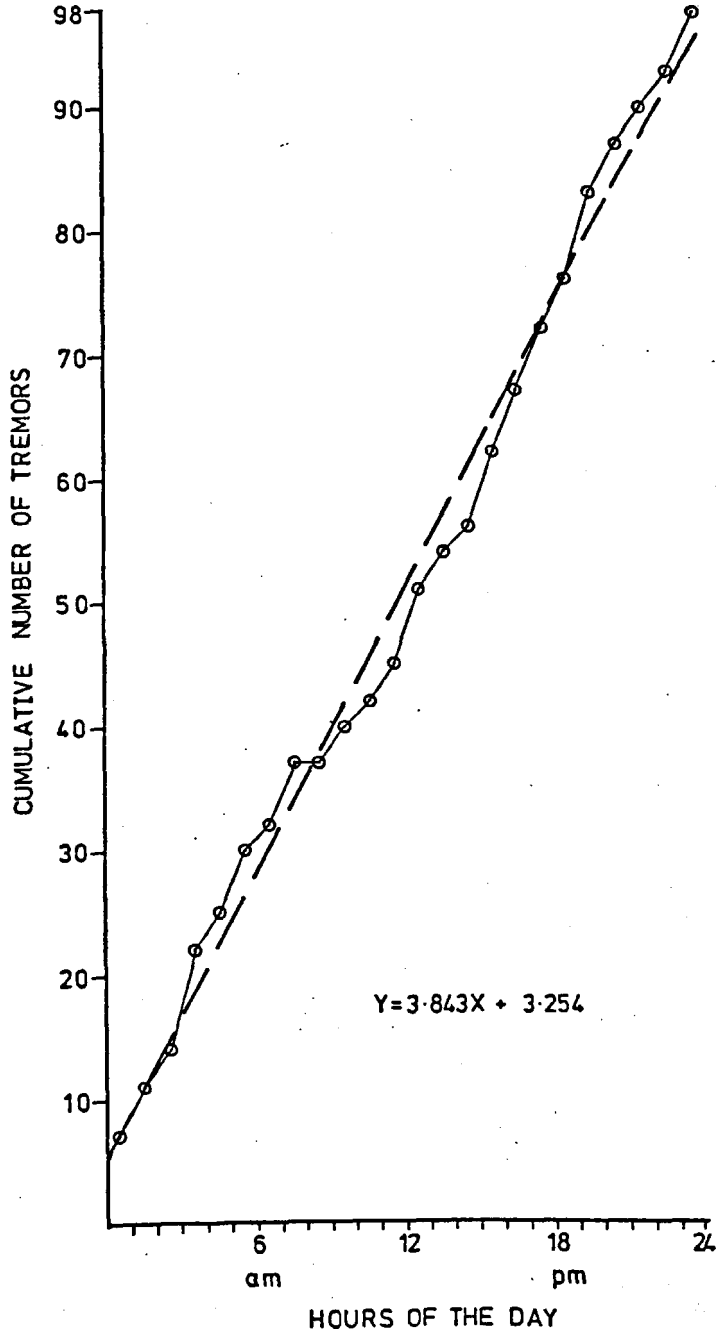

Fig. 8.3.9. Plot of the cumulative number of tremors against hours of the day for tremors which occurred in the northern part of the North Staffordshire Coalfield. The diagonal dashed line corresponds to the line on which the total number of tremors would plot if the tremor occurrence was uniform throughout the day.

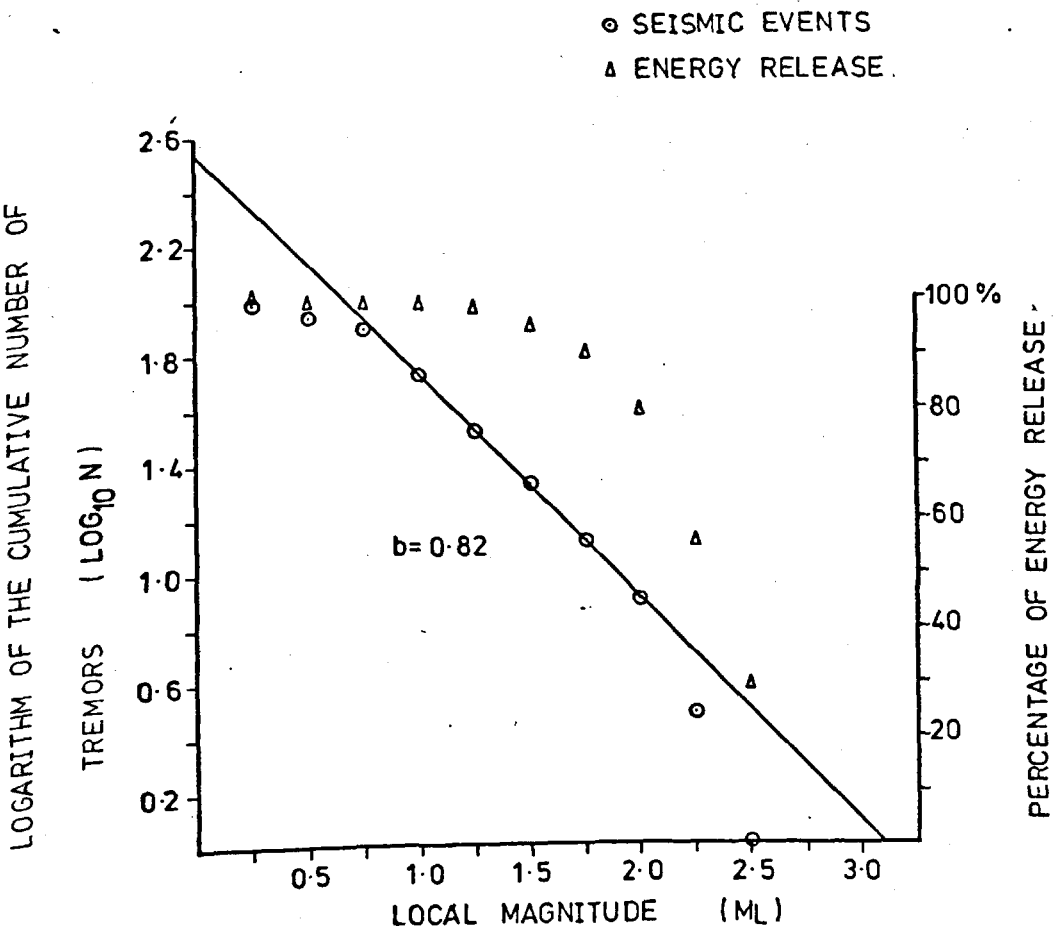

Figure 8.4.1. Plot of the logarithm of the cumulative number of tremors having local magnitudes, M_L, equal to or greater than a specific magnitude against that specific magnitude. The percentage of seismic energy released by each set of tremors having a specific range of magnitudes is also shown.

from formula 8.4.1. This may be explained in terms of the maximum strain energy which can be stored within the region, which consequently leads to the existence of a maximum tremor magnitude. The tremors followed Gumbel's third statistical distribution (see Section 7.4.2) which suggests that the largest magnitude (M_L) of the tremor in the coalfield is about 2.5. However, this should not be taken to be the maximum magnitude of tremors that would be likely to occur in the future in the northern parts of the coalfield, since the tremors in the coalfield are man-made tremors and their magnitudes depend to a great extent on mining practices (such as panel interaction, rate of face advance, etc.) as shown in Chapters 7 and 9. In fact, in August 1980 an earth tremor occurred in area A and was felt over the Stoke-on-Trent. The magnitude (M_L) of this tremor was estimated to be of about 3. (N. J. Kusznir, personal communication).

The fall-off of the number of tremors with low magnitude values is due to a detection threshold. Formula 8.4.1 applies for the seismicity of the whole of the northern part of the coalfield. The frequency-magnitude relationship for each seismic area of the coalfield has also been determined separately and described in Chapter 9.

The value of $\underline{b}$ for the foreshocks and aftershocks could not be determined since it has not been established which events are mainshocks, foreshocks and aftershocks or even whether this subdivision of events is applicable. The possible absence of foreshocks and aftershocks may suggest that the structural state of the rocks in the coalfield is extremely heterogeneous, or the applied stress in the coalfield is concentrated locally. Mogi (1963) explained that in a highly fractured material, when the applied stress gradually increases a high stress concentration appears around numerous cracks and faults and so local fractures begin to occur generating small tremors at such weak points under a low stress. Thus a single predominately large fracture cannot occur. Mogi suggested that this type of

tremor occurs as an earthquake swarm and results from extremely concentrated stress.

Figure 8.4.1 also shows the percentage of the total energy released by each set of tremors having a specific range of magnitude.

CHAPTER 9

EARTH TREMOR OBSERVATIONS AND SPECULATION ON THEIR MECHANISMS

9.1 Introduction

In this chapter the spatial and temporal distribution of the tremor hypocentres together with their relationship to mine workings and structural geology are discussed separately for each individual area. With the help of information from first motion analysis, mining techniques and rock mechanics, an attempt is made to establish the mechanisms of earth tremor generation.

9.2 Mine layout

In the northern part of the North Staffordshire coalfield, eleven different coal seams were mined in the period between September 1975 and September 1977, i.e. during the seismic monitoring period. A total of 27 longwall panels, as well as small areas worked by rooms-and-pillars, were used for the extraction of coal from these seams. Some of these panels had been mined since the early 1970's and continued to be mined throughout the monitoring period. These workings are distributed mainly in seven areas. Panel length and width, the dates of the commencement and end of production, the method of working, the direction of face advance (or retreat), depth from O.D. and thickness of the worked coal are shown in Table 9.1.

9.3 Area A

This area lies near Cobridge, NW of Hanley. In the period 1975 to 1977 two seams were mined in this area from Wolstanton colliery (see Table 9.1). This area was extensively mined previously in many other seams, some workings dating from the last century. The seams dip to the SW at an angle of about 15°. The two seams of interest are:

TABLE 9.1

The dimensions and specifications of the mine workings which were carried out during the seismic monitoring period (i.e. the active mine workings).

* Indicates that the panel was continued to be mined after September 1977 and the given panel length indicates the panel length at the end of September 1977.

A = Face Advance. R = Face Retreat. Minus depth indicates depth above O.D.

Area	Location	Colliery Name	Seam Name	Panel No.	Date of Extraction Start	Date of Extraction Finish	Method of Working	Direction of face Advance or Retreat	Panel Length (m)	Panel Width (m)	Panel depth from O.D. (m)	Thickness of worked seam (cm)
A	Cobridge	Wolstanton	Bowling Alley	101	6-12-1975	15- 1-77	A	NW	510	223	705-745	≈142
				102	11- 1-1975	29-11-75	A	NW	385	163	640-705	
			Banbury	402	25- 9-1976	Sept.77*	A	NW	500	227	920-960	152-167
				403	15- 1-1977	Sept.77*	A	SE	295	227	884-936	
B	Wolstanton	Wolstanton	Holly Lane	208	July 1974	Sept.76	A	NW	1060	136	925-948	85-102
C	Silverdale	Silverdale	Winghay	7	20-11-1976	10- 5-77	R	SW	618	118	320-381	250-300
				8	4-10-1975	31- 1-76	R	N-NW	500	106	335-358	
				12A	1- 2-1975	18-10-75	R	SE	824	135	290-320	
				14	8- 5-1976	7- 8-76	R	SW	306	118	350-375	
				15	24- 1-1976	15-12-76	R	NW	677	224	357-400	
				16	14- 5-1977	22-10-77	R	NW	470	170	360-400	

Area	Location	Colliery Name	Seam Name	Panel No.	Date of Extraction Start	Finish	Method of Working	Direction of face Advance or Retreat	Panel Length (m)	Panel Width (m)	Panel depth from O.D. (m)	Thickness of worked seam (cm)
C	Silverdale	Holditch	Hams	7	1973	26- 3-76	A	SE	730	160	670-731	135-222
				9	19- 7-1975	26- 6-76	R	SE	718	165	710-755	
				10	31- 5-1976	Sept.77*	R	SE	706	200	716-756	
				11	11- 4-1977	Sept.77*	R	SE	294	200	739-780	
D	Tunstall	Wolstanton	Ten Feet	56	Dec. 1974	14- 2-76	A	SE	473	140	660-690	152-250
				57	Sept.1976	Sept.77*	A	NW	455	235	635-665	
E	Chesterton	New High Carr	Cannel Row		1975	Sept.77*	Rooms and Pillars Method				-137 to -60	≈100
			Winghay		Early 1970s	1976					-100 to -60	150
		Wedgwood	Winghay		Early 1970s	1976					-160 to 40	150
			Rowhurst		Sept.1976	Sept.77*	Rooms and Pillars Method				-120 to -80	210
			Hams		1975	Sept.77*					-158 to -100	150
F	Burslem	Norton	Bullhurst	11	Sept.1974	Sept.75	R	NW	475	146	408-448	132
				12	Aug. 1974	28- 1-76	R	SE	415	166	494-533	
				14	Jan. 1976	24- 9-76	R	SE	463	159	427-472	
			Brights	2	2-10-1976	11- 6-77	A	NW	358	225	408-490	96

Area	Location	Colliery Name	Seam Name	Panel No.	Date of Extraction Start	Date of Extraction Finish	Method of Working	Direction of face Advance or Retreat	Panel Length (m)	Panel Width (m)	Panel depth from O.D. (m)	Thickness of worked seam (cm)
G	Goldenhill	Victoria	Hams	9	1971	31- 1-76	A	SE	1078	125	457-549	160-180
				12	24- 1-1976	23- 4-77	R	E-SE	625	220	496-542	
				13	March 1975	10- 1-76	R	SE	392	147	546-560	
				17	22- 1-1977	May 77	A	SE	200	127	460-506	
		Chatterley Whitfield	Hardmine	4	25- 5-1974	20- 9-75	A	W-NW	893	176	658-716	127-150
				5	Sept. 1975	March 77	A	W-NW	646	222	652-701	

(i) The Bowling Alley seam: Two panels - panels 101 and 102 - were mined in this seam during the monitoring period in an area which formed a coal pillar barrier between properties of two old collieries which operated before nationalization. This pillar had a maximum width of about 800 m. The depth of the two panels ranged from 640 m to 745 m below O.D. Figure 9.3.1a shows that these two panels are surrounded on all sides by extensive old workings, some of which were worked during the last century. No pillars were left between these two panels. Mudstone forms the roof and floor of the panels. The seam is disturbed by minor faults at the seam level, having maximum throws of as much as 5 m and dipping mostly to the NE and SW.

The active workings in the seam are overlain by previous workings in the Ten Feet, Ragman and Moss seams (Figures 9.3.1c, d and e), at heights of about 35 m, 137 m and 195 m respectively above the active workings. They are underlain by workings in the Holly Lane, Banbury and Cockshead seams (Figures 9.3.1f, b and g), at depths of approximately 32 m, 145 m and 208 m respectively below the Bowling Alley seam level.

(ii) The Banbury seam: Coal was extracted from this seam by two panels - panels 402 and 403 - worked during the monitoring period at depths ranging between approximately 884 m and 960 m below O.D. (see Table 9.1). Old mine workings bound these two panels to the east as shown in Figure 9.3.1b. Coal pillars of variable width were left between them and the old workings, as well as between the two panels. Mudstone, siltstone and silty sandstone form the roof of the panels, while mudstone forms the floor. Minor faults having throws of about 0.5 m were found at the seam level.

The active panels are underlain by workings in the Cockshead seam (Figure 9.3.1g) at a depth of about 60 m below the panel levels. They are overlain by workings in the Holly Lane, Bowling Alley and Ten Feet seams (Figures 9.3.1f, a and c) at heights of 125 m, 153 m and 198 m respectively above the Banbury seam level.

Fig. 9.3.1. The layouts of the mine workings in area A showing the active mine workings (dotted ornament), faults at the surface and at the level of the active seam in

(a) the Bowling Alley seam (B.A.)

(b) the Banbury seam (BANB).

Also shown are the mine workings in the Bowling Alley and Banbury seams superimposed on previous mine workings in

(c) the Ten Feet seam (10 Ft)

(d) Ragman seam

(e) Moss seam

(f) Holly Lane seam (H.L.)

(g) Cockshead seam.

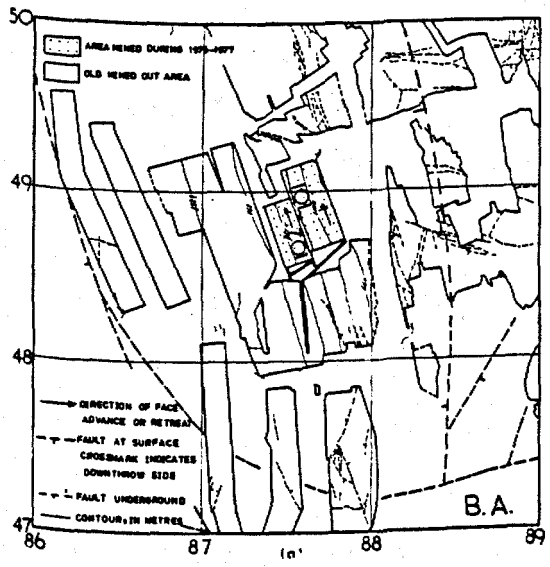
AREA MINED DURING 1976–1977
OLD MINED OUT AREA
DIRECTION OF FACE ADVANCE OR RETREAT
FAULT AT SURFACE CROSSBAR INDICATES DOWNTHROW SIDE
FAULT UNDERGROUND
CONTOURS IN METRES
B.A.
50
49
48
47
86
87
88
89
(a)

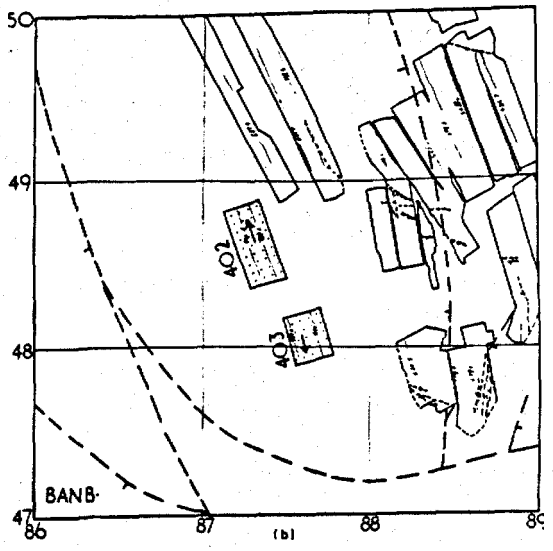
402
403
BANB
50
49
48
47
86
87
88
(b)

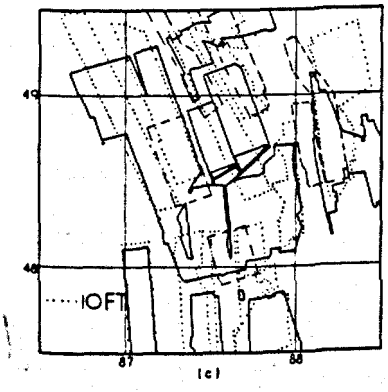
IOFT
49
48
87
88
(c)

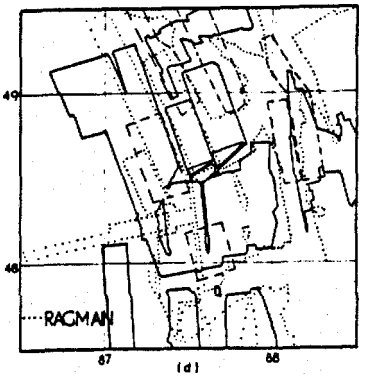
RAGMAN
49
48
87
88
(d)

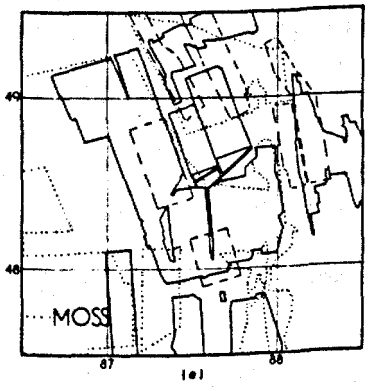
MOSS
49
48
87
88
(e)

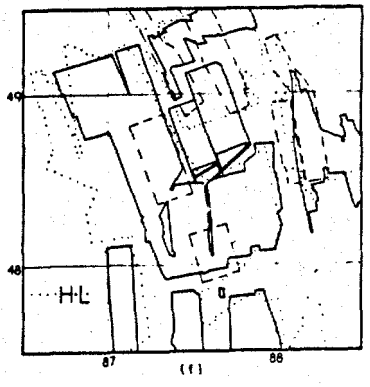
H·L·
49
48
87
88
(f)

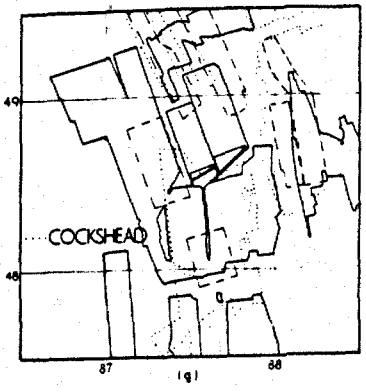
COCKSHEAD
49
48
87
88
(g)

9.3.1 Spatial distribution of tremor hypocentres

19 tremors (19% of the total) occurred in this area. The spatial distribution of the tremor epicentres with respect to the mine workings and structural geology is shown in Figure 9.3.2. The tremors cluster adjacent to the active mine workings in the Bowling Alley and Banbury seams. However, the tremors do not concentrate immediately over these active panels but appear to be displaced to the south and south west of panels 101 and 102 of the Bowling Alley seam, to the east of panel 402 and to the north of panel 403 of the Banbury seam. Without a well determined seismic velocity structure and high resolution seismic network it is difficult to decide whether this displacement of tremors is a real effect or is a location error.

The vertical distribution of tremor hypocentres is shown in Figure 9.3.3. The figure was drawn along the profiles AB and CD of Figure 9.3.2. The tremors, except three, cluster well away from the Far Green fault. This suggests that this fault had no effect in generating these tremors. No distinctive planer zone of activity is defined by the hypocentre distribution, but the figure indicates a zone of concentrated activity located between the surface and about 800 m in depth below O.D., at the level of the Bowling Alley seam. They occur at a level considerably higher than the Banbury seam.

The vertical distribution of tremor foci is also shown by an histogram (Figure 9.3.4) which plots the number of tremors which occurred within each 100 m depth interval, and the corresponding seismic energy release , against depth. The depth ranges of the active mine workings in both the Bowling Alley and the Banbury seams are also marked. Most tremor foci lie within the depth interval between 500 m and 600 m below O.D., with an average height of less than 160 m above the active panels in the Bowling Alley seam. Most of the energy was released in the depth range between 400 m below O.D. and the surface. This may suggest that these tremors

Fig. 9.3.2. Map of earth tremor epicentres for tremors which occurred in area A. Tremors are represented by a circle whose radius is proportional to the magnitude, M_L, of the tremor. Circle with a cross represents tremors having a shear source mechanism. Tremors are located near the active mine workings (dotted ornament) in

(a) the Bowling Alley seam

(b) the Banbury seam.

Faults at the surface and at the active seam datums are also shown. Also shown are the two active seams (Bowling Alley and Banbury seams) together with previous mine workings in different adjacent seams; in the

(c) Ten Feet seam

(d) Ragman seam

(e) Moss seam

(f) Holly Lane seam

(g) Cockshead seam.

(For legend see Fig. 9.3.1).

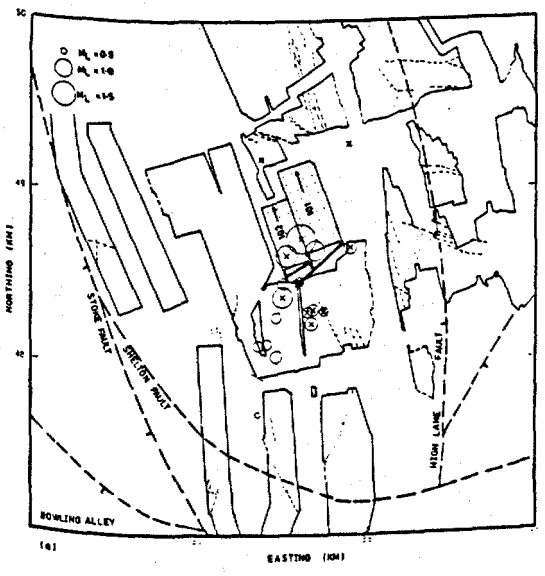
NORTHING (KM)
EASTING (KM)
STONE FAULT
BRERETON FAULT
HIGH LANE FAULT
BOWLING ALLEY
(a)

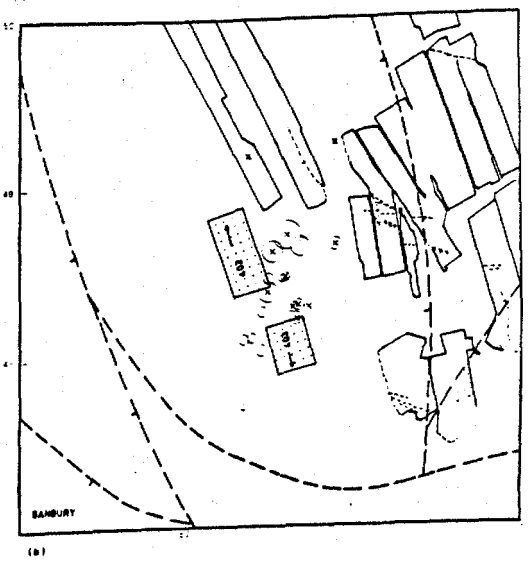
BANBURY
(b)

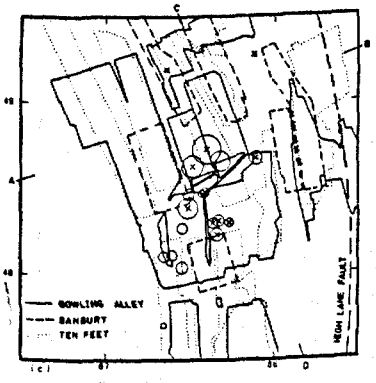
BOWLING ALLEY
BANBURY
TEN FEET
HIGH LANE FAULT
(c)

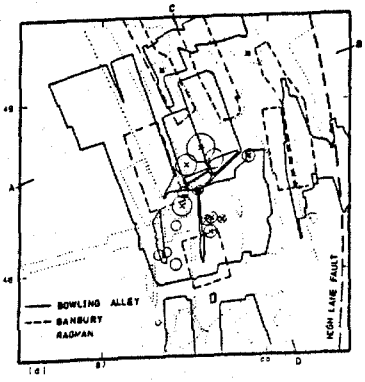
BOWLING ALLEY
BANBURY
RADMAN
HIGH LANE FAULT
(d)

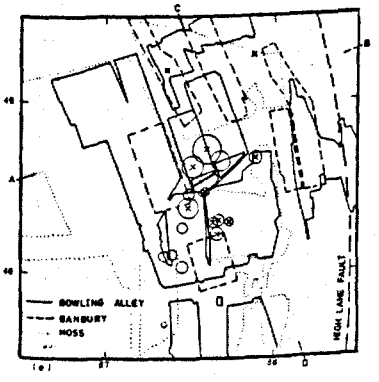
BOWLING ALLEY
BANBURY
MOSS
HIGH LANE FAULT
(e)

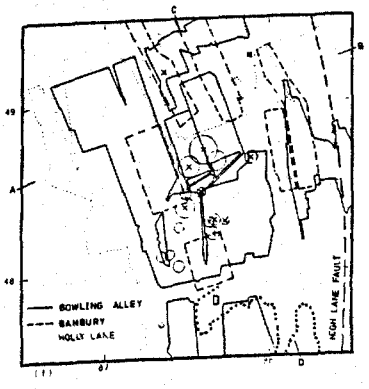
BOWLING ALLEY
BANBURY
HOLLY LANE
HIGH LANE FAULT
(f)

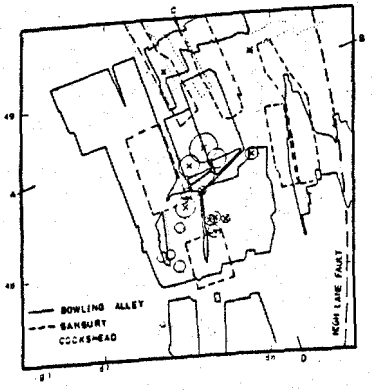
BOWLING ALLEY
BANBURY
COCKSHEAD
HIGH LANE FAULT
(g)

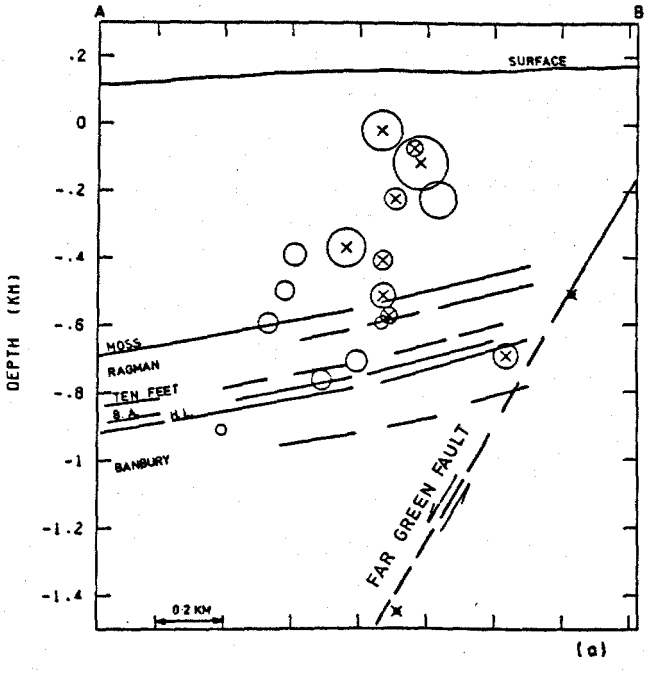

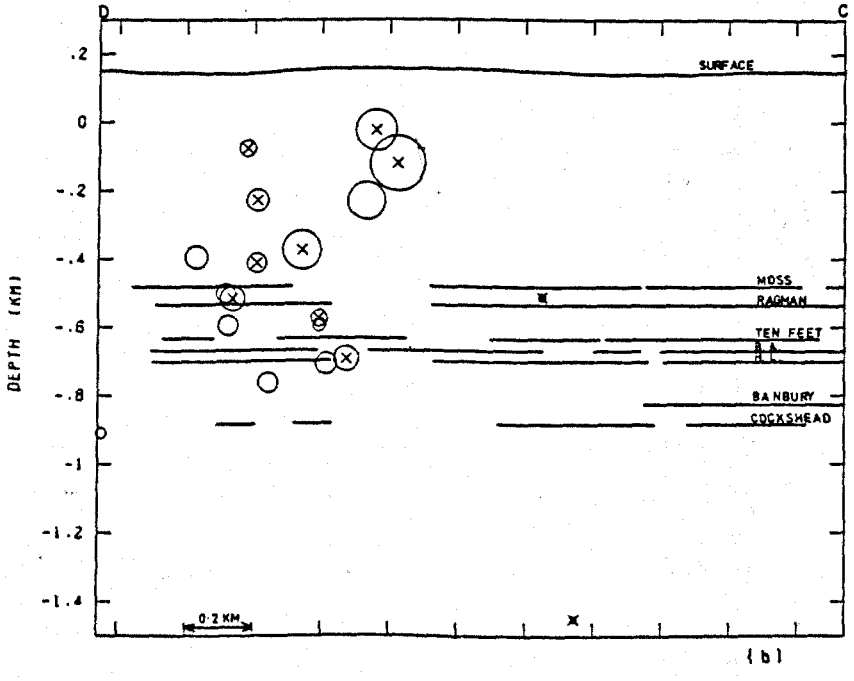

Fig. 9.3.3 Hypocentre sections (A-B, C-D, Figure 9.3.2) of tremors located in area A, showing the position of tremor hypocentres with respect to the active and old mine workings and to the Far Green fault.

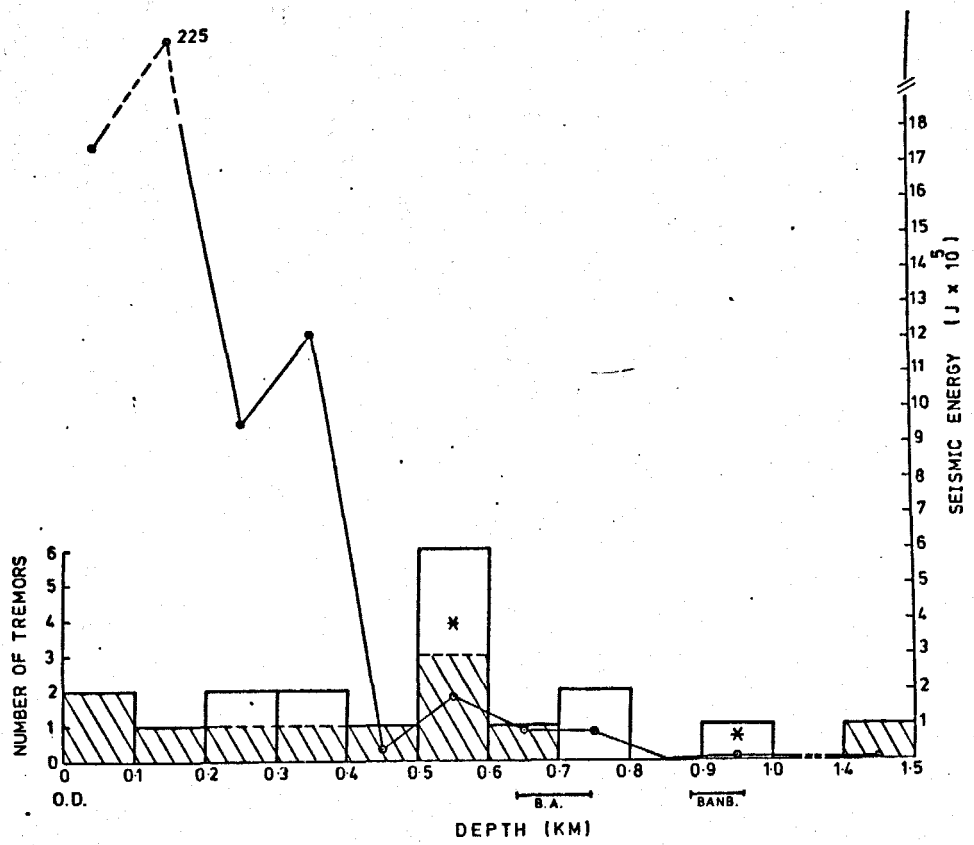

Fig. 9.3.4. A plot showing the number of earth tremors and the corresponding seismic energy release, occurring within each 100 m depth interval in area A. The depth ranges of the active mine workings in the Bowling Alley (BA) and Banbury (BANB) seams are also shown. The shaded area represents tremors having a shear source mechanism.

were generated mainly due to mine workings in the Bowling Alley seam, in particular by the mining of panel 101, since 17 tremors occurred during the working life of this panel. The two stars represent the only two tremors which occurred in 1977 during the working life of panels 402 and 403 of the Banbury seam, and after panels 101 and 102 of the Bowling Alley seam had finished production. These two events had an implosional/collapse source mechanism (see Section 9.3.3). One of these tremors occurred within the depth range of the mine workings in the Banbury seam, which may suggest that these two events occurred as a result of the mine workings of panels 402 and 403 of the Banbury seam. Alternatively, they could result from collapses due to mine stabilization after panels 101 and 102 of the Bowling Alley seam had finished production.

The relationship between the tremor size, M_L, and the depth is shown in Figure 9.3.5. In general, it can be seen that the largest tremors occurred at relatively shallow depths. This could be real and a direct effect of mining, or it could be that the seismic energy generated from deeper tremors suffered more absorption during their propagation. An alternative explanation is that the P-wave first arrivals of these large tremors could have been picked earlier than for weaker tremors, and this would have caused the larger tremors to be located at shallower depths than the weaker tremors (see Section 7.2). No obvious relationship between the size of any kind of tremors (collapse/implosional or shear source mechanism) and depth was found.

Figure 9.3.6 shows the distribution of the tremor foci with respect to the general lithological succession in the area, in particular with respect to the presence of sandstone beds. The section was drawn down dip. No obvious relationship between the foci locations and the presence of any sandstone bed can be seen. However, the accuracy in determining the focal depth is poor and the sandstone beds relatively thin. Moreover, information

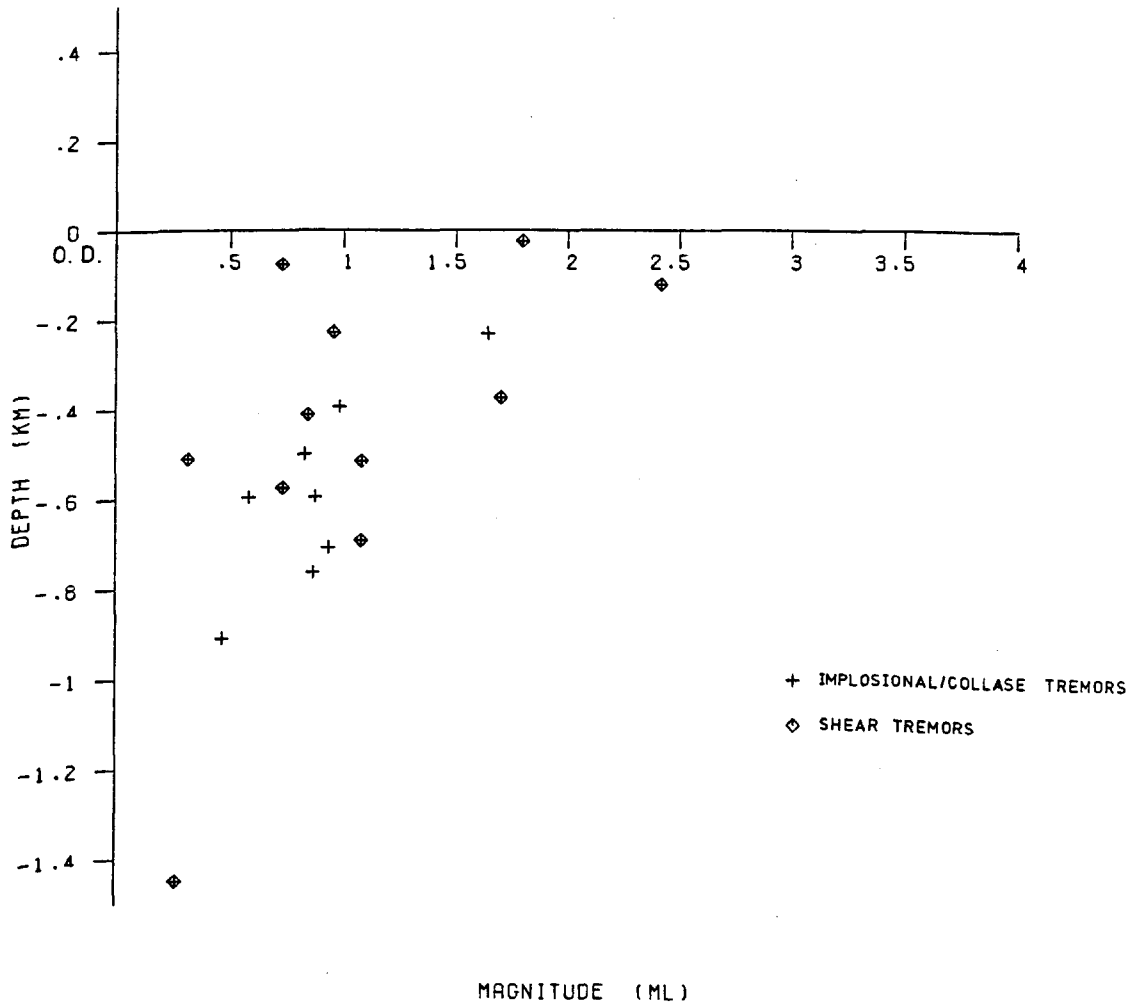

Figure 9.3.5. Plot of tremor depth against local magnitude, M_L, for tremors occurring in area A.

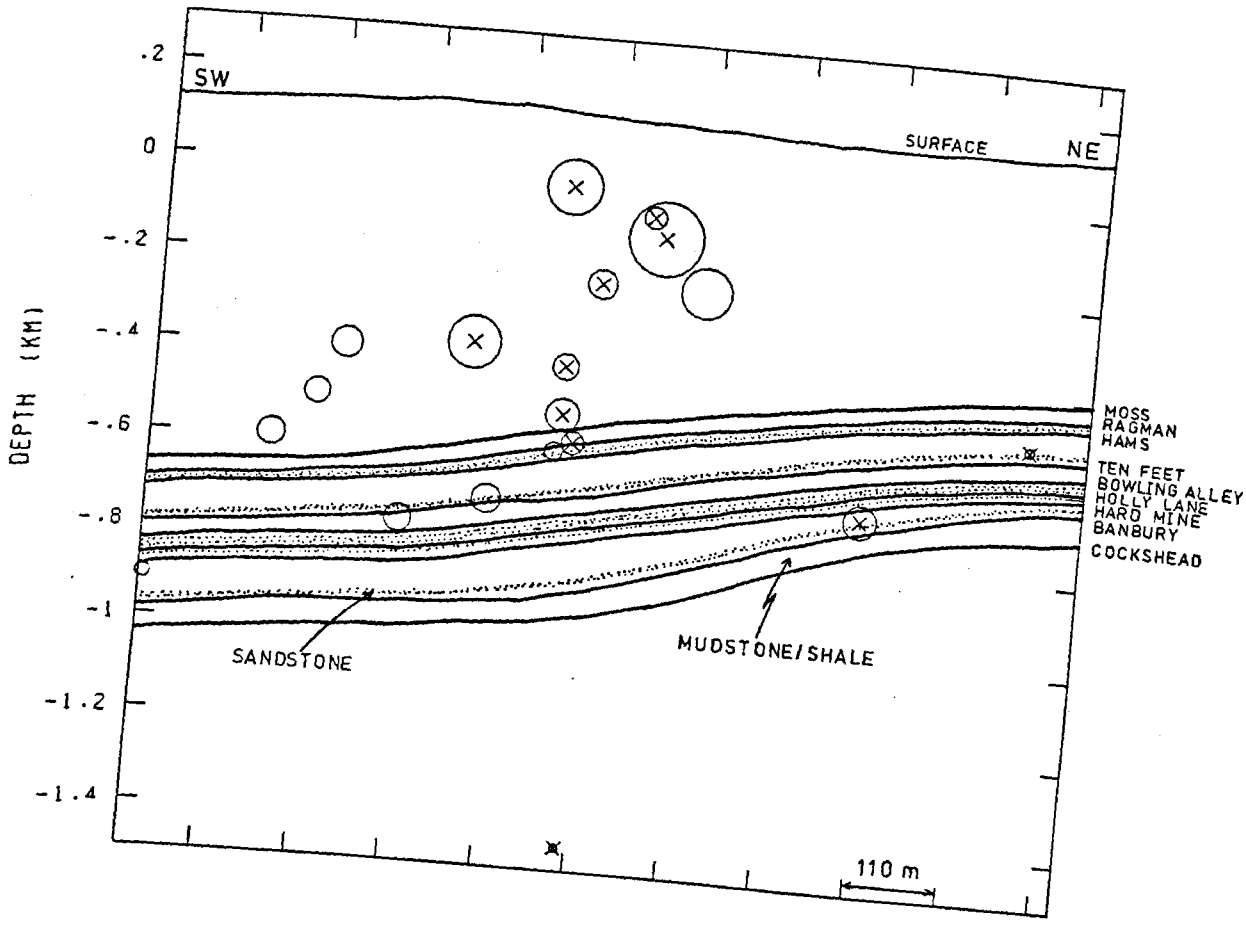

Fig. 9.3.6. Geological section drawn downdip showing the positions of tremor foci for tremors occurring in area A.

about the seam levels and the lithological sequence above the Moss seam is unavailable.

As already explained above, 17 tremors occurred during the working life of panel 101 of the Bowling Alley seam. Figure 9.3.7 gives the position of these earth tremors with respect to the position of panel 101 working face, at the time of occurrence. Figure 9.3.7a is a plan view, while Figure 9.3.7b is a vertical section perpendicular to the face. The figure shows that all but two tremors occurred behind the face. This may be a real effect or may be due to location error.

The relationship between the occurrence of earth tremors and the position of face 101 as it advanced along the panel is shown in Figure 9.3.8. The seismic activity started when the face had advanced a distance of about 270 m. Before this distance there was no seismic activity except for three tremors which occurred just as the face opened. These are probably associated with the mining of panel 102, since they occurred less than two weeks after panel 102 had finished production (see Table 9.1 and Appendix 2). When the face had advanced 270 m, it had passed a distance of about 75 m under two pillars left in the Ten Feet and Ragman seams, having widths of about 30 m and 60 m respectively. At this point also the face entered a pillar about 105 m wide left in the Banbury seam below the panel level. Hence, the occurrence of the seismic events correlates with the passage of the panel face under and above pillars in old workings. Figure 9.3.9 gives the depth of tremor foci as the face advanced along the panel. The four largest tremors generally lie at a higher level (adjacent to the Ragman seam and approximately 190 m in depth below O.D. on average) than the smaller tremors (570 m average depth). The depth of panel 101 ranges between 640 m and 705 m below O.D. Bearing in minde the low resolution of depth determinations, the smaller tremors appear to be located near the level of panel 101 (approximately 100 m above the panel on average).

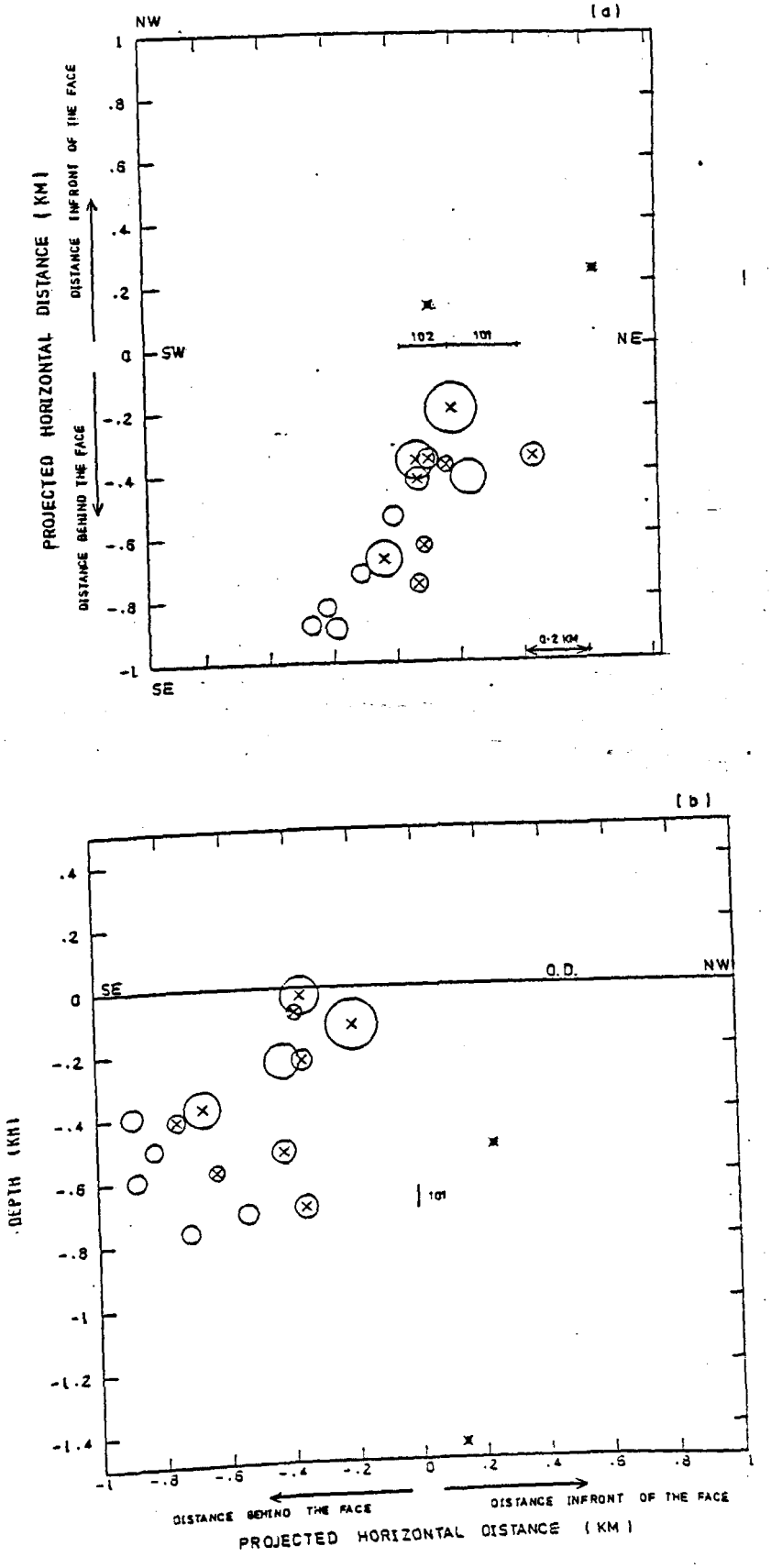

Figure 9.3.7. Plots showing the positions of tremor hypocentres with respect to the position of the working face, at the time of occurrence, for tremors occurring during the mining of panel 101 in area A. (a) Plan view. (b) Vertical section perpendicular to the coal face.

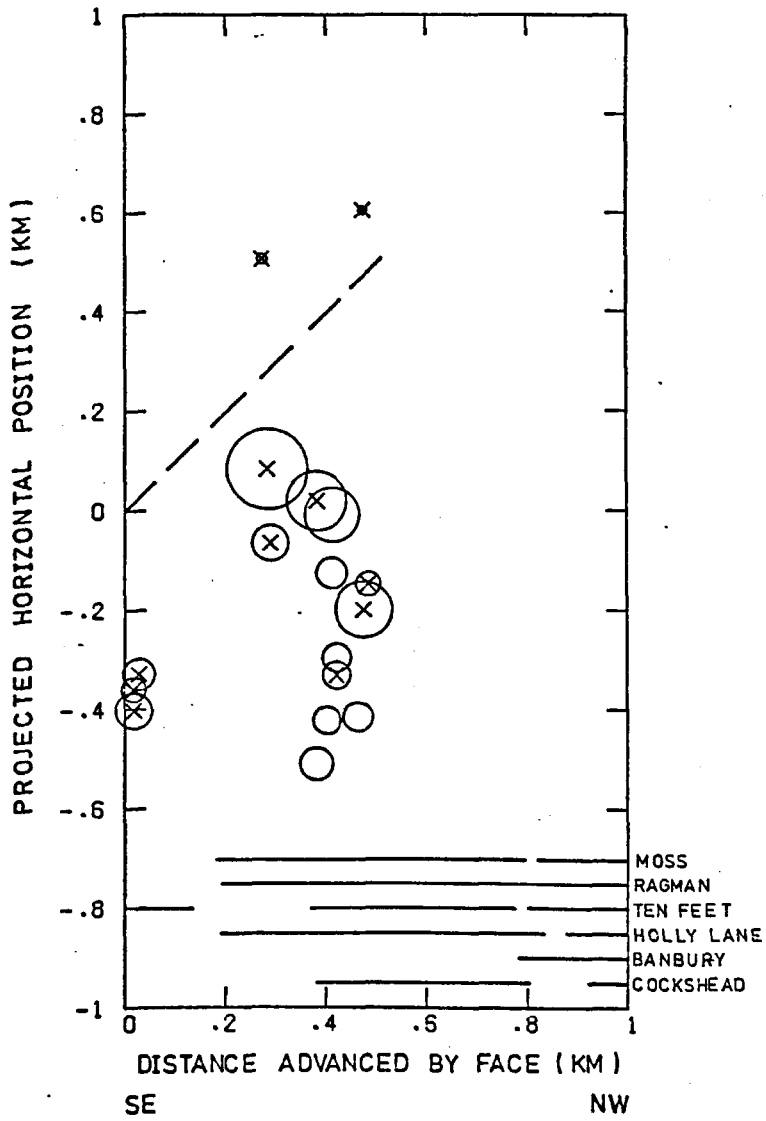

Fig. 9.3.8. Plot of the horizontal position of tremor epicentres projected onto the line of face advance and measured from the start of the panel, against distance advanced by the face for tremors occurring during the mining of panel 101 in area A. The diagonal dashed line corresponds to the line on which tremors would plot if they occurred on the face 101. The regions where the face 101 lies below previous Moss, Ragman, Ten Feet or above Holly Lane, Banbury and Cockshead seam workings are also shown.

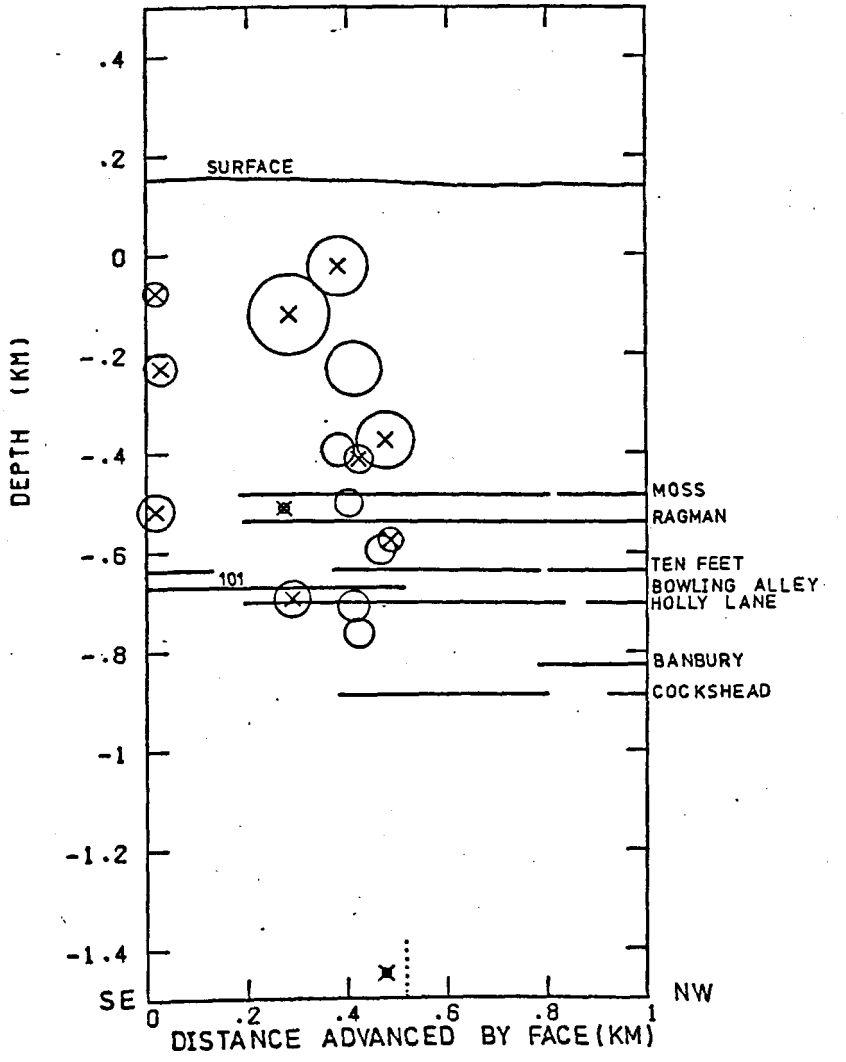

Fig. 9.3.9. Plot of tremor depth against the distance advanced by the face for tremors occurring during the mining of panel 101 in area A. The position of mine workings in panel 101 of the Bowling Alley seam and previous workings in different adjacent seams are also shown.

The correlation between the passage of panel 101 face over the Banbury pillar and under the Ten Feet and Ragman pillars and the occurrence of earth tremors is also evident in Figure 9.3.10. Figures 9.3.10a and 9.3.10b give respectively the size, M_L, of the tremor and the energy released, as the face advanced along the panel. The figure shows that the largest tremor occurred when the face had moved a distance of about 85 m over and under the pillars. This largest tremor had a shear source mechanism and occurred about 550 m above the panel level as shown in Figure 9.3.9. It is interesting to see in Figure 9.3.10 that after the occurrence of this large tremor, tremors occurred more frequently but were smaller in size.

9.3.2 Temporal distribution of tremors and seismic energy release

The maximum number of tremors (14) occurred in 1976, while only three tremors occurred in 1975 and two tremors in 1977. This suggests that most of the tremors were generated by the mining of panel 101 of the Bowling Alley seam. This panel started production in December 1975 and finished in January 1977, while panel 102 finished production in late November 1975. Panels 402 and 403 of the Banbury seam started production in late September 1976 and in January 1977 respectively (see Table 9.1).

The weekly and daily distribution of the tremors and their corresponding seismic energy release are shown in Figure 9.3.11. The direct relationship between mining and seismic activities is evident.

9.3.3 First motion analysis of seismic data

Analysis of the P-wave first motions shows that 11 tremors had a shear source mechanism, while the other 8 could have had an implosional/collapse source mechanism. The reliability of the dilatational source mechanism is uncertain since the seismic events were recorded on a few stations only (4 or 5) which were badly distributed (in both azimuth and

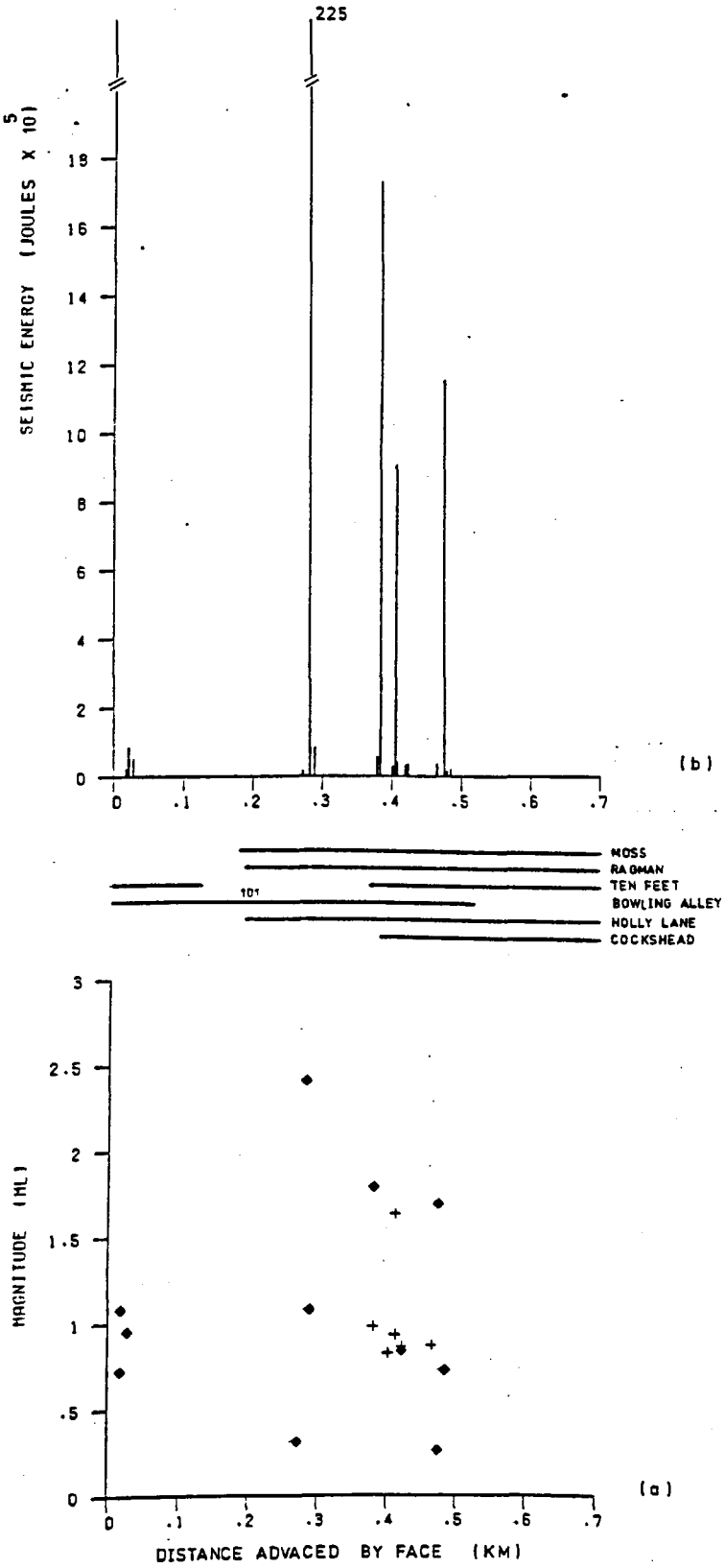

Fig. 9.3.10. Plots of (a) tremor magnitude, M_L, and (b) seismic energy release, against the distance advanced by the face for tremors occurring during the mining of panel 101 in area A. The regions where the panel face lies below or above previous workings in the Moss, Ragman, Ten Feet, Holly Lane and Cockshead seams are also shown.

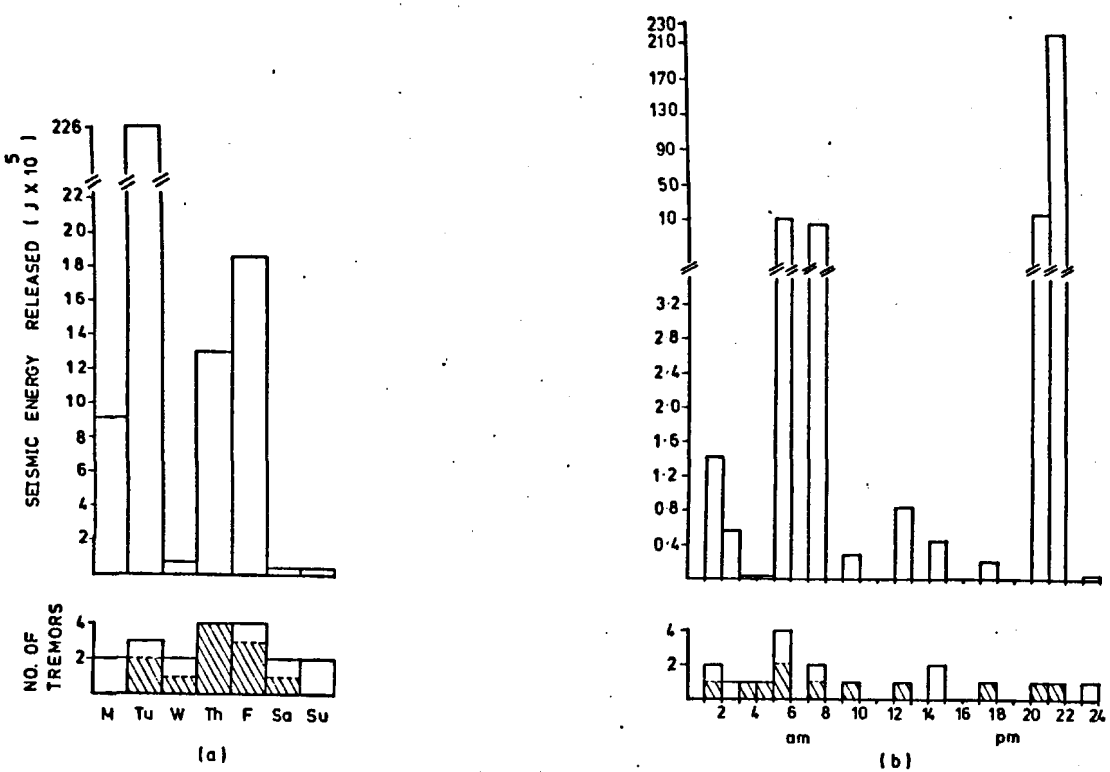

Fig. 9.3.11. Histograms showing (a) the weekly and (b) the daily distribution of tremors and the corresponding seismic energy release for tremors which occurred in area A. The shaded area represents tremors having a shear source mechanism.

epicentral distance) around the seismic region. The seismic area lies to the NE side of the seismic network with no seismic station to the north, northeast and east of this area (see Figure 4.2.1). Consequently, those dilatational focal mechanism events could have had a shear source origin. Figure 9.3.12I shows an upper hemisphere stereographic projection for those seismic events which generated dilatational first motion at all stations. As we can see from the figure, the seismic stations were located within an arc of about 140° from the tremor epicentres, i.e. these stations could be located in one or two opposite quadrants of a fault plane solution, as shown in the figure. The same explanation also applied for the seismic events in the other four seismic areas (areas B, C, D and E).

In our study the direction (azimuth and angle with respect to the vertical) of the seismic ray from the focus to each seismometer was calculated using a computer program (Appendix 1). The direction parameters were plotted on the upper hemisphere of a Wulff stereographic net, each carrying the sign of the P-wave first arrival, assuming the centre of the net to be the focus of the event.

A composite fault-plane solution using the data from all the events having a shear type mechanism was attempted unsuccessfully. The first motions exhibited major inconsistencies. The fault-plane solution for each event is given in Figure 9.3.12. The figure shows that the plotted first motion data lies mostly in two quadrants only, which makes it very difficult to give an unambiguous solution. The nodal-plane solutions for the seismic events in this area are therefore not very satisfactory and could be in error by as much as 30° in their dip and strike. Most events show fault-plane solutions (Figures 9.3.12A, B, D, E and F) which can be interpreted as representing rock movements either by normal or reverse faulting. The determination of which of the nodal planes is the fault plane is very difficult since there is no major structural

Fig. 9.3.12. Upper hemisphere fault-plane solutions for tremors occurring in area A. Dashed lines represent alternative fault-plane solution. A, B, D, E and F show fault-plane solutions which can be interpreted as representing movements by either normal or reverse faulting. Date of the event or events is shown below each fault-plane solution.

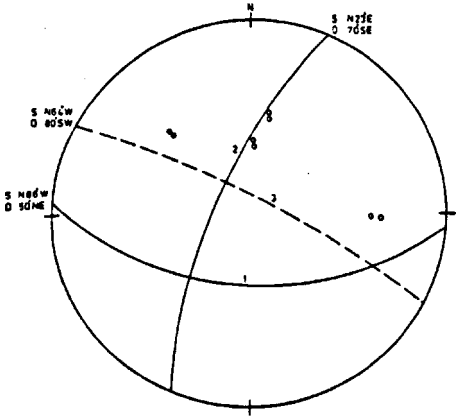

(A) 1975 12-10 05-36
1975 12-16 07-56

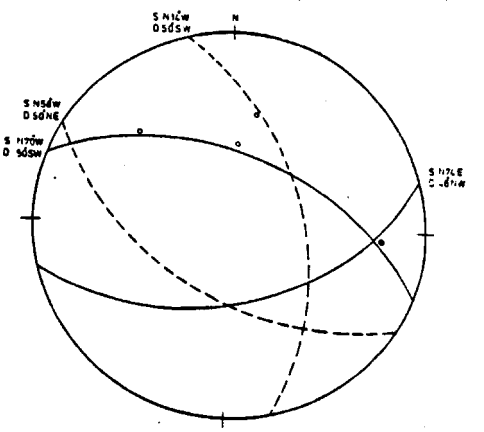

(B) 1975 12-12 01-21

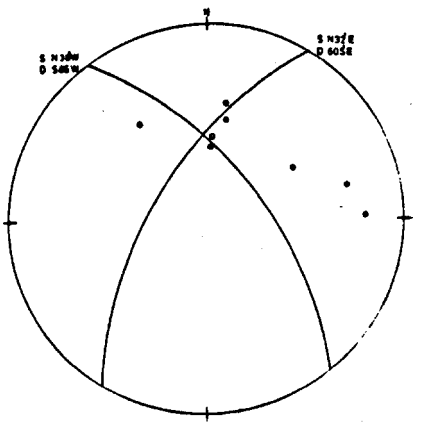

(C) 1976 6-21 04-08
1976 12-08 17-18

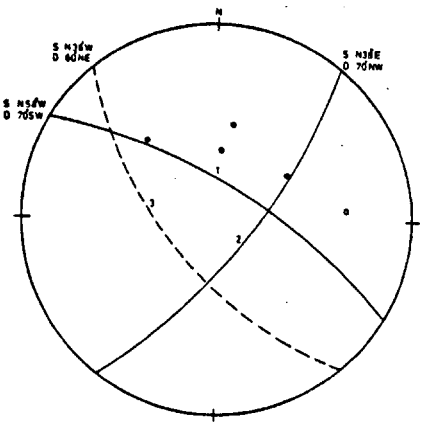

(D) 1976 8 15 21 08

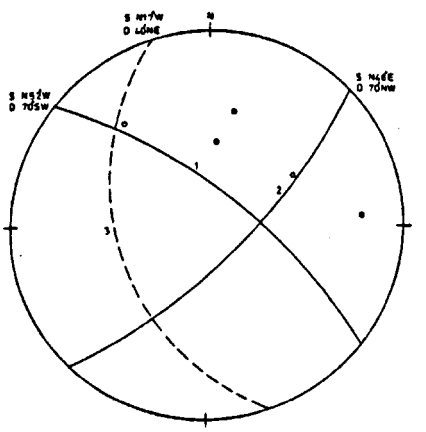

(E) 1976 6-24 12-57

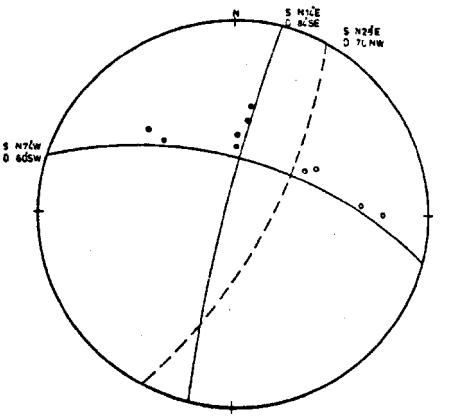

(F) 1976 10-1 20-02
1976 12-2 05-08

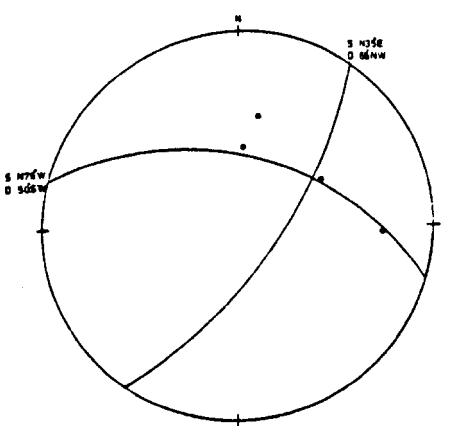

(G) 1976 10-26 08-33

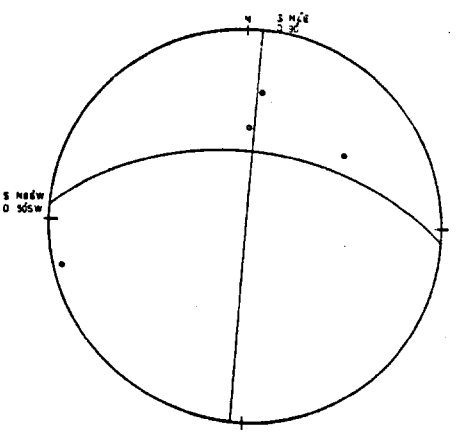

(H) 1976 12-4 03-08

LEGEND
S = STRIKE
D = DIP, LETTERS INDICATE DIP DIRECTION
⊕ = DILATATION
⊖ = COMPRESSION

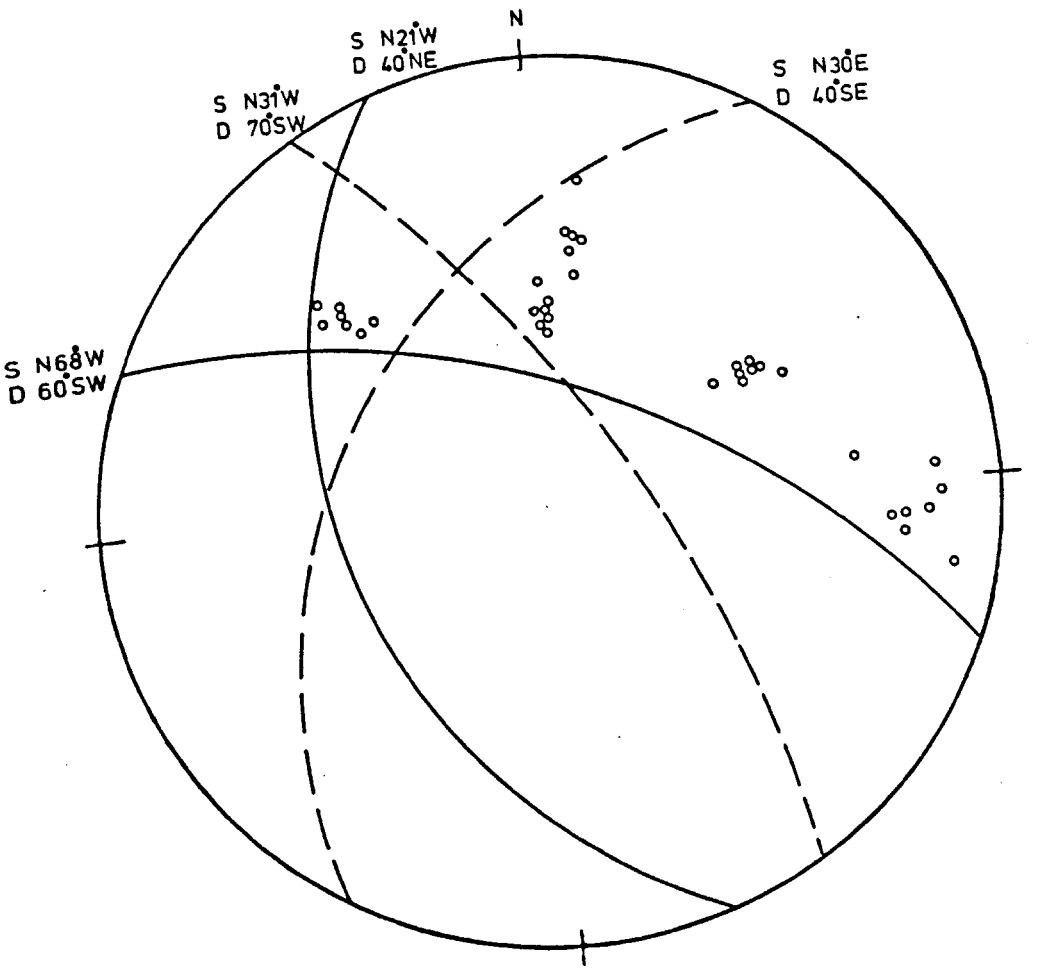

(I)

Fig. 9·3·12 I

feature which these solutions can be related to. However, for those events which show fault-plane solutions representing movements by normal faulting, the different solutions have nodal planes striking NW and dipping either to the SW or to the NE. These nodal planes may correspond to the fault planes since they generally agree with the orientation of many small faults at different seam levels. These small faults mostly strike NW-SE and dip to the SW and NE, as explained previously. For those events which gave fault-plane solutions representing movements by reverse fautling. This could be an error in observation, or it could be these events have occurred along pre-existing reverse faults, or may have occurred in the roof behind the active face. When coal is extracted the roof sags and the compressive principal stress in the goaf is reduced while the horizontal stress pushes the rocks towards the excavation and increase the sagging. If strong beds, such as sandstone, exist in the roof and if a strong bond exists between two strong layers, the two layers behave like one beam

(Denkhaus, 1964). If the shear forces caused by the deflection loosen the bond between these two competent layers, shear movements may occur along the bedding plane between these two beds which may give a fault-plane solution similar to that of a reverse fault solution.

Briefly, it can be concluded that earth tremors which occurred in this area with a shear source mechanism, occurred on a number of slip planes of different orientations, and that these tremors were not related to any major structural feature in the area. These tremors may have occurred due to rock movements along pre-existing small fractures or planes of weakness, or on new fracture planes developed by shear fracture in pillars and surrounding rocks.

9.3.4 b-value

The frequency-magnitude distribution of earth tremors in this area can be represented by the formula:

$$\log_{10} N = 2.26 - 1.4\, M_L \qquad 9.3.1$$

The constants were obtained graphically from the frequency-magnitude plots (Figure 9.3.13). The plot shows that there is a linear relationship between logN and M_L in the magnitude ranges between 0.9 and 1.2. The data having a magnitude greater than 1.2 do not fit this linear relationship, and fit another linear relationship represented by the formula:

$$\log_{10} N = 2.95 - 1.48\, M_L \qquad 9.3.2$$

The b-values in both of these formulae are almost equal, but the a-value is greater in equation 9.3.2. This situation most probably is a result of statistical error. However, if this situation is a real effect, it may indicate a sudden change in the state of the applied stress. After the occurrence of a few large tremors the rocks break and sometimes the pillar

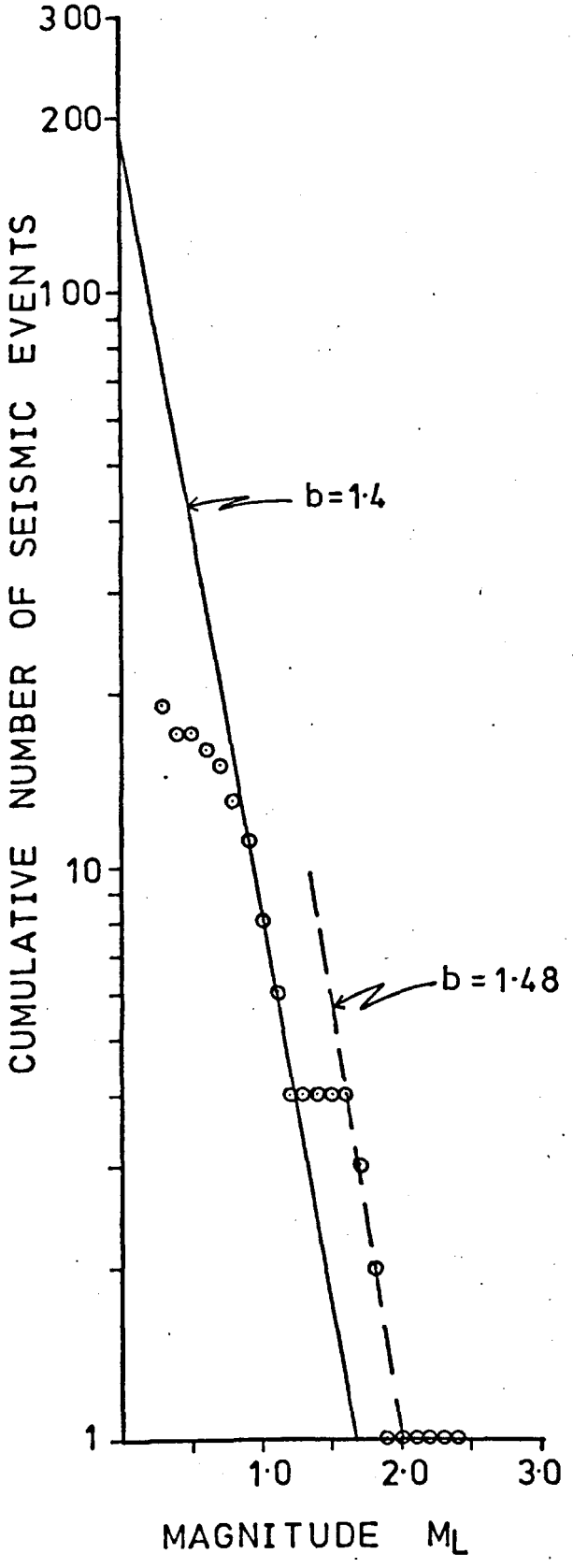

Fig. 9.3.13. A plot showing the frequency-magnitude distribution for tremors occurring in area A.

disintegrates and can no longer store large amounts of strain energy, so small tremors tend to occur. This situation consequently will lead to an abrupt change in the frequency-magnitude relationship. Formula 9.3.2 suggests that large tremors could occur more frequently in a given time than it is suggested from formula 9.3.1.

9.3.5 Earth tremor generation mechanisms

In order to determine the earth tremor generation mechanisms we have to determine first of all which seam (Bowling Alley or Banbury), and in particular which panel or panels generated these tremors. Consideration of the times when tremors occurred and which panels were then working indicates that panel 403 of the Banbury seam was not responsible. The spatial and temporal distributions of the tremors indicate that the mine workings in the Bowling Alley seam, in particular the mining of panel 101, was the main panel responsible for generating most of the tremors.

As we can see from Figures 9.3.1 and 9.3.3, panels 402 and 403 of the Banbury seam were driven under a previous extensively mined out area in the Holly Lane and Bowling Alley seams at heights of about 125 m and 155 m respectively above the active panel levels of the Banbury seam. Panel 403 was also driven over a large mined out area in the Cockshead seam at a depth of about 60 m below the panel. No pillars were left over or under panels 402 and 403 in these old mined adjacent seams, except very small pillars of coal left in the Bowling Alley seam. These small pillars most probably disintegrated under the overburden pressure. From the above it can be concluded that panels 402 and 403 of the Banbury seam were driven in de-stressed zones due to the fracture of the rocks above and below the panels as a result of previous old mine workings in the adjacent seams. Hence it is unlikely that the mining of these panels generated seismic activity, except behind the face as a result of roof caving.

Panels 101 and 102, however, of the Bowling Alley seam were mined in a large barrier pillar of coal. The extracted area of panel 102 is about half the extracted area of panel 101. Figures 9.3.1 and 9.3.3 reveal that many seams were mined previously under and above panels 101 and 102. Different sizes of coal pillars were left in these adjacent seams, in particular, over and under panel 101. As we have indicated above, 17 tremors occurred during the working life of panel 101. Three of these tremors most probably occurred due to the mine workings of panel 102. These three tremors had a shear souce mechanism. They probably occurred when the face of panel 102 approached a previous long, narrow, mined out area in the same seam (see Figure 9.3.1a), forming a small, very stressed, pillar. Consequently the pillar may have failed in shear under very high compressive stress. The smaller dimensions of panel 102 may have reduced the occurrence of seismic events during the mining of this panel, since the number of rock failures and tremors increases as the excavation size increases, as explained in Sections 2.8 and 3.4.1. The other 14 tremors occurred due to the workings of panel 101.

Two possible mechanisms could have generated earth tremors during the mining of panel 101.

(i) Tremors occurring ahead of the panel face and in pillars left above and below the panel.

The seismic activity associated with panel 101 started when the face had moved a distance of about 75 m below and above pillars left in adjacent seams. At this distance the face was advancing in a highly stressed region due to the presence of these pillars which are surrounded by extensive mined out areas, causing the weight of the overburden to be put onto these pillars, particularly on their sides (abutment pressures), as discussed in Sections 2.2 and 2.3. As face 101 advanced, a high pressure zone would have built up in front of the face (front abutment pressure) as well as

along the two sides of the panel (flank abutment pressure). In the early stage of panel opening the front abutment pressure increases as the face advances due to the increase in the excavation area and the enlargement of the pressure arch. After some distance, however, the front abutment pressure may become constant due to roof caving which reduces the concentration of the pressure on the face. When the face moved under and over the highly loaded pillars left in the adjacent seams, the front abutment pressure of the advancing face (dynamic pressure) and the pillar abutments (static pressures) were superimposed producing together a very high pressure zone occurring a few metres ahead of the face. The presence of mudstone above and below the seam may have caused the pressure to concentrate nearer the panel face with the pressure peak at a distance of about 1-3 m from the face, as explained by Whittaker and Pye (1975). Thus a situation occurred a few metres inside the solid coal ahead of the panel face and inside the pillars in the adjacent seams, where a very large vertical pressure existed - the maximum principal stress - while the two lateral stresses - the intermediate and minimum principal stresses - acted parallel and perpendicular to the face respectively. This situation could have resulted in the rocks ahead of the panel face and the pillars above failing in shear as explained in Section 2.6 by Hudspeth and Phillips (1932-33). The same situation would have occurred as the face advanced further. As already indicated most of the large tremors had a shear source mechanism. These large tremors occurred at a higher level, probably in the Ragman pillar since this pillar is wide enough to permit the occurrence of differential pressure, while the narrow pillar left in the Ten Feet seam may have failed in compression (pressure bursts). This may explain why most of the smaller tremors occurred near the Bowling Alley and Ten Feet seam levels than the larger tremors. Once the pillars fractured they could not store large amounts of strain energy, so subsequent tremors are smaller. This may explain why the tremors became

more frequent but smaller in size as face 101 advanced after the occurrence of the large tremor.

Another mechanism that could generate tremors ahead of panel 101 face and in pillars over the panel might exist. If a strong stratum is present in the roof succession, such as sandstone. This bed need not necessarily be present in the immediate roof but it could be higher. Such a competent bed may not break when the roof caves in, but may overspan the goaf and acts as a beam or cantilever. This beam or cantilever is loaded by its own weight plus the weight of the overlying beds and supported by the panel face at one of its ends. The other end may rest on the compacted broken rocks in the goaf (in the case of a beam) or it could be free (in the case of a cantilever). In both of these two cases the rocks ahead of the panel face are put under heavy pressure. If the rocks in the face are hard, these beds may fail in shear, while the rocks ahead of the face may fail in compression, as explained by Holland (1958) in Section 3.2.1. It is also known that at a shale-sandstone contact, numerous fractures, randomly oriented mainly within the shale, are to be expected due to the differential compaction during the solidification process of sand deposited in a generally clayey depositional area (Peng, 1978). Movements along these fracture planes are expected. In addition to the occurrence of the fractures, the stress is highly concentrated at the shale-sandstone contact due to the large difference in their elastic constants. The higher stress concentration usually occurs in the sandstone since it has a larger elastic Young's Modulus. Therefore, during mining, when the excavation approaches these highly stressed regions, the stress may be released suddenly, producing seismic events.

(ii) Tremors occurring behind the face

Most of the tremors appear to be located behind the face of panel 101 as we have seen earlier. As explained before, this could be due to an

error in location. However, some tremors could have occurred behind the panel face (in the goaf) or may have even occurred in the goaf of old workings in adjacent seams. The tremors occurring behind the face were tensile in origin and must be attributed to the collapse of roof layers above the worked seams. The reduction of the compressive vertical principal stress in the goaf area resulted in tensile fracture of the roof layers subject to reduced confinement, as explained by Kusznir et al. (1980b) in Section 7.3. This situation is also well explained by Figure 2.4.1. The figure shows that tensile strain occurs in the goaf behind the face, while compressive strain occurs ahead of the face.

Another possible cause of earth tremors behind the face is the falling of a thick block of competent bed from the roof onto the waste. The impact of falling could be very great and could generate an earth tremor, as explained by Rice (1935) in Section 3.2.1.

9.4 Area B

This area is near to Wolstanton. The coal was extracted from this area by panel 208 in the Holly Lane seam, worked from Wolstanton colliery at a depth ranging between about 925 m and 948 m below O.D. (see Table 9.1). This seam was the only seam mined during the monitoring period in this area. The panel was bounded to the east by many older workings as shown in Figure 9.4.1a. The panel extends along the eastern side of the Stoke fault, and is parallel to the fault. This fault strikes at N 30°W. Mudstone and silty mudstone form the roof and floor of the panel. The Holly Lane seam dips at 6° to the SW. It is disturbed by some minor faults at the seam level. The maximum throw of these faults is less than 2 m, mostly dipping to the NE and SW.

The panel is overlain by workings in the Bowling Alley, Ten Feet and Ragman seams (Figures 9.4.1b and c) at heights of about 23 m, 69 m and 179 m respectively above the Holly Lane seam. There are other workings in

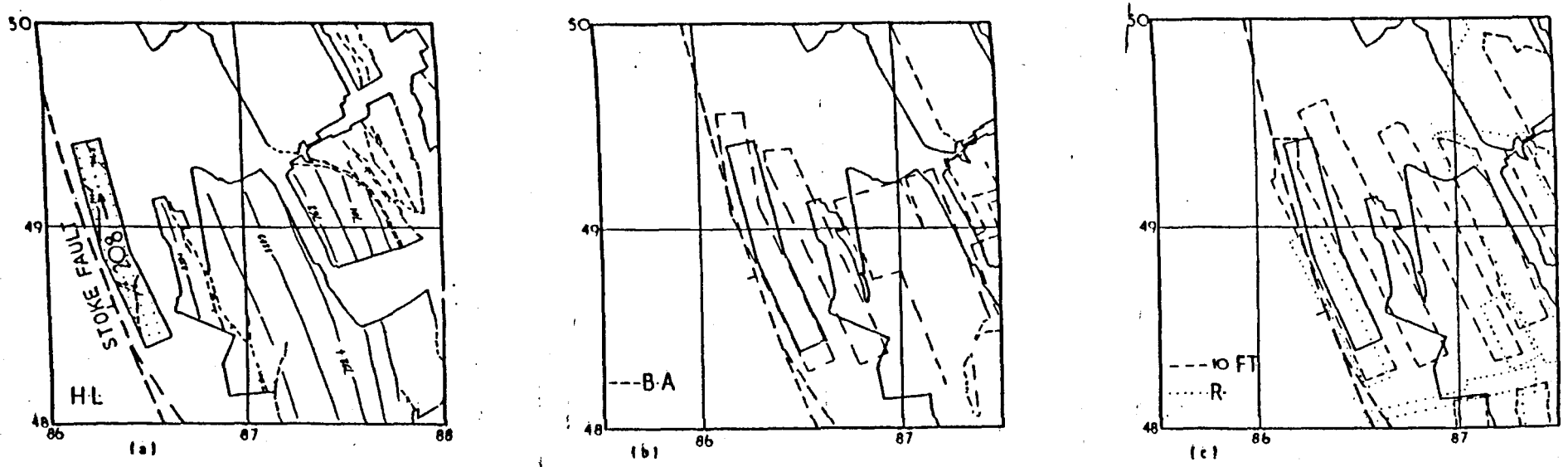

Fig. 9.4.1. The layouts of the mine workings in area B showing the active mine workings (dotted ornament) with faults at the surface and at the seam level in (a) the Holly Lane seam. Also shown are the mine workings in the Holly Lane seam superimposed on previous mine workings in (b) the Bowling Alley seam (B.A.), and (c) the Ten Feet (10 ft) and Ragman (R) seams. (For legend see Fig. 9.3.1).

the Yard and Moss seams at much higher levels. No workings are present beneath this panel.

9.4.1 Spatial distribution of tremor hypocentres

Nine events (9% of the total) occurred in this area. Figure 9.4.2 is a plan view showing the location of the tremor epicentres with respect to the mine workings and structural geology in the area. The vertical distribution of the tremor hypocentres is shown in Figure 9.4.3. This figure is drawn along profiles AB and CD of Figure 9.4.2. Figures 9.4.2 and 9.4.3 show that the tremors are located adjacent to the mine workings. The tremors are not located immediately over or under the active panel but are displaced a few hundred metres to the west and southwest of the panel. The tremors, particularly those having a shear source mechanism, are concentrated adjacent to the Stoke normal fault and are located at distances of not more than 350 m from the fault plane (see Figure 9.4.3a). Even though the accuracy of our location is about 500 m in plan and depth, it is felt that the location of the tremors near the Stoke fault is real. This area is in a better situation with respect to the seismic network geometry and should give more accurate locations compared with the other areas. Tremor foci mostly lie between depths of 600 m below O.D. and the surface. Only one event is located deeper with a depth value of about 1200 m below O.D.

The vertical distribution of the tremor hypocentres and the corresponding total amount of seismic energy release within each interval of one hundred metres in depth is shown in Figure 9.4.4. The depths of the active mine workings are also shown. No prominent depth of seismic activity can be seen. However, most of the energy was released near the surface. The relationship between the tremor size, M_L, and the depth is shown in Figure 9.4.5. No simple relationship can be seen. However, the figure clearly shows that most of the tremors occurred in the magnitude ranges between 1 and 1.5. Unfortunately, there are no boreholes in this area, hence the

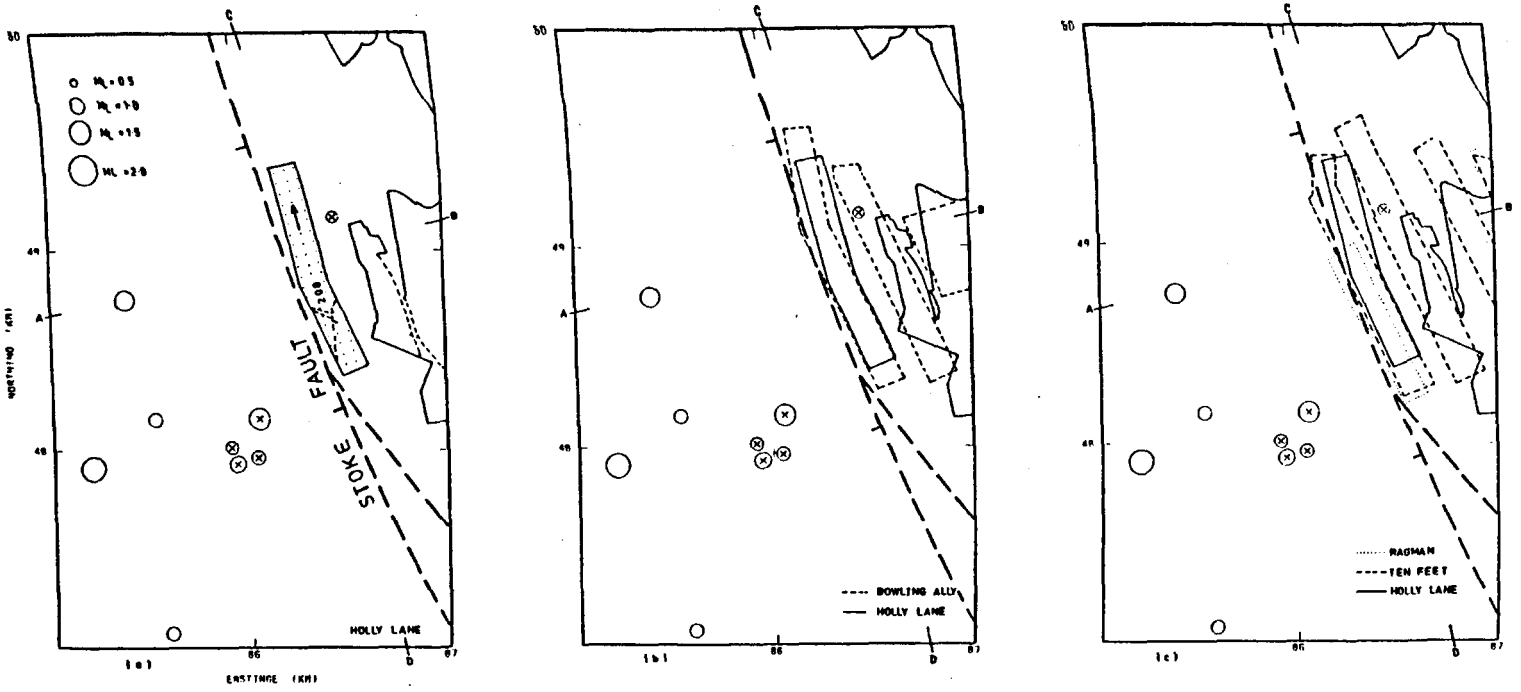

Fig. 9.4.2. Map of earth tremor epicentres for tremors which occurred in area B. Tremors are located along the Stoke fault and within a few hundred metres to the south-west of the active panel (panel 208) in (a) the Holly Lane seam. Faults at the level of the Holly Lane seam are also shown. Also shown are the Holly Lane seam mine workings together with previous mine workings in different adjacent seams in (b) the Bowling Alley seam and (c) the Ragman and Ten Feet seams. (For legend see Fig. 9.3.1).

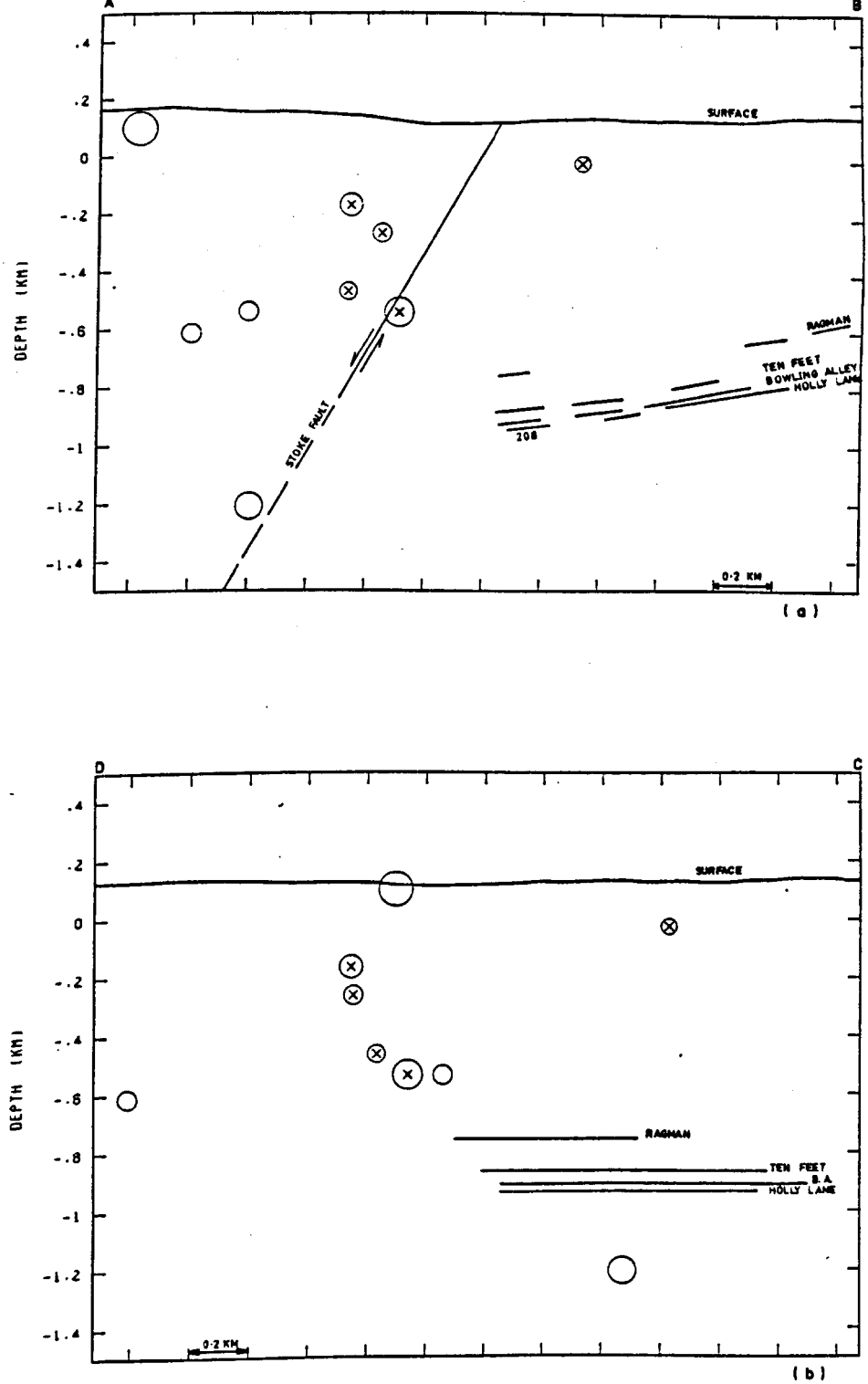

Fig. 9.4.3. Hypocentre sections (A-B, C-D, Figure 9.4.2) of tremors located in area B, showing the position of tremor hypocentres with respect to the active and old mine workings and to the Stoke fault.

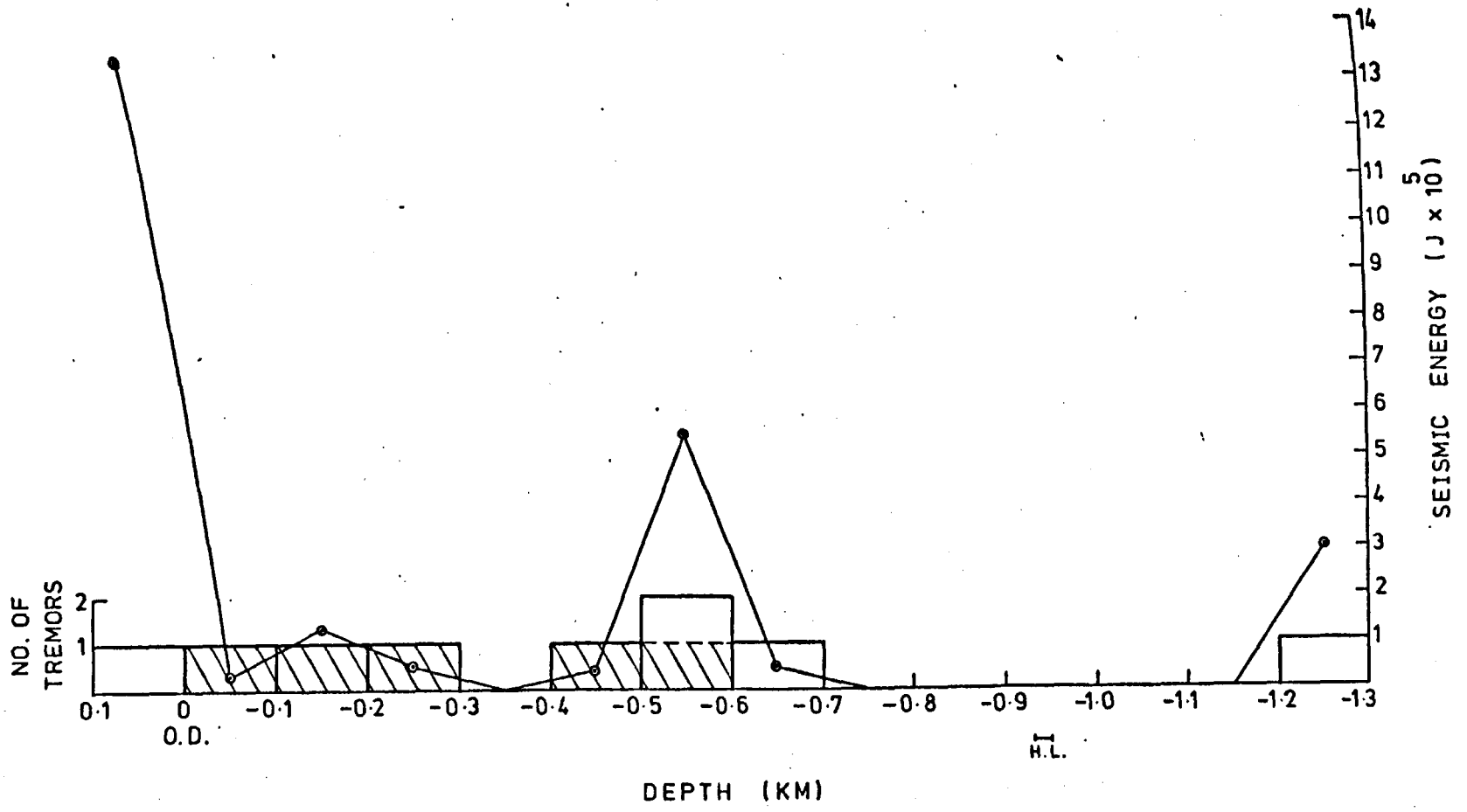

Fig. 9.4.4. A plot showing the number of tremors and the corresponding seismic energy release, occurring within each 100 m depth interval in area B. The depth ranges of the active mine workings in the Holly Lane (H.L.) seam is also shown. The shaded area represents tremors with a shear source origin.

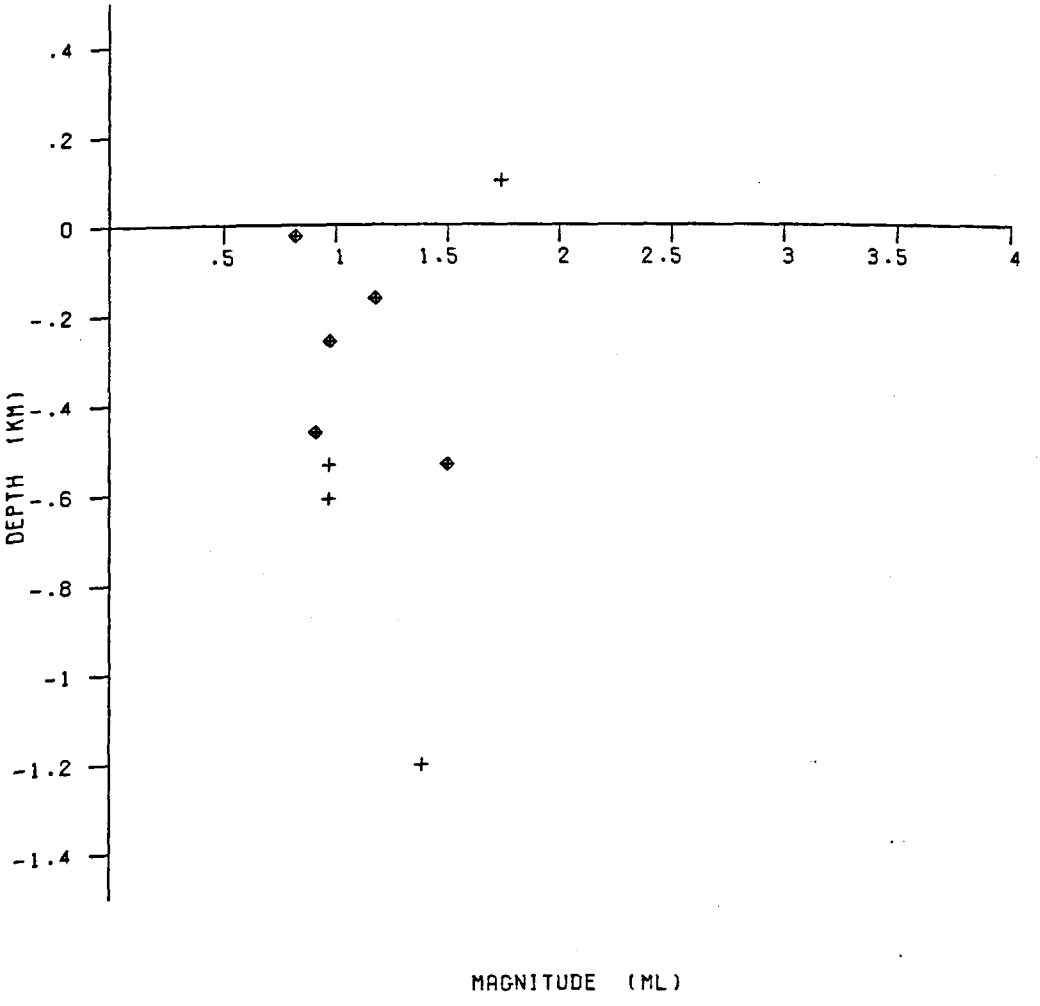

Figure 9.4.5. Plot of tremor depth against local magnitude, M_L, for tremors occurring in area B.

relationship between the tremor foci position and the presence of sandstone beds could not be determined.

9.4.2 Temporal distribution of tremors and seismic energy release

One event occurred in 1975 while the other eight events occurred in 1976. No event occurred in 1977. This indicates that these tremors were associated with the mine workings of panel 208 of the Holly Lane seam, which started production in 1974 and finished in September 1976. The distribution of the seismic events and the energy release throughout the week and the day are shown in Figure 9.4.6. The figure shows no obvious relationship between mining and seismic activity, however, very few earth tremors are available to prove or disprove this relationship.

9.4.3 First motion analysis of seismic data

Observation of the P-wave first motions shows that five tremors had a shear source mechanism, while the other four could have had an implosional/collapse source origin. The five events having a shear source mechanism were concentrated near the Stoke fault. A composite fault-plane solution using the data from all the five shear events was obtained (Figure 9.4.7). The composite focal mechanism is well determined. The consistency of the first motions on the focal plot suggests that the five tremors share a similar mechanism. However, the plot shows that the events could fit two fault-plane solutions. Both solutions indicate a predominantly dip-slip motion associated with normal faulting. The nodal plane striking N 32°W (plane 1) with a dip of 70° SW is considered to be the preferred choice of the fault-plane since it agrees well with the N 30° W strike of the Stoke fault. The dip of the Stoke fault is estimated to be between 50°-70° SW (N.C.B. private communication). The nodal plane striking N 18° E (plane 2) with a dip of 80° to the SE is considered to be the auxiliary plane.

Four events with an implosional/collapse source mechanism were located further away from the fault-plane (Figures 9.4.2 and 9.4.3), and

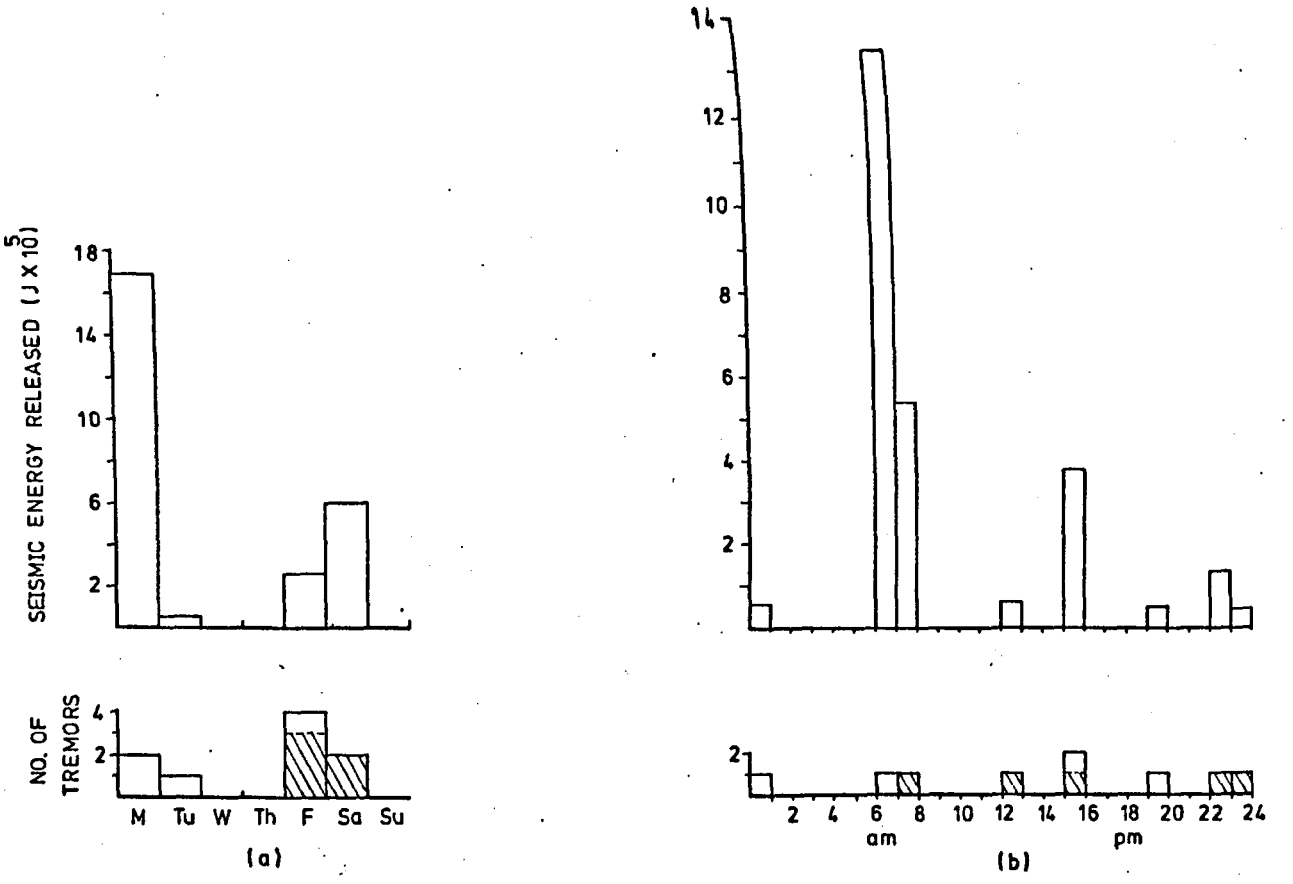

Fig. 9.4.6. Histograms showing (a) the weekly and (b) the daily distribution of tremors and the corresponding seismic energy release for tremors which occurred in area B. The shaded area represents tremors with a shear source mechanism.

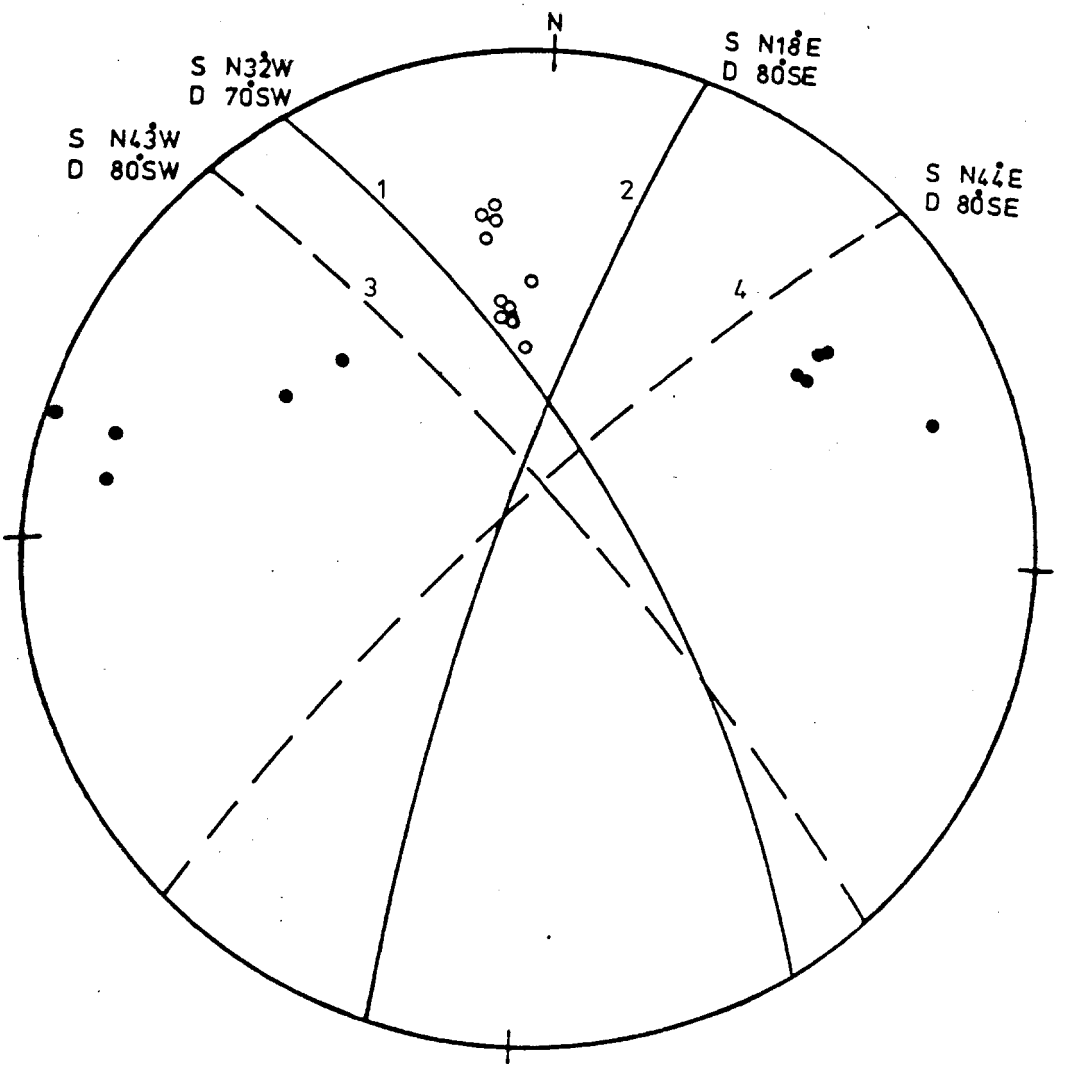

Fig. 9.4.7. A composite focal mechanism for tremors which occurred in area B.

all of them lie on the down throw side of the Stoke fault (in the hanging-wall). However, the reliability of the dilatational source mechanism is uncertain since there was cross-interference between the output signals from some seismometers. The events could also be of shear type mechanism but they developed kataseismic P-wave first motion at all stations due to the downward movement of the rocks in the hanging-wall of the fault as a result of the redistribution of strata pressure due to mining and the gravitational force, as described by Gane et al. (1952) in Section 3.3. Collapses in old workings disturbed by the active mining operations could also have generated these four tremors.

9.4.4 b-value

The frequency-magnitude relationship in this area follows the formula:

$$\log_{10} N = 1.94 - 1.09\, M_L \qquad 9.4.1$$

The constants in this formula were obtained from Figure 9.4.8. The figure shows a linear relationship between logN and M_L in the magnitude ranges between 1.0 and 1.5.

9.4.5 Earth tremor generation mechanisms

The concentration of tremors adjacent to the Stoke fault suggests that these tremors were associated in some way with the fault. Figure 9.4.3 shows that panel 208 of the Holly Lane seam had been driven under three old panels mined out previously in three different successive seams. There are also other workings at higher levels. These panels were driven parallel to the Stoke fault on its up-throw side (foot-wall) and at distances of less than 600 m from the fault plane. The interbedded rocks between these panels (intradosal ground) are fractured and heavily de-stressed due to the extraction of the coal from these panels. This situation may have led to

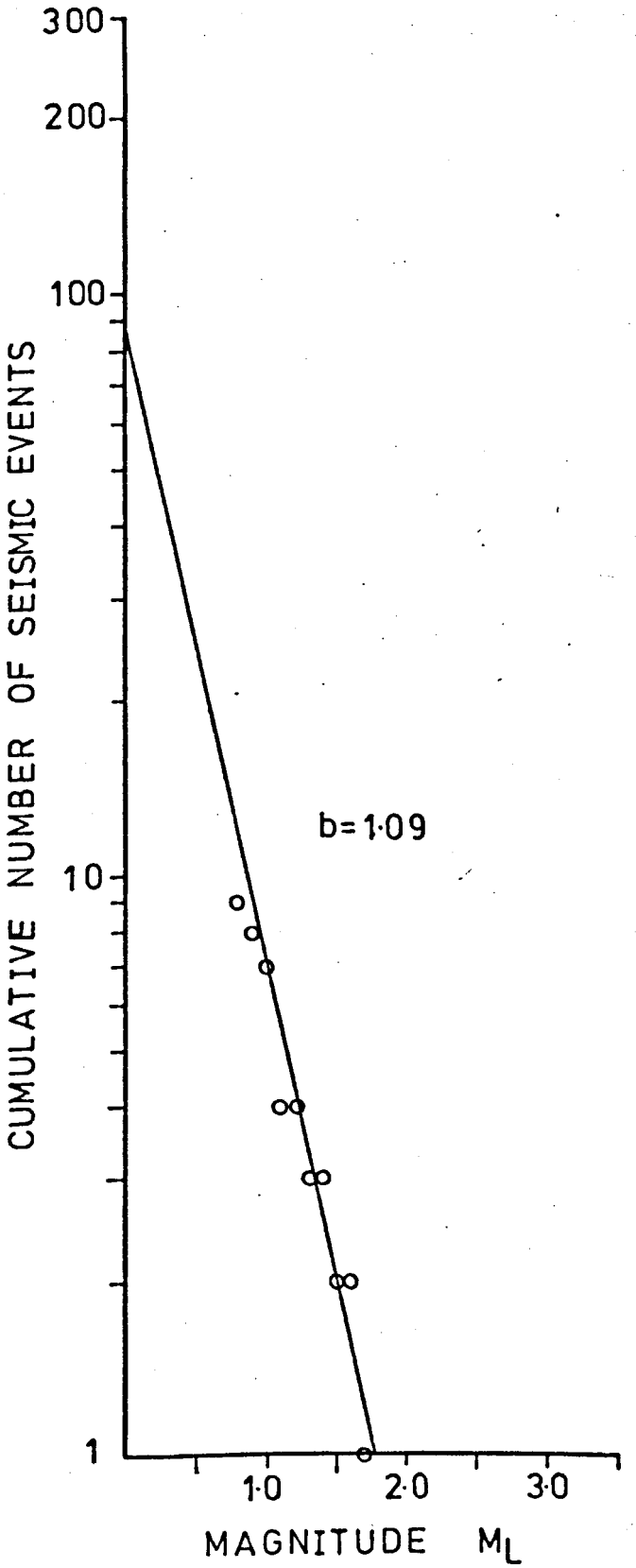

Fig. 9.4.8. A plot showing the frequency-magnitude distribution for tremors occurring in area B.

the reduction in the normal stress component across the fault plane and consequently the internal friction forces along the fault plane decreased. As a result of this, shear movements may have been triggered along the fault due to the readjustment of the stress along the fault plane. Since the fault is exposed at the surface, water may infiltrate along the fault plane as well, so lubricating it and helping movement along the fault plane.

The occurrence of earth tremors when mine workings advance perpendicular or parallel to an existing fault has been observed by many authors (see Section 3.2.3 and 3.4.2). In the Kolar gold field, India, Isaacson (1961) observed the occurrence of seismic events when a stope advanced perpendicular towards a normal fault. Shadbolt (1978) indicated that abnormal movement (vertical and/or lateral) develops at the fault plane, and that the extent of such movement depends to a great extent on the methods and extent of the mining in relation to the fault plane, such as:

(i) A single working of small width/depth ratio approaching a fault at right angles is less likely to cause stepping than a large width/depth working parallel to it.

(ii) The chance of a fault stepping are much greater when the fault has been affected by previous workings in shallow seams than they are for a single working in a virgin area.

(iii) Workings on the upthrow side (under the fault plane) are more likely to cause stepping than similar workings on the other side of the fault.

(iv) As successive workings increase the effect on the fault plane, so the chances of abnormal movement or stepping increase."

From the above it can be concluded that if another seam is mined below or between the previous mined-out panels in the other seams, more frequent and severe tremors will be expected to occur along the Stoke fault, particularly if the new seam is extensively mined. The tremors may also

occur if more panels are mined adjacent to the old panels in the different successive seams mentioned above.

9.5 Area C

This area lies around Silverdale. In this area the coal was mined during the monitoring period in two seams worked from two different collieries. The area was also extensively mined in many seams in the past. Most of the working panels lie between the Apedale and Millbank faults. The seams dip to the south-southwest at an angle of approximately 6°. The two seams worked in the monitoring period are in descending order:

(i) The Winghay seam. The coal was extracted from this seam by 16 panels worked from Silverdale colliery in the period between 1969 and 1977, over an area of about 4 km^2 as shown in Figure 9.5.1a. They form a triangular shape with its apex on the southeast, and with a large pillar in its centre. These panels are bounded by much older workings to the NW. Of these 16 panels, 6 panels were mined during the monitoring period at depths ranging between 290 m and 400 m below O.D. (see Table 9.1). These panels were separated from one another and from other old workings by coal pillars of variable widths. The roof and floor of the panels consist mostly of mudstone. The seam is disturbed by a number of small faults at the seam level, particularly in the region of the pillar left between panel 12A and the other old panels. These faults, having maximum throws of as much as 17 m, dip mostly in NE and SW directions.

The active panels in the seam are overlain by several older workings. The next adjacent working is in the Chalkey seam (Figure 9.5.1c) at a height of approximately 88 m above the Winghay seam. They are also underlain by previous workings in several seams. The nearest workings are in the Moss seam at a depth of about 320 m below the panel levels (Figure 9.5.1d).

(ii) The Hams seam. The coal in this seam was extracted from ten panels mined from Holditch colliery since 1968 in an area of about 4 km^2 as

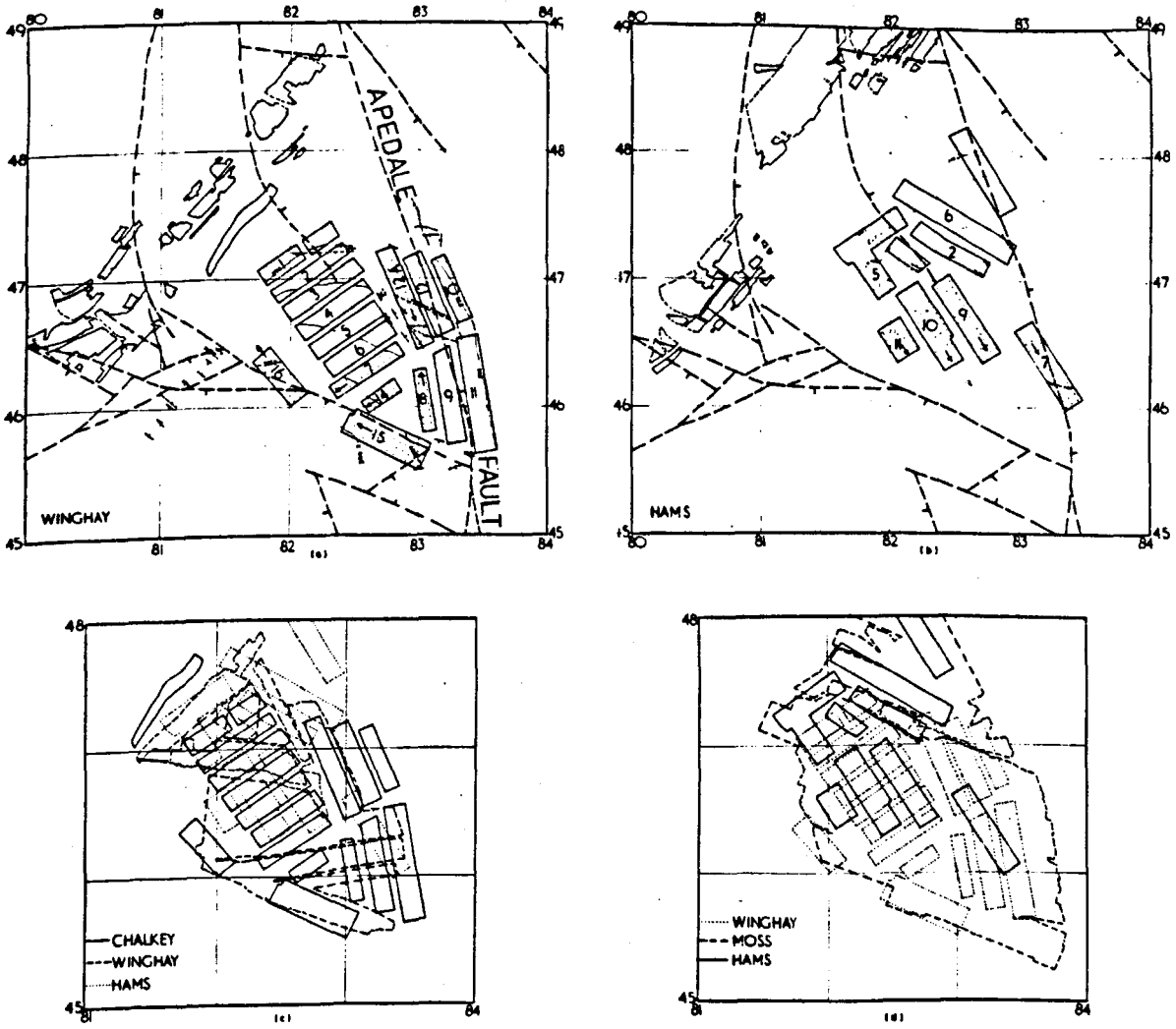

Fig. 9.5.1. The layout of the mine workings in area C showing the active mine workings (dotted ornament), faults at the surface and at the level of the active seam in (a) the Winghay seam and (b) the Hams seam. Also shown are the mine workings in the two active seams superimposed on previous mine workings in (c) the Chalkey seam and (d) the Moss seam. (For legend see Fig. 9.3.1).

shown in Figure 9.5.1b. The panels are bounded to the NW by other old and shallow workings, mined in the last century. Four of these panels were mined during the monitoring period at depths ranging between 670 m and 780 m below O.D. (see Table 9.1). Coal pillars of variable widths were left between the panels. The roof of the panels consists mainly of mudstone and silty mudstone, while the floor consists mostly of mudstone and sandstone, or mudstone and siltstone.

The active workings are overlain by previous workings in the Moss seam (Figure 9.5.1d) at a height of about 90 m above the Hams seam level. No working is present beneath the active panels.

9.5.1 Spatial distribution of tremor hypocentres

A total of 33 tremors representing 34% of the total number occurred in this area. The tremors are plotted in Figure 9.5.2 to show their relationship with mining and structural geology in the area. Figure 9.5.2 is a plan view, while Figures 9.5.3a and b show vertical sections along profiles AB and CD respectively. Most of the tremors cluster adjacent to the mine workings and within a few tens of metres from the active panels. The tremors do not concentrate over or under any specific panel, but are mostly located in the pillars left between the panels. Most of the tremors which occurred in a particular year are located near the panel or panels which were being mined during that year. The two largest tremors in this area occurred in the Winghay pillar which was left between panel 12A and the other six old panels (panels 1-6). Only a few tremors are scattered outside the mined area. Three tremors are located to the west outside the limit of the map in figure 9.5.2. These locations could be due to error, or they could be located in areas adjacent to old mine workings. The mining operations in the Winghay and Hams seams may have disturbed the balance of the existing stress in these old mine workings causing rock movements, such as roof falls which may have generated small tremors. Roof collapses may also take place in old mines after a long period of time as a process of

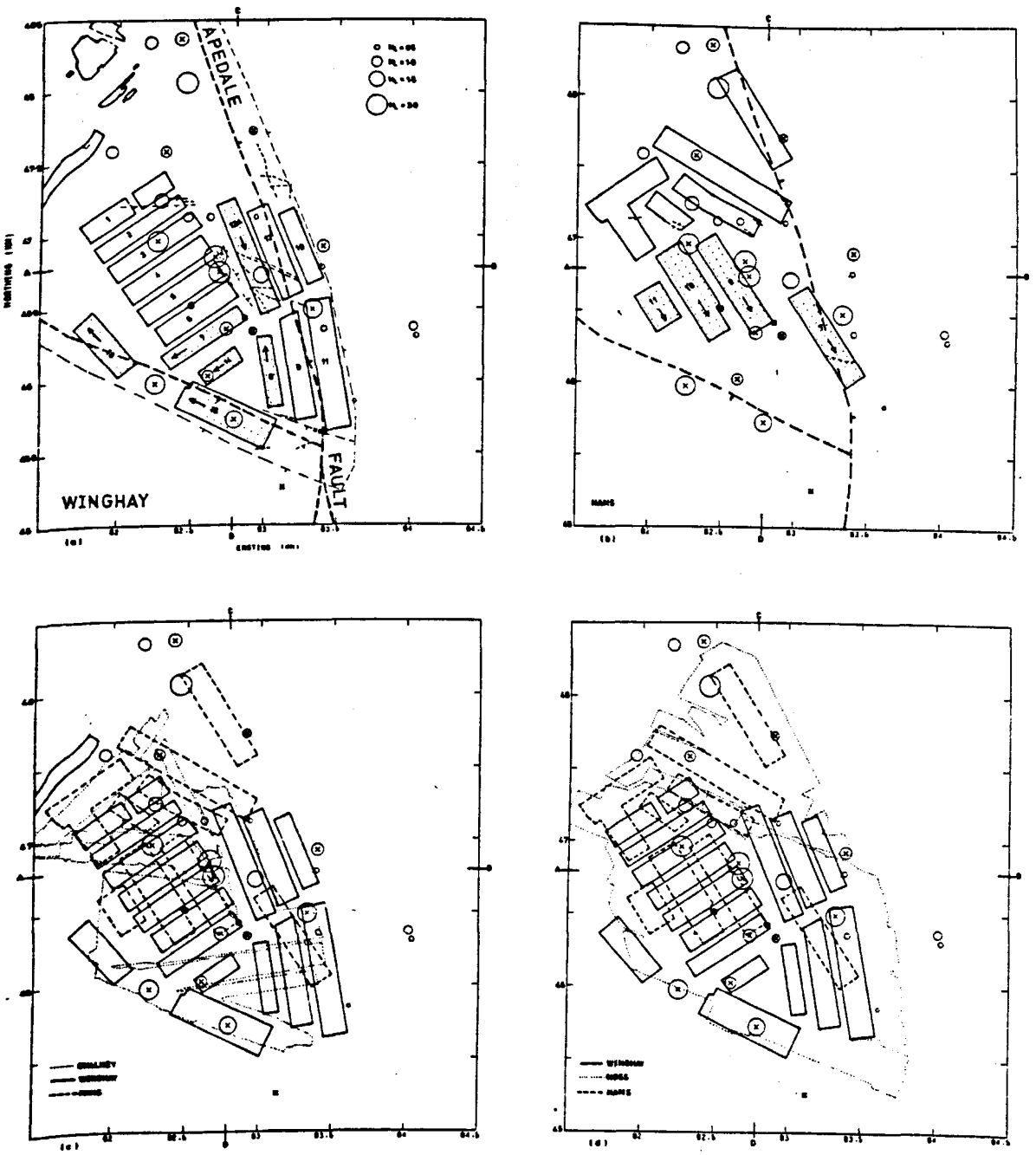

Fig. 9.5.2. Map of earth tremor epicentres for tremors which occurred in area C. Tremors are located near the active panels (dotted ornament) in (a) the Winghay seam and (b) the Hams seam. Faults at the surface and at the active seam datums are also shown. Also shown are the previous mine workings in two adjacent seams; in (c) the Chalkey seam and (d) the Moss seam. (For legend see Fig. 9.3.1).

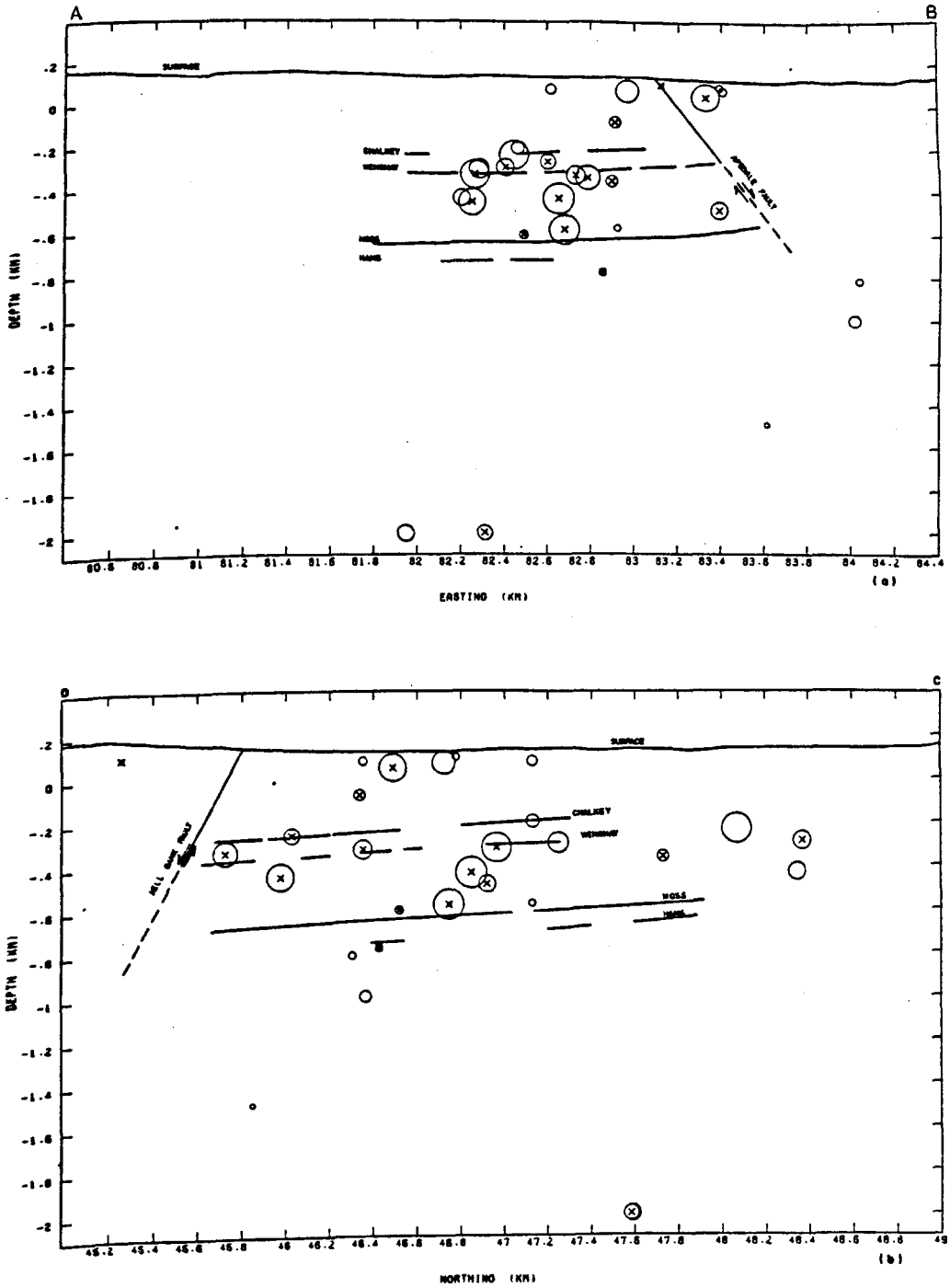

Fig. 9.5.3. Hypocentre sections (A-B, C-D, Figure 9.5.2) of tremors located in area C, showing the position of tremor hypocentres with respect to the active and old mine workings and to the Apedale and Millbank faults.

stabilization in the mine (Bell, 1975). The tremors do not cluster in the vicinity of the Millbank fault. Only a few tremors are located near the Apedale fault. This suggests that the Millbank fault is inactive and plays no part in generating the tremors, while the Apedale fault could have affected the occurrence of some of these tremors. The tremor foci mostly lie between depths of 600 m below O.D. and the surface, mainly between the Winghay and Moss seams.

Figure 9.5.4 is a histogram giving the number of earth tremors and the corresponding total amount of seismic energy release in each 100 m depth interval. Most of the tremors, and energy release, occurred near the level of the active mine workings in the Winghay seam. The average depth of 28 tremors, the total number except for those located at the maximum depth limit (2 km) and those outside the boundary of the map (Figure 9.5.2), is about 397 m below O.D. The depth of the active workings in the Winghay seam ranges between 290 m and 400 m below O.D., while in the Hams seam it ranges between 670 m and 780 m. This suggests that most of the tremors were generated due to the mine workings in the Winghay seam.

Figure 9.5.5 shows tremor size, M_L, plotted against the depth from O.D. No specific relationship between tremor depth and size was found. The plot demonstrates that most of the tremors have a local magnitude, M_L, ranging between 0.5 and 2.0.

The distribution of the tremor foci with respect to the general lithology, in particular to the presence of sandstone beds, is shown in Figure 9.5.6. No obvious relationship between the foci location and the presence of sandstones could be observed.

9.5.2 Temporal distribution of tremors and seismic energy release

The maximum number of tremors (17) occurred in 1976, with the minimum number (6) in 1975. 1976 had the longest recording time and also most of the panels were mined during this year. The weekly and daily distribution of the seismic events, and the corresponding seismic energy release,

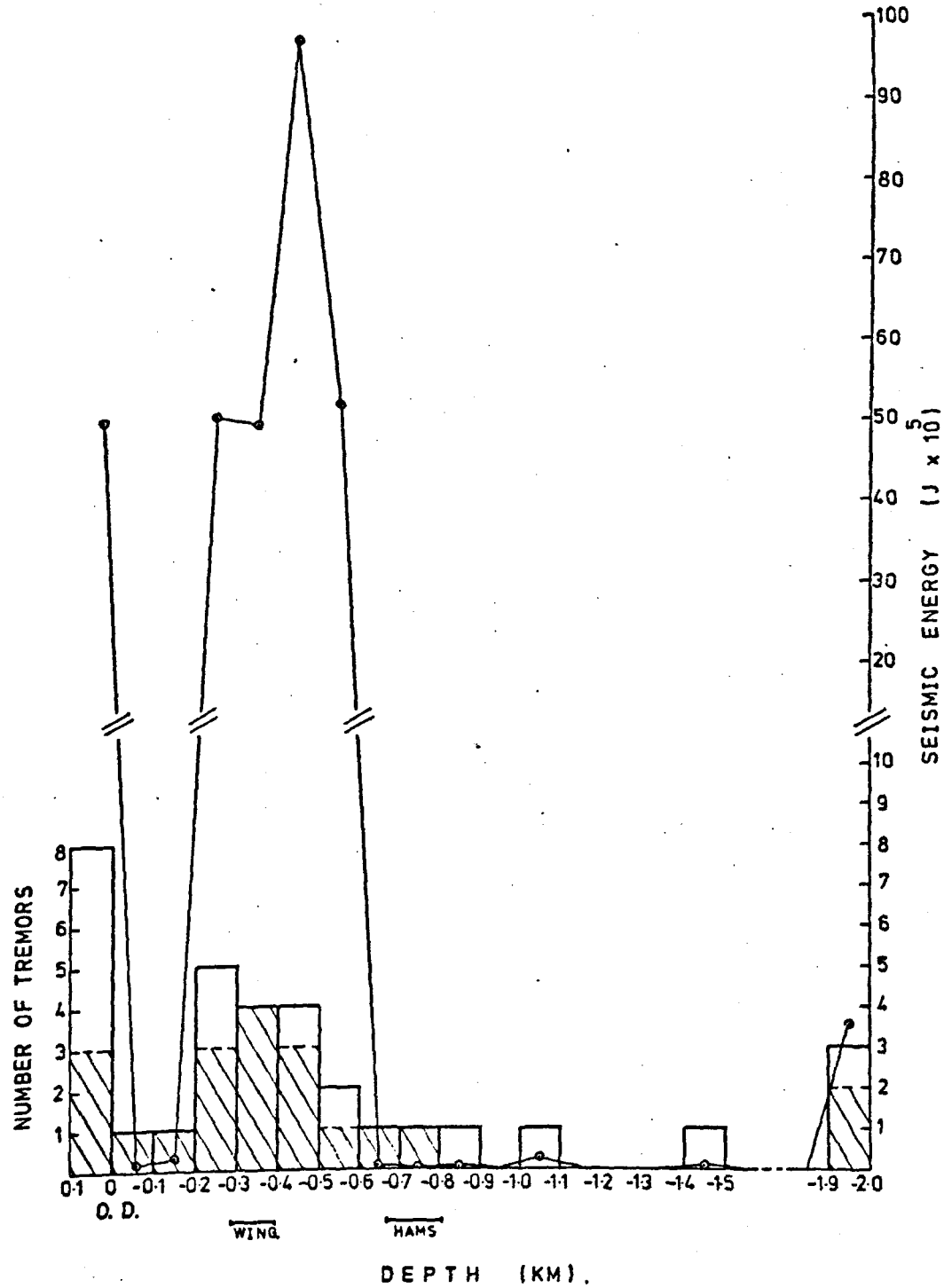

Fig. 9.5.4. A plot showing the number of tremors and the corresponding seismic energy release, occurring within each 100 m depth interval in area C. The depth ranges of the active mine workings in the Winghay (WING) and Hams seams are also marked. The shaded area represents tremors with a shear source origin.

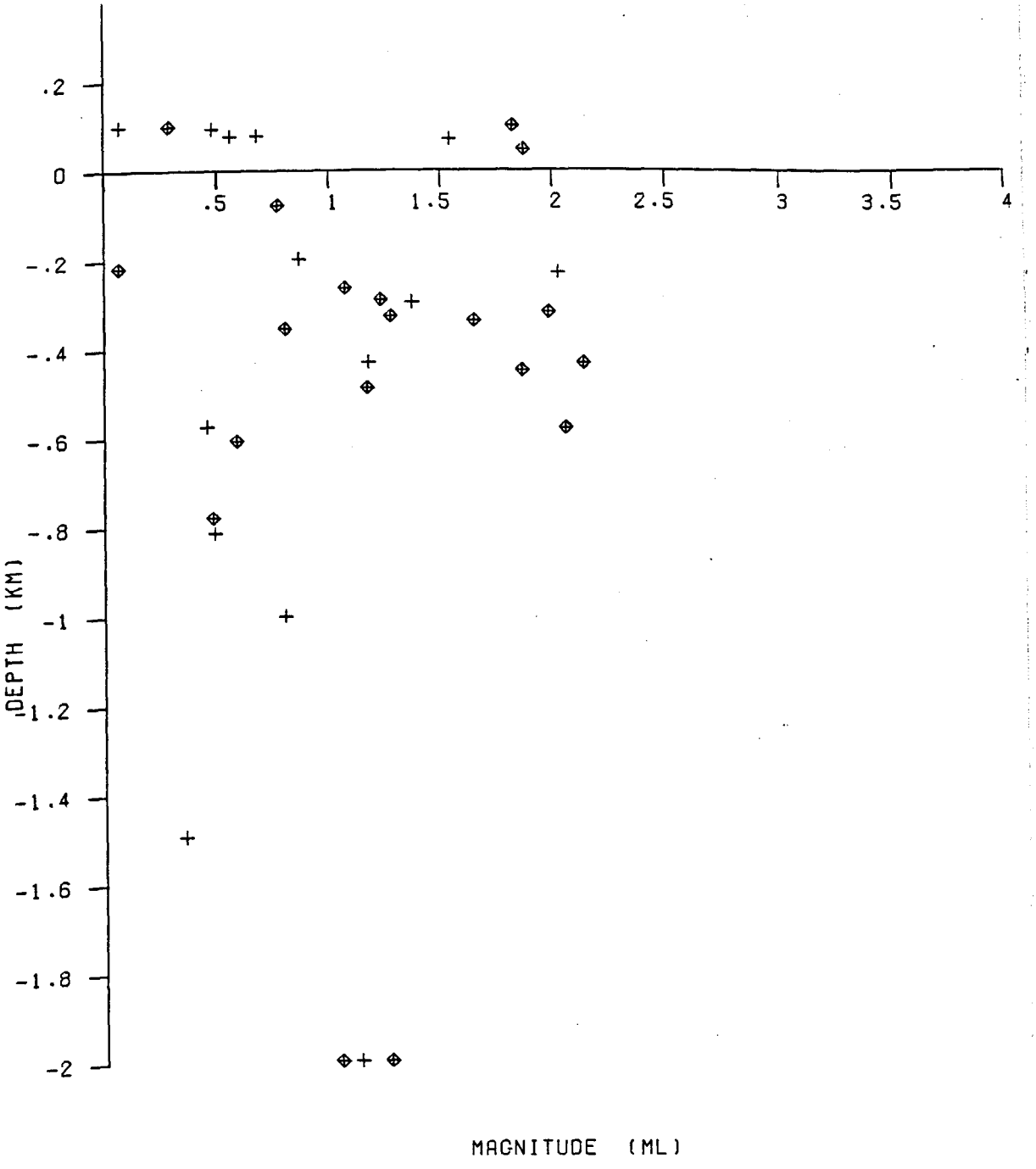

Figure 9.5.5. Plot of tremor depth against local magnitude, M_L, for tremors occurring in area C.

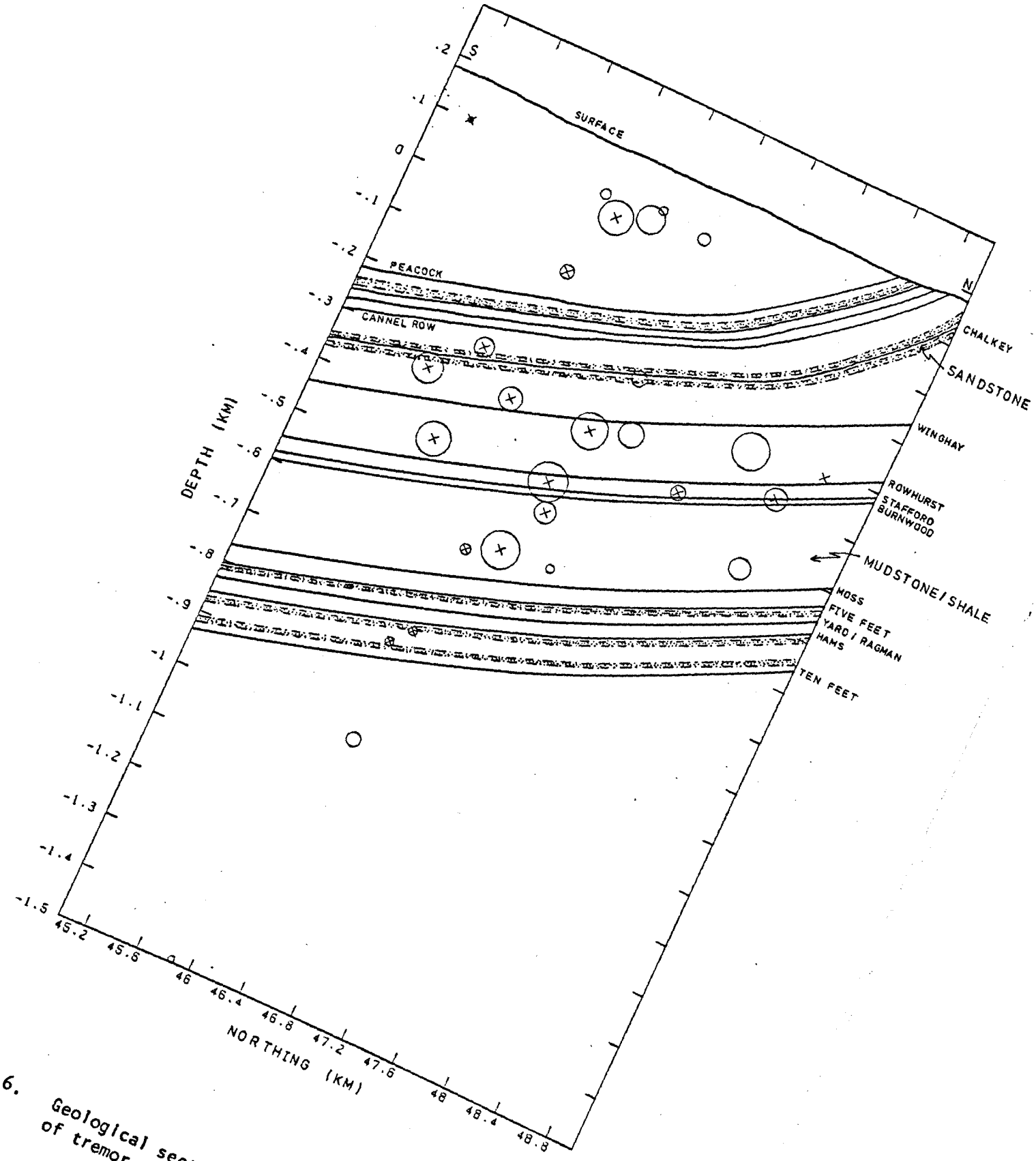

Fig. 9.5.6. Geological section drawn downdip showing the positions of tremor foci for tremors occurring in area C.

are shown in Figure 9.5.7. The figure gives strong evidence for a casual relationship between mining activity and the occurrence of earth tremors.

9.5.3 First motion analysis of seismic data

Analysis of the P-wave first motions has found that 19 tremors had a shear source mechanism, 12 tremors probably had an implosional/collapse source mechanism, while two tremors were found to have an explosive source mechanism. These two tremors are the only events found to have an explosive source mechanism in this study. However, the reliability of the compressional source mechanisms are uncertain since these two events were recorded on four stations only located within an arc of about 106° from the tremor epicentre. They have relatively large magnitude, M_L, values of 2 and 1.2. These two tremors could have been generated by some explosion in the mine. It is unlikely that they were generated by the breaking of rocks in tension due to bending, as discussed by Gane et al. (1952) in Section 3.3. The energy released when the rock break in tension is very small compared with the energy released in compression, since the rock has a compression strength equal to about ten times its tensile strength (Osterwald and Dunrud, 1966; Kusznir et al., 1980b).

A composite fault-plane solution was obtained using data from nine tremors (Figure 9.5.8A). The nodal planes are well determined. The solution indicates movements by normal faulting. None of the nodal planes match any of the known structures in the area. The nodal plane striking N-S may represent the fault-plane since it is running more or less parallel to the strike of the small faults encountered at the Winghay seam level. These faults strike at approximately N 30° W. Alternatively, it could be that the solution obtained represents rock movements along an unknown underground fault or faults. The other ten events having a shear source mechanism did not fit the composite solution. Two of these events fit more than one fault-plane solution (Figures 9.5.8C and I). However, the fault

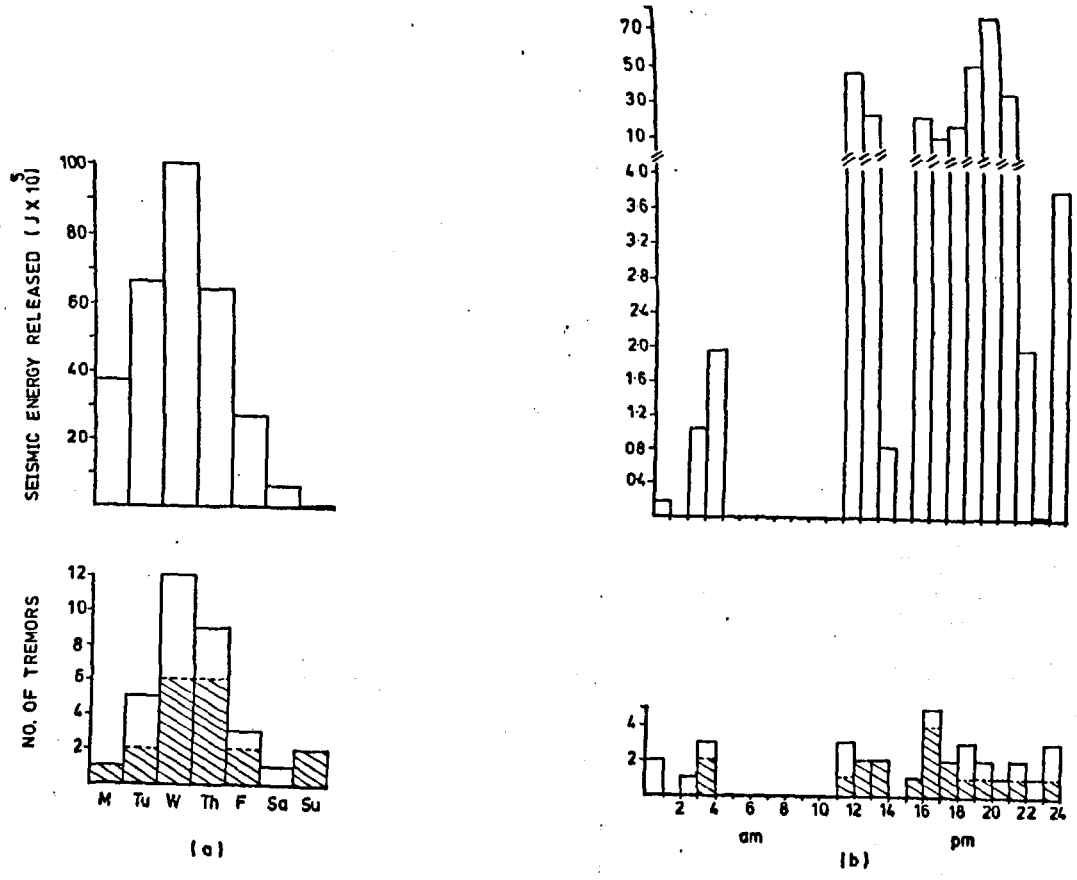

Fig. 9.5.7. Histograms showing (a) the weekly and (b) the daily distribution of tremors and the corresponding seismic energy release for tremors which occurred in area C. The shaded area represents tremors with a shear source mechanism.

Fig. 9.5.8. Upper hemisphere fault-plane solutions for tremors which occurred in area C. Each event shows a different fault-plane solution, but in (A) a composite fault-plane solution was obtained using the data from the nine following tremors.

1975 9-3 19-35

1975 10-16 18-38

1976 3-10 13-33

1976 3-25 23-43

1976 4-22 13-16

1976 5-5 15-13

1976 7-19 20-00

1977 5-31 21-03

1977 7-27 17-44

(For legend see Fig. 9.3.12).

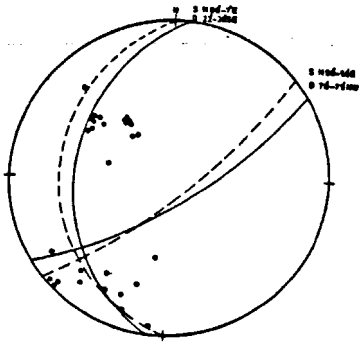

(A)

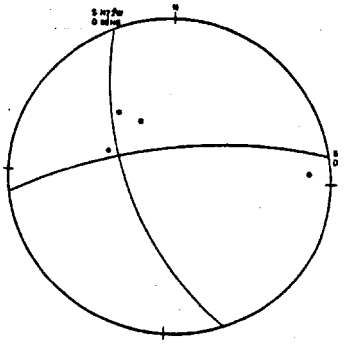

(B)

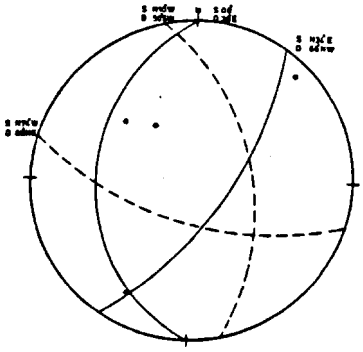

(C)

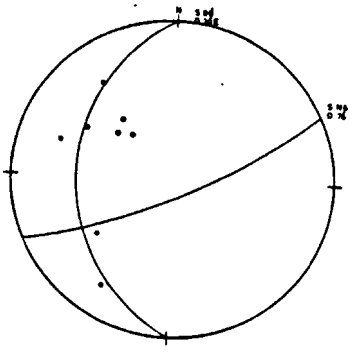

(D)

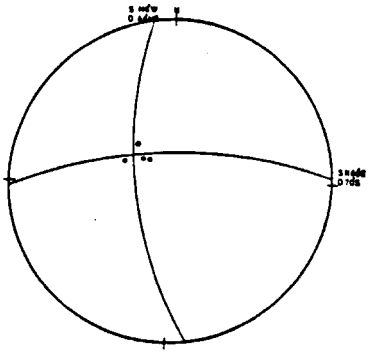

(E)

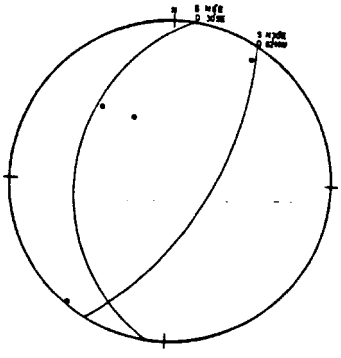

(F)

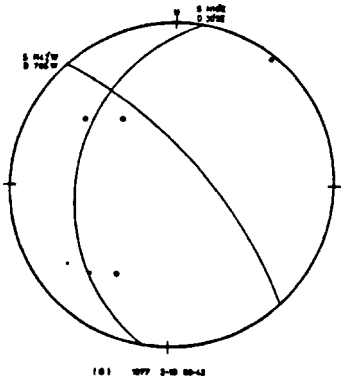

(G)

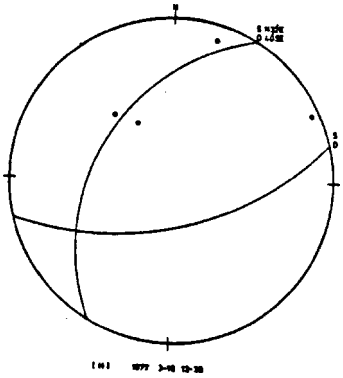

(H)

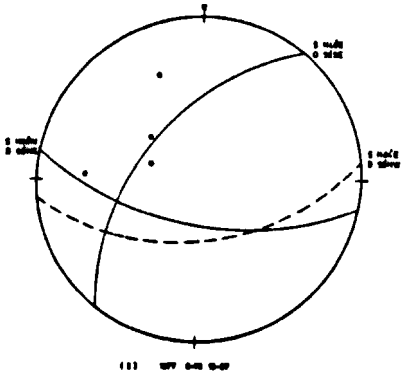

(I)

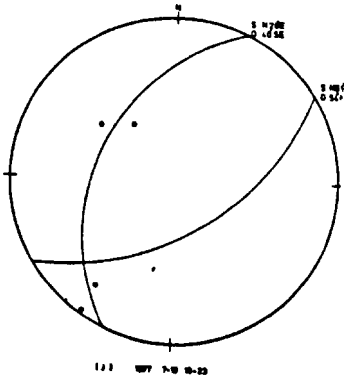

(J)

plane solution for all these events (Figure 9.5.8) represent rock movements by normal faulting, except six tremors (Figures 9.5.8B, C, D, I and J) which show movements by reverse faulting. These six tremors may have occurred along pre-existing reverse faults, or may have occurred in the roof behind the face (in the goaf), in the same mechanism as discussed for Area A. Alternatively, error in observations could have produced this type of fault-plane solution.

The tremors having implosional/collapse source mechanisms most probably occurred in the goaf area, in the same situation as explained for Area A. However, some of these tremors may also have occurred due to the failure in compression of some pillars (i.e. pressure bursts).

Finally, it can be concluded that some of the tremors in Area C had a shear source mechanism resulting from rock movements along pre-existing planes of weakness due to the re-adjustment of the stresses along these planes as a result of the mining operations. These tremors are represented by the composite focal mechanism (Figure 9.5.8A). However, most of the tremors occurred along fracture planes having different orientations. This may suggest that these tremors could have occurred as a result of the failure of pillars and adjoining rocks in shear along different planes due to increasing pressure on these rocks.

9.5.4 b-value

The frequency-magnitude relationship in this area follows the formula:

$$\log_{10} N = 1.72 - 0.5\, M_L \qquad 9.5.1$$

This formula was obtained graphically from the frequency-magnitude plot (Figure 9.5.9). There is a linear relationship between the magnitude and the frequency in the magnitude ranges between 0.5 and 1.75. The tremors in the higher magnitude range do not fit this relationship. This may suggest that the rocks have an upper limit for strain energy which can be stored, or it could just be a statistical error. It is interesting to

plane solution for all these events (Figure 9.5.8) represent rock movements by normal faulting, except six tremors (Figures 9.5.8B, C, D, I and J) which show movements by reverse faulting. These six tremors may have occurred along pre-existing reverse faults, or may have occurred in the roof behind the face (in the goaf), in the same mechanism as discussed for Area A. Alternatively, error in observations could have produced this type of fault-plane solution.

The tremors having implosional/collapse source mechanisms most probably occurred in the goaf area, in the same situation as explained for Area A. However, some of these tremors may also have occurred due to the failure in compression of some pillars (i.e. pressure bursts).

Finally, it can be concluded that some of the tremors in Area C had a shear source mechanism resulting from rock movements along pre-existing planes of weakness due to the re-adjustment of the stresses along these planes as a result of the mining operations. These tremors are represented by the composite focal mechanism (Figure 9.5.8A). However, most of the tremors occurred along fracture planes having different orientations. This may suggest that these tremors could have occurred as a result of the failure of pillars and adjoining rocks in shear along different planes due to increasing pressure on these rocks.

9.5.4 b-value

The frequency-magnitude relationship in this area follows the formula:

$$\log_{10} N = 1.72 - 0.5\, M_L \qquad 9.5.1$$

This formula was obtained graphically from the frequency-magnitude plot (Figure 9.5.9). There is a linear relationship between the magnitude and the frequency in the magnitude ranges between 0.5 and 1.75. The tremors in the higher magnitude range do not fit this relationship. This may suggest that the rocks have an upper limit for strain energy which can be stored, or it could just be a statistical error. It is interesting to

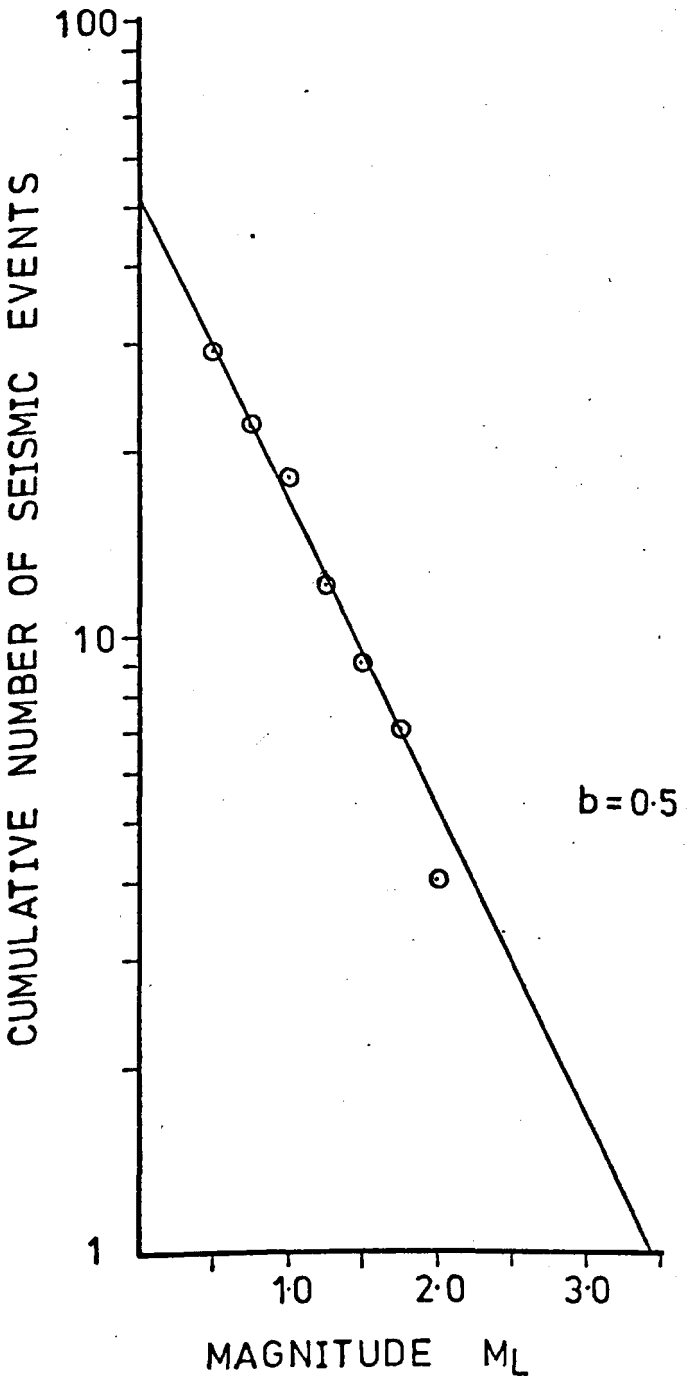

Fig. 9.5.9. A plot showing the frequency-magnitude distribution for tremors occurring in area C.

note that the b-value in this area is the lowest value encountered in the coalfield. This may suggest that this area is under higher pressure than the other areas (Scholz, 1968). The rocks also could be hard and homogeneous so sustaining greater stress before they break (Mogi, 1962). This may explain why most of the tremors in this area were of a shear type mechanism.

9.5.5 Earth tremor generation mechanisms

Since the mine workings in the Hams seam are much deeper than the workings in the Winghay seam, one might expect the workings in the Hams seam to generate tremors because of the greater pressure, as discussed in Sections 2.3, 3.2.1 and 3.4.2. However, the spatial distribution of the tremors suggested that most of the tremors were generated by mine workings in the Winghay seam and not the Hams seam.

As we can see from Figures 9.5.1 and 9.5.3 all the active panels in the Hams seam were mined under previous old workings in the Moss seam at an average height of about 90 m above the panel levels. The coal in the Moss seam was extracted extensively without leaving pillars. As a result of this the rocks above and below the Moss seam (intradosal ground) have been fractured and their stress relieved, and consequently they could not store great amounts of strain energy. This indicates that the panels in the Hams seam were driven in a very relaxed zone. Moreover, there are no mine workings beneath these panels which can cause interaction effects. Therefore, it is unlikely that the mine workings in the Hams seam could generate seismic activity, especially large tremors. Some small tremors could have occurred behind the face in the goaf as a result of roof caving and fractures of sagging beds in the roof. Six tremors occurred on the downthrow side of the Apedale fault. Five of these tremors had implosional/collapse type mechanisms. These tremors could have occurred due to downward movements of the rocks in old workings on the downthrow side of the fault producing a

dilatational source mechanism . This may have occurred as a result of the readjustment of the stress along the fault due to the advancing face of panel 7 of the Hams seam at an acute angle towards the fault on its up-throw side. Alternatively, and most probably, error in location might have placed the tremors on the downthrow side of the fault.

The active mine workings in the Winghay seam were also carried out under an extensively mined-out area in the Chalkey seam at an average height of about 88 m above the Winghay seam level. But as we can see from Figures 9.5.1 and 9.5.3 the mine workings in the Chalkey seam were not as clean as those carried out in the Moss seam. Different sizes and irregular shape of pillars were left in the Chalkey seam. These pillars carry the over-burden load and therefore were highly stressed. When the panel face in the Winghay seam advanced below these pillars, the abutment pressures of the panel (front and flank abutments) and the abutment pressure of the pillar added together causing the pillar and the rocks in front of the panel face to fail either in shear or in compression.

(As explained earlier, the two largest tremors occurred in the pillar left between panel 12A and the other six old panels (panels 1-6). This pillar is also common with a smaller and irregular shaped pillar left in the Chalkey seam. These two tremors occurred in 1975. They most probably occurred due to the mining of panel 12A which was being worked at the time of occurrence. As the panel face retreated SE, front and side abutment pressures developed, acting in front and on both sides of the panel. The west abutment pressure, which was probably greater than the eastern abut-ment pressure, acted on the large pillar left between the active panel and the six old panels. The greater value of the western abutment pressure was due to the mining of panel 12A to the west of the two old panels (panels 11 and 12). Carman (1965) indicated that the side abutment pressure increases to a maximum as each consecutive panel is extracted. At the same time the

pillar became narrower as the face retreated southwards, and consequently the stress and strain energy per unit volume increased within the pillar. When the face of panel 12A approached beneath the projected part of the Chalkey pillar, the front and west side abutment pressures of the panel added to the abutment pressure of the Chalkey pillar producing together a very highly stressed zone. The rocks in the Winghay and Chalkey seam pillars and adjacent rocks failed when the average stress of the pillars exceeded their strength. The Winghay pillar, as we can see from Figure 9.5.1a, is disturbed by many small faults. Therefore, the pillar probably failed along these planes of weakness or along new fracture planes).

9.6 Area D

This area lies in Tunstall. The coal was extracted in this area through two panels - panels 56 and 57 - driven in the Ten Feet seam at depths ranging from 635 m to 690 m below O.D. and operated from Wolstanton colliery (see Table 9.1). This seam was the only seam mined in this area during the monitoring period. The two active panels are bounded on all sides by extensive old mine workings as shown in Figure 9.6.1. Coal pillars of different widths were left between the two panels and the old workings. The active panels were driven along the seam strike. The seam dips at approximately 7° to the SW. Mudstone and silty mudstone form the roof of the seam while fireclay forms the floor. A general section through the coal seam (Figure 9.6.1a) shows that a thin band of shale having a thickness of about 12.5 cm is interbedded within the coal. At the seam level, the seam is disturbed by minor faults. These faults have maximum throws of less than one metre and dip mostly to the SW. However, to the southwest of the active panels, faults having throws of as much as 16 m were found. These faults extend approximately parallel to the seam strike (strike faults) and dip in both NE and SW directions.

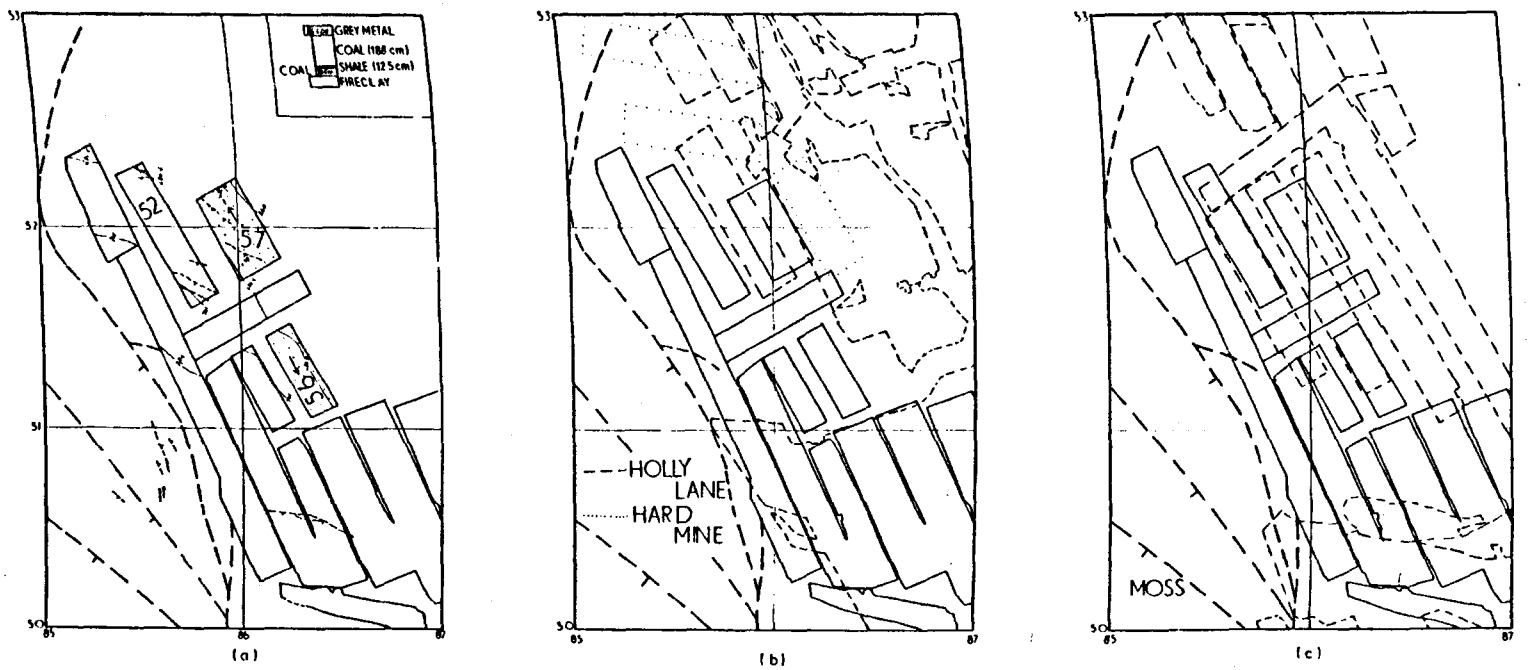

Fig. 9.6.1. The layouts of the mine workings in area D showing (a) the mine workings in the Ten Feet seam including the two active panels (dotted ornament) together with faults at the surface and at the seam datum. Also shown is a general geological section through the Ten Feet seam. Ten Feet seam workings are also shown together with previous adjacent workings in (b) the Holly Lane and Hardmine seams and (c) the Moss seam. (For legend see Fig. 9.6.3).

The active workings are underlain by previous workings in the Holly Lane and Hardmine seams (Figure 9.6.1b) at depths of about 61 m and 84 m respectively below the Ten Feet seam level. They are also overlain by old workings in the Moss seam (Figure 9.6.1c) at a height of approximately 165 m above the Ten Feet level.

9.6.1 Spatial distribution of tremor hypocentres

22 tremors (22.5% of the total) occurred in this area. The tremors are plotted in Figure 9.6.2 and 9.6.3 to illustrate their relationship with recent and previous mine workings and with the structural geology of the area. Figure 9.6.2 is a plan view showing the position of tremor epicentres, while Figure 9.6.3 is a vertical section showing the position of the tremor foci along the profiles AB, CD and EF of Figure 9.6.2 (i.e. parallel and perpendicular to the advancing faces of panels 56 and 57 of the Ten Feet seam). The tremors cluster adjacent to the mine workings, but they do not concentrate immediately over or under any of the active panels. The tremors are displaced to the west and southwest of the panels. This displacement of tremors could be real, or again it could be caused by systematic location errors, especially since the area is located well outside the S.O.T. seismic network. Figure 9.6.3 shows that the tremor hypocentres are located well away from any of the major mapped faults in the area. This suggests that these faults have no effect in generating these tremors. The tremor foci lie predominately between depths of 700 m and 200 m below O.D.

Figure 9.6.4 is a histogram showing the total number of tremors and the corresponding seismic energy release , occurring in each 100 m depth interval. The maximum number of tremors occurred in the depth interval between 500 m and 600 m below O.D., while the maximum amount of energy was released in the depth interval between 400 m and 500 m below O.D. The relationship between the tremor size, M_L, and the depth is shown in

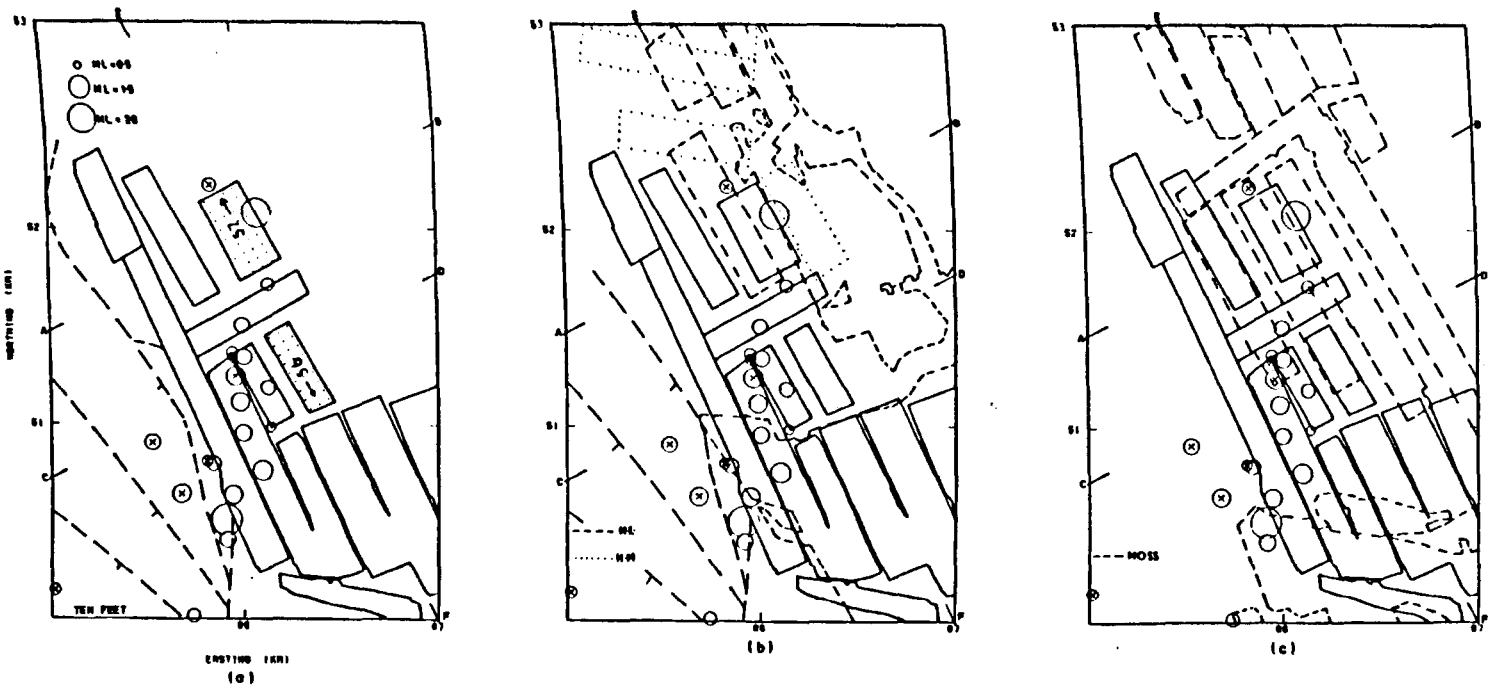

Fig. 9.6.2. Map of earth tremor epicentres for tremors occurring in area D during the mining of panels 56 and 57 of the Ten Feet seam. Tremors are located W-SW of the active panels in (a) the Ten Feet seam. Major faults at the surface are also shown. Ten Feet seam workings are also shown together with previous adjacent workings in (b) The Holly Lane (H.L.) and Hardmine (H.M.) seams, and (c) the Moss seam. (For legend see Fig. 9.3.1).

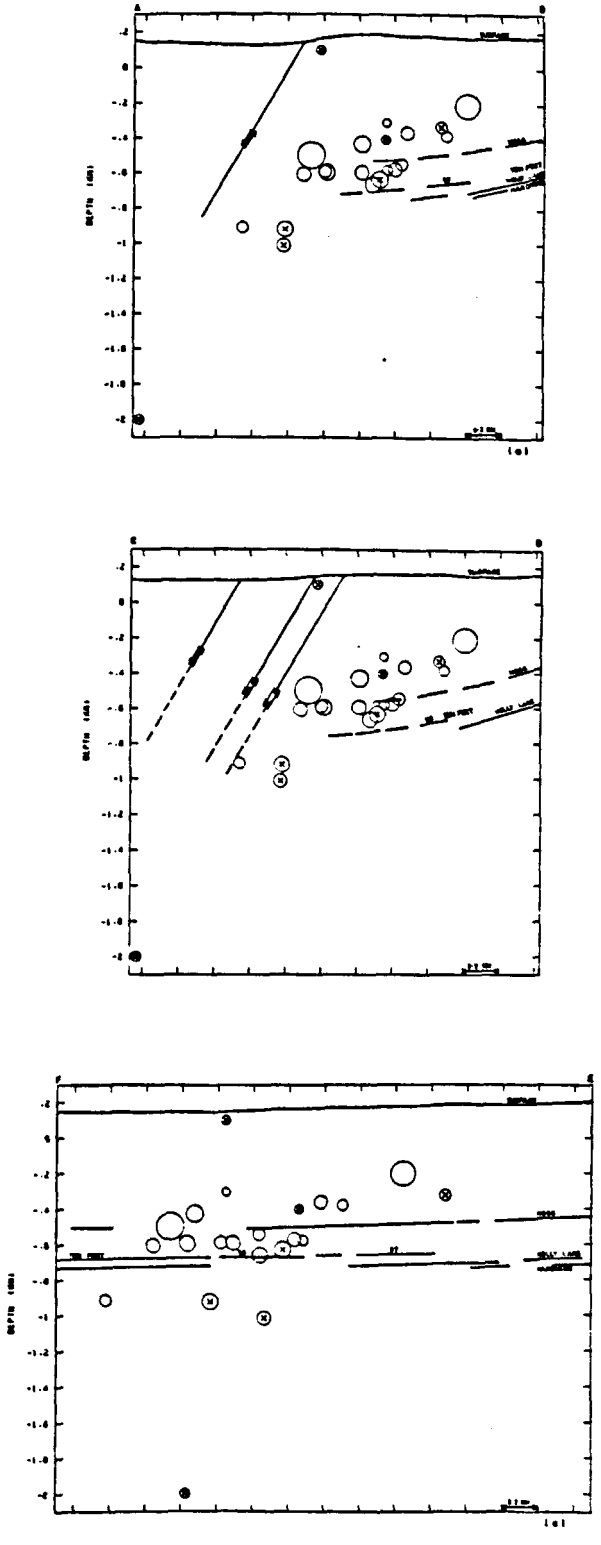

Fig. 9.6.3. Hypocentre sections (A-B, C-D, E-F, Figure 9.6.2) of tremors located in area D, showing the position of tremor hypocentres with respect to the active and old mine workings and to the major faults in the area.

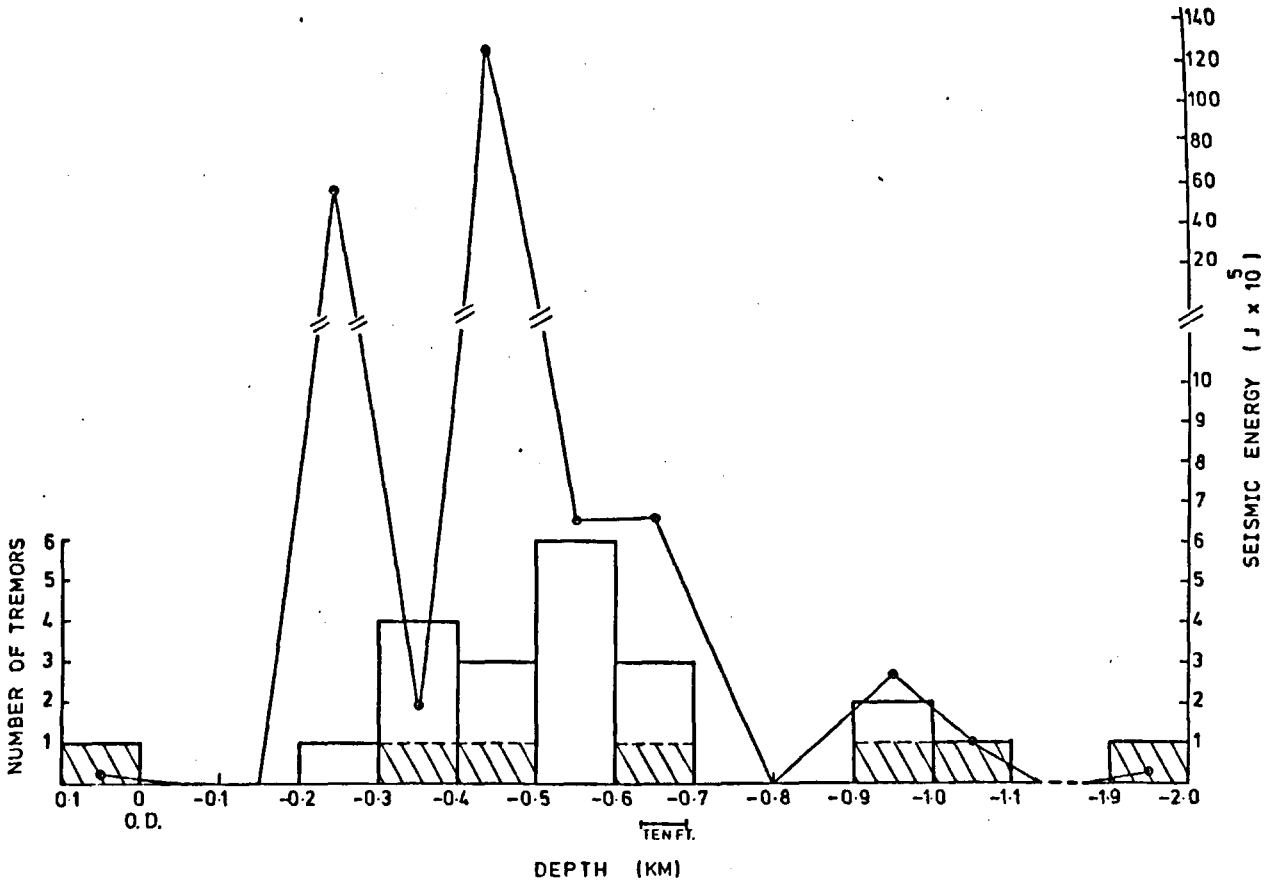

Fig. 9.6.4. A plot showing the number of tremors and the corresponding seismic energy release occurring within each 100 m depth interval in area D. The depth ranges of the active mine workings in the Ten Feet (TEN FT.) seam is also shown. The shaded area represents tremors with a shear source origin.

Figure 9.6.5. No specific relationship can be obtained, but the plot shows that most of the tremors have a local magnitude, M_L, ranging between 0.5 and 1.5. However, the figure shows that the two largest tremors are located at relatively shallow depths.

The tremor foci are plotted in Figure 9.6.6 to show their relationship with the presence of sandstone beds. Unfortunately, the borehole data for the lithological succession above the Moss seam is not available, hence definite conclusions about the relationship between the occurrence of earth tremors and the presence of sandstone strata could not be reached.

Dates of occurrence of earth tremors (Appendix 2) indicate that three tremors occurred in 1975 during the mining of panel 56 and before panel 57 was opened. The other 19 tremors occurred more than five months after panel 56 had finished production, and during the working life of panel 57. This suggests that all or most of these 19 tremors occurred as a result of the mine workings in panel 57.

Figure 9.6.7 is a plot showing the position of earth tremors with respect to the position of the working face of panel 57 at the time of occurrence. Figure 9.6.7a is a plan view, while Figure 9.6.7b gives a vertical section. The figure shows that nearly all the tremors are located behind the face, forming more or less a line running at about 40° SW of the face and lying predominately at the face level. Some of the tremors are located more than 1800 m behind the face. However, the location resolution is insufficient to confirm this. The figure also shows that the largest tremor occurred a few metres behind the face at a height of less than 450 m above the face level. This may explain why there were no reports of rock bursts in the mine.

The position of the tremor epicentres and the position of the working face of panel 57 as it advanced along the panel is shown in Figure 9.6.8. The positions of the old mine workings in the other adjacent seams

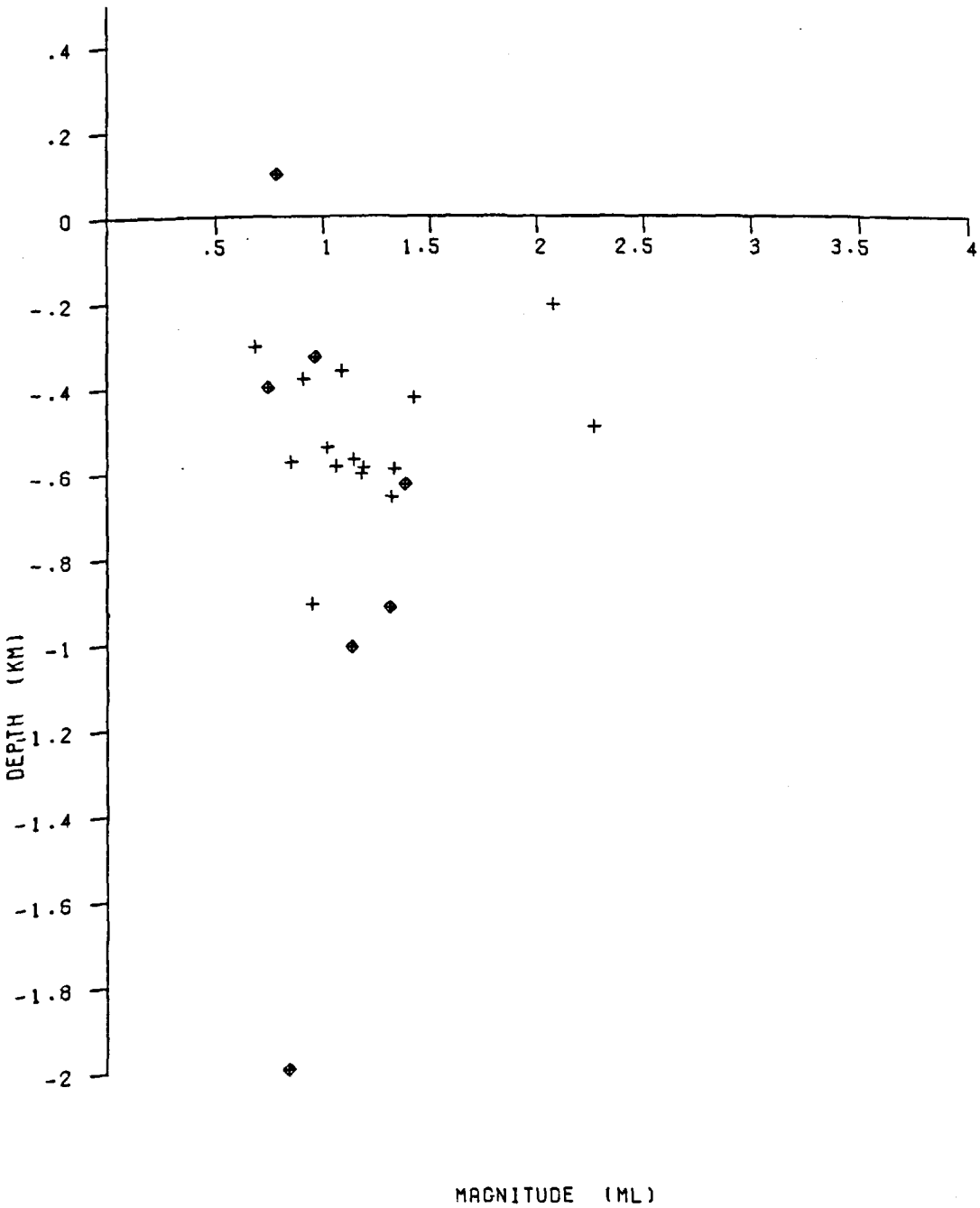

Figure 9.6.5. Plot of tremor depth against local magnitude, M_L, for tremors occurring in area D.

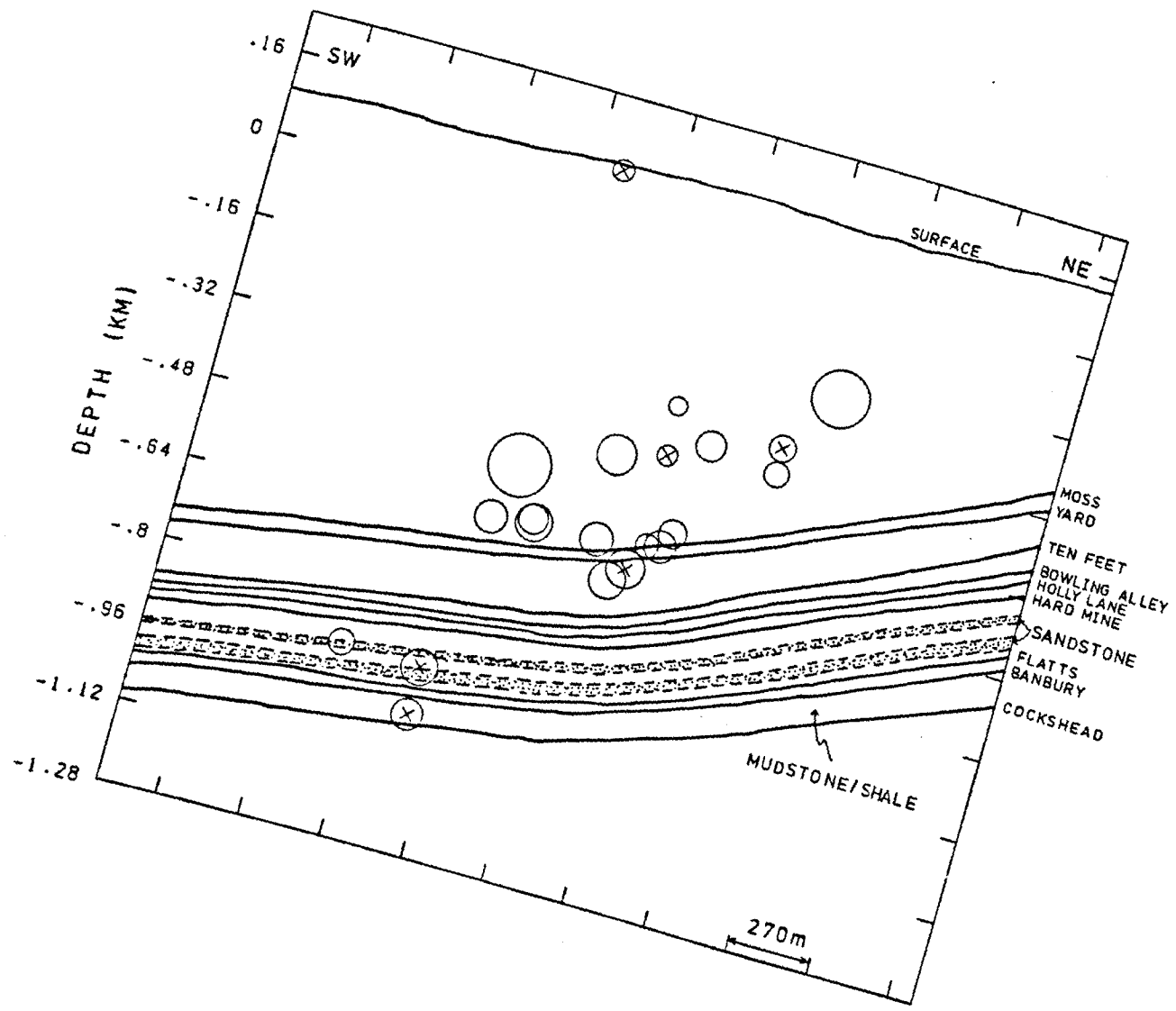

Fig. 9.6.6. Geological section drawn downdip showing the positions of tremor foci for tremors occurring in area D.

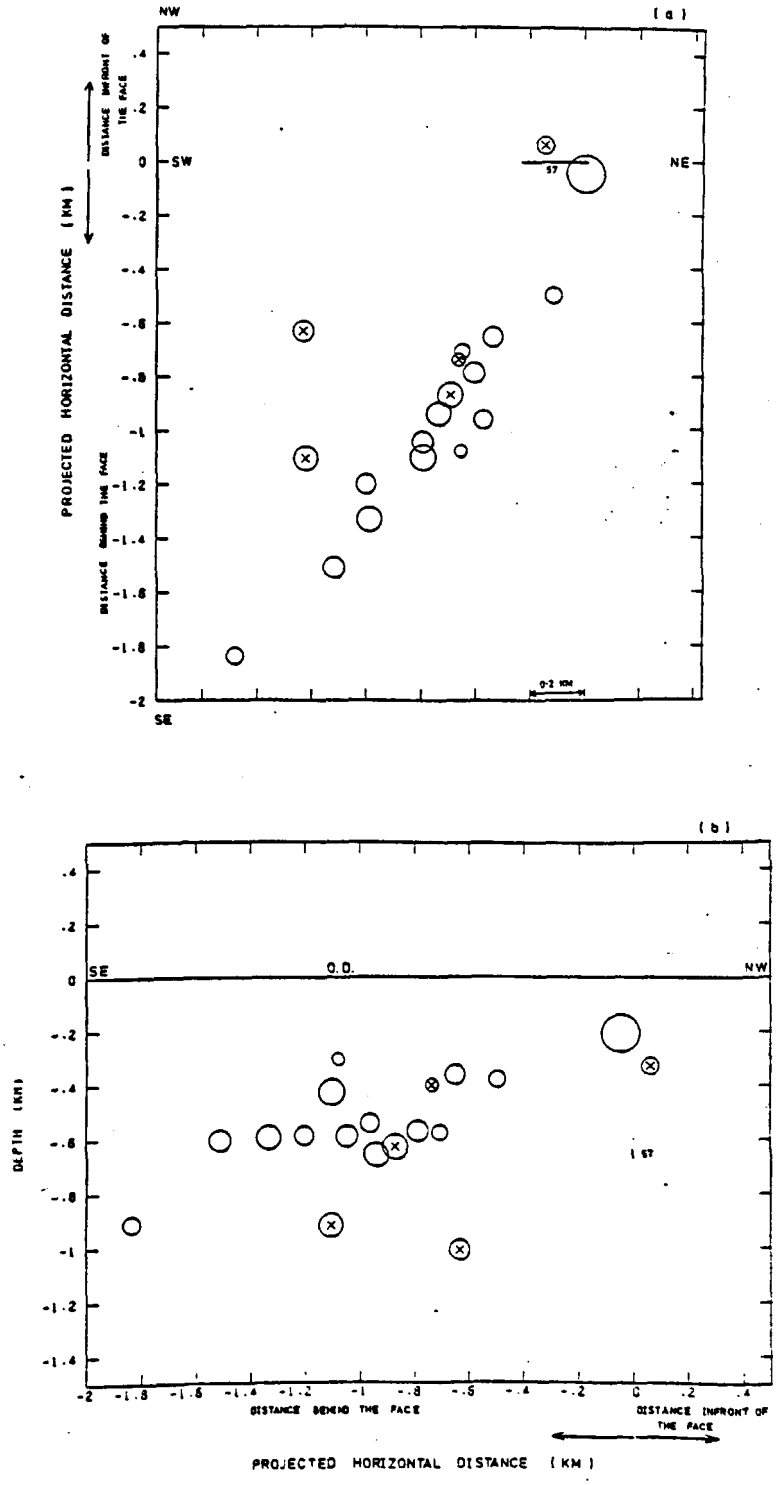

Figure 9.6.7. Plots showing the positions of tremor hypocentres with respect to the position of the working face, at the time of occurrence, for tremors occurring during the mining of panel 57 in area D.

(a) Plan view.
(b) Vertical section perpendicular to the coal face.

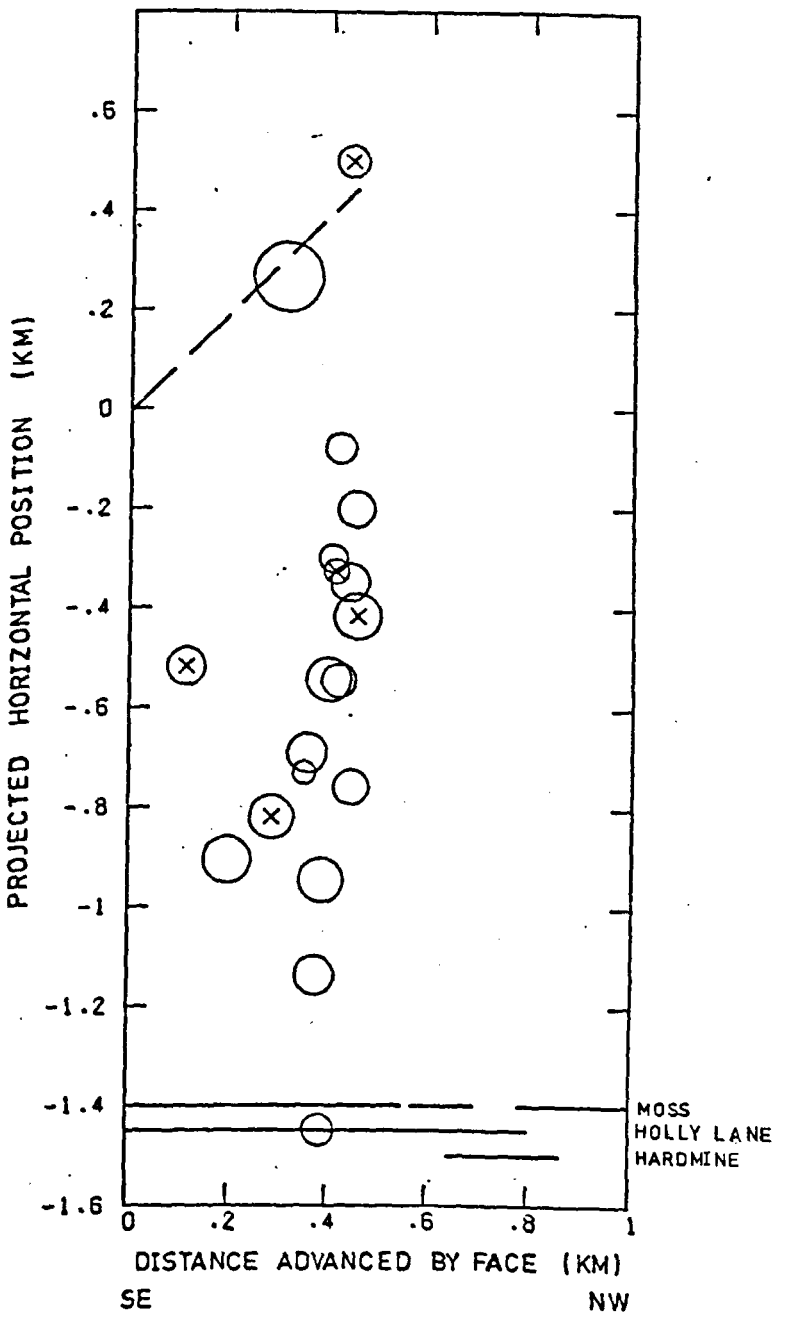

Fig. 9.6.8. Plot of the horizontal position of tremor epicentres projected onto the line of face advance and measured from the start of the panel, against distance advanced by the face for tremors occurring during the mining of panel 57 in area D. The diagonal dashed line corresponds to the line on which tremors would plot if they occurred on the face 57. The regions where the face 57 lies below previous Moss or above Holly Lane and Hardmine seam workings are also shown.

are also shown. The plot shows that the tremors may have advanced with the face. The seismic activity did not start until the face had moved a distance of about 290 m. Before this distance only two tremors occurred. These two tremors most probably occurred due to the mining of panel 56, or they could have occurred in the southern pillar left between face 57 and an old panel (see Figure 9.6.1a). After this distance of face advance, the seismic activity suddenly increased. This situation is clearly evident when tremor size, M_L, and the energy release are plotted against the advancing face (Figure 9.6.9). The figure shows that when the face had moved a distance of 290 m, a small tremor occurred. When the face advanced 21 m further (at a distance of 311 m from the start) the largest tremor during the mining of this panel occurred and had a local magnitude, M_L, of approximately 2.1. After the occurrence of this tremor the face advanced a distance of about 39 m (350 m from the start) without the occurrence of a single tremor. Then the tremors became more frequent but generally smaller in size.

The depth of the tremor foci as the face advanced along the panel is shown in Figure 9.6.10. The depths of the active and old workings are also shown. The figure shows that most of the tremors lie at an average height of about 50 m above the panel level (approximately at an average depth of about 615 m below O.D.). A few tremors occurred at a higher level (approximately at an average depth of about 330 m below O.D.). Only three tremors occurred below the panel level.

9.6.2 Temporal distribution of tremors and seismic energy release

The maximum number of tremors occurred during 1977. This coincides with the extraction of panel 57 which started production in September 1976.

The distribution of the seismic events and the corresponding total amount of energy release throughout the week and throughout the day are shown in Figure 9.6.11. The figure demonstrates a very close relationship

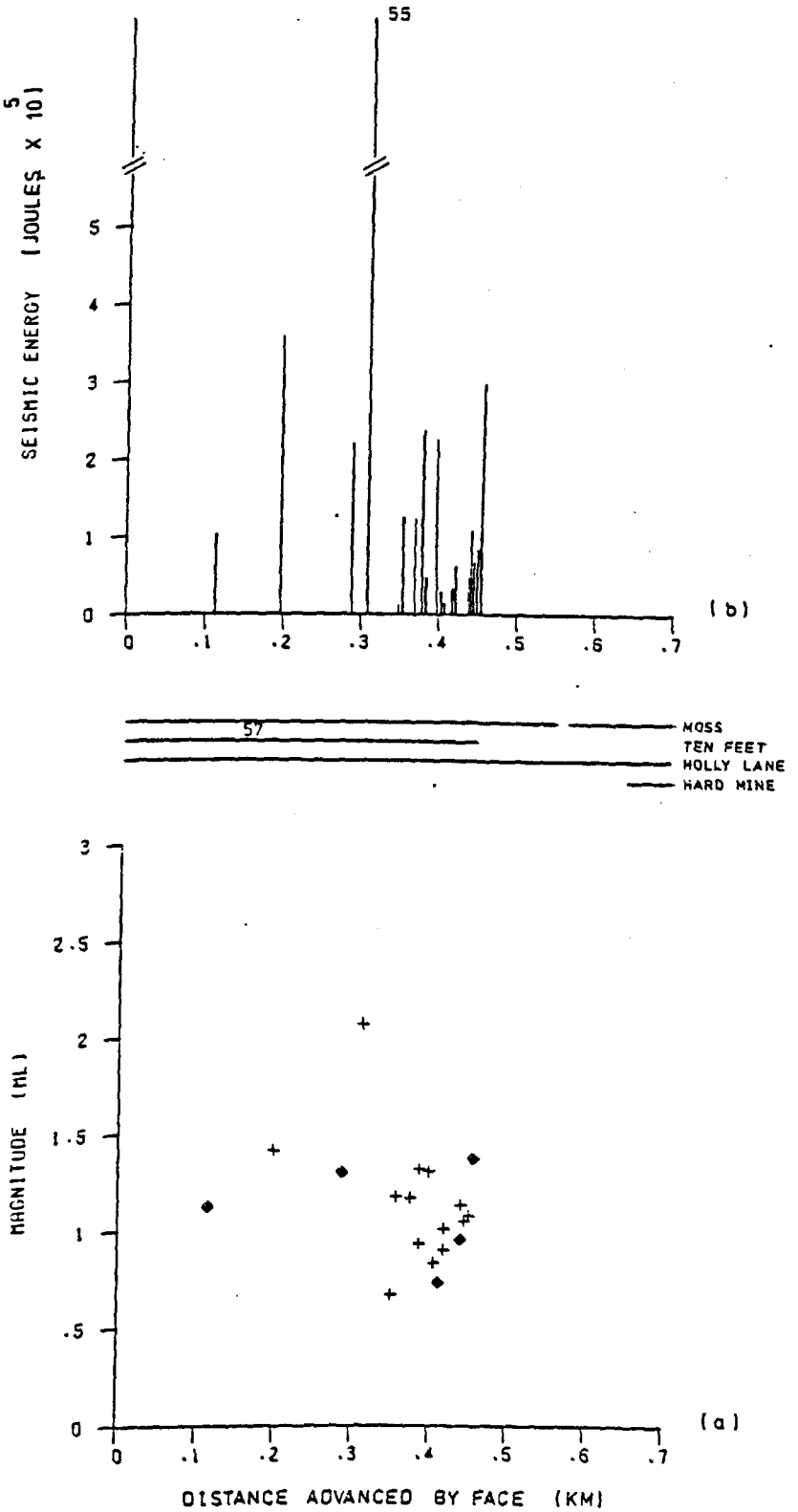

Fig. 9.6.9. Plots of (a) tremor magnitude, M_L, and (b) seismic energy release, against the distance advanced by the face for tremors occurring during the mining of panel 57 in area D. The regions where the panel face lies below or above previous workings in the Moss, Holly Lane and Hard Mine seams are also shown.

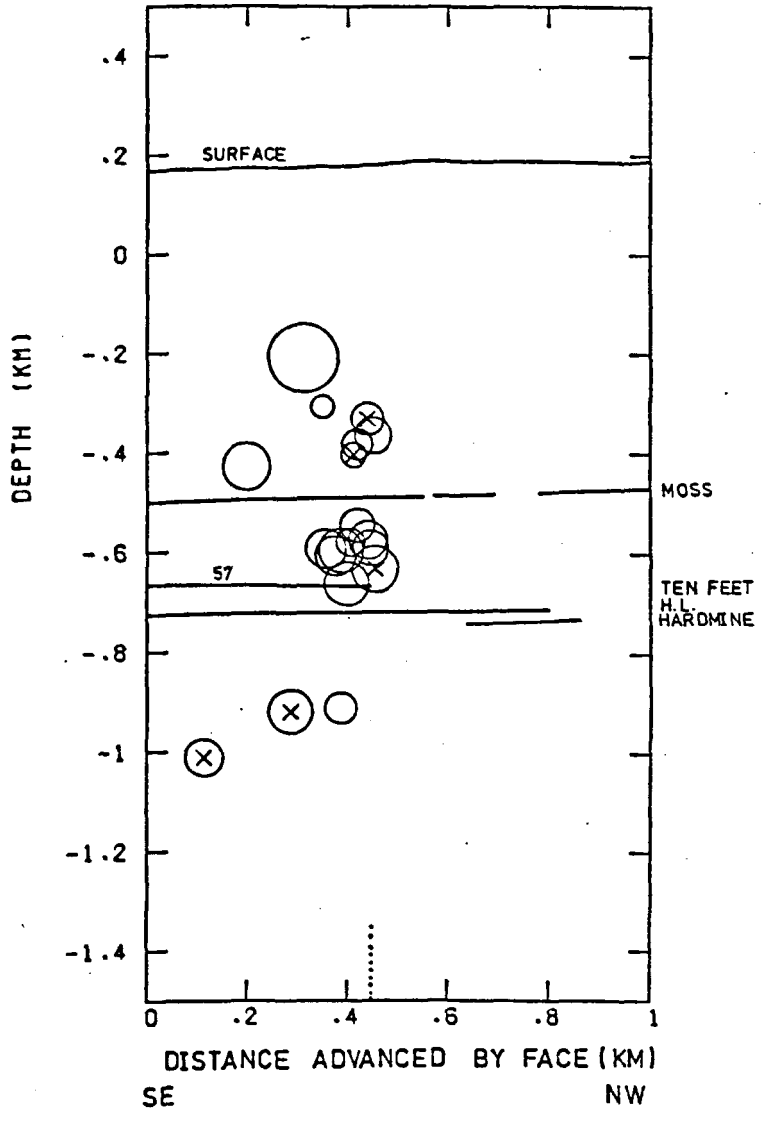

Figure 9.6.10. Plot of tremor depth against the distance advanced by the face for tremors occurring during the mining of panel 57 in area D. The position of mine workings in panel 57 of the Ten Feet seam and previous workings in the Moss, Holly Lane (H.L.) and Hard mine seams are also shown.

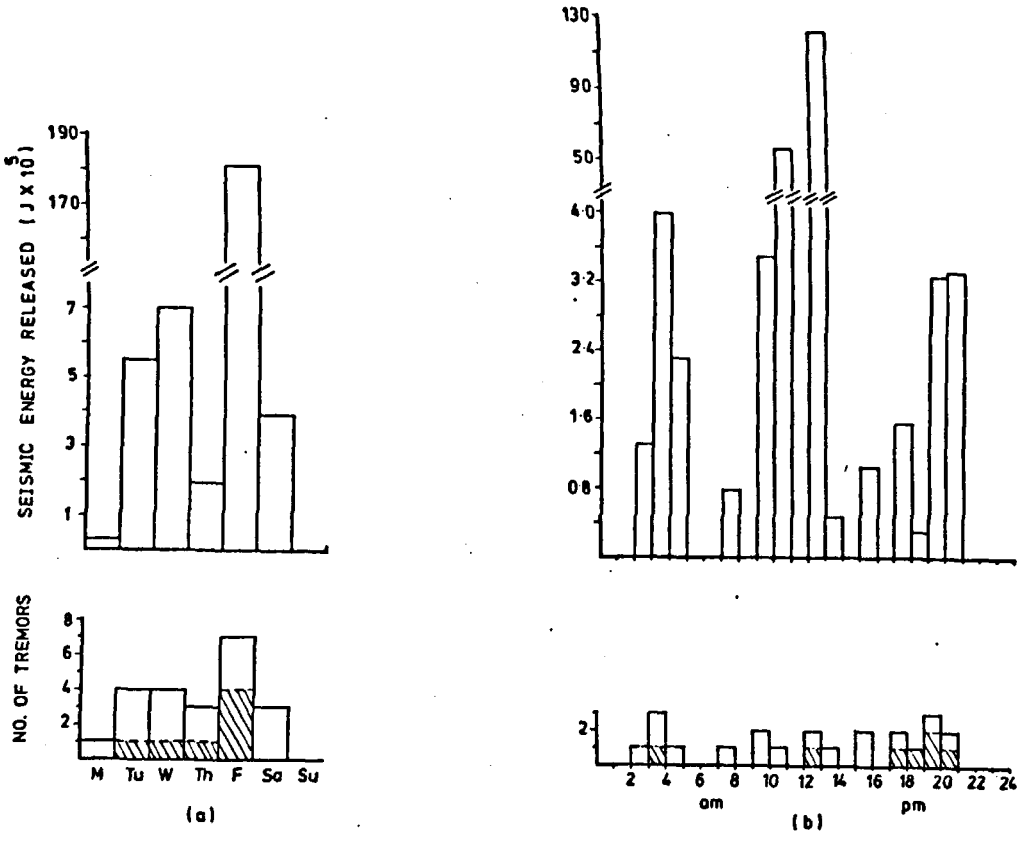

Fig. 9.6.11. Histograms showing (a) the weekly and (b) the daily distribution of tremors and the corresponding seismic energy release for tremors which occurred in area D. *The shaded area represents tremors with* a shear source mechanism.

between the times of the mining activities and the occurrence of the earth tremors.

9.6.3 First motion analysis of seismic data

First motions analysis has shown that only seven events had a shear source mechanism, while the other 15 tremors probably had implosional/collapse source mechanisms. Some of these 15 tremors might have a shear source origin, but the poor distribution of the seismic stations in both azimuth and epicentral distances with respect to this area, made the precise determination of the mechanism of some tremors impossible. It is not surprising to find that most of the tremors in this area had a collapse source mechanism since the roof condition of panel 57 was very bad. Examination of the mining reports (the deputy's reports) during the mining of panel 57 showed that there were many roof breaks and roof falls during the mining.

A composite fault-plane solution using the data from three shear tremors was obtained (Figure 9.6.12A). The other shear events did not fit this solution. The fault-plane solutions for these other four events are shown in Figures 9.6.13B, C, D and E. The different fault-plane solutions suggest that the tremors occurred on a number of dip-slip planes striking in different orientations. It is difficult to decide which of the nodal planes represent the fault plane, but it is assumed that the nodal planes striking to the NW represent the fault planes since they agree with the general trend of the surface faults and the numerous small faults encountered at the seam level. Two tremors (Figures 9.6.12B and C) show reverse fault-plane solutions. This could be due to errors in observation, or they could represent shear movements, which occurred in the roof of the goaf along the bedding planes due to the effect of roof bed sagging (as discussed for Area A). Alternatively, they could represent movements along pre-existing reverse faults.

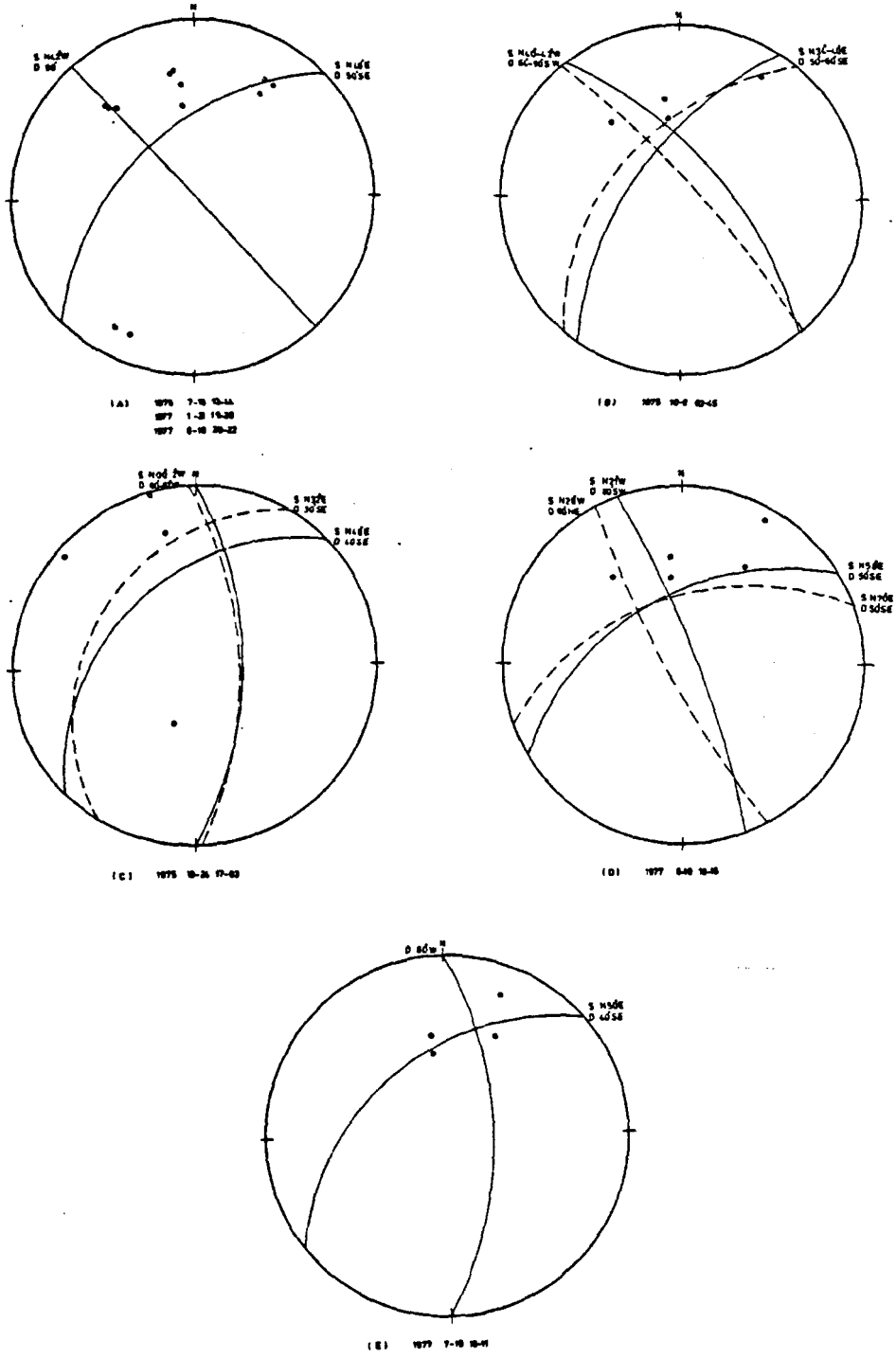

Fig. 9.6.12. Upper hemisphere fault-plane solutions for tremors which occurred in area D. Dashed lines represent alternative solutions. In (A) a composite fault-plane solution was obtained from three tremors. In (D) the fault-plane solution can be interpreted as representing movements by either normal or reverse faulting. (For legend see Fig. 9.3.12).

9.6.4 b-value

The frequency-magnitude relationship in this area follows the formula:

$$\log_{10} N = 2.92 - 1.64 M_L \qquad 9.6.1$$

This formula was obtained graphically from the frequency-magnitude plot in Figure 9.6.13. There is a linear relationship between logN and M_L in the magnitude range between 1.1 and 1.6. The tremors having a magnitude greater than 1.6 do not fit this linear relationship. This is most probably due to insufficient data, but it could be due to a sudden change in the state of the applied stress in the area (as discussed for Area A).

The b-value in this area is the highest value encountered in the coalfield. This may suggest that the external applied stress in this area is lower than the other areas (see Sections 7.4 and 9.5.4). It may also suggest that the rocks in this area are less homogeneous than the other areas. This could cause the stress to concentrate locally, in contrast to uniform distribution of the stress, resulting in frequent rock breaks producing small tremors (since the tremor size depends not only on the value of stress but also on the volume of rocks that fall). The deputy's mining reports for panel 57 indicated that the roof condition was very bad and that a lot of coal and dirt fell from the panel roof. This may indicate that the rocks were heterogeneous and could not withstand high stress, consequently breaking and falling more often, so releasing small amounts of energy which appeared as small tremors.

9.6.5 Earth tremor generation mechanisms

The spatial and temporal distributions of the tremors indicate that 19 tremors occurred due to the mining of panel 57, while three tremors occurred as a result of mining panel 56. It is not surprising to see that panel 57 generated a large number of tremors. Figures 9.6.1 and 9.6.3a show

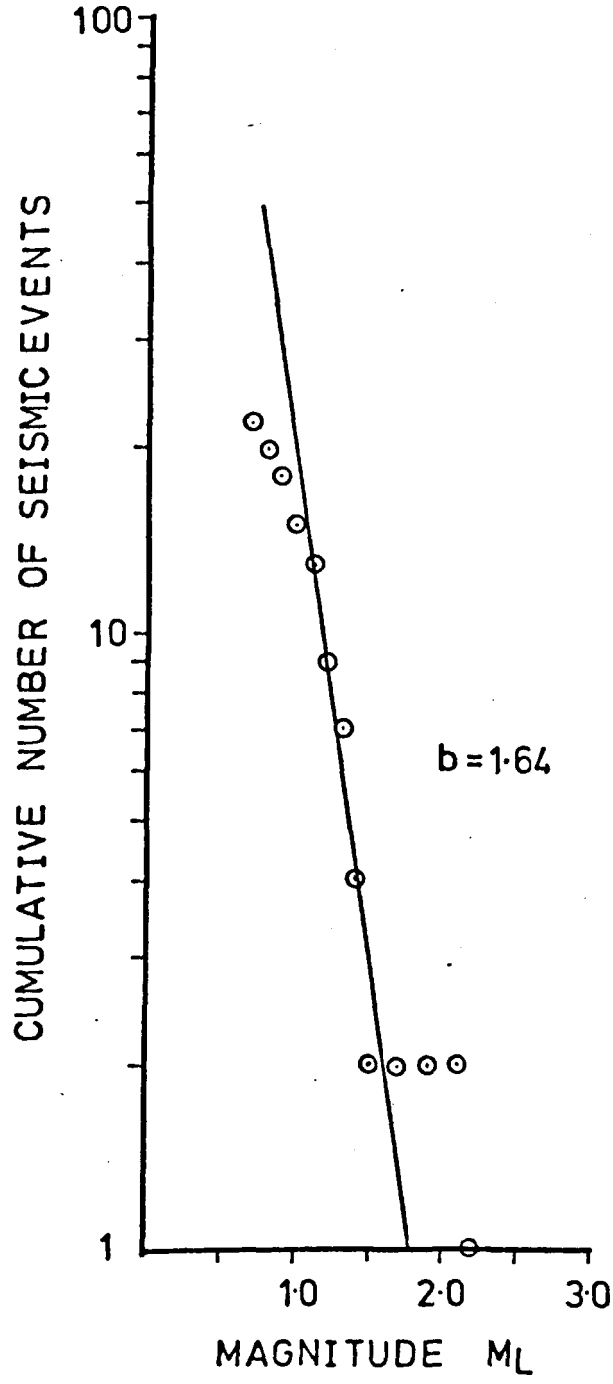

Fig. 9.6.13. A plot showing the frequency-magnitude distribution for tremors occurring in area D.

that panel 57 advanced below a long coal pillar having a width of approximately 80 m left in the Moss seam at a height of about 165 m above panel 57. This pillar is in a rectangular form bounded on three sides by mined out areas (a peninsula abutment). At the same time the panel face advanced over a much wider coal pillar of about 120 m width left in the Holly Lane seam at a depth of approximately 61 m below the panel. This pillar narrows in its northern part. This is because to the east side of the pillar, the Holly Lane seam was worked by the room and pillar method forming an irregular shaped mined out area. The Holly Lane pillar is bounded on its eastern side by deeper workings in the Hardmine seam at a depth of about 84 m below the Ten Feet level (i.e. 22 m below the Holly Lane level). These two pillars over and under the path that the face of panel 57 passed, resulted in the panel face advancing in a very stressed region due to the concentration of the overburden strata pressure on these two pillars. This situation is illustrated diagrammatically in Figures 9.6.14 and 9.6.15. As the face advanced some distance along the panel, say to point A in Figure 9.6.15, a high pressure zone was developed in the solid a few metres ahead of the face (front abutment pressure). The front abutment pressure was superimposed on the pillar abutments and a very high pressure zone developed in front of the face, particularly at the corners formed by the intersection of the vertical plane of the face and the sides of the pillars. As a result of this, the rocks ahead of the face, particularly at the corners of the pillars, stored a large amount of strain energy, while small amounts of energy dissipated non-violently. At this stage the coal strength was still higher than the pressure strength, hence the coal did not fail. As the face advanced further, the stress distribution in the solid abutment changed by virtue of mining and anisotropy of the rocks. At a point, say B, where the three maximum pressures interact constructively, a condition arose where the stress exceeded that which the rocks could withstand.

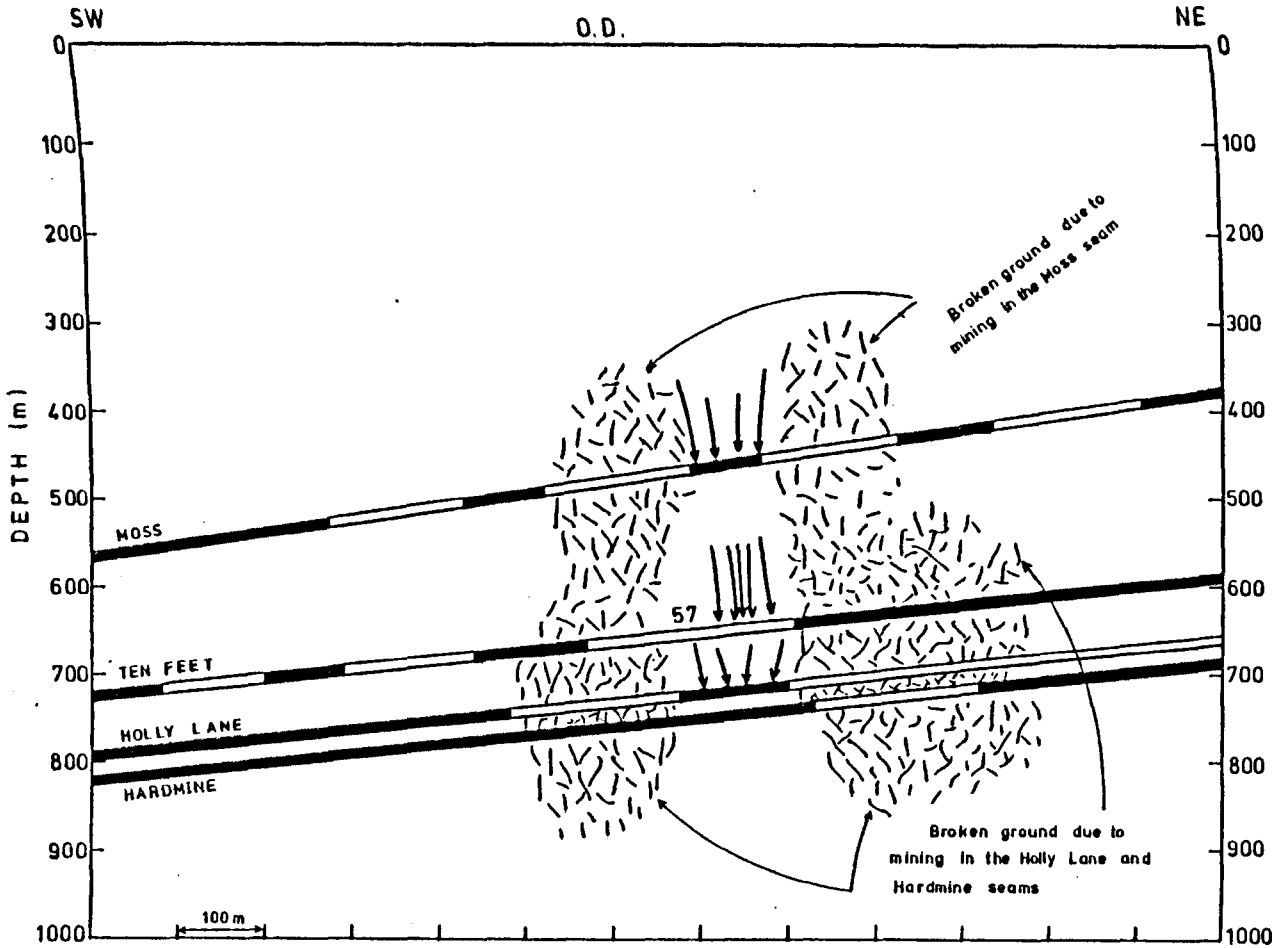

Fig. 9.6.14. Diagrammatic section parallel to face 57 of the Ten Feet seam in area D showing the distribution of stresses around the panel face due to the presence of pillars in previous mine workings above and below the panel, in the Moss, Holly Lane and Hard mine seams. The stress is concentrated on pillars while the broken ground above and below the extracted region is de-stressed.

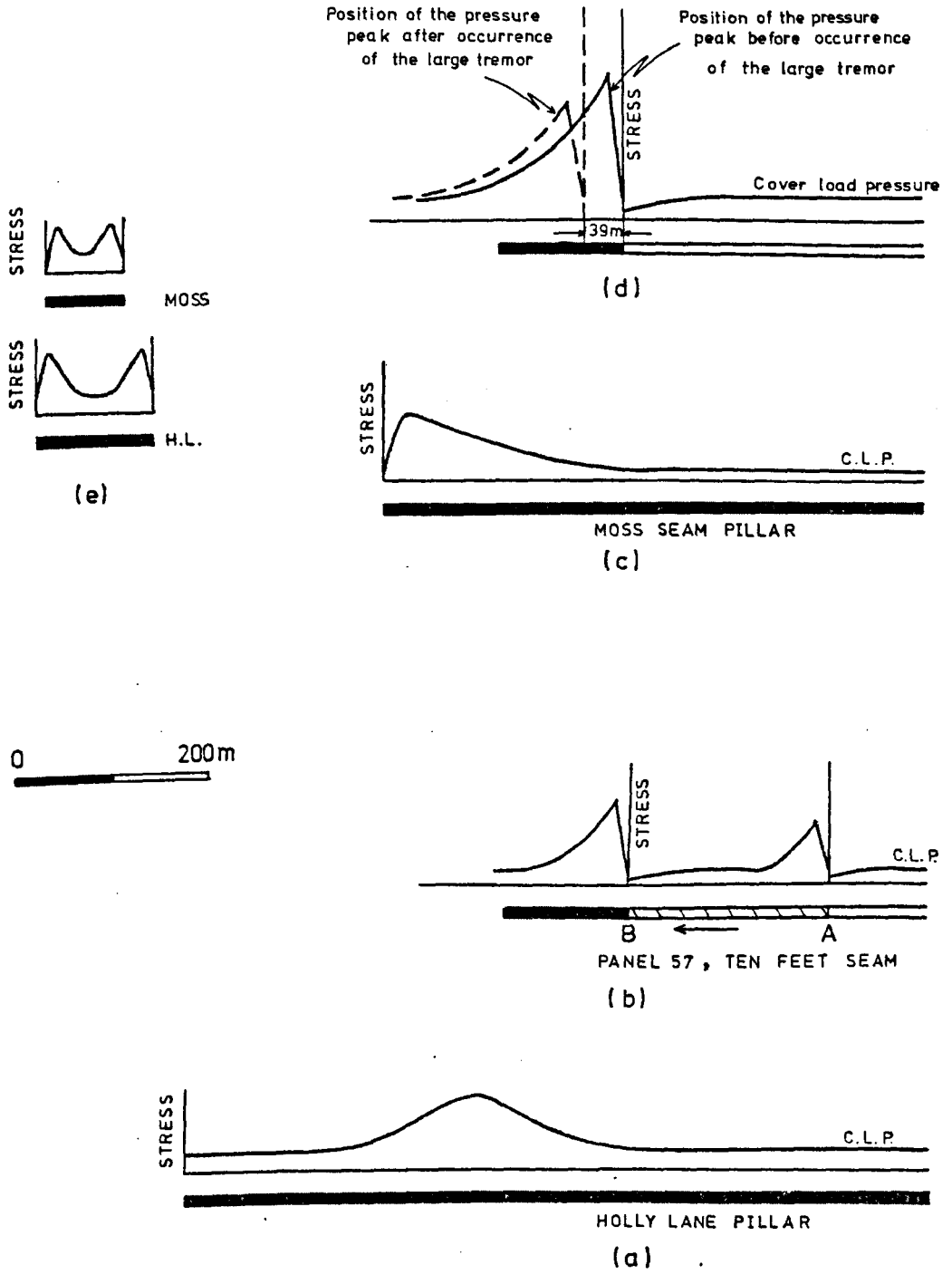

Fig. 9.6.15. Diagrams illustrating the distribution of strata pressure along (a) the Holly Lane seam pillar, (b) panel 57 of the Ten Feet seam, (c) the Moss seam pillar, (d) the resultant stress due to adding constructively the maximum stresses in diagrams a, b and c, and (e) across the Moss and Holly Lane (H.L.) pillars. The position of the peak resultant pressure was shifted 39 m deeper inside the solid rocks as a result of the occurrence of event 1977 2-18 10-47, the largest tremor which occurred during the mining of panel 57.

Consequently, the rocks failed suddenly causing a violent release of a large amount of stored strain energy so appearing as a strong tremor. Van Proctor (1978) quoted Salamon (1976) who indicated that "there must be a stress change to trigger an event and there must be significant amounts of strain energy stored in the rock in the vicinity where the event is triggered. Clearly, seismic events are most likely to be initiated in the vicinity of moving faces".

As indicated earlier, the largest tremor occurred when the face had advanced a distance of 311 m. As a result of this large tremor the rocks fractured some distance ahead of the face and could not store large amounts of strain energy. Hence, the position of the maximum pressure shifted deeper inside the solid rocks as illustrated in Figure 9.6.15. This explains why after the occurrence of this largest tremor the panel face moved a further distance of 39 m without a single tremor occurring. As the face advanced further (beyond 350 m) it approached the end of the pillar left in the Moss seam, and at the same time approached the narrowing part of the Holly Lane pillar. This situation may have led the coal in these parts, particularly in the Moss pillar, to burst in compression (as explained by Phillips, 1944-45 in Section 3.2.1), so causing the release of small amounts of energy appearing as small tremors. If the face had advanced further than 455 m (its position at the end of August 1977) one would have expected to see the tremor frequency and their magnitude reduced significantly due to the complete destruction of the coal, particularly in the Moss pillar.

Panel 56, on the other hand, was driven immediately under a previously mined out panel in the Moss seam at a height of approximately 165 m above panel 56 level (see Figures 9.6.1c and 9.6.3b). No pillar was left in the Moss seam workings over panel 56, and no mine workings were present beneath the panel, i.e. the panel was driven in a relatively de-stressed

region. Hence it is not surprising to see that the mine workings in this panel generated only a few tremors, though one of these tremors was very large and reached a magnitude, M_L, of approximately 2.3 (the largest tremor in this area). These tremors most probably occurred some distance after the panel face had emerged from beneath the southern boundary of the mined out panel in the Moss seam, i.e. after the face had advanced a distance of about 316 m (see Figures 9.6.1c and 9.6.3c). At this point the panel face is about 200 m from another old mined out area in the same seam (Ten Feet seam) to the south of the panel. Therefore, a very large abutment pressure developed in front of panel 56 face. The front abutment pressure of the panel (dynamic abutment) and the pre-existing abutment pressure (static abutment) in the southern border of the Moss panel were superimposed, forming together a very highly stressed zone. This change in the pressure state could have occurred rapidly once the face had approached the southern end of the Moss panel. This relatively sudden change in the pressure may have led the rocks ahead of the panel face to fail suddenly causing a violent release of a large amount of strain energy which appeared as a strong tremor.

The above interpretation in both panels 56 and 57 has assumed that the earth tremors occurred in the solid rocks ahead of the panel and pillar faces. But as already discussed in Section 9.6.1, most of the tremors were located behind the face. This is assumed to be an error in location. However, some tremors may have occurred behind the face (in the goaf) as a result of roof sagging and caving, in the same way as discussed for Area A.

9.7 Area E

This area lies around Chesterton. Four coal seams were mined in this area during the seismic monitoring period from two collieries (see Table 9.1). The seams were mined using the room and pillar technique (see Chapter 6). The area was also mined previously in many other seams. Most

of the mining in this area was carried out at shallow depth. The topography in this area ranges between about 180 m and 215 m above O.D. The area is disturbed by many surface faults as shown in Figures 8.3.1 and 9.7.1. The seams dip at angles ranging between 15° to more than 40° SE at the eastern flank of the Staffordshire anticline. The four active seams are:

(i) The Cannel Row seam: A small area of about 0.025 km^2 was mined in this seam from the New High Carr colliery at depths ranging between 60 m and 137 m above O.D. as shown in Table 9.1. The active workings are bounded to the south by workings from the first half of this century, as shown in Figure 9.7.1a. The roofs in these old workings have caved in. The workings in this seam during the monitoring period consisted of the driving of roadways only, leaving large pillars between them. These pillars were not extracted for technical reasons. No supports (barrels) were left in these workings since there was no extensive extraction. The workings stopped in downdip due to the reaching of the water table. The thickness of the seam is about 1 m. A general geological section through the coal seam (Figure 9.7.1a) shows that cannel (light bituminous coal) and ironstone form the roof while the floor is composed of fireclay. The active workings are overlain by previous workings in many seams at different heights above the Cannel Row seam. No working is present under the active workings. The active workings are bounded on the NE side by a fault at the seam level dipping to the SW.

(ii) The Winghay seam: The coal from this seam was mined in 1975 and 1976 from two collieries in the area; the New High Carr colliery and the Wedgwood colliery. The workings from the New High Carr colliery were carried out at depths rangingbetween about 60 m and 100 m above O.D., and consisted of the driving of a few roadways only without pillar extraction as shown in Figure 9.7.1b. However, the workings in this seam from the Wedgwood colliery which were carried out at depths ranging from 40 m below

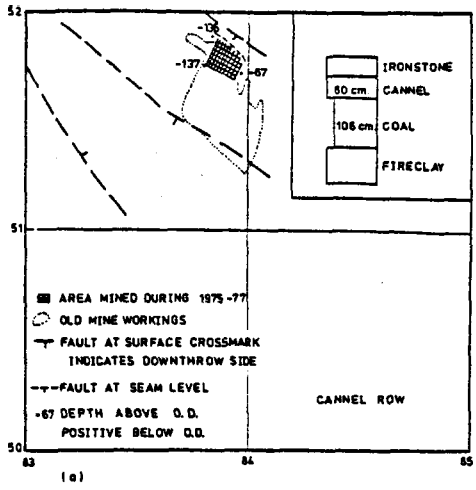

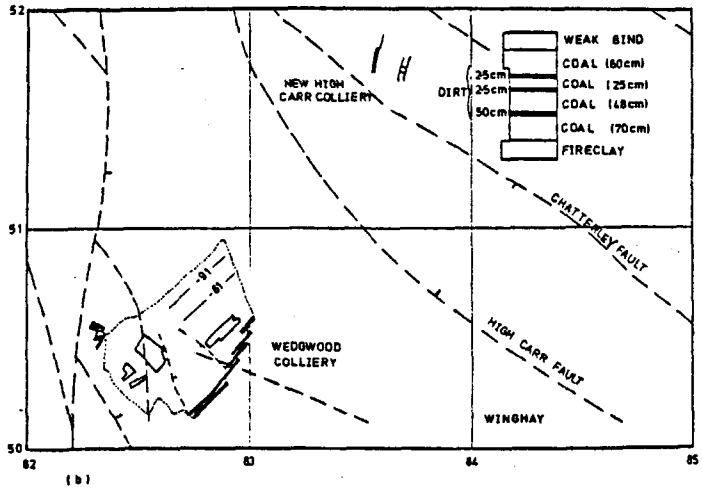

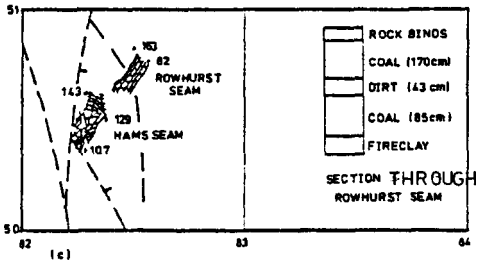

Fig. 9.7.1. The layouts of the mine workings in area E showing the active and old mine workings, faults at the surface and at the active seam level and general geological sections through the coal seams in (a) the Cannel Row seam, (b) the Winghay seam and (c) the Rowhurst and Hams seams.

O.D. to 160 m above O.D. consisted of driving roadways and pillar extraction as shown in Figure 9.7.1b. The pillars were extracted from areas having dimensions as large as 150 m x 90 m (0.01 km^2). The roof in the goaf was not allowed to cave in, instead it was supported by 45 gallon oil barrels (see Chapter 6). The active workings are surrounded by extensive workings which have been mined since the early 1960's. The seam is disturbed by numerous small faults at the seam level, mostly dipping either to the NE or to the SW. The thickness of the mined coal is about 1.5 m. A general geological section in the seam (Figure 9.7.1b) shows that the roof is composed of shale while the floor is composed of fireclay. The section also reveals that three very thin bands of dirt with a maximum thickness of 5 cm are interbedded in the coal seam. The active workings are overlain and underlain by previous workings in other seams at different distances from the Winghay seam level.

(iii) The Rowhurst seam: A very small area of less than 0.03 km^2 was mined in this seam from the Wedgwood colliery during the monitoring period at depths ranging between 80 m and 120 m above O.D. The mining started in September 1976 and consisted of the driving of roadways only without pillar extraction as shown in Figure 9.7.1c. The thickness of the worked seam is about 2.1 m. A very hard shale (Rock binds) forms the roof while the floor is soft and composed of fireclay. A general section through the seam (Figure 9.7.1c) shows that a band of dirt having a thickness of about 43 cm is interbedded within the seam. Minor faults dipping to the NE and SW were found at the seam level. The active workings are overlain and underlain by previous workings in other seams at different distances from the Rowhurst seam level.

(iv) The Hams seam: A small area of about 0.03 km^2 was mined in this seam during the monitoring period from the Wedgwood colliery at a depth of about 100 m to 158 m above O.D. as shown in Table 9.1 and

Figure 9.7.1c. The thickness of the worked coal is about 1.5 m. The roof of the active workings consists mainly of mudstone and silty-mudstone, while the floor consists mostly of mudstone and sandstone, or mudstone and siltstone. The seam is disturbed by numerous small faults at the seam level, dipping mostly to the east and south-east.

9.7.1 Spatial distribution of tremor hypocentres

Thirteen tremors (13% of the total) occurred in this area. These tremors are plotted in Figure 9.7.2 to show their relationship with the mine workings and structural geology. The tremors are located near the active mine workings but they do not concentrate over or under any specific active mining area. Instead the tremors are scattered over a large area and one tremor is located outside the boundary of the map in figure 9.7.2. Most of the tremors can be seen to be located between the major faults in the area, in particular between the High Carr and Stoke faults. This could be coincidental or due to poor location, or it could be the faults played a role in generating these tremors. As we can see from Figure 4.2.1, the area is located outside the boundary of the seismic network and without a well known seismic velocity structure in the area it is difficult to obtain accurate location. Figure 9.7.3 gives the vertical distribution of tremor hypocentres. The figure was drawn along the profiles AB and CD of Figure 9.7.2. The depths of the active mine workings are also marked in these sections. Figure 9.7.3a shows that most of the events are concentrated adjacent to the Chatterley and Stoke faults. The tremor foci lie predominately between the depth of 700 m below O.D. and the surface, only two events were located at a deeper level.

The vertical distribution of the tremor foci, and the corresponding amount of energy release, within each 100 m depth interval, are shown in Figure 9.7.4. No prominent depth of seismic activity can be seen, however, most of the energy was released near the surface. Figure 9.7.5 is a plot

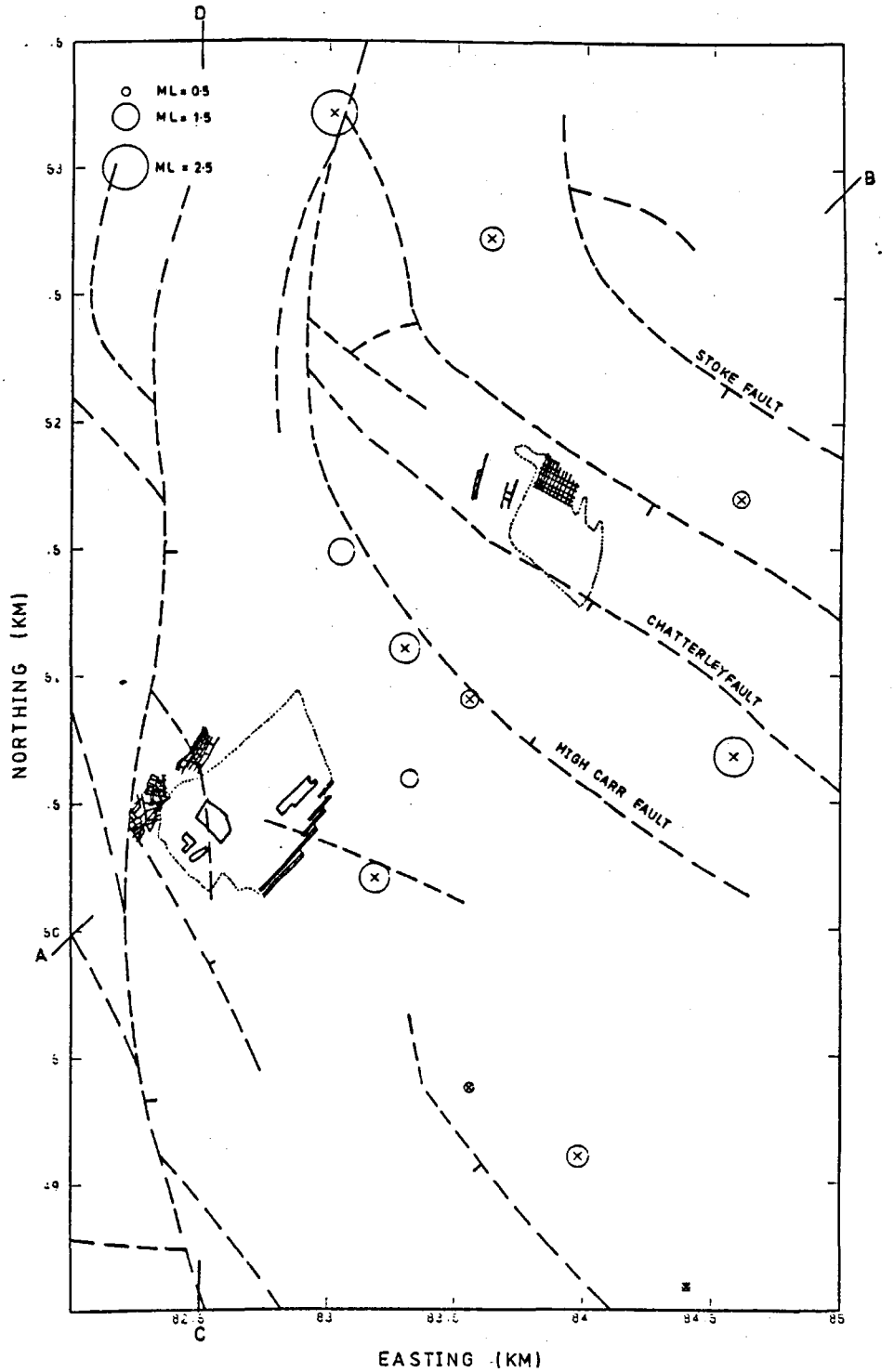

Fig. 9.7.2. Map of earth tremor epicentres for tremors which occurred in area E. Tremors are located near the active mine workings but mostly along the major surface faults. (For legend see Fig. 9.7.1).

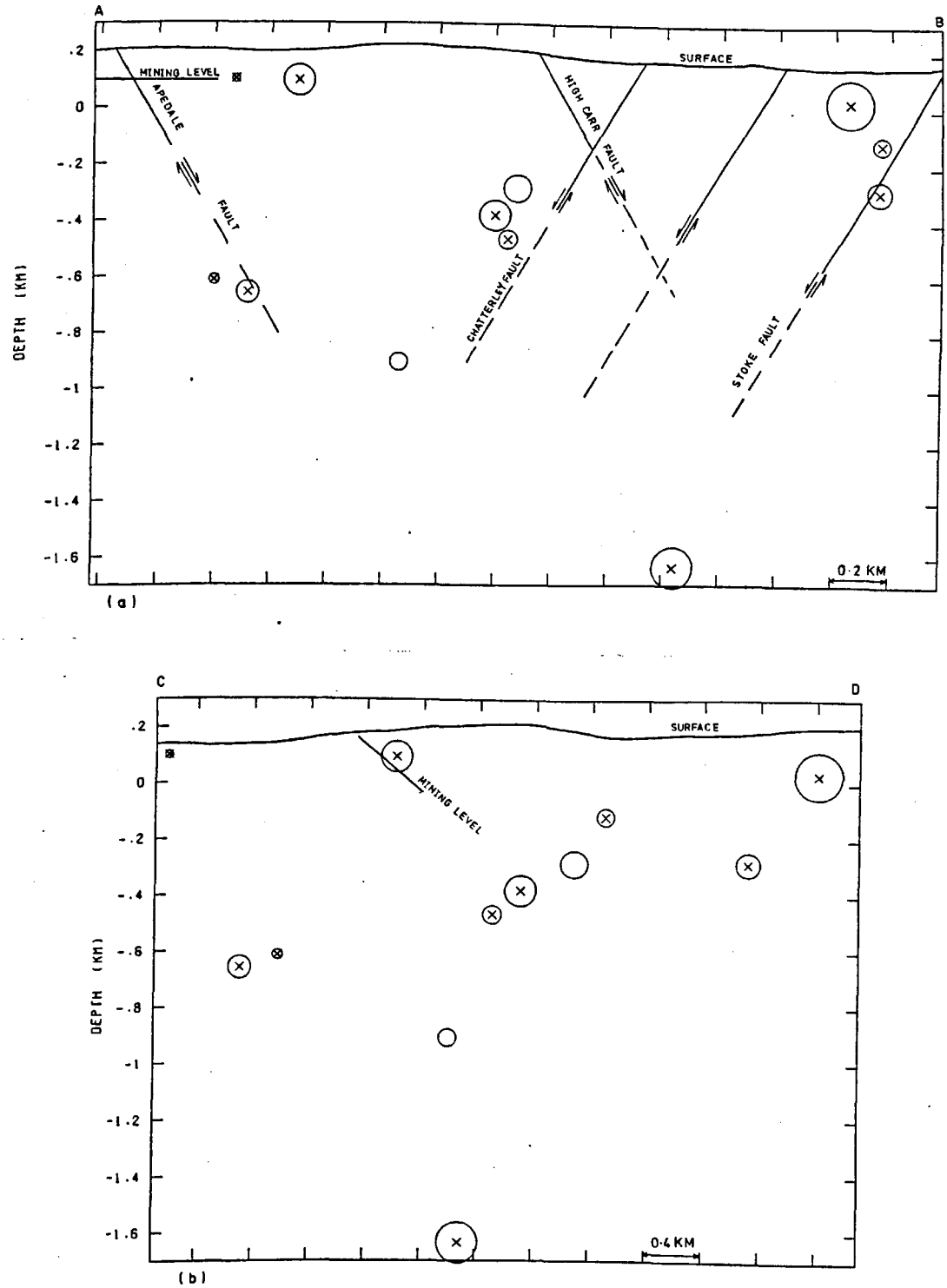

Fig. 9.7.3. Hypocentre sections (A-B, C-D, Figure 9.7.2) of tremors located in area E, showing the position of tremor hypocentres with respect to the active and old mine workings and to the major faults in the area.

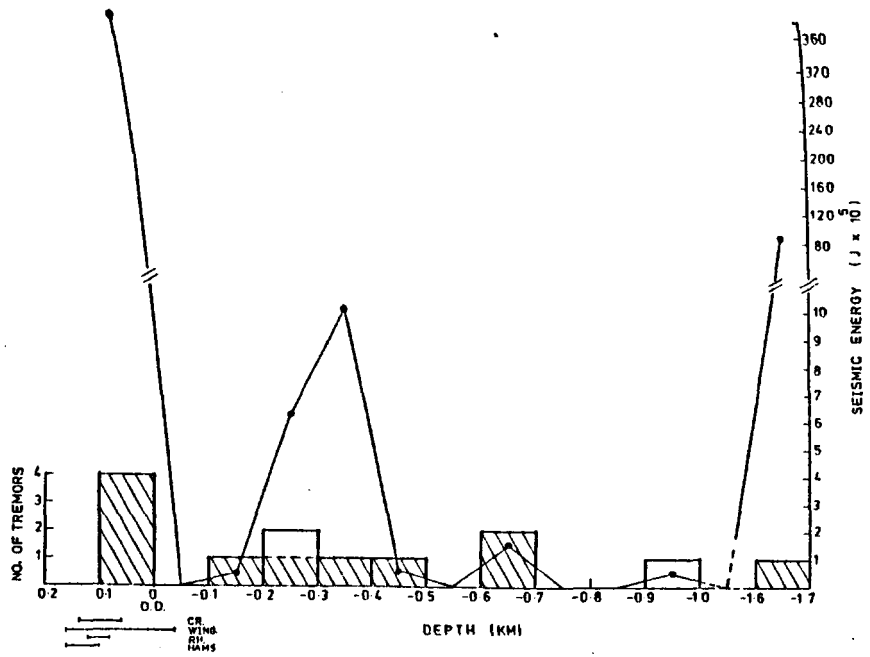

Fig. 9.7.4. A plot showing the number of tremors and the corresponding seismic energy release occurring within each 100 m depth interval in area E. The depth ranges of the active mine workings in the Cannel Row (CR), Winghay (WING), Rowhurst (RH) and Hams seams are also shown. The shaded area represents tremors with a shear source origin.

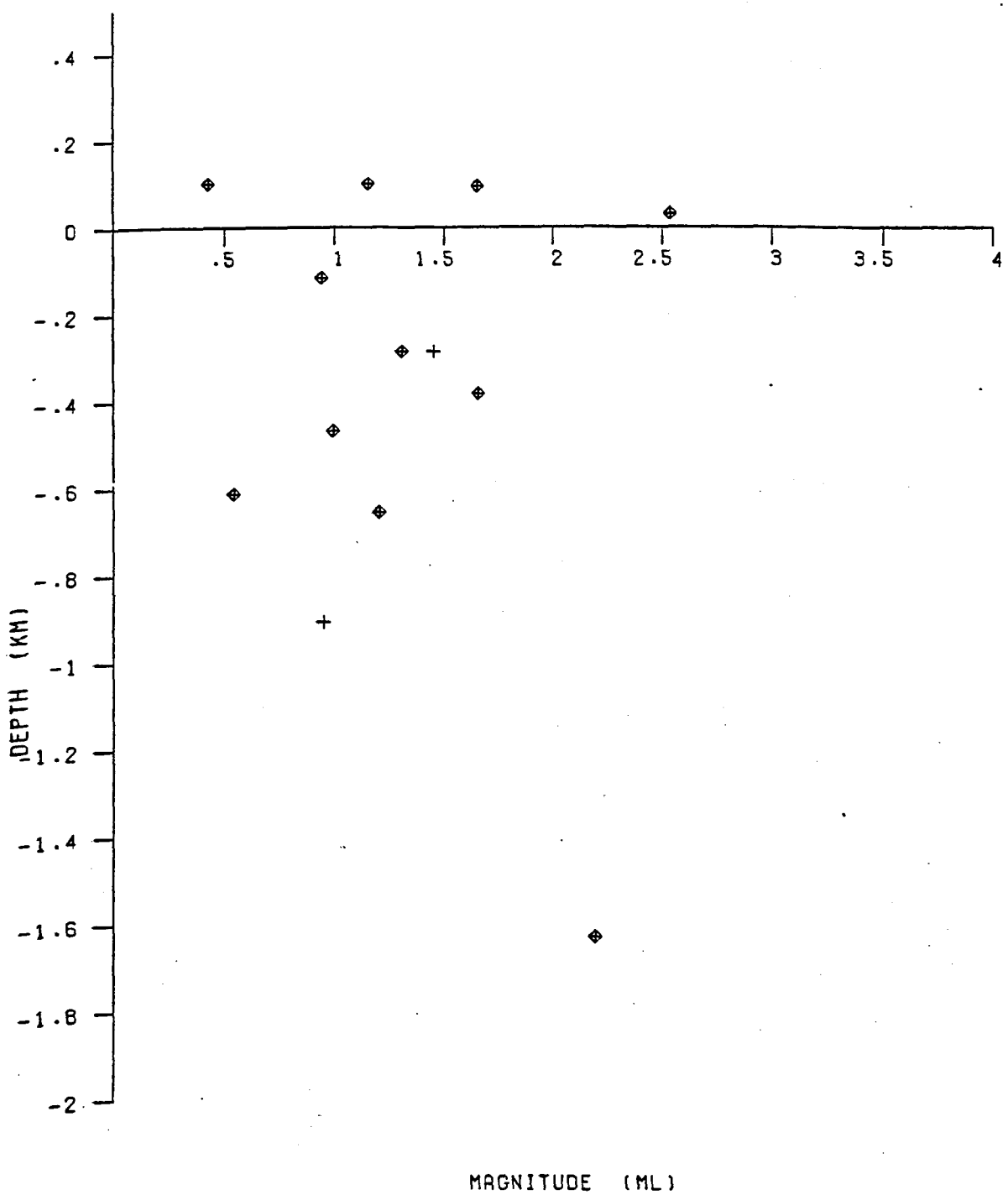

Figure 9.7.5. Plot of tremor depth against local magnitude, M_L, for tremors occurring in area E.

showing the tremor size, M_L, against the depth from O.D. No relationship between depth and tremor size has been found.

The relationship between the tremor foci location and the presence of sandstone beds in the coal measures could not be determined since there are no boreholes in this area.

9.7.2 Temporal distribution of tremors and seismic energy release

The maximum number of tremors (8) occurred in 1977, four in 1976, and only one tremor was recorded during the four months' monitoring period in 1975. Table 9.1 shows that in 1977 there was no mining activity in the Winghay seam. This may suggest that the seismic activity which occurred in 1977 was probably not associated with mining in the Winghay seam, or more probably the effect of the mining in this seam on the occurrence of earth tremors continued into 1977, one year after the mining in this seam had stopped.

The weekly distribution of the seismic events (Figure 9.7.6a(i)) does not show a clear relationship between mining and seismic activity. However, Figure 9.7.6a(ii), which gives the weekly distribution of the seismic energy release shows that the maximum amounts of energy were released on Sundays and Fridays. The occurrence of a peak on Sunday is due to the occurrence of the largest event found in this study which occurred on Sunday (see Section 8.3.2). Without this event the peak would be on a Friday. The daily distribution of the seismic events and the corresponding amounts of energy release are shown in Figure 9.7.6b. The figure shows that the peak of the energy release occurred during the second working shift, which may suggest that a relationship exists between the mine workings and the occurrence of earth tremors.

9.7.3 First motion analysis of seismic data

Analysis of the P-wave first motions has shown that 11 tremors had

showing the tremor size, M_L, against the depth from O.D. No relationship between depth and tremor size has been found.

The relationship between the tremor foci location and the presence of sandstone beds in the coal measures could not be determined since there are no boreholes in this area.

9.7.2 Temporal distribution of tremors and seismic energy release

The maximum number of tremors (8) occurred in 1977, four in 1976, and only one tremor was recorded during the four months' monitoring period in 1975. Table 9.1 shows that in 1977 there was no mining activity in the Winghay seam. This may suggest that the seismic activity which occurred in 1977 was probably not associated with mining in the Winghay seam, or more probably the effect of the mining in this seam on the occurrence of earth tremors continued into 1977, one year after the mining in this seam had stopped.

The weekly distribution of the seismic events (Figure 9.7.6a(i)) does not show a clear relationship between mining and seismic activity. However, Figure 9.7.6a(ii), which gives the weekly distribution of the seismic energy release shows that the maximum amounts of energy were released on Sundays and Fridays. The occurrence of a peak on Sunday is due to the occurrence of the largest event found in this study which occurred on Sunday (see Section 8.3.2). Without this event the peak would be on a Friday. The daily distribution of the seismic events and the corresponding amounts of energy release are shown in Figure 9.7.6b. The figure shows that the peak of the energy release occurred during the second working shift, which may suggest that a relationship exists between the mine workings and the occurrence of earth tremors.

9.7.3 First motion analysis of seismic data

Analysis of the P-wave first motions has shown that 11 tremors had

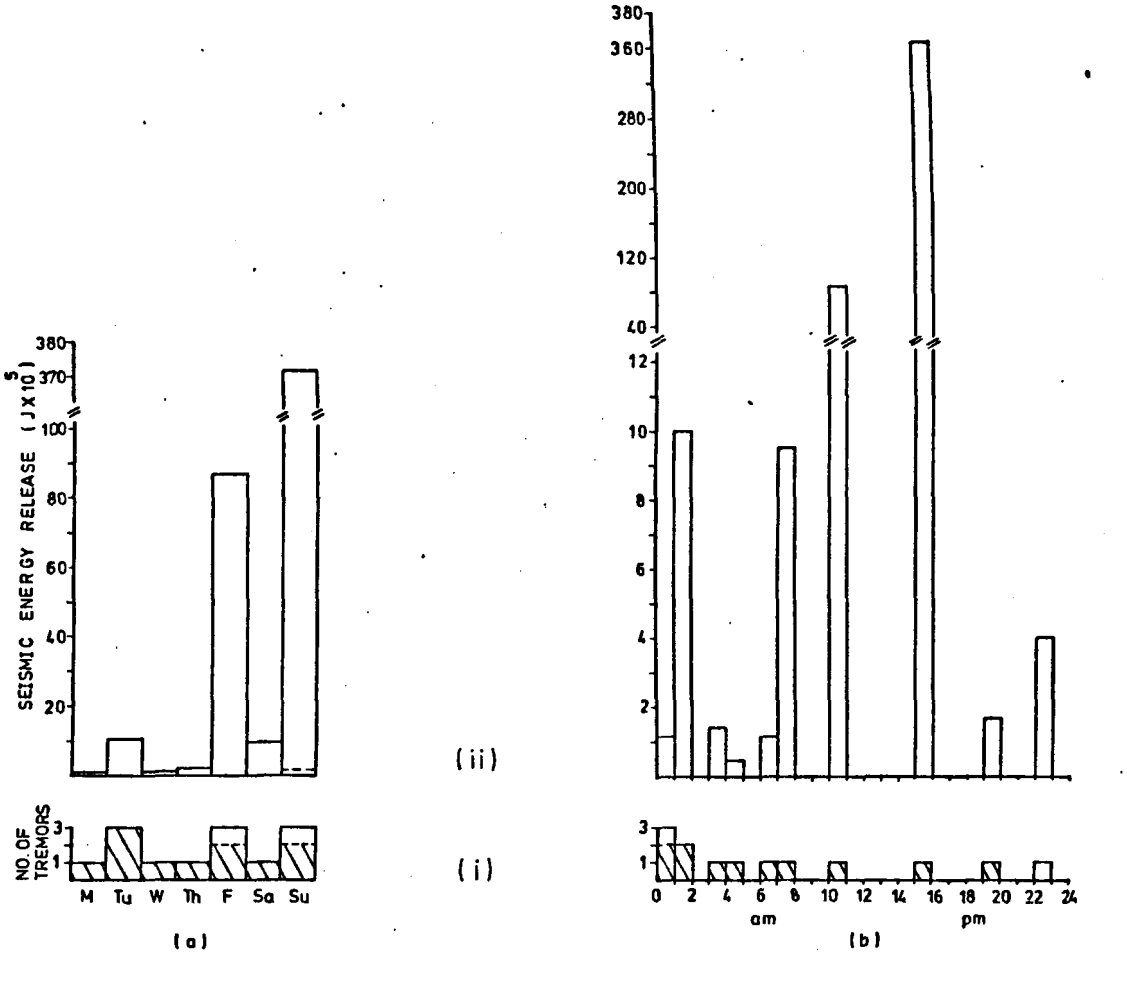

Fig. 9.7.6. Histograms showing (a) the weekly and (b) the daily distribution of tremors and the corresponding seismic energy release for tremors which occurred in area E. The shaded area represents tremors with a shear source mechanism. The dashed line in Fig.a (ii) represents the amount of energy release on Sundays if the seismic energy released by event 1976 10-31 15-47 is subtracted.

a shear source mechanism while the other two could have had an implosional/ collapse source mechanism. A composite fault-plane solution using the data from six shear events was obtained (Figure 9.7.7A). The composite focal mechanism is well determined, and the consistency of the first motions on the focal plot substantiates that the tremors share a similar mechanism. The solution indicates movements by normal faulting. The nodal plane striking N 80° W with a dip of 50° to the SW is considered to be the fault-plane since it agrees reasonably well with the N 55° W strike of the Chatterley and other parallel faults in the area (see Figure 9.7.1). The dips of these faults were estimated to be between 50° and 70° SW (N.C.B. private communication). Event 1976 9-11 07-28, however, did not fit the composite solution, but its fault-plane solution (Figure 9.7.7D) shows that it has the same nodal plane chosen as the fault-plane in the composite solution. Another composite fault-plane solution was obtained (Figure 9.7.7B) using the data from three events located on the upthrow side of a fault striking N 42° W and dipping to the SW as shown in Figure 9.7.2. The solution represents movements by normal faulting. The nodal plane striking N 34° W with a dip of 82° to the SW was consequently considered to be the fault plane. One tremor (Figure 9.7.7C) shows a reverse fault-plane solution. This could be due to error in observation, or it could represent movements along a pre-existing underground reverse fault.

9.7.4 b-value

The frequency-magnitude distribution of the tremors in this area follows the formula:

$$\log_{10} N = 1.66 - 0.7\, M_L$$

The constants in this formula were determined from Figure 9.7.8. The figure shows a linear relationship between logN and M_L in the magnitude ranges between 1.0 and 1.5.

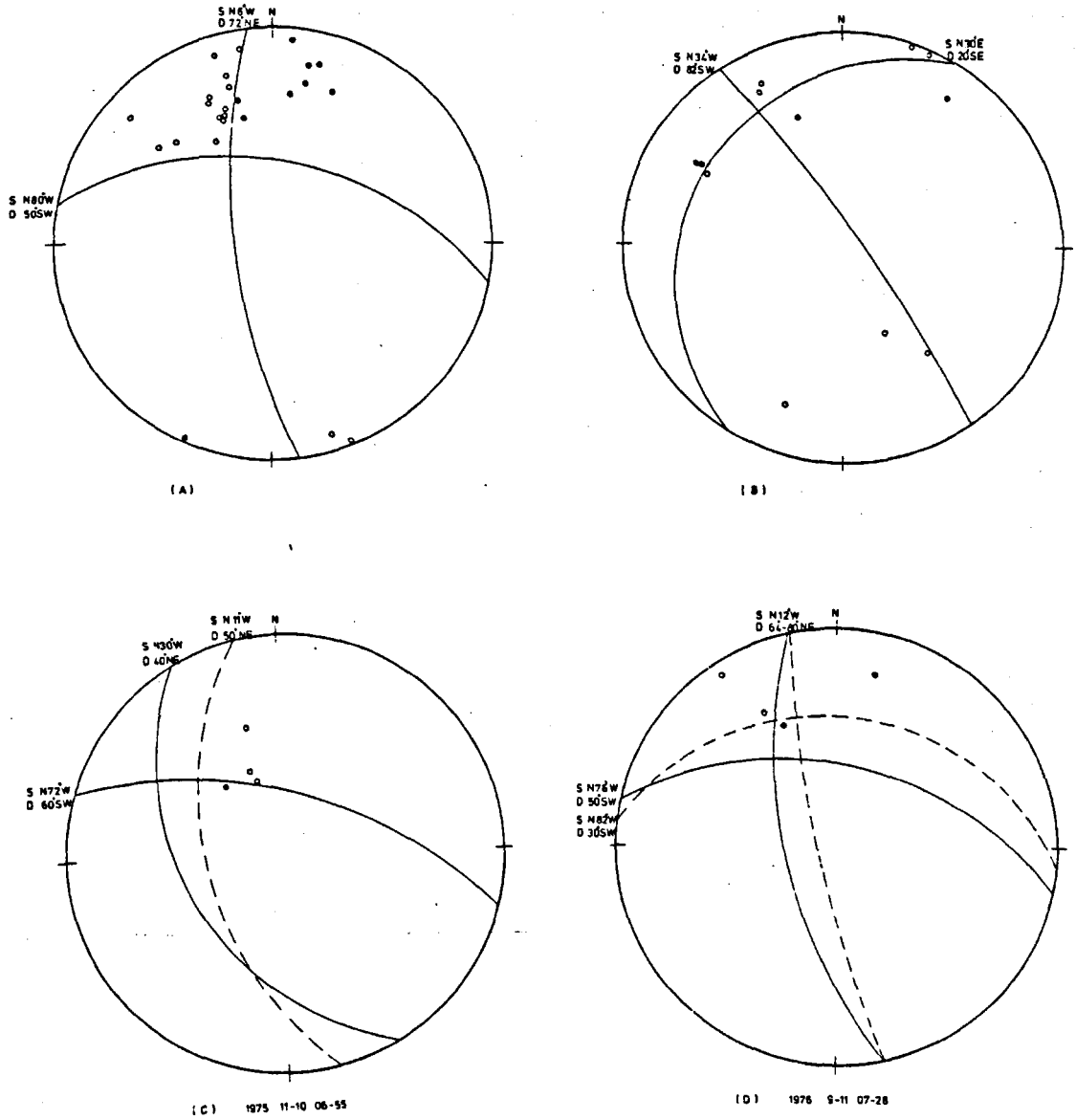

Fig. 9.7.7. Upper hemisphere fault-plane solutions for tremors which occurred in area E. Two composite fault-plane solutions are shown.

(A) A composite fault-plane solution obtained from events:

1976 6-4 10-29, 1976 10-31 15-47
1977 2-15 01-03, 1977 2-25 00-49
1977 3-8 04-06, 1977 4-28 19-27

(B) A composite fault-plane solution obtained from events:

1977 1-19 03-49, 1977 5-8 00-34
1977 6-14 01-53

(For legend see Fig. 9.3.12).

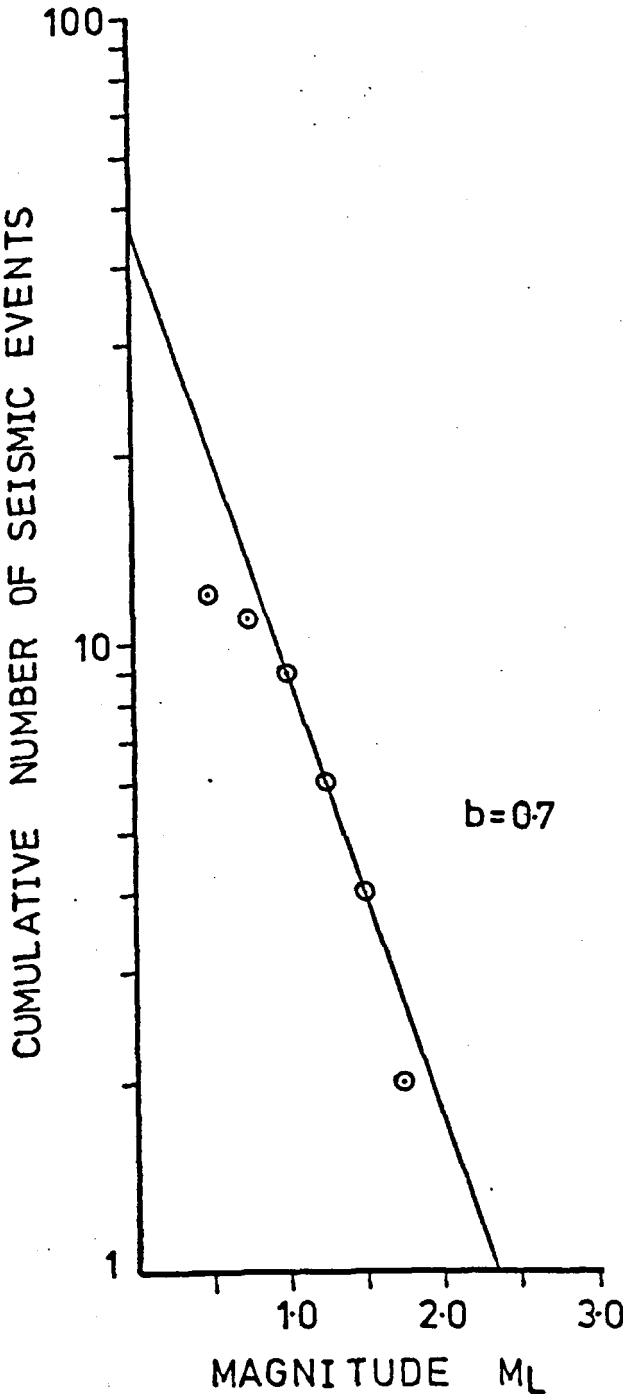

Fig. 9.7.8. A plot showing the frequency-magnitude distribution for tremors occurring in area E.

The value of b in this area is the second smallest b value in the coalfield, after Area C. This may suggest that the area was under high stress or the rocks more homogeneous, as discussed in Section 7.4. However, the above b value is not well determined since only a few events were available.

9.7.5 Earth tremor generation mechanisms

In order to determine the earth tremor generation mechanisms it is useful to determine first which of the four seams generated the tremors. The mine workings in the Hams seam, Cannel Row seam and the Winghay seam, which was mined from the New High Carr colliery, consisted of the driving of roadways only leaving large pillars between them. These pillars were not extracted. There were no reports of any pillar crushing, roof falls or floor heaves in these workings. Therefore, the mine workings in these three seams are unlikely to have caused earth tremor generation. The mine workings in the Rowhurst seam started in September 1976 and also consisted of the driving of roadways only without pillar extraction, but the mine reports show that floor heavings, pillar crushing and roof breaking occurred during the working of this seam. The mine reports also indicated that pillar crushing and roof breaking occurred in the Winghay seam, which was mined from the Wedgwood colliery. Therefore, the mine workings in the Winghay and Rowhurst seams were probably responsible for generating earth tremors in this area.

The mine workings in the Winghay seam, which were carried out from the Wedgwood colliery, consisted of the driving of roadways and pillar extraction. The roof and floor were strong and there was no floor heaving. During the driving of the roadways there was no roof sagging or any pressure problems. However, weight problems started when a large area had been extracted. The roof in the extracted area was not allowed to cave in, instead it was supported by barrels filled with waste. The extraction

of a large area resulted in the roof converging, throwing most of its weight onto the supports and onto the remaining pillars. The increase in pressure on supports and pillars occurred suddenly and sometimes overnight causing the supports and the pillars to break along their edges. The rocks continued to fall from the pillar sides until they were finally completely crushed. When the pillars and supports crushed, roof falls occurred.

The mine workings in the Rowhurst seam consisted of the driving of roadways only. The floor of this seam was very soft (fireclay) while the roof was strong. There were reports of pillars punching through the soft layer forming the floor causing floor heaves which sometimes tended to close the roadways. Also, the thick dirt band present in this seam squeezed out along the pillar sides causing the pillars to swell and to have the shape of a barrel. As a result of this the coal peeled off from the pillar sides and consequently the pillars became small and eventually crushed. The crushing of the pillars may have led to roof breaking. The position of the long axis of the pillars parallel to the seam strike, i.e. perpendicular to the dip, caused more dirt to squeeze out of the pillar and consequently the pillars crushed much faster than they would have been if the long axis of the pillars was situated downdip.

Pillar and roof in the above two working seams could have failed in shear and consequently generated earth tremors having shear source mechanisms, or more probably the crushing of pillars and supports and the breaking of roofs caused the redistribution of the strata pressure in the area in such a way that sliding movements took place along the major faults. The crop out of these faults at the surface may have allowed the penetration of water through them, lubricating the surface of these faults resulting in sliding movements along them.

During the writing of this thesis, a few large tremors occurred and were felt over a large area of Stoke-on-Trent. Initial macroseismic and microseismic observations have suggested that the epicentres of these tremors were in the Talke area, less than 3 km north of the Chesterton area (Dr. N. J. Kusnir, personal communication). The small size of the area being mined in Chesterton and the severity of the felt tremors may suggest that these felt tremors occurred as a result of sliding movements along a fault or faults in this area. The location of most of the seismic events, recorded during the monitoring period, in this area along faults may confirm the above assumption. Alternative interpretation is that these felt tremors could be of natural origin.

9.8 Area F

This area lies near Burslem. The coal was extracted in this area from two seams mined from Norton colliery during the monitoring period (see Table 9.1). The coal was extracted along panels driven along the strike of the seams. The seams dip 19° SW. The area was also extensively mined previously in many different seams. The two active seams in descending order are:

(i) The Bullhurst seam: Three panels (panels 11, 12 and 14) were mined in this seam during the monitoring period at depths ranging between 408 m and 533 m below O.D. as shown in Table 9.1. Figure 9.8.1a shows that these three panels were surrounded by extensive old workings. Pillars of coal ranging in width from 10 m to about 210 m were left between these three panels, and between these panels and the old workings. Small faults having throws of less than 2 m were encountered at the seam level during the mining operations. A geological section through the seam (Figure 9.8.1a) shows that a layer 23 cm thick of coaly-shale forms the immediate roof of the seam and is overlain by a layer of cannel (light bituminous coal) 53 cm thick and then mudstone. The floor is composed of fireclay.

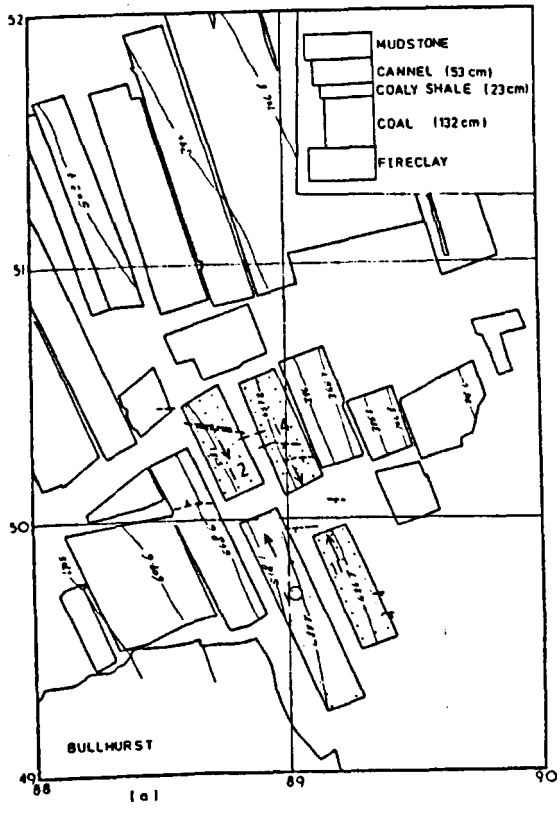

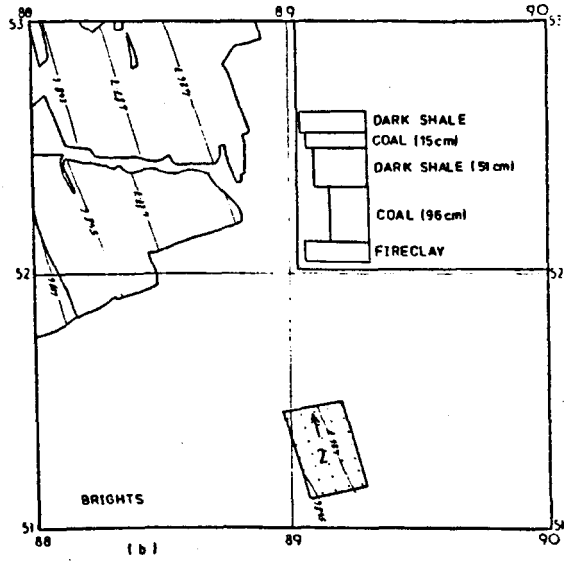

Fig. 9.8.1. The layout of the mine workings in area F showing the active mine workings (dotted ornament), faults at the seam level, and a general geological section through the seam in (a) the Bullhurst seam and (b) the Brights seam. (For legend see Fig. 9.3.1).

The active panels are overlain by workings in the Cockshead and Banbury seams, at heights of about 60 m and 198 m respectively above the active panels. They are also overlain by other workings in many other seams at much higher levels. No working is present underneath the active panels.

(ii) The Brights seam: One panel (panel 2) was mined in this seam during the monitoring period at depths ranging between 408 m and 490 m below O.D., as shown in Table 9.1. This panel was driven in an area not previously mined in this seam as shown in Figure 9.8.1b. The nearest old workings from this panel are more than 700 m away. The seam is disturbed by a number of small faults at the seam level. A general section in the seam, Figure 9.8.1b, shows that a layer of shale having a thickness of about 0.51 m immediately overlies the seam followed by about a 15 cm thickness of coal and then shale again. The seam is underlain by a layer of fireclay. The panel is overlain by extensive old workings in the Bullhurst seam at a height of approximately 130 m above the panel level. The panel is also overlain by many other workings at much higher levels. No working underlies the panel.

Only two tremors were located in this area. Either the mine workings in this area have not generated earth tremors, or most probably they generated small earth tremors, but they were not detected by the seismic network due to the remote location of this area with respect to the S.O.T. seismic network. Although events from this area may have been detected at stations D and G, tremors recorded on three or less seismic stations have not been considered in this study.

The possibility that mine workings in the Brights seam (panel 2) generated earth tremors was unlikely since the panel was mined under extensive old mine workings in the Bullhurst seam, i.e. it was driven in a de-stressed area. Some small tremors could perhaps have occurred behind the face due to roof caving. Mine workings in the Bullhurst seam, however, had a

greater possibility of generating tremors. The mine workings in this seam (panels 11, 12 and 14) were mined under old workings in the Cockshead and Banbury seams which have coal pillars left in their workings. Interaction between the abutment pressures of these pillars and the front and side abutment pressures of the active panels could have occurred.. As a consequence of this, the rocks in the pillars and ahead of the panel faces may have broken or failed causing the release of some amounts of stored strain energy which may have appeared as small tremors.

9.9 Area G

This area lies near Goldenhill to the north of Tunstall. Two seams were mined in this area during the monitoring period from two different collieries. Four panels (panels 9, 12, 13 and 17) were mined in the Hams seam from the Victoria colliery at depths ranging between 457 m and 560 m below O.D., as shown in Table 9.1 and Figure 9.9.1a. The four active panels were overlain by workings in the Moss seam at a height of about 91 m above the panels, and underlain by workings in the Holly Lane and Hardmine seams at depths of about 145 m and 182 m below the Hams seam respectively.

Two panels (panels 4 and 5) were driven in the Hardmine seam from the Chatterley Whitfield colliery at depths ranging between 652 m and 716 m below O.D. as shown in Table 9.1 and Figure 9.9.1b. The two active panels are overlain by previous workings in the Holly Lane seam at a height of about 32 m above the panel levels. No workings exist beneath these two panels.

The panels in the above two seams were driven along the seam strikes. The seams dip to the south and south-west at about 7°. The area was extensively mined previously in many different seams.

No seismic events were located in this area. This is either because the mine workings in this area have not generated seismic activity, or more probably because the area is located far away from the seismic network, so that the seismic events have not been recorded on four or more seismometers.

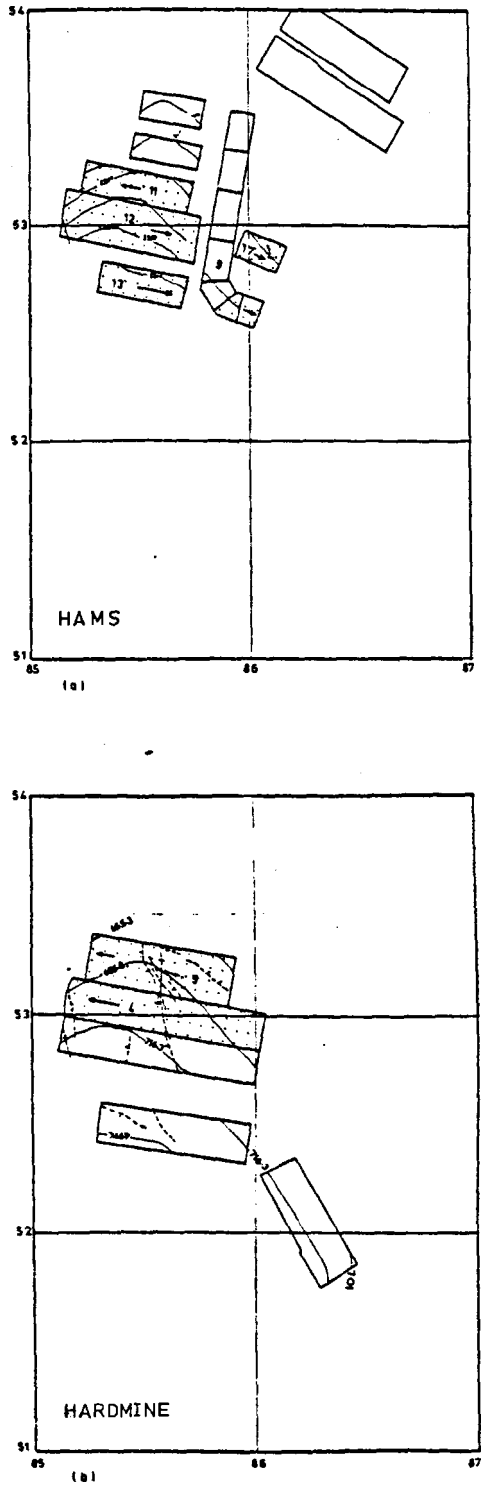

Fig. 9.9.1. The layout of the mine workings in area G showing the active mine workings (dotted ornament), faults at the surface and at the active seam datum in (a) the Hams seam and (b) the Hardmine seam. (For legend see Fig. 9.3.1).

CHAPTER 10

CONCLUSIONS

10.1 Summary

Mining induced seismicity in the North Staffordshire coalfield was monitored for a two year period (between September 1975 and September 1977). During this period more than 300 seismic events were recorded and 98 of these were located. Only events recorded on four or five seismometers were located. The accuracy of the tremor locations was estimated to be of about 500 m in plan and depth. None of the recorded seismic events were felt on the surface or underground. The earth tremors were found to originate from regions where mining activities were being carried out, and the tremors were found to be located within a few hundred metres of the active mine workings. Only a few tremors were scattered outside the mining areas. These mostly occurred as a result of rock falls in old workings triggered by the active mine workings or collapses in the old workings occurring as a consequence of the process of stabilization within the mine. The tremor foci lie predominantly at depths of between 1,000 m below O.D. and the surface, i.e. within the depth ranges of the active mine workings.

The tremor hypocentres were found to concentrate in five active mining areas:

(I) In three areas (areas A, C and D) the seismic events occurred mainly due to interaction between the stress field produced by active mining and the stress field associated with old workings in adjacent seams. In particular, this occurred when the active face passed under or over a pillar left in an adjacent seam.

(II) In area B the seismic events mainly occurred as a result of sliding movements along the Stoke fault due to the effect of mining many seams on the upthrow side of the fault.

(III) In area E the tremors may have possibly occurred as a result of failures in shear of pillars and roofs of the mine workings, or more probably they could have occurred as a result of sliding movements along the Chatterley and other parallel faults in the area due to the redistribution of the strata pressure in the area as a result of mining operations. The possibility that these tremors were of natural origin, however, is not ruled out.

During the mining of a particular panel, the following points were observed:

1. The tremors did not start until the face had advanced a distance of about 270 m.

2. Most of the tremors were located behind the active face (in the goaf). However, this is most probably due to errors in location.

3. Most of the large tremors occurred when the active face entered a high pressure zone (abutment pressure) due to a pillar left in an adjacent seam over or under the active panel.

4. When a panel was driven under or over an extensive previously mined out area in an adjacent seam, i.e. driven in a de-stressed zone, no tremors or only a few tremors occurred.

The temporal distribution of seismic events and the corresponding seismic energy released showed a close relationship between the times of mining activities and the incidence of earth tremors. The monthly distribution of tremors and energy release showed that seismic activity was reduced drastically during and within a few weeks after the miners' holidays in December and July of each year. The weekly distribution demonstrated that the incidence of earth tremors was far higher during weekdays, when coal was being extracted, than at weekends. The daily distribution showed that the peak of the seismic energy released was during the two productive shifts.

A study of earth tremor mechanisms based on the analysis of the P-wave first motions showed that two groups of tremors were common in the coalfield. The first group of tremors produced both kataseismic and anaseismic first motions. This type of tremor occurred either as a result of sliding movements of the rocks along pre-existing fault planes, or due to failure in shear of the rocks in pillars and ahead of the active faces. The second group of tremors produced only kataseismic first motion on all the seismometers. This type of tremor either has an implosional source mechanism and occurred as a result of rock failures in compression (pressure bursts), or has a collapse source origin and occurred mainly behind the active face or in the goaf of old workings, as a result of strata collapse and roof caving.

The magnitude, M_L, of seismic events ranged between 0.1 and 2.5, releasing seismic energy of between 10^3 J and 10^7 J. This is within the range of tremor size experienced in other coalfields such as Sunnyside, Utah (Smith et al., 1974), Midlothian, Scotland (Mashkour, 1976) and the Czechoslovakian coalfield (Holub, 1966). However, the magnitudes in the northern part of the North Staffordshire coalfield are small compared with those tremors which have occurred in the Trent Vale-Hanford area in the southern part of the North Staffordshire coalfield. The largest tremor in the Trent Vale area had a local magnitude, M_L, of about 2.8 (Kusznir et al., 1980a). This may be because the interaction effect between the stress fields of the active and old mine workings in the Trent Vale-Hanford area was more severe than in the other areas in the northern part of the coalfield. As a whole, the tremors in the North Staffordshire coalfield are small compared with those tremors which have occurred in the South African and Canadian goldfields. The largest tremor in the Witwatersrand goldfield (South Africa) released seismic energy of about 10^{11} Joules (Gane et al., 1946). The difference in size between earth tremors which occurred in the North Staffordshire coalfield and those which occurred in goldfields is most

probably due to the greater depth of the goldfield mining and also due to the greater hardness of the rocks.

The frequency-magnitude relationship of seismic events in the North Staffordshire coalfield resembles that for natural earthquakes. In the Trent Vale-Hanford area it has been shown that the b-value appeared to decrease when the active face passed over or under a pillar left in previous workings in an adjacent seam (i.e. increasing pressure), while the value of b increased when the face passed under or over a previously mined out area (de-stressed zone). It was also found that leaving a coal pillar barrier between the active panel and the laterally adjacent previous panel in the same seam increased the value of b, and increased the seismicity level by 31 times.

Finally, it was found that the Stoke-on-Trent seismic network was suitable for studying seismic activity in the coalfield as a whole, but it was too large for the precise study of seismic activity associated with mining operations for a specific panel. In particular, the tremors located in area E are felt to have very poor location since they are situated far away from the centre of the network.

10.2 Suggestions for further study

For the accurate location of seismic events in the coalfield, the seismic velocity structure in the coalfield needs to be determined in more detail, preferably in each area. Furthermore, the geometry of the seismometer network used to investigate a particular panel should ideally be designed for that particular panel.

In order to establish the causes and mechanisms of the earth tremors in the Chesterton area (area E), which has also experienced felt tremors recently (1980), a small aperture seismic network needs to be installed in the area.

The P-wave first motions distribution produced from the collapses or downward movements of the roof in the mine needs to be determined experimentally and mathematically in order to distinguish between the collapse and implosional source mechanism. Also the P-wave first motions pattern generated by shock bursts, described by Phillips (1944-45) in Section 3.2.1, needs determining in order to understand the actual mechanism of this kind of burst more clearly.

BIBLIOGRAPHY

ALDER, H., POTTS, E. L. J. and WALKER, A. (1951). Research on strata control in the northern coalfield of Great Britain. In: Proceedings of the First Conference on Rock Pressure and Support in Working, Leige, 24-28 April, Paper A8, pp.106-120.

ANTSYFEROV, M. S. (1966). Principles of the application of seismo-acoustics to coal seams subject to rock bursts. In: Seismo-Acoustic Methods in Mining, Edited by Antsyferov, M. S. Translated from Russian by Hall, S. E. Colorado School of Mines, Colorado, Consultant Bureau, New York, pp.1-8.

AVERSHIN, S. G. and PETUKHOV, I. M. (1964). Rock bump conditions and ways of combating them in Soviet mines. In: Proceedings of the Fourth International Conference on Strata Control and Rock Mechanics, Columbia University, May 4-8, pp.412-419.

BANSON, J. K. A. (1970). Methods for Studying Seismicity at Short Range. M.Sc. Thesis, University of Edinburgh.

BARNES, B. K., DUNRUD, C. R. and HERNANDEZ, J. (1969). Seismic activity in the Sunnyside mining district, Utah, during 1967. United States Geological Survey. Open file report, No. R290, 26 pp.

BATH, M. (1973). Introduction to Seismology. New York, Birkhauser Verlag, 395 pp.

BAULE, H. and RAO, M.V. M. S. (1979). Seismoacoustic activity in a coal seam in relevance to destressing. Rock Mechanics, 11,pp.177-187.

BELL, F. G. Editor (1975). Site investigation in areas of mining subsidence. London, Butterworth and Co. Ltd., 168 pp.

BLAKE, W. (1972). Rock burst mechanics. Quarterly of the Colorado School of Mines, 67(1), 64 pp.

BLAKE, W., LEIGHTON, F. and DUVALL, W. I. (1974). Microseismic techniques for monitoring the behaviour of rock structures. United States Bureau of Mines, Bulletin 665, 45 pp.

BOIKO, G. K. (1966). Relation between rock pressure diagrams and the seismo-acoustic conditions in a coal seam. In: Seismo-Acoustic Methods in Mining. Edited by Antsyferov, M. S., Translated from Russian by Hall, S. E., Colorado School of Mines, Colorado, Consultant Bureau, New York, pp.75-78.

BROWITT, C. W. A. (1977). Detection and location of earthquakes and unplanned explosions. In: Instrumentation for Ground Vibration and Earthquakes. The Institution of Civil Engineers, London, pp.63-76.

BUKLE, F. (1965). The rock-burst hazard in Wright-Hargreaves mine at Kirkland Lake, Ontario. Canadian Mining Journal, 86, pp.81-87.

BUDRYK, W. (1955). The effects of earth tremors in the Upper Silesian mines. Archiwum Gornictwa i Hutnictwa, 3(2), pp.227-240. (British Lending Library, Translation No. RTS 9453).

CARMAN, C. O. (1965). Understanding roof action is imperative in longwall mining. Coal Mining and Processing, 2(3), pp.38-41.

CAZALET, P. (1920). Notes on the study of records of earth tremors on the Central Rand. The Journal of the South Africa Institution of Engineers, 18, pp.211-228.

CETE, A. (1977). Seismic source location in the Ruhr district. In: Proceedings of the First Conference on Acoustic Emission/Micro-seismic Activity in Geological Structures and Materials, Pennsylvania State University, June 9-11, Edited by Hardy, H. R. Jr., and Leighton, F. W., pp.231-241.

COOK, N. G. W. (1962). The seismic location of rock bursts. In: Proceedings of the Fifth Rock Mechanics Symposium, May 1962, Oxford, Pergamon Press, pp.493-516.

COOK, N. G. W. (1963). The basic mechanics of rock bursts. Journal of the South African Institute of Mining and Metallurgy, 64(3), pp.56-66.

COOK, N. G. W. (1976). Seismicity associated with mining. Engineering Geology, 10, pp.99-122.

COOK, N. G. W., HOEK, E., PRETORIUS, J. P. G., ORTLEPP, W. D. and SALAMON, M. D. G. (1966). Rock mechanics applied to the study of rock bursts. Journal of the South African Institute of Mining and Metallurgy, 66(10), pp.435-528.

CROWLE, P. J. (1931). Ground movements and methods of support in deep mining (The Kolar Gold Field). Transactions of the Institution of Mining and Metallurgy, 40, pp.77-100.

DAVISON, C. (1919). The Stafford earthquakes of 1916. Geological Magazine, 6, pp.302-312.

DAVISON, C. (1924). A History of British Earthquakes. Cambridge University Press.

DENKHAUS, H. G. (1964). Critical review of strata movements theories and their application to practical problems. Journal of the South African Institute of Mining and Metallurgy, 64, pp.310-332.

DEWEY, J. W. (1971). Seismicity Studies with the method of Joint Hypocentre Determination. Ph.D. Dissertation, University of California, Berkeley.

DINSDALE, J. R. (1937). Ground failure around excavations. Transactions of the Institution of Mining and Metallurgy, 46, pp.673-700.

DOUGLAS, A. (1967). Joint epicentre determination. Nature, 215, pp.47-48.

DUNRUD, C. R. and OSTERWALD, F. W. (1965). Seismic study of coal mine bumps, Carbon and Emery counties, Utah. Transactions of the American Institute of Mining, Metallurgy and Petroleum Engineers, 232, pp.174-182.

FARMER, I. W. and ALTOUNYAN, P. F. R. (1980). The mechanics of ground deformation above a caving longwall face. Paper to Second Conference on Large Ground Movements and Structures, Cardiff, U.K.

FINSEN, W. S. (1950). The statistics of Witwatersrand earth tremors, 1938.5 to 1949. Union Observatory, Circular No. 110, p.444-456.

FRANCIS, T. J. G., PORTER, I. T. and McGRATH, J. R. (1977). Ocean bottom seismograph observations on the Mid-Atlantic ridge near latitude 37°N. Bulletin of the Geological Society of America, 88(1), pp.664-677.

GANE, P. G. (1939). A statistical study of the Witwatersrand earth tremors. Journal of the Chemical, Metallurgical and Mining Society of South Africa, 40, pp.155-171.

GANE, P. G., HALES, A. L. and OLIVER, H. A. (1946). A seismic investigation of the Witwatersrand earth tremors. Bulletin of the Seismological Society of America, 36(2), pp.49-80.

GANE, P. G., LOGIE, H. J. and STEPHEN, J. H. (1949). Triggered tele-recording seismic equipment. Bulletin of the Seismological Society of America, 39, pp.117-133.

GANE, P. G., SELIGMAN, P. and STEPHEN, J. H. (1952). Focal depths of Witwatersrand tremors. Bulletin of the Seismological Society of America, 42(3), pp.239-250.

GIBOWICZ, S. (1963). An energy classification of underground tremors in Upper Silesia and their frequency of occurrence in relation to energy level. Archiwum Gornictwa, 8(1), pp.17-41. (British Lending Library, Translation No. RTS 8901).

GIBSON, W., WEDD, C. B. and SCOTT, A. (1925). The geology of the country around Stoke-upon-Trent. Memoirs of the Geological Survey, England.

GOFORTH, T. T. and McDONALD, J. A. (1970). A physical interpretation of seismic waves induced by sonic booms. Journal of Geophysical Research, 75(26), pp.5087-5092.

GUPTA, H. K. and RASTOGI, B. K. (1976). Dams and Earthquakes. Oxford, Elsevier Scientific Publishing Company.

HAINS, B. A. and HORTON, A. (1969). British Regional Geology, Central England. London, Institute of Geological Sciences, 142 pp.

HARDY, H. R. Jr., and MOWREY, G. L. (1976). Study of microseismic activity associated with a longwall coal mining operation using a near-surface array. Engineering Geology, 10, pp.263-281.

HILL, F. G. and DENKHAUS, H. G. (1961). Rock mechanics research in South Africa with special reference to rock bursts and strata movement in deep level gold mines. In: Transactions of the Seven Commonwealth Mining and Metallurgical Congress, South Africa, 2, pp.807-829.

HODGSON, E. A. (1958). Dominion observatory rock burst research, 1938-1945. Publication of the Dominion Observatory, Ottowa, Canada, Department of Mines and Technical Surveys, 20(1), 248 pp.

HODGSON, K. and JOUGHIN, N. C. (1967). The relationship between energy release rate, damage and seismicity in deep mines. In: Failure and Breakage of Rock, pp.194-203. Edited by Fairhurst, C. Proceedings of the Eighth Symposium on Rock Mechanics, University of Minnesota, 1966.

HOLLAND, C. T. (1958). Cause and occurrence of coal mine bumps. Mining Engineering, 10, pp.994-1004.

HOLLAND, C. T. and THOMAS, E. (1954). Coal-mine bumps: some aspects of occurrence, cause and control. United States Bureau of Mines, Bulletin 535, 37 pp.

HOLUB, K. (1966). A contribution to the study of rock bursts from the Pribram region. Geofysikalni Sbornik, 14 (248), pp.291-305.

HOOKER, V. E., LEIGHTON, F. and STEBLAY, B. J. (1974). Microseismic investigations in coal mines. Mining Congress Journal, 60 (10), pp.66-71.

HUDSPETH, H. M. and PHILLIPS, D. W. (1932-33). The forces induced by the extraction of coal and some of their effects on coal-measures strata. Transactions of the Institution of Mining Engineers, 85, pp.37-50.

ISAACSON, E.DE.ST.Q. (1957). Research into the rock burst problem on the Kolar gold field. Mine and Quarry Engineering, 23, pp.520-526.

ISAACSON, E.DE.ST.Q. (1961). Stress waves resulting from rock failure. In: Proceedings of the Fourth Symposium on Rock Mechanics, Pennsylvania State University. Edited by Hartman, H. L., pp.153-161.

IVANOV, V. S. (1966). Seismo-acoustic deformation of the boundaries of zones in coal seams subject to rock bursts. In: Seismo-Acoustic Method in Mining. Edited by Antsyferov, M. S., Translated from Russian by Hall, S. E., Colorado School of Mines, Colorado, Consultant Bureau, New York, pp.57-61.

IVANOV, V. S. and PARSHIKOV, N. B. (1966). Seismo-acoustic method for determining the efficiency of measures to combat rock bursts. In: Seismo-Acoustic Method in Mining. Edited by Antsyferov, M. S., Translated from Russian by Hall, S. E., Colorado School of Mines, Colorado, Consultant Bureau, New York, pp.87-91.

JACOB, A. W. B. and NEILSON, G. (1977). Magnitude determination on LOWNET. Institute of Geological Sciences, Global Seismology Unit, Report 86.

JAMES, D. E., SACKS, I. S., EDUARDO LAZO, L. and PABLO APARICIO, G. (1969). On locating local earthquakes using small networks. Bulletin of the Seismological Society of America, 59 (3), pp.1201-1212.

JAMES, F. and ROOS, M. (1971). MINUIT - A package of programs to minimize a function of n variables, compute the covariance matrix, and find the true errors. CERN Computer 7600 Interim Program Library.

JANCZEWSKI, E. W. (1950). The problem of underground tremors in the Polish coal basin and methods of studying the phenomena. Biuletyn Slaskiej Stacji Geofizycznej W Raciborzu, 1, pp. 25-55. (British Lending Library, Translation No. RTS 8949).

JANCZEWSKI, E. W. (1955). Earth tremors in Upper Silesia. Archiwum Gornictwa i Hutnictwa, 3(2), pp.205-225. (British Lending Library, Translation No. RTS 8899).

JANCZEWSKI, E. W. (1956). Earth tremors in Upper Silesia, Part 2. Archiwum Gornictwa, 1 (4), pp.321-344. (British Lending Library, Translation No. RTS 8900).

JOSEPH, E. H. A. (1938). Rock bursts: the mechanism of crush bursts. Journal of the Chemical, Metallurgical and Mining Society of South Africa, 39, pp.114-131.

KAGAN, Ya.Ya. and LAVROV, I. M. (1966). Locating the sources of seismo-acoustic pulses. In: Seismo-Acoustic Methods in Mining, Edited by Antsyferov, M. S., Translated from Russian by Hall, S. E., Colorado School of Mines, Colorado, Consultant Bureau, New York, pp.81-86.

KING, H. J., WHITTAKER, B. N. and BATCHELOR, A. S. (1972). The effects of interaction in mine layouts. In: Proceedings of the Fifth International Strata Control Conference, London, Paper 17, 11p.

KNOPOFF, L. and GILBERT, F. (1960). First motions from seismic sources. Bulletin of the Seismological Society of America, 50(1), pp.117-134.

KRASNIKOVSKY, G. W. and BARANOVSKY, W. I. (1963). Some problems of safe development of coal seams at great depth. In: Proceedings of the Third International Mining Congress, Salzburg, 15-21 September.

KRAWIEC, A. and STANISLAW, T. (1977). Rock bursting in Polish deep coal mines in light of research and practical observation. Transactions of the American Institute of Mining, Metallurgy and Petroleum Engineers, 262, pp.30-36.

KULPINSKI, J. (1966). A micro-survey of bounces and tremors in the Miechowice mine. Przeglad Gorniczy, 12, pp.530-534. (British Lending Library, Translation No. RTS 9295).

KUSZNIR, N. J., ASHWIN, D. P. and BRADLEY, A. G. (1980a). Mining induced seismicity in the North Staffordshire Coalfield, England. International Journal of Rock Mechanics, Mining Science and Geomechanics Abstract, 17, pp.45-55.

KUSZNIR, N. J., FARMER, I. W., ASHWIN, D. P., BRADLEY, A. G. and AL-SAIGH, N. H. (1980b). Observations and mechanics of seismicity associated with coal mining in North Staffordshire, England. In: Proceedings of the Twenty-first United States Rock Mechanics Symposium, pp.163-171.

LAMA, R. D. (1967). Some aspects of planning of deposits liable to rock bursts. Journal of the Mines, Metals and Fuels, May, pp. 149-158.

LEIGHTON, F. and DUVALL, W. I. (1972). A least squares method for improving the source location of rock noise. United States Bureau of Mines, Report of Investigation 7626, 19 pp.

LEIGHTON, F. and STEBLAY, B. J. (1977). Applications of microseismics in coal mines. In: Proceedings of the First Conference on Acoustic Emission/Microseismic Activity in Geologic Structures and Materials, Pennsylvania State University, 9-11 June, 1975. Edited by Hardy, H. R. Jr. and Leighton, F. W., pp.205-229.

LEITERITZ, rer.nat. H. (1978). The significance of geological-tectonic factors in rock bursts in the Ruhr coalfield. Gluckauf (English translation), 114, pp.472-476.

LILWALL, R. C. and FRANCIS, T. J. G. (1978). Hypocentral resolution of small ocean bottom seismic networks. Geophysical Journal Research Astronomical Society, 54, pp.721-728.

LOGIE, H. J. (1951). The volocity of seismic waves on the Witwatersrand. Bulletin of the Seismological Society of America, 41, pp.109-121.

MASHKOUR, M. (1976). A seismological study in a mining area. Ph.D. Thesis, University of Strathclyde.

McGARR, A. (1971). Violent deformation of rock near deep-level tabular excavations - seismic events. Bulletin of the Seismological Society of America, 61(5), pp.1453-1466.

McGARR, A., SPOTTISWOODE, S. M. and GAY, N. C. (1975). Relationship of mine tremors to induced stresses and to rock properties in the focal region. Bulletin of the Seismological Society of America, 65(4), pp. 981-993.

McGARR, A. and WIEBOLS, G. A. (1977). Influence of mine geometry and closure volume on seismicity in a deep-level mine. International Journal of Rock Mechanics, Mining Science and Geomechanics Abstract, 14, pp.139-149.

MILNE, W. G. and WHITE, W. R. H. (1958). A seismic investigation of mine "Bumps" in the Crowsnest Pass Coalfield. The Canadian Mining and Metallurgical Bulletin, 51, pp.678-685.

MIRER, S. V. (1966). Determining the relief zone of rise boreholes by the seismo-acoustic method. In: Seismo-Acoustic Methods in Mining. Edited by Antsyferov, M. S., Translated from Russian by Hall, S. E., Colorado School of Mines, Colorado, Consultant Bureau, New York, pp.97-101.

MOGI, K. (1962). Study of elastic shocks caused by the fracture of hetrogeneous materials and its relations to earthquake phenomena. Bulletin of the Earthquake Research Institute, 40, pp.125-173.

MOGI, K. (1963). Some discussions on aftershocks, foreshocks and earthquake swarms - the fracture of a semi-infinite body caused by an inner stress origin and its relation to the earthquake phenomena. Bulletin of the Earthquake Research Institute, 41, pp.615-658.

MUKHERJEE, S. K. and SINGH, B. (1964). Scientific approach to the problem of rock bursts and bumps. Journal of Mines, Metals and Fuels, 12(9), pp.273-280.

NEYMAN, B. (1955). The location of rock bursts in the coal mines of the Upper Silesian coal basin. Archiwum Gornictwa, 11(1), pp.249-265.

NEYMAN, B. (1964). The relationship between the phenomena of bounce and earth tremors in the Upper Silesia area. Przeglad Gorniczy, 20(11), pp.552-558. (British Lending Library, Translation No. RTS 8617).

OBERT, L. and DUVALL, W. (1945). Microseismic method of predicting rock failure in underground mining, Part I, General Method. United States Bureau of Mines, Report of Investigation 3797.

OSTERWALD, F. W. (1970). Comments on rock bursts, outbursts, and earthquake prediction. Bulletin of the Seismological Society of America, 60(6), pp.2083-2085.

OSTERWALD, F. W., BENNETTI, J. B. Jr., DUNRUD, C. R. and MABERRY, J. O. (1971). Field instrumentation studies of earth tremors and their geologic environments in central Utah coal mining areas. United States Geological Survey, Professional Paper No. 693, 20 pp.

OSTERWALD, F. W. and DUNRUD, C. R. (1965). Geology applied to the study of coal mine bumps at Sunnyside, Utah. Transactions of the American Institute of Mining, Metallurgical and Petroleum Engineers, 232, pp. 168-174.

OSTERWALD, F. W. and DUNRUD, C. R. (1966). Instrumentation study of coal mine bumps, Sunnyside district, Utah. Utah Geological and Mineralogical Survey, Bulletin 80, pp.97-110.

OSTERWALD, F. W., DUNRUD, C. R., BENNETTI, J. B. Jr. and MABERRY, J. O. (1972). Instrumentation studies of earth tremors related to geology and to mining at the Somerset coal mine, Colorado. United States Geological Survey, Professional Paper 762, 27 pp.

PENG, S. S. (1978). Coal mine ground control. New York, John Wiley, 450 pp.

PEPERAKIS, J. (1958). Mountain bumps at the Sunnyside mines. Mining Engineering, 10, pp.982-986.

PETROSYANTS, E. V. and GORBACHENKO, V. A. (1969). Seismoacoustic study of the stability of rocks above a mine working. Soviet Mining Science, 4, pp.391-394.

PHILLIPS, D. W. (1944-45). Rock bursts or bumps in coal-mines. Transactions of the Institution of Mining Engineers, 104, pp.55-84.

PRETORIUS, J. P. G. (1964). The use of statistics in rock burst research. Journal of the South African Institute of Mining and Metallurgy, 64(8), pp.398-405.

RACAL-THERMIONIC LIMITED. Field recording system for seismic data. Instrument Manual for Geostore.

RICE, G. S. (1935). Bumps in coal mines of the Cumberland field, Kentucky and Virginia - causes and remedy. United States Bureau of Mines, Report of Investigation 3267, 36 pp.

RICHTER, C. F. (1935). An instrumental earthquake magnitude scale. Bulletin of the Seismological Society of America, 25(1), pp.1-32.

RICHTER, C. F. (1958). Elementary seismology. San Francisco, W. H. Freeman and Company, 768 pp.

ROBSON, W. T. (1946). Rock-burst incidence, research and control measures at Lake Shore Mines Limited. Transactions of the Canadian Institute of Mining and Metallurgy, 49, pp.347-374.

ROUX, A. J. A. and DENKHAUS, H. G. (1954). An investigation into the problem of rock bursts: Part II. An analysis of the problem of rock bursts in deep level mining. Journal of the Chemical, Metallurgical and Mining Society of South Africa, 55, pp.103-124.

RYDER, J. A. and OFFICER, N. C. (1964). An elastic analysis of strata movement observed in the vicinity of inclined excavations. Journal of the South African Institute of Mining and Metallurgy, 64(6), pp.219-244.

SALAMON, M. D. G. (1976). The role of pillars in mining. In: The Use of Rock Mechanics Principles in Practical Underground Mine Design, S.A.I. M.M. Vacation School.

SCHOLZ, C. H. (1968). The frequency-magnitude relation of microfracturing in rock and its relation to earthquakes. Bulletin of the Seismological Society of America, 58(1), pp.399-415.

SEBOR, G., RUDAJEV, V., SIMANE, J. and ROCEK, V. (1976). Rock bursts and possibilities of their prevention. In: Proceedings of the Ninth World Mining Congress, Federal Republic of Germany, Paper II-14.

SHADBOLT, C. H. (1978). Mining subsidence - historical review and state of art. In: Large Ground Movements and Structures, pp.705-748. Edited by Geddes, J. D. Proceedings of Conference at the University of Wales Institute of Science and Technology, Cardiff, 1977, New York, John Wiley.

SHEPHERD, R. (1973). The forward abutment in longwall mining. Colliery Guardian, 221(5), pp.177-182.

SHEPHERD, R. and KELLET, W. H. (1973). Strata behaviour, a study on faces and roadways in workings under a sandstone roof liable to rock bumps. Colliery Guardian, 221(3), pp.93-102.

SIBEK, V. (1963). On securing the safety of operation ore mines exposed to rock burst hazards. In: Proceedings of the Third International Mining Congress, Salzburg, 15-21 September.

SIBEK, V., SIMANE, J. and BUBEN, J. (1964). Methods of research into rock bursts in the Czechoslovak Socialist Republic. In: Proceedings of the Fourth International Conference on Strata Control and Rock Mechanics, New York, Columbia University Press, pp.420-431.

SINCLAIR, W. E. (1936). Rock bursts - their cause and prevention. Journal of the Chemical, Metallurgical and Mining Society of South Africa, 37, pp.4-11.

SINHA, K. N., SARKAR, S. K., SAXENA, N. C. and SINGH, R. D. (1972). Strata control research at longwall workings in India. In: Proceedings of the Fifth Strata Control Conference, London, Paper 15, 8 pp.

SMITH, R. B., WINKLER, P. L., ANDERSON, J. G. and SCHOLZ, C. H. (1974). Source mechanisms of microearthquakes associated with underground mines in eastern Utah. Bulletin of the Seismological Society of America, 64(4), pp.1295-1317.

SPRUTH, F. (1951). Distribution of pressure up, on and near the coal face. In: Proceedings of the First Conference on Rock Pressure and Support in Working, Liege, 24-28 April, Paper A1, pp.36-44.

STOKES, R. S. G. (1936). Recent development in mining practice on the Witwatersrand. Transactions of the Institution of Mining and Metallurgy, 45, pp.115-122.

TALMAN, W. G. and SCHRODER, J. L. Jr. (1958). Control of Mountain bumps in the Pocahontas No. 4 seam. Mining Engineering, 10, pp.888-891.

TAYLOR, J. T. M. (1962-63). Research on ground control and rock bursts on the Kolar gold field, India. Transactions of the Institution of Mining and Metallurgy, 72, pp.317-338.

THE SOUTH STAFFORDSHIRE AND WARWICKSHIRE INSTITUTE OF MINING ENGINEERS. (1932-33). First progress report of the safe working of mines committee of the South Staffordshire and Warwickshire Institute of Mining Engineers: the occurrence of bumps in the thick coal seam of South Staffordshire. Transactions of the Institution of Mining Engineers, 85, pp.116-137.

THE SOUTH STAFFORDSHIRE AND WARWICKSHIRE INSTITUTE OF MINING ENGINEERS. (1945-46). First progress report of the safe working of mines committee of the South Staffordshire and Warwickshire Institute of Mining Engineers on the problem of "bumps" in the South Staffordshire thick coal seam. Transactions of the Institution of Mining Engineers, 105, pp.458-499.

VAN PROCTOR, R. J. (1978). An investigation of the nature and mechanism of rock fracture around longwall faces in a deep gold mine. Ph.D. Thesis, University of the Witwatersrand, Johannesburg, South Africa.

WEISS, O. (1938). The theory of rock bursts and the possibilities of geophysical methods in predicting rock bursts on the producing mines of the Witwatersrand. Journal of the Chemical, Metallurgical and Mining Society of South Africa, 38, pp.273-329.

WESTBROOK, G. K. (1977). Investigation of earth tremors at Stoke-on-Trent. In: Instrumentation for Ground Vibration and Earthquakes. The Institution of Civil Engineers, London, pp.76-82.

WESTBROOK, G. K., KUSZNIR, N. J., BROWITT, C. W. A. and HOLDSWORTH, B. K. (1980). Seismicity induced by coal mining in Stoke-on-Trent (U.K.). Engineering Geology, 16, pp.225-241.

WHITTAKER, B. N. (1974). An appraisal of strata control practice. The Mining Engineer, 134, pp.9-24.

WHITTAKER, B. N. and PYE, J. H. (1975). Design and layout aspects of longwall methods of coal mining. In: Proceedings of the Sixteenth Symposium on Rock Mechanics, September 22-24, University of Minnesota, Minneapolis, pp.198-209.

WIERZCHOWSKA, Z. (1962). New views on the origin of earth tremors in Upper Silesia. Przeglad Gorniczy, 18(7-8), pp.417-422. (British Lending Library, Translation No. 8894).

WILSON, A. and ASHWIN, D. P. (1972). Research into the determination of pillar size. The Mining Engineer, 131(141), pp.409-427.

WOOD, H. E. (1914). The Witwatersrand earth tremors. Journal of the Chemical, Metallurgical and Mining Society of South Africa, 14, pp.423-427.

ZNANSKI, J. (1959). Bounce occurring simultaneously with an earth tremor. Przeglad Gorniczy, 15(10-11), pp.501-504. (British Lending Library, Translation No. RTS 8896.

ADDITIONAL REFERENCES

BEALE, R. A. (1981): The application of numerical modelling techniques to the mechanisms of reservoir- and mining-induced seismicity. Ph.D. Thesis, University of Keele, U.K.

BURTON, P. W. (1979): Seismic risk in southern Europe through the India examined using Gumbel's third distribution of extreme values. Geophysical Journal Research Astronomical Society, 59, pp.249-280.

GUMBEL, E. J. (1958): Statistics of extremes. New York and London, Columbia University Press.

HEALY, J. H., RUBEY, W. W., GRIGGS, D. T. and RALEIGH, C. B. (1968): The Denver earthquakes. Science, 161, pp.1301-1310.

HODGSON, J. H. (1953): A seismic survey in the Canadian Shield; Refraction studies based on rock bursts at Kirkland Lake, Ontario. Publications of the Dominion Observatory, Ottowa, Canada. Department of Mines and Technical Survey, 16(5), pp.113-163.

HOEK, E. and BROWN, E. T. (1980): Underground excavations in rock. London, The Institution of Mining and Metallurgy, 527 pp.

HUBBERT, M. K. and RUBEY, W. W. (1959): Role of fluid pressure in mechanics of overthrust faulting. Bulletin of the Geological Society of America, 70, pp.115-166.

MORRISON, R. G. K. (1947): The rock burst - a study of factors and conditions. Engineering and Mining Journal, 148, pp.62-67.

RALEIGH, C. B., HEALY, J. H. and BREDEHOEFT, J. D. (1976): An experiment in earthquake control at Rangely, Colorado, Science, 191, pp.1230-1237.

SIMPSON, D. W. (1976): Seismicity changes associated with reservoir loading. Engineering Geology, 10, pp.123-150.

YERKES, R. F. and CASTLE, R. O. (1976): Seismicity and faulting attributable to fluid extraction. Engineering Geology, 10, pp.151-167.

APPENDICES

APPENDIX 1

The program listed in this appendix consists of a main program and two subroutines which need to be run separately with the main program.

Main Program (HYPCTR)

This is a package of the MINUITL subroutines developed by James and Roos (1971) which use non-linear optimization procedures to minimize an objective function which in our case is the variance between the observed and calculated travel times from the hypocentre to the seismic station (see Section 4.7.2). The following subroutines were written by Dr. G. K. Westbrook.

Subroutine SHL

This subroutine is used to compute tremor hypocentre parameters (easting, northing, depth and origin time) for a single seismic event. The program uses the relative delays between P-arrival times at the different seismometers (S-P times can also be used if available) to calculate tremor hypocentre and origin time, using a velocity structure model which assumes a linear increase of seismic velocity with depth (Fig. A-1).

The following quantities are given or assumed.

1. The arrival times of the P-waves at each seismic station. S-P time can also be used if available.
2. The co-ordinates and delay time for each seismic station.
3. An initial estimate of the position of the hypocentre.
4. The seismic velocity structure of the area.

The program calculates the travel times and compares them against the observed times. The co-ordinates of the hypocentre are varied until the difference between the observed and computed times are minimized. A flow diagram for the subroutine is given in Figure A-2.

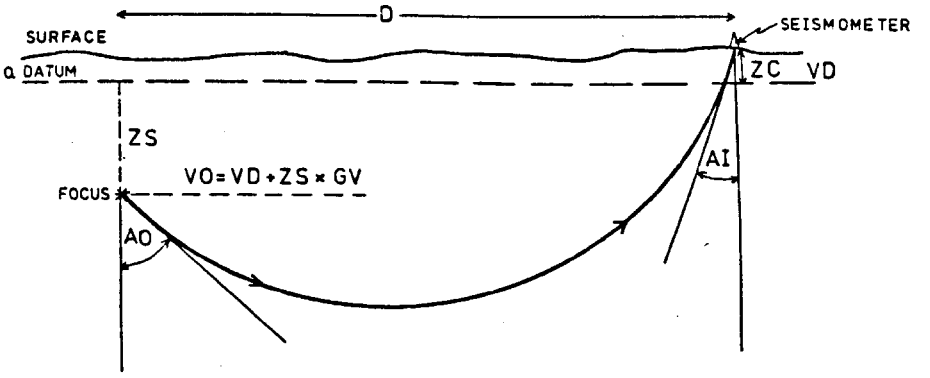

Fig. A-1: Seismic structure model with linear increase of seismic velocity with depth.

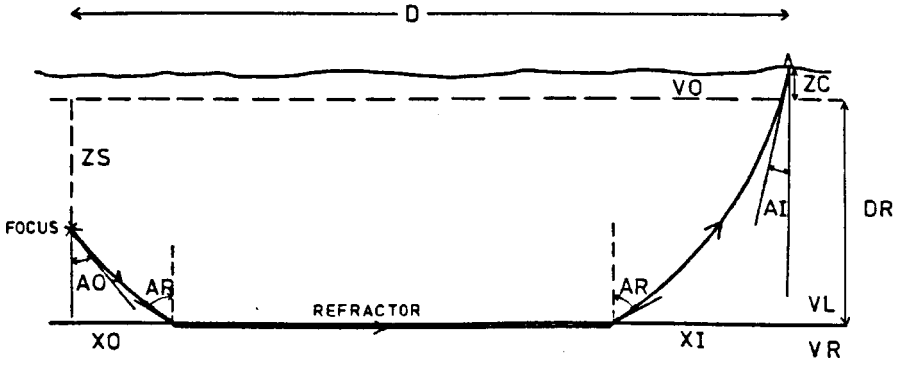

Fig. A-3: Seismic structure model with linear increase of seismic velocity with depth which is underlain by a constant higher velocity layer (refractor). The tremor focus lies above the refractor.

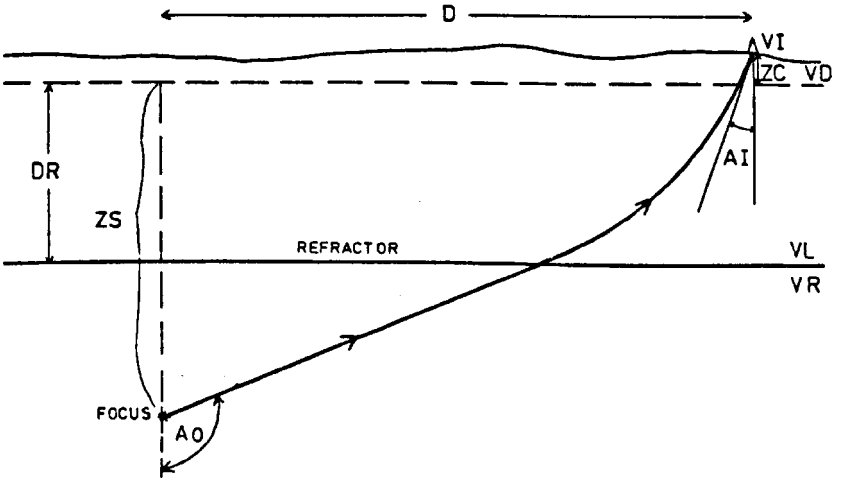

Fig. A-4: Seismic structure model with linear increase of seismic velocity with depth which is underlain by a constant higher velocity layer (refractor). The tremor focus lies below the refractor.

Fig. A-2: Flow Diagram for Subroutine SHL

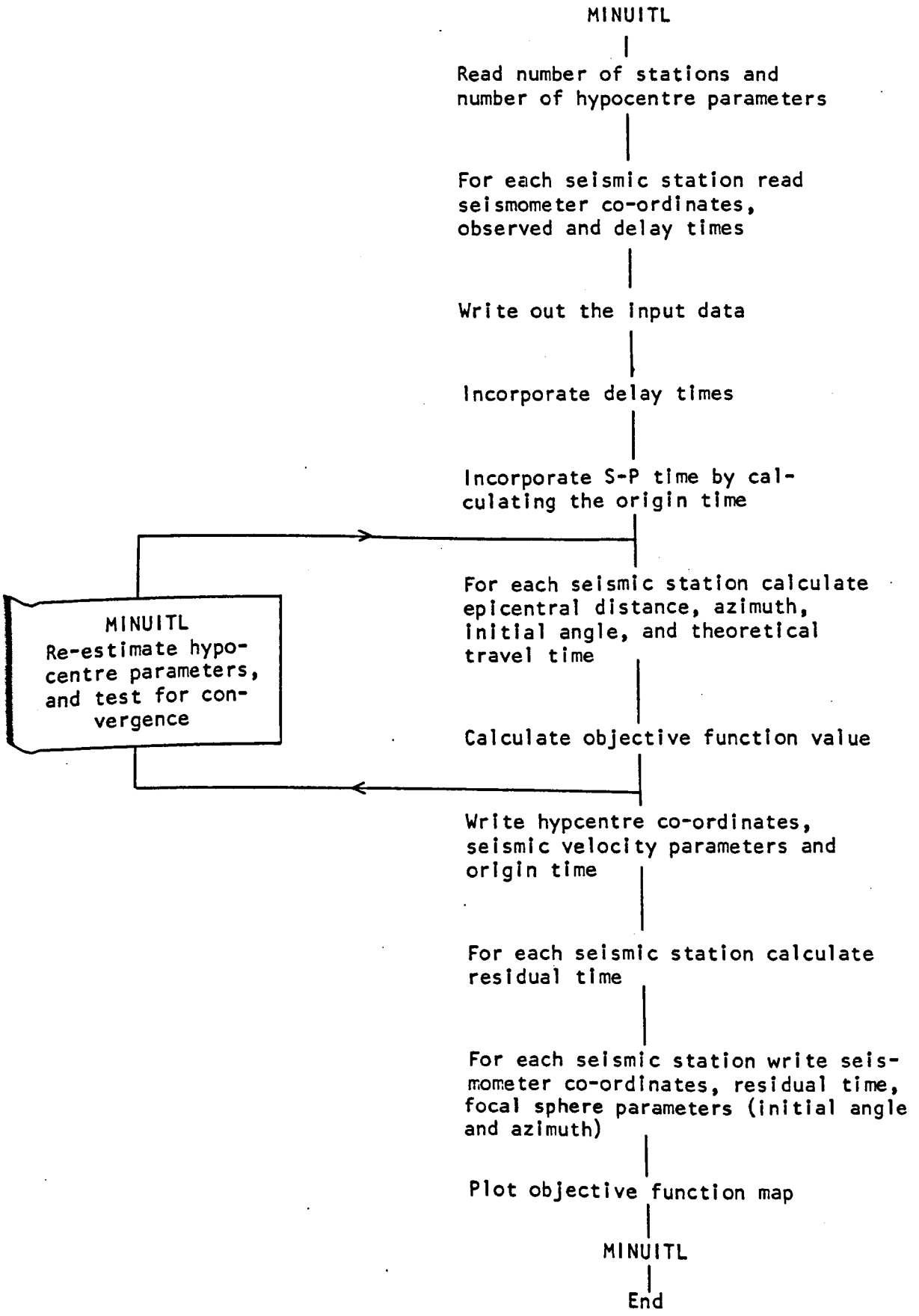

Subroutine JHL

This is a modified version of subroutine SHL. The program calculates simultaneously the tremor hypocentre parameters and origin times for a group of tremors in a given region. The program also optimizes the seismic velocity structure parameters for the given area. As in subroutine SHL, the program uses the relative delays in P-arrival times, as well as S-P arrival times (if available) at different seismometers to calculate tremor hypocentres and origin times. It assumes the same velocity model as for the SHL program. However, an alternative model can be applied, assuming a linear increase of seismic velocity with depth which is underlain by a high-speed layer (refractor), as shown in Figures A-3 and A-4. The same parameters are given or assumed as in subroutine SHL, with the exception of the seismic velocity parameters which are not known in this program. A flow diagram for the subroutine is given in Figure A-5.

All the programs were designed to run on the CDC 7600, using the CDC FORTRAN EXTENDED COMPILER.

```
          SUBROUTINE SINGLE HYPOCENTRE LOCATION (SHL)
          ******************************************

C         G= A VECTOR INTO WHICH THE DERIVATIVE ARE TO BE PUT

C         F= THE FUNCTION VALUE CALCULATED IN FCN

C         P = A VECTOR CONTAINING THE EXTERNAL PARAMETER VALUES

C         IND =A MARKER INSTRUCTS FCN ON WHAT IT SHOULD DO AT THE PARTICULAR
               CALL IN QUESTION . FOR EXAMPLE IF IND=3 IT MEANS TERMINATING
               ENTRY AND WRITE OUT ANY SPECIAL SUMMARIES , OUTPUT TABLES ...
               ....ETC. FOR THE MINIMUM POINT.

C         XC =EASTING

C         YC =NORTHING

C         T  =OBSERVED ARRIVAL TIME

C         SD =DELAY TIME AT EACH SEISMIC STATION

C         CT =CALCULATED TRAVEL TIME

C         ZC =STATION HEIGHT

C         AZ =AZIMUTH

C         PST =S-P ARRIVAL TIME

C         NPS =NUMBER OF STATIONS HAVING S-P TIME

C         IPS =STATION NUMBER WHICH CONTAINS S-P ARRIVAL

C         ANG =INITIAL ANGLE

C         NPAR =THE NUMBER OF VARIABLE PARAMETRES

C         NSTA =NUMBER OF STATIONS

C         NPA  =NUMBER OF HYPOCENTRE PARAMETERS

C*************************************************************************
```

```
      PROGRAM HYPCTR(INFILE,OUTPUT,PUNCH,TAPE7,TAPE1=INFILE,TAPE2=OUTPUT
     1,TAPE3=PUNCH)
      CALL MINUITL
      STOP
      END
C*
C*
C********SUBROUTINE SINGLE HYPOCENTRE LOCATION (SHL)
C*
      SUBROUTINE FCN(NPAR,G,F,P,IND)
      DIMENSION P(15),XC(20),YC(20),T(20),SD(20),CT(20),ZC(20),IB(5),IE(
     15),PP(5),AXV(10),FV(10),PST(20),IPS(20),ANG(20),AZ(20)
      GO TO(10,20,30,40,50),IND
C*      READ NUMBER OF STATIONS AND NUMBER OF HYPOCENTRE PARAMETRES
C*      ISD =1 MEANS IGNORE DELAY TIME
C*      ISPS=1 MEANS INCORPORATE S-P TIME
   10 READ(1,11) NSTA,NPA,ISD,ISPS
   11 FORMAT(4I5)
C*      READ SEISMOMETRE COORDINATES , OBSERVED ARRIVAL AND DELAY TIMES
      READ(1,12) (XC(I),YC(I),ZC(I),T(I),SD(I),I=1,NSTA)
   12 FORMAT(5F10.0)
      WRITE(2,14) (XC(I),YC(I),ZC(I),T(I),SD(I),I=1,NSTA)
   14 FORMAT(1H0,'DATA INPUT'/'     X          Y          Z          T
     1   SD'/(5F10.3))
C*      INCORPORATE DELAY TIME
      IF(ISD.EQ.1) GO TO 16
      DO 15 I=1,NSTA
   15 T(I)=T(I)-SD(I)
   16 IF(ISD.EQ.1) WRITE(2,17)
   17 FORMAT(1H0,'STATION DELAYS IGNORED'/'**********************')
C*      INCORPORATE S-P TIME BY CALCULATING ORIGIN TIME
      READ(1,91) NPS,(IPS(I),PST(I),I=1,NPS)
   91 FORMAT(I5,(I2,F8.0))
      WRITE(2,777) NPS,(IPS(I),PST(I),I=1,NPS)
  777 FORMAT(1H0,'SP TIME INPUT'/' NO. OF ST.   ST. NO.   SP TIME'/(2I1
     10,F10.3))
      OTS=0.
      DO 95 I=1,NPS
      IK=IPS(I)
      OTS=OTS+T(IK)-PST(I)/1.03101
   95 CONTINUE
      OTS=OTS/NPS
      IF(ISPS.EQ.1) GO TO 90
   20 CONTINUE
C*
   40 TM=0.
      XS=P(1)
      YS=P(2)
      ZS=P(3)
      VD=P(4)
      GV=P(5)
      DO 44 I=1,NSTA
      VO=VD+ZS*GV
C*      EPICENTRAL DISTANCE
      D=SQRT((XC(I)-XS)**2+(YC(I)-YS)**2)
C*      AZIMUTH
      AZ(I)=ATAN2((XC(I)-XS),(YC(I)-YS))*57.295779
      PH=ATAN(D/(2*VO/GV+ZC(I)-ZS))
      TH=ATAN((ZC(I)-ZS)/D)
      AO=1.5707963-TH-PH
```

```
C*      INITIAL ANGLE
        ANG(I)=AO*57.295779
        AI=1.5707963-TH+PH
C*      THEORETICAL TRAVEL TIME
        CT(I)=ALOG(TAN(AI/2)/TAN(AO/2))/GV
        TM=TM+T(I)-CT(I)
   44 CONTINUE
C*      ORIGIN TIME CALCULATED FROM P - ARRIVAL TIMES
        TM=TM/NSTA
        IF(ISPS.EQ.1) TM=OTPS
        SE=0.
C*      FUNCTION VALUE
        DO 46 I=1,NSTA
   46 SE=SE+(T(I)-TM-CT(I))**2
        F=SE*1000/(NSTA-1)
        RETURN
C*
   30 WRITE(2,32) P(1),P(2),P(3),P(4),P(5),TM
   32 FORMAT(1H1,'HYPOCENTRE LOCATION'/' X =',F10.3,3X,'Y =',F10.3,3X,'Z
     1 =',F10.3/' VELOCITY AT DATUM =',F10.3/' VELOCITY GRADIENT =',F10.
     13/' ORIGIN TIME       =',F10.3)
        WRITE(2,33)
   33 FORMAT(1H0,'STATION     X          Y     RESIDUAL   INIT. ANG.  AZIM
     1UTH   CAL.ARRIVAL'/)
C*      RESIDUAL VALUE
        DO 34 I=1,NSTA
        RES=T(I)-TM-CT(I)
        WRITE(2,35) I,XC(I),YC(I),RES,ANG(I),AZ(I),CT(I)
   35 FORMAT(1H ,2X,I3,2X,6F10.3)
   34 CONTINUE
        WRITE(2,37)
   37 FORMAT(1H0,'RESIDUAL = OBSERVED - CALCULATED'//)
C*
C*      PLOT OBJECTIVE FUNCTION MAP
        GO TO 40
   50 DO 51 I=1,NPA
        IE(I)=P(I)*10+5
        IB(I)=IE(I)-9
   51 CONTINUE
        NPB=NPA-1
        DO 59 I=1,NPB
        IP=I+1
        MB=IB(I)
        ME=IE(I)
        DO 59 J=IP,NPA
        LB=IB(J)
        LE=IE(J)
        IET=LE+1
        PP(1)=P(1)
        PP(2)=P(2)
        PP(3)=P(3)
        PP(4)=P(4)
        PP(5)=P(5)
        WRITE(2,551) I,J
  551 FORMAT(1H1,'OBJECTIVE FUNCTION MAP.   VARIABLES',I5,' (X)',I5,' (Y
     1)')
        IK=0
        DO 52 K=MB,ME
        IK=IK+1
   52 AXV(IK)=K*0.1
```

```
      WRITE(2,552) (AXV(IL),IL=1,IK)
  552 FORMAT(1H0,10X,10F5.1)
      DO 57 L=1,10
      LL=IET-L
      PP(J)=LL*0.1
      MM=0
      DO 56 M=MB,ME
      MM=MM+1
      PP(I)=M*0.1
      TM=0
      IF(PP(5).LT.0.000000001.AND.PP(5).GT.-0.000000001) GO TO 57
      DO 94 N=1,NSTA
      VO=PP(4)+PP(3)*PP(5)
      D=SQRT((XC(N)-PP(1))**2+(YC(N)-PP(2))**2)
      U=2*VO/PP(5)+ZC(N)-PP(3)
      IF(U.LT.0.0000001.AND.U.GT.-0.0000001) GO TO 54
      PH=ATAN(D/U)
      GO TO 55
   54 PH=1.5707963
   55 TH=ATAN((ZC(N)-PP(3))/D)
      AO=1.5707963-TH-PH
      AI=1.5707963-TH+PH
      CT(N)=ALOG(TAN(AI/2)/TAN(AO/2))/PP(5)
      TM=TM+T(N)-CT(N)
   94 CONTINUE
      TM=TM/NSTA
      IF(ISPS.EQ.1) TM=OTPS
      SE=0.
      DO 96 N=1,NSTA
   96 SE=SE+(T(N)-TM-CT(N))**2
      FV(MM)=SE*1000/(NSTA-1)
   56 CONTINUE
      WRITE(2,553) PP(J),(FV(IM),IM=1,MM)
  553 FORMAT(//,F8.1,2X,10F5.1)
   57 CONTINUE
   59 CONTINUE
      RETURN
      END
```

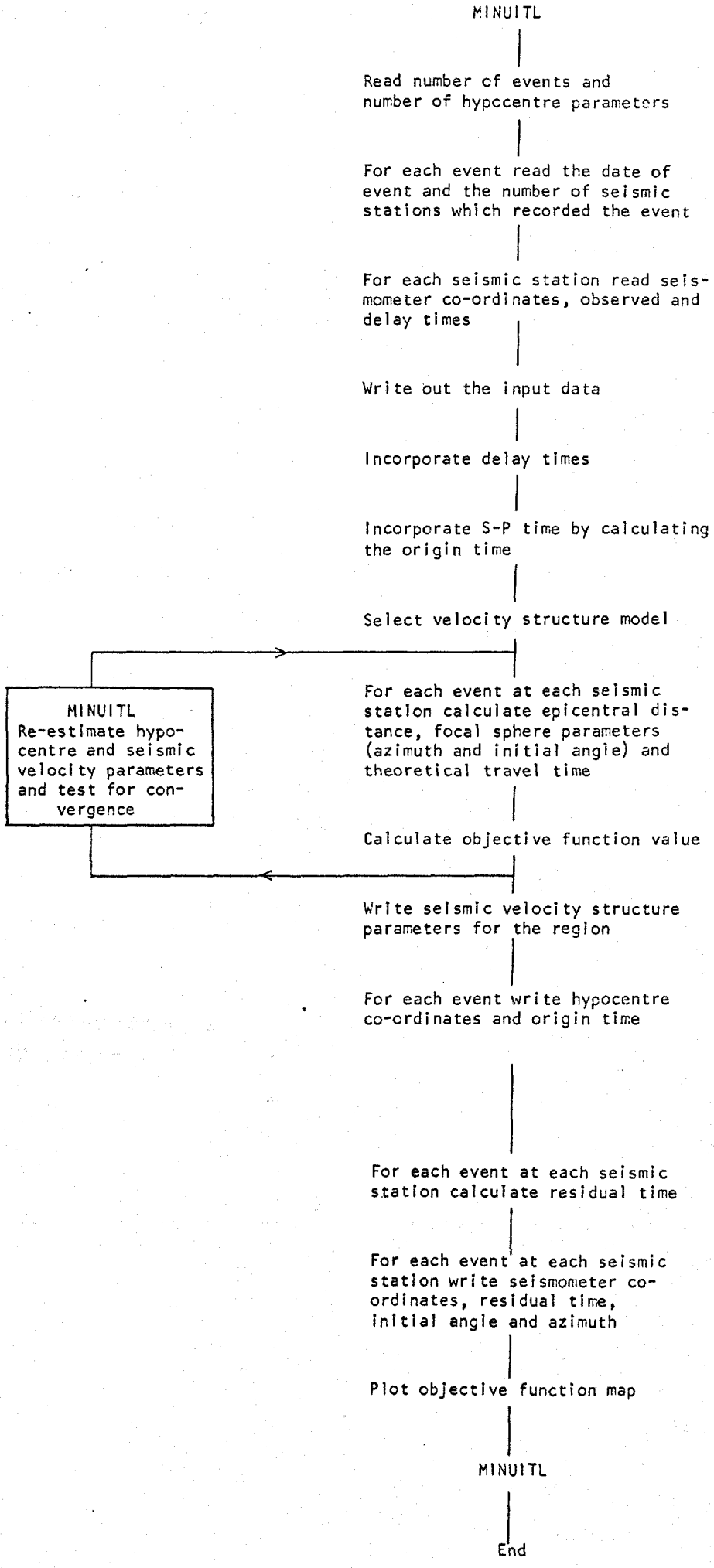
MINUITL
Read number of events and number of hypocentre parameters
For each event read the date of event and the number of seismic stations which recorded the event
For each seismic station read seismometer co-ordinates, observed and delay times
Write out the input data
Incorporate delay times
Incorporate S-P time by calculating the origin time
Select velocity structure model
For each event at each seismic station calculate epicentral distance, focal sphere parameters (azimuth and initial angle) and theoretical travel time
Calculate objective function value
MINUITL
Re-estimate hypocentre and seismic velocity parameters and test for convergence
Write seismic velocity structure parameters for the region
For each event write hypocentre co-ordinates and origin time
For each event at each seismic station calculate residual time
For each event at each seismic station write seismometer co-ordinates, residual time, initial angle and azimuth
Plot objective function map
MINUITL
End

```
      SUBRROUTINE JOINT HYPOCENTRE LOCATION (JHL)
      ******************************************

C     G= A VECTOR INTO WHICH THE DERIVATIVE ARE TO BE PUT
C     F= THE FUNCTION VALUE CALCULATED IN FCN
C     P = A VECTOR CONTAINING THE EXTERNAL PARAMETER VALUES
C     IND =A MARKER INSTRUCTS FCN ON WHAT IT SHOULD DO AT THE PARTICULAR
           CALL IN QUESTION . FOR EXAMPLE IF IND=3 IT MEANS TERMINATING
           ENTRY AND WRITE OUT ANY SPECIAL SUMMARIES , OUTPUT TABLES....
C          .....ETC. FOR THE MINIMUM POINT
C     XC =EASTING
C     YC =NORTHING
C     T  =OBSERVED ARRIVAL TIME
C     SD =DELAY TIME AT EACH SEISMIC STATION
C     CT =CALCULATED TRAVEL TIME
C     ZC =STATION HEIGHT
C     AZ =AZIMUTH
C     PST =S-P ARRIVAL TIME
C     NPS =NUMBER OF STATIONS HAVING S-P TIME
C     IPS =STATION NUMBER WHICH CONTAINS S-P ARRIVAL
C     ANG =INITIAL ANGLE
C     NPAR =THE NUMBER OF VARIABLE PARAMETRES
C     NSTA =NUMBER OF STATIONS
C     NPA  =NUMBER OF HYPOCENTRE PARAMETERS
C     NDG =NUMBER OF SEISMIC EVENTS
C     SBTTL =DATE OF SEISMIC EVENT
C     WT =WEIGHT
C*****************************************************************************
```

```
      PROGRAM HYPCTR(INFILE,OUTPUT,PUNCH,TAPE7,TAPE1=INFILE,TAPE2=OUTPUT
     1,TAPE3=PUNCH)
      CALL MINUITL
      STOP
      END
C*
C*
C********SUBROUTINE  JOINT HYPOCENTRE LOCATION (JHL)
C*
      SUBROUTINE FCN(NPAR,G,F,P,IND)
      DIMENSION P(32),XC(10,32),YC(10,32),T(10,32),SD(10,32),CT(10,32),Z
     1C(10,32),IB(7),IE(7),PP(7),AXV(32),FV(32),ANG(10,32),NSTA(32),TM(3
     22),SS(32),AZ(10,32),SBTTL(32),WT(10,32),IPS(10),PST(10),OTPS(32),I
     3SPS(32)
      GO TO(10,20,30,40,50),IND
C*      READ NUMBER OF EVENTS AND NUMBER OF HYPOCENTRE PARAMETRES
C*      IR =MEANS USE REFRACTION MODEL
C*      ISD=MEANS IGNORE DELAY TIME
   10 READ(1,11) NDG,NPA,IR,ISD
   11 FORMAT(4I5)
      NT=0
      DO 16 K=1,NDG
C*      READ DATE OF EVENT AND NUMBER OF SEISMIC STATIONS
C*      ISPS =1 MEANS INCORPORATE S-P TIME
      READ(1,13) SBTTL(K),NSTA(K),ISPS(K)
   13 FORMAT(A10,2I5)
      NT=NT+NSTA(K)
      NSTK=NSTA(K)
C*     READ SEISMOMETER COORDINATES , OBSERVED ARRIVAL AND DELAY TIMES AND WEIGHT
      READ(1,12) (XC(I,K),YC(I,K),ZC(I,K),T(I,K),SD(I,K),WT(I,K),I=1,NST
     1K)
   12 FORMAT(6F10.0)
      WRITE(2,14) SBTTL(K),(XC(I,K),YC(I,K),ZC(I,K),T(I,K),SD(I,K),WT(I,
     1K),I=1,NSTK)
   14 FORMAT(1H0,'DATA INPUT    ',A10/'    X          Y          Z
     1 T         SD         WT'/(6F10.3))
      IF(ISD.EQ.1) GO TO 18
C*     INCORPORATE DELAY TIME
      DO 15 I=1,NSTK
   15 T(I,K)=T(I,K)-SD(I,K)
   18 IF(ISPS(K).EQ.0) GO TO 16
C*     INCORPORATE S-P TIME BY CALCULATING ORIGIN TIME
      READ(1,91) NPS,(IPS(I),PST(I),I=1,NPS)
   91 FORMAT(I5,(I2,F8.0))
      WRITE(2,777) NPS,(IPS(I),PST(I),I=1,NPS)
  777 FORMAT(1H0,'SP TIME INPUT'/'  NO. OF ST.   ST. NO.   SP TIME'/(2I1
     10,F10.3))
      OTS=0.
      DO 95 I=1,NPS
      IK=IPS(I)
      OTS=OTS+T(IK,K)-PST(I)/1.03101
   95 CONTINUE
      OTPS(K)=OTS/NPS
   16 CONTINUE
      IF(ISD.EQ.1) WRITE(2,17)
   17 FORMAT(1H0,'STATION DELAYS IGNORD'/'**********************')
      NTD=NT-1
      NVP=NDG*3+2
   20 CONTINUE
   40 SE=0.
```

```
      VD=P(1)
      GV=P(2)
      IF(IR.EQ.0) GO TO 41
      VR=P(3)
      DR=P(4)
   41 DO 45 K=1,NDG
      TM(K)=0.
      SS(K)=0.
      XS=P(K*3+2)
      YS=P(K*3+3)
      ZS=P(K*3+4)
      NSTK=NSTA(K)
      DO 44 I=1,NSTK
      VO=VD+ZS*GV
      XD=XC(I,K)-XS
      YD=YC(I,K)-YS
C*      EPICENTRAL DISTANCE
      D=SQRT(XD**2+YD**2)
C*      AZIMUTH
      AZ(I,K)=ATAN2(XD,YD)*57.29578
      PH=ATAN(D/(2*VO/GV+ZC(I,K)-ZS))
      TH=ATAN((ZC(I,K)-ZS)/D)
      AO=1.5707963-TH-PH
      ZM=VO*(1/SIN(AO)-1)/GV+ZS
C*      INITIAL ANGLE
      ANG(I,K)=AO*57.29578
      AI=1.5707963-TH+PH
C*      THEORETICAL TRAVEL TIME
      CT(I,K)=ALOG(TAN(AI/2)/TAN(AO/2))/GV
      IF(IR.EQ.1) GO TO 400
   43 TM(K)=TM(K)+T(I,K)-CT(I,K)
   44 CONTINUE
      TM(K)=TM(K)/NSTK
      IF(ISPS(K).EQ.1) TM(K)=OTPS(K)
      DO 46 I=1,NSTK
   46 SS(K)=SS(K)+(T(I,K)-TM(K)-CT(I,K))**2*EXP(WT(I,K))
      SE=SE+SS(K)
   45 CONTINUE
C*      FUNCTION VALUE
      F=SE*1000./NTD
      RETURN
C*
C**** SEISMIC VELOCITY STRUCTURAL MODEL OF LINEAR INCREASE OF
        SEISMIC VELOCITY WITH DEPTH WHICH IS UNDERLAIN BY A REFRACTOR
  400 VL=DR*GV+VD
      IF(VL.GE.VR) GO TO 43
      SR=VL/VR
      SO=VO/VR
      VI=VD+ZC(I,K)*GV
      SI=VI/VR
      GVV=ABS(GV)
      IF(ZS.LE.DR) GO TO 402
      CO=SQRT(1.-SO**2)
      CI=SQRT(1.-SI**2)
      CR=SQRT(1.-SR**2)
      XO=VO*((CO-CR)/SO)/GVV
      XI=VI*((CI-CR)/SI)/GVV
      XCD=XO+XI
      IF(XCD.GE.D) GO TO 43
      AO=ATAN(SO/CO)
```

```
      AI=ATAN(SI/CI)
      AR=ATAN(SR/CR)
      TO=ALOG(TAN(AR*0.5)/TAN(AO*0.5))/GVV
      TI=ALOG(TAN(AR*0.5)/TAN(AI*0.5))/GVV
      TR=(D-XCD)/VR
      TT=TO+TI+TR
  411 IF(ZM.LT.DR) GO TO 401
      IF(CT(I,K).LT.TT) GO TO 43
  401 CT(I,K)=TT
      GO TO 43
  402 CI=SQRT(1.-SI**2)
      CR=SQRT(1.-SR**2)
      XI=VI*((CI-CR)/SI)/GVV
      IF(XI.GE.D) GO TO 43
      AI=ATAN(SI/CI)
      AR=ATAN(SR/CR)
      TI=ALOG(TAN(AR*0.5)/TAN(AI*0.5))/GVV
      TT=SQRT((DR-ZS)**2+(D-XI)**2)/VR+TI
      GO TO 411
   30 WRITE(2,301) P(1),P(2),P(3),P(4)
  301 FORMAT(1H1,'LOCATION OF HYPOCENTRES'//' VELOCITY AT DATUM =',F8.3/
     1' VELOCITY GRADIENT =',F8.3/' VELOCITY OF REFRACTOR =',F8.3/' DEPT
     2H OF REFRACTOR    =',F8.3/)
      DO 34 K=1,NDG
      WRITE(2,31) K,SBTTL(K)
   31 FORMAT(1H0/,' DATA GROUP',I3,5X,A10)
      WRITE(2,32) P(K*3+2),P(K*3+3),P(K*3+4),TM(K)
   32 FORMAT(1H0,'HYPOCENTRE LOCATION'/' X =',F10.3,3X,'Y =',F10.3,3X,'Z
     1 =',F10.3//' ORIGIN TIME =',F8.3)
      IF(ISPS(K).EQ.1) WRITE(2,1250)
 1250 FORMAT(1H0/',                    ** SP TIME USED **')
      WRITE(2,33)
   33 FORMAT(1H0,'STATION    X          Y      RESIDUAL  INIT. ANG  AZIMUT
     1H'/)
      NSTK=NSTA(K)
C*     RESIDUAL TIME
      DO 34 I=1,NSTK
      RES=T(I,K)-TM(K)-CT(I,K)
      WRITE(2,35) I,XC(I,K),YC(I,K),RES,ANG(I,K),AZ(I,K)
   35 FORMAT(1H ,2X,I3,2X,2F10.3,F8.3,2F10.3)
   34 CONTINUE
      WRITE(2,37)
   37 FORMAT(1H0,' RESIDUAL = OBSERVED - CALCULATED'//)
      GO TO 40
C*
C*     PLOT OBJECTIVE FUNCTION MAP
   50 DO 501 I=4,7
      PP(I)=P(I-3)
      IE(I)=PP(I)*10+5
      IB(I)=IE(I)-9
  501 CONTINUE
      DO 60 K=1,NDG
      DO 51 I=1,3
      IE(I)=P(3*(K-1)+4+I)*10+5
      IB(I)=IE(I)-9
   51 CONTINUE
      NPB=NPA-1
      DO 59 I=1,NPB
      IP=I+1
      MB=IB(I)
```

```
      ME=IE(I)
      DO 59 J=IP,NPA
      LB=IB(J)
      LE=IE(J)
      IET=LE+1
      PP(1)=P(K*3+2)
      PP(2)=P(K*3+3)
      PP(3)=P(K*3+4)
      DO 557 II=4,7
  557 PP(II)=P(II-3)
      WRITE(2,551) I,J
  551 FORMAT(1H1,'OBJECTIVE FUNCTION MAP.   VARIABLES',I5,' (X)',I5,' (Y
     1)')
      IK=0
      DO 52 LK=MB,ME
      IK=IK+1
   52 AXV(IK)=LK*0.1
      WRITE(2,552) (AXV(IL),IL=1,IK)
  552 FORMAT(1H0,10X,10F5.1)
      DO 57 L=1,10
      LL=IET-L
      PP(J)=LL*0.1
      MM=0
      DO 56 M=MB,ME
      MM=MM+1
      PP(I)=M*0.1
      IF(PP(5).LT.0.000000001.AND.PP(5).GT.-0.000000001) GO TO 57
      SE=0.
      DO 58 KK=1,NDG
      IF(KK.EQ.K) GO TO 58
      SE=SE+SS(KK)
   58 CONTINUE
      KK=K
      TM(KK)=0.
      NSTKK=NSTA(KK)
      DO 94 N=1,NSTKK
      VO=PP(4)+PP(3)*PP(5)
      D=SQRT((XC(N,KK)-PP(1))**2+(YC(N,KK)-PP(2))**2)
      U=2*VO/PP(5)+ZC(N,KK)-PP(3)
      IF(U.LT.0.0000001.AND.U.GT.-0.0000001) GO TO 54
      PH=ATAN(D/U)
      GO TO 55
   54 PH=1.5707963
   55 TH=ATAN((ZC(N,KK)-PP(3))/D)
      AO=1.5707963-TH-PH
      ZM=VO*(1/SIN(AO)-1)/PP(5)+PP(3)
      AI=1.5707963-TH+PH
      CT(N,KK)=ALOG(TAN(AI/2)/TAN(AO/2))/PP(5)
      IF(IR.EQ.1) GO TO 500
  555 TM(KK)=TM(KK)+T(N,KK)-CT(N,KK)
      GO TO 94
  500 VL=PP(7)*PP(5)+PP(4)
      IF(VL.GE.PP(6)) GO TO 555
      SR=VL/PP(6)
      SO=VO/PP(6)
      VI=PP(4)+ZC(N,KK)*PP(5)
      SI=VI/PP(6)
      GVV=ABS(PP(5))
      IF(PP(3).LE.PP(7)) GO TO 420
      CO=SQRT(1.-SO**2)
```

```
      CI=SQRT(1.-SI**2)
      CR=SQRT(1.-SR**2)
      XO=VO*((CO-CR)/SO)/GVV
      XI=VI*((CI-CR)/SI)/GVV
      XCD=XO+XI
      IF(XCD.GE.D) GO TO 555
      AO=ATAN(SO/CO)
      AI=ATAN(SI/CI)
      AR=ATAN(SR/CR)
      TO=ALOG(TAN(AR*0.5)/TAN(AO*0.5))/GVV
      TI=ALOG(TAN(AR*0.5)/TAN(AI*0.5))/GVV
      TR=(D-XCD)/PP(6)
      TT=TO+TI+TR
  508 IF(ZM.LT.PP(7)) GO TO 509
      IF(CT(N,KK).LT.TT) GO TO 555
  509 CT(N,KK)=TT
      GO TO 555
  420 CI=SQRT(1.-SI**2)
      CR=SQRT(1.-SR**2)
      XI=VI*((CI-CR)/SI)/GVV
      IF(XI.GE.D) GO TO 555
      AI=ATAN(SI/CI)
      AR=ATAN(SR/CR)
      TI=ALOG(TAN(AR*0.5)/TAN(AI*0.5))/GVV
      TT=SQRT((DR-ZS)**2+(D-XI)**2)/PP(6)+TI
      GO TO 508
   94 CONTINUE
      TM(KK)=TM(KK)/NSTKK
      IF(ISPS(K).EQ.1) TM(KK)=OTPS(KK)
      DO 96 N=1,NSTKK
   96 SE=SE+(T(N,KK)-TM(KK)-CT(N,KK))**2*EXP(WT(N,KK))
      FV(MM)=SE*1000/NTD
   56 CONTINUE
      WRITE(2,553) PP(J),(FV(IM),IM=1,MM)
  553 FORMAT(//,F8.1,2X,10F5.1)
   57 CONTINUE
   59 CONTINUE
   60 CONTINUE
      RETURN
      END
```

APPENDIX 2

Dates of tremor occurrence, hypocentre co-ordinates, local magnitude and seismic energy released

Date					Easting	Northing	Depth from	No. of	Local Magnitude	Energy Released
Y	M	D	H	Mn	km	km	O.D. (km)	Stations	(M_L)	(Joules x 10^5)
75	9	3	19	35	82.658	46.849	0.436	4*	2.1	71.4
75	9	10	11	54	82.410	48.368	0.290	4*	1.2	1.6
75	9	12	11	58	82.205	48.344	0.431	4	1.8	1.3
75	9	16	11	56	82.450	48.064	0.231	4	2.0	44.7
75	10	9	03	45	85.813	50.811	-0.100	4*	0.8	0.2
75	10	16	18	38	82.686	46.745	0.582	4*	2.1	51.6
75	10	24	17	03	85.016	50.149	2.000	4*	0.8	0.3
75	10	31	12	40	83.327	46.489	-0.047	4*	1.9	23.8
75	11	10	06	55	82.503	55.147	-0.100	4*	1.2	1.2
75	11	21	12	13	85.909	50.512	0.497	4	2.3	121.0
75	11	21	15	34	86.453	49.163	0.025	4*	0.8	0.3
75	12	10	05	36	87.734	48.299	0.077	5*	0.7	0.2
75	12	12	01	21	87.663	48.228	0.517	4*	1.1	0.9
75	12	18	07	56	87.671	48.309	0.229	5*	1.0	0.5
76	2	10	18	55	83.405	46.353	-0.078	4	0.6	0.09
76	3	10	13	33	83.125	45.259	-0.100	4*	0.3	0.03
76	3	15	06	42	85.196	47.909	-0.100	4	1.7	13.4
76	3	16	00	31	85.522	48.154	0.538	4	1.0	0.5
76	3	17	21	28	84.039	46.304	0.814	4	0.5	0.07
76	3	19	19	21	85.584	47.070	0.613	4	1.0	0.5
76	3	22	15	10	85.385	48.752	1.209	4	1.4	3.0
76	3	25	05	16	88.897	50.215	-0.100	4*	1.1	0.9
76	3	25	23	43	82.314	47.585	2.000	4*	1.0	0.7
76	3	26	03	27	78.403	50.388	2.000	4*	1.3	1.8
76	3	31	02	48	81.950	47.589	2.000	4	1.1	1.1
76	4	13	17	37	75.835	52.239	-0.100	4*	1.8	19.4
76	4	22	13	16	82.610	46.028	0.263	4*	1.1	0.8
76	5	4	23	34	84.019	46.366	1.001	4	0.8	0.3
76	5	5	15	13	82.255	45.977	0.451	4*	1.9	22.8
76	5	6	16	06	83.395	46.922	0.488	4*	1.2	1.2
76	5	6	16	23	82.792	45.726	0.339	4*	1.7	9.3
76	6	4	10	29	84.585	50.678	1.636	5*	2.2	87.1
76	6	9	18	57	82.468	47.127	0.198	4	0.9	0.3
76	6	11	04	28	87.878	49.275	0.511	4*	0.3	0.03
76	6	12	19	00	82.971	46.723	-0.070	4	1.5	6.0
76	6	15	21	08	87.600	48.723	0.121	5*	2.4	225.4
76	6	24	12	57	87.890	48.670	0.694	5*	1.1	0.9
76	7	15	00	00	88.718	49.644	-0.100	4*	1.2	1.2
76	7	16	12	44	85.528	50.907	1.012	4*	1.1	1.0
76	7	19	20	00	82.268	46.964	0.321	5*	2.0	37.5
76	9	11	07	28	83.183	50.207	-0.094	5*	1.7	9.5
76	9	29	01	45	87.454	48.038	0.395	5	1.0	0.6

Y	Date M	D	H	Mn	Easting km	Northing km	Depth from O.D. (km)	No. of Stations	Local Magnitude (M_L)	Energy Released (Joules x 10^5)
76	10	1	20	02	87.514	48.624	0.024	5*	1.8	17.3
76	10	5	03	38	86.099	50.766	0.427	5	1.4	3.6
76	10	17	05	13	87.397	48.110	0.502	5	0.8	0.3
76	10	18	07	17	87.680	48.655	0.231	5	1.6	9.1
76	10	22	05	24	87.494	48.462	0.709	4	0.9	0.5
76	10	26	09	23	87.638	48.295	0.413	4*	0.8	0.3
76	10	26	14	13	87.455	48.266	0.764	4	0.9	0.3
76	10	31	15	47	83.017	53.210	-0.031	4*	2.5	368.3
76	11	25	22	53	83.616	45.851	1.493	4	0.4	0.04
76	11	26	22	47	85.932	47.930	0.165	5*	1.2	1.3
76	11	26	23	00	85.905	48.014	0.465	4*	0.9	0.4
76	11	27	02	27	87.348	48.100	0.596	5	0.9	0.4
76	11	27	07	59	86.051	48.158	0.537	4*	1.5	4.9
76	11	27	12	10	86.035	47.963	0.262	4*	1.0	0.5
76	12	2	00	10	82.621	47.127	-0.079	4	0.7	0.2
76	12	2	05	08	87.490	48.383	0.375	5*	1.7	11.5
76	12	4	03	09	87.359	49.190	1.450	4*	0.3	0.03
76	12	5	22	36	83.051	51.481	0.287	4	1.5	4.0
76	12	9	17	10	87.591	48.475	0.576	5	0.7	0.2
77	1	19	03	49	83.981	49.106	0.658	4*	1.2	1.4
77	1	21	19	20	85.677	50.644	0.919	4*	1.3	2.2
77	2	13	03	43	82.862	46.426	0.780	4*	0.5	0.06
77	2	15	01	03	83.300	51.102	0.384	5*	1.7	10.0
77	2	18	10	47	86.084	52.079	0.208	4	2.1	55.3
77	2	25	00	49	83.551	50.904	0.470	4*	1.0	0.6
77	2	25	00	51	83.316	50.594	0.908	4	0.9	0.5
77	3	8	04	06	84.612	51.696	0.116	4*	0.9	0.5
77	3	10	12	39	82.903	47.723	0.355	4*	0.8	0.3
77	3	29	03	28	86.142	50.987	0.306	5	0.7	0.2
77	4	7	02	30	85.999	50.957	0.591	5	1.2	1.3
77	4	20	23	21	82.288	47.246	0.296	4	1.4	2.9
77	4	26	17	59	85.916	50.410	0.605	4	1.2	1.3
77	4	28	19	27	83.634	52.717	0.287	4*	1.3	2.2
77	5	8	00	34	83.557	49.378	0.614	4*	0.5	0.08
77	5	11	09	35	85.943	50.639	0.594	5	1.3	2.4
77	5	11	13	38	85.737	49.965	0.911	5	0.9	0.5
77	5	28	04	03	85.984	51.116	0.660	4	1.3	2.3
77	5	30	20	13	85.946	51.370	0.577	4	0.8	0.3
77	5	31	21	03	82.736	46.353	0.328	4*	1.3	1.9
77	6	10	19	16	85.947	51.342	0.402	5*	0.7	0.2
77	6	14	01	53	84.405	48.591	-0.100	4*	0.4	0.05
77	6	15	03	39	83.390	46.778	-0.094	4	0.5	0.06
77	6	15	16	35	82.931	47.124	0.575	4	0.5	0.06
77	6	16	15	50	86.138	51.719	0.381	5	0.9	0.4
77	6	17	15	01	86.130	51.190	0.543	4	1.0	0.6
77	6	19	16	27	80.826	48.610	0.217	4*	0.1	0.01
77	6	25	23	24	87.346	47.702	0.910	5	0.5	0.06
77	7	10	14	07	87.571	48.467	0.596	5	0.6	0.1
77	7	13	16	23	82.917	46.336	0.078	4*	0.8	0.2
77	7	19	18	11	85.846	52.219	0.330	4*	1.0	0.5
77	7	20	09	57	86.007	51.348	0.572	5	1.1	1.1

Y	Date M	D	H	Mn	Easting km	Northing km	Depth from O.D. (km)	No. of Stations	Local Magnitude (M_L)	Energy Released (Joules x 10^5)
77	7	27	17	44	82.496	46.517	0.607	4*	0.6	0.1
77	7	30	07	28	85.845	50.800	0.588	4	1.1	0.8
77	8	6	19	55	85.999	51.509	0.363	5	1.1	0.9
77	8	10	20	22	85.962	51.248	0.630	5*	1.4	3.0
77	8	18	00	29	83.367	46.765	-0.100	4	0.1	0.01

Y Year
M Month
D Day
H Hour
Mn Minute
- Indicates depth above O.D.
* Indicates tremor with a shear source mechanism